



**HAL**  
open science

# Analyse et modélisation du développement de plantes cultivées soumises à des contraintes environnementales

Olivier Turc

► **To cite this version:**

Olivier Turc. Analyse et modélisation du développement de plantes cultivées soumises à des contraintes environnementales. Sciences du Vivant [q-bio]. Université de Montpellier, 2018. tel-02789509

**HAL Id: tel-02789509**

**<https://hal.inrae.fr/tel-02789509>**

Submitted on 5 Jun 2020

**HAL** is a multi-disciplinary open access archive for the deposit and dissemination of scientific research documents, whether they are published or not. The documents may come from teaching and research institutions in France or abroad, or from public or private research centers.

L'archive ouverte pluridisciplinaire **HAL**, est destinée au dépôt et à la diffusion de documents scientifiques de niveau recherche, publiés ou non, émanant des établissements d'enseignement et de recherche français ou étrangers, des laboratoires publics ou privés.



Distributed under a Creative Commons Attribution 4.0 International License



*Habilitation à Diriger des Recherches*

## **Analyse et modélisation du développement de plantes cultivées soumises à des contraintes environnementales**

**Olivier Turc**  
Chargé de Recherche  
UMR LEPSE

Soutenue le 16 octobre 2018 devant le jury composé de :

**Mme Nadia BERTIN**, Directrice de Recherche, INRA Avignon, Rapporteur  
**Mme Evelyne COSTES**, Directrice de Recherche, INRA Montpellier, Rapporteur  
**M. Jan TRAAS**, Directeur de Recherche, INRA ENS Lyon, Rapporteur  
**M. Bruno TOURAINE**, Professeur, Université de Montpellier, Examineur  
**Mme Anne-Sophie VOISIN**, Chargée de Recherche, INRA Dijon, Examinatrice  
**Mme Alexandra JULLIEN**, Professeure AgroParisTech, Examinatrice





## Sommaire

<b><u>CV</u></b>	1
<i>Parcours professionnel</i>	1
<i>Contrats de recherche récents</i>	1
<i>Collaborations productives</i>	2
<i>Investissement au service de collectifs de recherche et pour la diffusion de la recherche</i>	3
<i>Encadrement d'étudiants</i>	4
<b><u>Travaux de recherche et projet</u></b>	10
<i>Contexte général</i>	10
<b><u>1. Construction de modèles de développement des plantes</u></b>	11
<i>1.1 Une représentation du développement commune à différentes espèces et différents types d'organes</i>	11
<i>1.2 Mise en évidence de stades de développement caractéristiques</i>	13
<i>1.3 Stabilité des modèles de développement sur une échelle de temps thermique</i>	17
<i>1.4 Les modifications de développement en réponse au déficit hydrique</i>	19
<b><u>2. Les modèles de développement des plantes, une plus-value pour analyser les réponses écophysiologicals à des contraintes environnementales</u></b>	21
<i>2.1 Analyse spatiale de la réponse de la croissance foliaire à une contrainte transitoire</i>	21
<i>2.2 Analyse du déroulement de la sénescence foliaire, utilisant conjointement le modèle de développement et des marqueurs moléculaires</i>	23
<i>2.3 Fonctionnement du méristème végétatif et reproducteur du tournesol</i>	25
<i>2.4 Analyse spatiale de la croissance des soies de maïs : divisions cellulaires, expansion et lien avec le développement reproducteur</i>	28
<i>2.5 Réponse aux températures élevées chez la microvigne</i>	29
<b><u>3. L'impact du déficit hydrique sur les organes reproducteurs s'explique-t-il par leur statut carboné ?</u></b>	31
<i>3.1 Le déficit hydrique s'accompagne d'une accumulation de sucres dans les organes reproducteurs en croissance</i>	31
<i>3.2 Séquence d'événements conduisant à l'avortement des ovaires de maïs en déficit hydrique</i>	33
<i>3.3 Analyse des événements moléculaires associés à l'avortement des ovaires</i>	35
<i>3.4 Un contrôle hydraulique de la croissance des soies, similaire à celui des feuilles</i>	36
<i>3.5 Avortement d'organes reproducteurs et processus d'expansion</i>	38

<u>4. Projet de recherche</u>	39
4.1 <i>Projet 1 : analyse rétrospective du progrès génétique chez le maïs</i>	40
4.2 <i>Projet 2 : Déterminants physiologiques : visualisation des flux d'eau (IRM)</i>	41
4.3 <i>Projet 3 : Exploration des déterminants génétiques</i>	43
4.4 <i>Projet 4 : phénotypage de la croissance des soies et modélisation de l'élaboration du rendement en grains</i>	43
<b><u>Liste des publications</u></b>	46
<b><u>Annexe : Publications choisies</u></b>	53

- Turc O, Tardieu F** (2018) Drought affects abortion of reproductive organs by exacerbating developmentally-driven processes, via expansive growth and hydraulics. *Journal of Experimental Botany* **69**: 3245-3254.
- Turc O, Bouteillé M, Fuad-Hassan A, Welcker C, Tardieu F** (2016) The growth of vegetative and reproductive structures (leaves and silks) respond similarly to hydraulic cues in maize. *New Phytologist* **212**: 377-388.
- Oury V, Tardieu F, Turc O** (2016) Ovary apical abortion under water deficit is caused by changes in sequential development of ovaries and in silk growth rate in maize. *Plant Physiology* **171**: 986-996.
- Oury V, Caldeira CF, Prodhomme D, Pichon J-P, Gibon Y, Tardieu F, Turc O** (2016) Is change in ovary carbon status a cause or a consequence of maize ovary abortion in water deficit during flowering? *Plant Physiology* **171**: 997-1008.
- Muller B, Pantin F, Génard M, Turc O, Freixes S, Piques M, Gibon Y** (2011) Water deficits uncouple growth from photosynthesis, increase C content, and modify the relationships between C and growth in sink organs. *Journal of Experimental Botany* **62**: 1715-1729.
- Dosio GAA, Tardieu F, Turc O** (2011) Floret initiation, tissue expansion and carbon availability at the meristem of the sunflower capitulum as affected by water or light deficits. *New Phytologist* **189**: 94-105.

Olivier Turc

Né le 9 avril 1960 à Montpellier

Nationalité française

Marié, 3 enfants

Chargé de Recherche INRA

UMR LEPSE, 2 place Pierre Viala, 34060 Montpellier cedex 2

Section CNU 68 : Biologie des organismes

Docteur de l'Université de Montpellier, spécialité Physiologie et Biologie des organismes et des populations (19/10/1988)

Ecole Doctorale 584 GAIA - Biodiversité, Agriculture, Alimentation, Environnement, Terre, Eau

Filière BIDAP - Biologie, Interactions, Diversité Adaptative des Plantes

### **Parcours professionnel**

1994 - Chargé de Recherche, UMR LEPSE, INRA Montpellier

1989- 1993 Chargé de Recherche, Station d'Agronomie LECSA, INRA Montpellier

1986- mars 1987 Volontaire de l'Aide Technique, Station de Physiologie Végétale, INRA Antilles-Guyane

1984-1985, puis avril 1987-1988 : Attaché Scientifique Contractuel, Station d'Agronomie, INRA Dijon

### **Contrats de recherche récents**

Programme national *Investissements d'avenir* PHENOME 2012-2021. Développements méthodologiques autour des plateformes de phénotypage. 2 projets autour de l'imagerie des épis de maïs. (2700 k€ pour l'équipe)

ANR Investissement d'avenir AMAIZING 2012-2020. Participant. 800 k€ pour l'équipe

Agropolis Fondation Flagship project APLIM 2016-2019, utilisation RMN en physiologie végétale, participant

Pari scientifique département EA 2016-2017. IRM pour caractériser l'avortement d'organes reproducteurs. Responsable sous-projet maïs 30 k€

UE DROPS 2011-2015. DROught-tolerant yielding Plants. Responsable du sous-programme "mise au point de méthodes de caractérisation de l'avortement des grains, fondées sur des modèles et processus écophysiologicals" dans le work package "De la plate-forme de

phénotypage au champ" 1200 k€ pour l'équipe

ANR DROMADaIR 2008-2013. DROught adapted MAize : ear Development and leaf Area. Responsable du work package 2 "Determinism of kernel abortion in water deficit" 325 k€ pour l'équipe

Generation Challenge Programme (2006 - 2011) : analyse phénotypique d'un panel tropical et analyse d'un réseau d'essais au champ en conditions de sécheresse 47 k€

### **Collaborations productives**

- Collaborations dans l'unité :

Equipe MAGE (15 articles scientifiques : Art1 ; Art3 ; Art5 ; Art6 ; Art7 ; Art8 ; Art9 ; Art11 ; Art16 ; Art17 ; Art18 ; Art19 ; Art21 ; Art22 ; Art24)

LEPSE hors équipe MAGE (14 articles scientifiques : Art2 ; Art4 ; Art8 ; Art9 ; Art10 ; Art11 ; Art12 ; Art13 ; Art21 ; Art23 ; Art25 ; Chap1; Chap2 ; Chap7 ; Chap9)

- Collaborations locales (Montpellier) :

UMR AGAP, INRA, CIRAD, Montpellier SupAgro (2 articles scientifiques : Art1 ; Art12)

UMR BPMP, INRA, Montpellier SupAgro (2 articles scientifiques : Art19 ; Art25)

UMR AMAP, CIRAD, Montpellier (2 articles scientifiques : Art3 ; Art4)

LIRMM, Université Montpellier (1 article scientifique : Art1)

UMR SPO, INRA, Montpellier (1 article scientifique : Art12)

- Collaborations nationales :

UMR Agronomie, INRA, Dijon (7 articles scientifiques : Art14 ; Art15 ; Art20 ; Chap3 ; Chap4 ; Chap5 ; Chap8)

UMR Biologie et Pathologie du Fruit, INRA Bordeaux (4 articles scientifiques : Art12 ; Art13 ; Art16 ; Art18)

UMR PSH, INRA, Avignon (1 article scientifique : Art13)

UMR GQE, INRA, Le Moulon (1 article scientifique : Conf12)

Biogemma, Clermont-Ferrand (1 article scientifique : Art16)

- Collaborations internationales :

INTA, Université Mar del Plata, Argentine (4 articles scientifiques : Art3 ; Art4 ; Art5 ; Art6)

Max Planck Institut, Gölm, Allemagne : (2 articles scientifiques : Art13 ; Art18)

Université Queensland, Brisbane, Australie (1 article scientifique : Conf16)

Pioneer, Des Moines, USA (1 article scientifique : Conf16)

Estação Nacional de Melhoramento de Plantas (ENMP), Elvas, Portugal (1 article scientifique : Conf27)

### **Investissement au service de collectifs de recherche et pour la diffusion de la recherche**

Membre élu du Conseil scientifique de Centre de 2002 à 2016

Correspondant documentation de l'unité. En l'absence de documentaliste dans l'UMR, je suis chargé d'assurer la mise à jour du référencement des productions de l'unité (base de données des publications de l'IBIP, base institutionnelle ProDINRA, enquêtes du Département EA etc..)

Responsable "Imagerie" de l'unité : animation d'un atelier d'imagerie (gestion du parc microscopie de l'unité, formation des utilisateurs, veille technologique) ; correspondant imagerie pour l'UMR dans la plateforme régionale "Montpellier RIO Imaging ».

Reviewer régulier d'articles scientifiques dans plusieurs revues internationales (JExpBot, AnnBot, PlantJ, PCE...)

Participation à la formation "Ecophysiologie et phénotypage du maïs" à destination des expérimentateurs "maïs" publics et privés, organisée par la Formation Continue de Montpellier SupAgro, soutenue par les projets ANR Investissements d'Avenir Phenome et Amaizing (environ 1 session de 3h par an )

Participation à la conception du stand de l'unité au Salon de l'Agriculture en 2012 (prototype miniaturisé de phénotypage et documents pédagogiques, à nouveau présentés au SIA de 2014) ; interview sur le phénotypage pendant le SIA 2012 diffusée sur France 24

Correspondant de l'unité pour la rédaction des dossiers d'Agropolis (publications Trans3 ; Trans4 ; Trans5)

## **Encadrement d'étudiants**

### **Co-encadrement de doctorants**

- Etu1. Oury V* (2014) Déterminisme du nombre de grains chez le maïs (*Zea mays* L.) en déficit hydrique : rôles de la dynamique d'émergence des soies et du métabolisme carboné. Thèse de Doctorat Biologie Intégrative des Plantes. Montpellier SupAgro, Montpellier, France, 73 p. (*encadrant principal*).
- Etu2. Luchaire N* (2015) Réponses développementales et physiologiques de la Microvigne aux températures élevées : caractérisation de l'effet sur le bilan carboné et son implication dans l'avortement précoce des organes reproducteurs. Thèse de Doctorat Biologie Intégrative des Plantes. Montpellier SupAgro, Montpellier, France, 315 p. (*participation à l'encadrement*)
- Etu3. Fuad-Hassan A* (2006) Analyse de la croissance des soies de plantes de maïs soumises à des déficits hydriques édaphiques et atmosphériques. Thèse de Doctorat Biologie Intégrative. ENSAM, Montpellier, France, 61 p. (*encadrant principal*)
- Etu4. Dosio GAA* (2002) Analyse conjointe des développements végétatifs reproducteurs chez des plantes de tournesol soumises à des déficits précoces en eau et en lumière. Thèse de Doctorat Biologie Intégrative. ENSAM, Montpellier, France, 65 p. (*encadrant principal*)
- Etu5. Pic E* (1998) Analyse de la sénescence foliaire chez le pois (*Pisum sativum* L., cv Messire) : utilisation conjointe d'un modèle de développement et de marqueurs moléculaires. Thèse de Doctorat Sciences Agronomiques. ENSAM, Montpellier, France, 168 p. (*encadrant principal*)

### *Devenir des doctorants :*

Vincent Oury a créé une start-up pour le phénotypage des plantes (Phymea-systems) basée sur le campus de Montpellier SupAgro (incubateur INRA – SupAgro)

Nathalie Luchaire est en recherche d'emploi après un CDD de 2 ans à l'INRA

Avan Fuad-Hassan est traductrice-interprète (anglais, français, arabe, kurde) au Royaume-Uni (après 4 ans dans une entreprise de biotechnologies végétales)

Guillermo Dosio est enseignant chercheur au CONICET, Université de Mar del Plata, Argentine

Emmanuelle Pic est responsable de projets scientifiques à l'Agence Nationale de Sécurité Sanitaire

### **Direction d'étudiants de Master (ou DEA)**

- Etu6. Abani H* (2009) Caractérisation du gradient de développement sur l'épi et contrôle de l'état hydrique du sol dans un programme d'amélioration de la tolérance au déficit hydrique chez le maïs. Mémoire M2Pro Conception et Evaluation des Systèmes de Production. SupAgro, Montpellier, France, 37 p.

- Etu7.* **Bies N** (1992) Conséquences de stress hydriques sur la qualité des semences de pois (*Pisum sativum* L.). Mémoire de Master Biologie Cellulaire et Physiologie, option physiologie végétale appliquée. Université Montpellier II, Montpellier, France, 18 p.
- Etu8.* **Bouteillé M** (2006) Analyse de la croissance des soies et des feuilles chez des lignées de maïs (*Zea mays*) contrastées pour le maintien du développement reproducteur en situation de déficit hydrique. Mémoire de Master Biologie Géosciences Agroressources Environnement, spécialité Biologie Fonctionnelle des Plantes. Université Montpellier II, Montpellier, France, 17 p.
- Etu9.* **Brichet N** (2014) Analyse d'image pour la détection d'organes spécifiques de plantes : l'épi de maïs au début de son développement. Mémoire de M2 Électronique, Électrotechnique et Automatismes. Université Montpellier II, Montpellier, France, 38 p. (*participation à l'encadrement*)
- Etu10.* **Cuny J-F** (1992) Un modèle de fonctionnement du pois protéagineux : CROPOIS. Mise au point et première validation. DAA Génie Agronomique. ENSAM, Montpellier, France, 30 p.
- Etu11.* **Dourguia J** (2005) Analyse spatiale et temporelle de la division et de l'expansion cellulaires dans des soies de plantes de maïs soumises à un déficit hydrique. Mémoire de Master Biologie Géosciences Agroressources Environnement, option Biologie Fonctionnelle des Plantes. Université Montpellier II, Montpellier, France, 17 p.
- Etu12.* **Lamy T** (2011) Caractérisation du transport de saccharose vers l'épi de maïs (*Zea mays* L.) lors de son développement. Mémoire de Master Biologie Santé. Université Montpellier II, Montpellier, France, 11 p.
- Etu13.* **Laugier N** (2003) Coordination de l'expansion des tissus et de l'initiation des boutons floraux sur des capitules de tournesol en réponse à des déficits précoces en eau et en lumière. Mémoire de Master Biologie Cellulaire et Physiologie, option physiologie végétale appliquée. Université Montpellier II, Montpellier, France, 21 p.
- Etu14.* **Lefevre T** (1998) Analyse de la mise en place de la surface foliaire à l'échelle de la plante chez le tournesol (*Helianthus annuus* L., variété Albena) : élaboration d'un modèle de développement. Diplôme d'Etudes Approfondies Bases de la Production Végétale. ENSAM - Université Montpellier II, Montpellier, France, 18 p.
- Etu15.* **Marin V** (2003) Mise au point d'une méthode d'analyse en continu de la croissance des soies chez différents géotypes de maïs. Mémoire de Master Biologie Cellulaire et Physiologie, option physiologie végétale appliquée. Université Montpellier II, Montpellier, France, 18 p.
- Etu16.* **Martin J** (1993). Effet de déficits hydriques pré-floraison sur le développement reproducteur chez le pois. Diplôme d'Etudes Approfondies "Bases de la Production Végétale". ENSA.M - Université Montpellier II. 16p.
- Etu17.* **Massonnet C** (2000) Effet du rayonnement intercepté sur la croissance foliaire d'*Arabidopsis thaliana* : rôle de la disponibilité en carbone et de la transition entre les statuts importateur et exportateur des feuilles. DEA Développement et Adaptation des

Plantes. ENSAM - Université Montpellier 2 - Université de Perpignan, Montpellier, France, 18 p.

- Etu18.* **Oury V** (2010) Analyse du déterminisme conduisant à l'avortement des grains de maïs sous déficit hydrique (*Zea mays* L.). Mémoire de M2R Biologie Géosciences Agroressources Environnement, option Biologie Fonctionnelle des Plantes. Université Montpellier II, Montpellier, France, 22 p.
- Etu19.* **Patrois M** (2004) Contribution à la mise au point d'un cadre d'analyse des étapes précoces de la morphogenèse de l'épi de maïs en réponse à un déficit hydrique. Mémoire de Master Biologie Cellulaire et Physiologie, option physiologie végétale appliquée. Université Montpellier II, Montpellier, France, 18 p.
- Etu20.* **Pic E** (1994). Recherche de marqueurs du développement du pois (*Pisum sativum* L., cv Messire) : Evaluation de l'utilisation de sondes d'ADNc codant pour des marqueurs du développement foliaire de tabac et de pétunia. Diplôme d'Etudes Approfondies "Bases de la Production Végétale". ENSA.M - Université Montpellier II. 14p.
- Etu21.* **Sao Chan Cheong G** (1990). Mode d'action d'un déficit hydrique sur l'orientation des assimilats chez le pois protéagineux (cv Frilène). Diplôme d'Etudes Approfondies "Bases de la Production Végétale". ENSA.M - Université Montpellier II. 17p.
- Etu22.* **Soewarto J** (2012) Caractérisation de la réponse au déficit hydrique du sol chez trois génotypes de maïs : photosynthèse, transpiration, dynamique de sortie des soies et avortement des grains. Mémoire de Master Biologie des plantes et des microorganismes, Biotechnologies, Bioprocédés ; spécialité Biotechnologies des Plantes Tropicales. Université Montpellier II, Montpellier, France, 17 p.
- Etu23.* **Tixier A** (2009) L'intensité des avortements de grains de maïs en réponse au déficit hydrique est-elle liée au gradient de développement des ovules sur l'épi ? Analyse chez quelques lignées contrastées. Mémoire de Master Génomique Ecophysiologie et Production Végétale. Université Blaise Pascal, Clermont-Ferrand, France, 20 p.
- Etu24.* **Verney D** (2013) Test d'une méthode de phénotypage du maintien de la croissance des organes reproducteurs femelles de maïs (*Zea mays* L.) en réponse au déficit hydrique. Mémoire de M1 Biologie Fonctionnelle des Plantes. Université Montpellier II, Montpellier, France, 13 p.

### ***Publications avec les étudiants encadrés (noms soulignés)***

*Articles dans des revues internationales à comité de lecture. Facteur d'impact moyen : 5,65*

- PubliEtu1.* **Brichet N, Fournier C, Turc O, Strauss O, Artzet S, Pradal C, Welcker C, Tardieu F, Cabrera-Bosquet L** (2017) A robot-assisted imaging pipeline for tracking the growths of maize ear and silks in a high-throughput phenotyping platform. *Plant Methods* **13**: 96.
- PubliEtu2.* **Cookson SJ, Turc O, Massonnet C, Granier C** (2010) Phenotyping the development of leaf area in *Arabidopsis thaliana*. *Methods in Molecular Biology* **655**: 89-103.

- PubliEtu3.* **Dosio GAA, Rey H, Lecoeur J, Izquierdo NG, Aguirrezabal LAN, Tardieu F, Turc O** (2003) A whole-plant analysis of the dynamics of expansion of individual leaves of two sunflower hybrids. *Journal of Experimental Botany* **54**: 2541-2552.
- PubliEtu4.* **Dosio GAA, Rey H, Lecoeur J, Turc O** (2003) La radiacion solar durante etapas tempranas del desarrollo afecta al area foliar del girasol. *Revista Argentina de Agrometeorologia* **2**: 113-118.
- PubliEtu5.* **Dosio GAA, Tardieu F, Turc O** (2006) How does the meristem of sunflower capitulum cope with tissue expansion and floret initiation? A quantitative analysis. *New Phytologist* **170**: 711-722.
- PubliEtu6.* **Dosio GAA, Tardieu F, Turc O** (2011) Floret initiation, tissue expansion and carbon availability at the meristem of the sunflower capitulum as affected by water or light deficits. *New Phytologist* **189**: 94-105.
- PubliEtu7.* **Fuad-Hassan A, Tardieu F, Turc O** (2008) Drought-induced changes in anthesis-silking interval are related to silk expansion: a spatio-temporal growth analysis in maize plants subjected to soil water deficit. *Plant, Cell & Environment* **31**: 1349-1360.
- PubliEtu8.* **Granier C, Massonnet C, Turc O, Muller B, Chenu K, Tardieu F** (2002) Individual leaf development in *Arabidopsis thaliana*: a stable thermal-time-based programme. *Annals of Botany* **89**: 595-604.
- PubliEtu9.* **Luchaire N, Rienth M, Romieu C, Nehe A, Chatbanyong R, Houel C, Ageorges A, Gibon Y, Turc O, Muller B, Torregrosa L, Pellegrino A** (2017) Microvine: A New Model to Study Grapevine Growth and Developmental Patterns and their Responses to Elevated Temperature. *American Journal of Enology and Viticulture* **68**: 283-292.
- PubliEtu10.* **Oury V, Caldeira CF, Prodhomme D, Pichon J-P, Gibon Y, Tardieu F, Turc O** (2016) Is change in ovary carbon status a cause or a consequence of maize ovary abortion in water deficit during flowering? *Plant Physiology* **171**: 997-1008.
- PubliEtu11.* **Oury V, Tardieu F, Turc O** (2016) Ovary apical abortion under water deficit is caused by changes in sequential development of ovaries and in silk growth rate in maize. *Plant Physiology* **171**: 986-996.
- PubliEtu12.* **Pic E, Teyssendier de la Serve B, Tardieu F, Turc O** (2002) Leaf senescence induced by mild water deficit follows the same sequence of macroscopic, biochemical, and molecular events as monocarpic senescence in pea. *Plant Physiology* **128**: 236-246.
- PubliEtu13.* **Turc O, Bouteillé M, Fuad-Hassan A, Welcker C, Tardieu F** (2016) The growth of vegetative and reproductive structures (leaves and silks) respond similarly to hydraulic cues in maize. *New Phytologist* **212**: 377-388.

#### *Autres publications*

- PubliEtu14.* **Brichet N, Cabrera Bosquet L, Turc O, Welcker C, Tardieu F** (2017) An image-based automated pipeline for maize ear and silk detection in a highthroughput phenotyping platform. In ICRISAT, ed, *Interdrought V*, Hyderabad, India, pp P-055.

- PubliEtu15.* **Cookson SJ, Turc O, Massonnet C, Granier C** (2010) Phenotyping the development of leaf area in *Arabidopsis thaliana*. In JM Walker, ed, *Plant Developmental Biology*. Humana Press Inc., Totowa, NJ, USA., pp 89-103.
- PubliEtu16.* **Dosio GAA, Lefeuvre T, Suard B, Izquierdo N, Aguirrezabal L, Turc O** (2000) Stability of sunflower leaf development in France and Argentina. In *Proceedings of the 15<sup>th</sup> International Sunflower Conference*. International Sunflower Association, Toulouse, France. pp D47-51.
- PubliEtu17.* **Dosio GAA, Turc O** (2002). Efecto de una disminución temprana de la radiación solar incidente sobre el área foliar en girasol. In Asociación Argentina de Agrometeorología (ed) *Agrometeorología y agricultura sustentable en el nuevo milenio*. 18-20 September 2002. Vaquerías, Valle Hermoso, Córdoba, Argentina.
- PubliEtu18.* **Fuad Hassan A, Turc O** (2004). A framework of analysis of the response of maize silk elongation to soil water deficits. Workshop of the Challenge Program Generation. Montpellier, July 2004.
- PubliEtu19.* **Fuad-Hassan A, Tardieu F, Turc O** (2005) Analysis of maize silk growth during water stress. In *Comparative Biochemistry and Physiology a-Molecular & Integrative Physiology*, Vol 141 pp S310-S310.
- PubliEtu20.* **Fuad-Hassan A, Turc O** (2005) A model to predict anthesis silking interval in maize : analysis of differential responses to water deficit of ear-axis organs. In A Blum, R Tuberosa, eds, *Proceedings of the 2nd International Conference on Integrated Approaches to Sustain and Improve Plant Production Under Drought Stress Interdrought II*, Roma, Italy.
- PubliEtu21.* **Fuad-Hassan A, Tardieu F, Turc O** (2007) Spatial and temporal analysis of cell division and tissue elongation in silks of maize plants subjected to soil water deficit. In *Workshop on Growth Phenotyping and Imaging in Plants*, Montpellier, France. p 25.
- PubliEtu22.* **Lucaire N, Rienth M, Romieu C, Torregrosa L, Gibon Y, Turc O, Muller B, Pellegrino A** (2015) Role of plant carbon status in yield components responses to elevated temperatures in microvine. In *19. Journées Internationales de Viticulture GiESCO*, Gruissan, France. pp 66-70.
- PubliEtu23.* **Lucaire N, Torregrosa L, Gibon Y, Rienth M, Romieu C, Turc O, Pellegrino A** (2016) Yield reduction under high temperature is paired with a low carbon status in microvine. In *10. International Symposium on Grapevine Physiology and Biotechnology*, Verone, Italy
- PubliEtu24.* **Oury V, Prodhomme D, Gibon Y, Tardieu F, Turc O** (2013) Seed abortion of maize under water deficit is linked to a developmental process and not to carbon deprivation. In *Proceedings of Interdrought IV Conference*, Perth, Australia. p 361.
- PubliEtu25.* **Pic E, Turc O, Teysseidier de la Serve B, Tardieu F** (1998). Analyse de la sénescence foliaire du pois (*Pisum sativum* L., cv Messire) : utilisation conjointe d'un modèle de développement et de marqueurs moléculaires. Actes du 5<sup>ème</sup> Forum des Jeunes Chercheurs de la Société Française de Physiologie Végétale. 15-17 juillet 1998. Montpellier. France.

- PubliEtu26. Tardieu F, Caldeira CF, Oury V, Cabrera-Bosquet L, Turc O, Welcker C (2013) Dissection of drought tolerance; vegetative and reproductive growths in water deficit. In Interdrought IV Conference, Perth, Australia.*
- PubliEtu27. Turc O, Oury V (2011) Abortion and water deficit in maize: sugars or not sugars? In 2nd DROPS modelling meeting, Montpellier, France.*
- PubliEtu28. Turc O, Oury V, Gibon Y, Prodhomme D, Tardieu F (2017) Yield maintenance under drought: expansive growth and hydraulics also matter in reproductive organs. In ICRISAT, ed, Interdrought V, Hyderabad, India, pp P-076.*
- PubliEtu29. Turc O, Oury V, Tardieu F (2012) Ovary or kernel abortion and water deficit: a central role for silking dynamics. In 3rd DROPS modelling meeting, Des Moines, USA.*
- PubliEtu30. Turc O, Oury V, Tardieu F (2012) A central role for silking dynamics in maize ovary abortion. In 2nd annual meeting Drought-tolerant yielding plants, Sabanci University, Istanbul, Turkey.*
- PubliEtu31. Turc O, Tardieu F, Oury V (2015) Grain abortion and yield stability under drought: a key role for growth processes in reproductive organs. In C Welcker, R Tuberosa, F Tardieu, eds, Recent progress in drought tolerance: from genetics to modelling. Drops and Eucarpia, Montpellier, France. p 26.*
- PubliEtu32. Turc O, Wery J, Sao Chan Cheong G (1990). A limited drought stress as a tool for the management of the balance between vegetative and reproductive components of peas (*Pisum sativum* L.). ESA 1st Congress Paris 5-7 Dec 1990.*

## **Travaux de recherche et projet**

### *Contexte général*

Les travaux de recherche que je conduis au sein du Département Environnement et Agronomie de l'INRA relèvent, du point de vue disciplinaire, du champ thématique Ecophysiologie végétale et, au plan appliqué, de l'enjeu structurant Adaptation des cultures aux nouveaux contextes agricoles.

J'ai été affecté au Laboratoire d'Ecophysiologie des Plantes sous Stress Environnementaux dès sa création le 1/01/94. L'unité a été mise en place dans le contexte général d'évolution de l'agriculture européenne vers une situation moins artificialisée, plus économe d'intrants, s'adaptant mieux aux contraintes du milieu naturel, mais qui n'en reste pas moins soumise à des contraintes économiques de régularité de production et de qualité maîtrisée. L'utilisation de l'eau, de pluie ou d'irrigation, devra être restreinte, efficace et non polluante. On ne cherche plus forcément à atteindre le rendement potentiel, mais plutôt à identifier les combinaisons géotype x conduite de culture les plus adaptées au scénario climatique. Une approche explicative du fonctionnement du couvert est alors nécessaire pour prévoir le comportement de plantes soumises à des contraintes hydriques au champ et aider à leur amélioration génétique comme à leur gestion agronomique. Le projet du LEPSE consiste donc à bâtir avec nos collègues généticiens et biologistes végétaux, une stratégie scientifique d'ingénierie de plantes adaptées aux contextes de déficits hydriques, en privilégiant les situations agricoles où les déficits hydriques sont fréquents et d'intensité modérée.

La démarche de modélisation développée par l'unité vise à expliciter puis représenter la variabilité génétique. Elle comprend trois étapes : (i) expliciter les réponses des géotypes en termes quantitatifs : établir des modèles qui relient les caractéristiques étudiées aux conditions environnementales (dissection des caractéristiques phénotypiques en courbes de réponse aux conditions environnementales, puis assemblage dans un modèle) ; (ii) analyser la variabilité génétique de ces réponses : analyse de la variabilité génétique des principaux paramètres des modèles (= réponse des processus élémentaires aux conditions environnementales) ; (iii) reconstruire *in silico* le comportement des géotypes (combinaison de modèles architecturaux, écophysiologiques et génétiques. Elle a un débouché direct en génétique et en génomique pour l'identification des déterminismes génétiques de caractères plus élaborés que ceux souvent utilisés dans ces disciplines, en modélisation pour la simulation du comportement de géotypes en fonction des conditions environnementales et, de façon plus lointaine, en sélection variétale assistée par marqueurs, au travers de partenariats.

Mes travaux de recherche se situent essentiellement au niveau de la première étape de cette démarche. Ils s'articulent autour de l'analyse et la modélisation de l'effet de l'environnement sur le déroulement du programme de développement de plantes cultivées annuelles produisant des grains (pois, tournesol, maïs) et s'attachent à identifier et quantifier les processus physiologiques impactés. Une attention particulière a été donnée aux processus d'expansion des organes.

L'objectif des travaux décrits dans la première partie de ce mémoire est la construction de modèles de développement des plantes, fondés sur l'établissement de lois d'apparition des organes, sur la prévision des dates de changement de programme à l'échelle de l'organe et de la plante, sur l'explicitation des coordinations de croissance entre organes et de l'interaction entre les développements végétatif et reproducteur, en réponse aux modifications de l'environnement. La formalisation de ces résultats génère d'une part des algorithmes pour la construction de plantes numériques "répondant à l'environnement", d'autre part des cadres d'analyse de la réponse des plantes aux contraintes environnementales. L'utilisation des modèles de développement, pour mieux comprendre où, quand, combien et sur quels processus sont impactés les organes d'une plante soumise à une contrainte environnementale, fait l'objet de la deuxième partie du mémoire. La troisième partie s'attache à répondre à une question centrale dans les modèles de simulation du fonctionnement des plantes : est-ce que la croissance et le développement des organes reproducteurs d'une plante soumise à un déficit hydrique sont limités par l'approvisionnement en carbone de ces organes, en raison de la diminution de la photosynthèse ? L'exemple de l'avortement précoce des ovaires et grains de maïs y est détaillé. La quatrième partie du mémoire décrit mon projet de recherche pour les prochaines années, qui se situe dans le prolongement de cette dernière thématique.

Toutes ces études ont été réalisées en caractérisant finement l'environnement subi par les plantes, que ce soit en serre, en chambre de culture ou au champ, à l'aide de capteurs placés au plus près des organes des plantes (rayonnement, température de l'air et des organes, humidité de l'air et du sol). Les plateformes de phénotypage réalisées récemment dans l'unité permettent d'enregistrer la croissance des feuilles sur de grands effectifs, tout en contrôlant, de façon fine, automatique et individuelle, l'arrosage des plantes et l'état hydrique du sol. Ainsi il devient possible de caractériser la variabilité génétique des réponses selon différents scénarios de déficit hydrique. L'un des enjeux de mon projet de recherche est méthodologique : il s'agit d'adapter à la mesure et l'observation des organes reproducteurs ces outils initialement conçus pour enregistrer la croissance des feuilles.

## 1. Construction de modèles de développement des plantes

### *1.1 Une représentation du développement commune à différentes espèces et différents types d'organes (Fig. 1).*

L'organisation spatiale des organes d'une plante résulte du fonctionnement des méristèmes végétatifs et reproducteurs qui initient de façon séquentielle les primordia des organes (Chap2). Il y a ainsi une correspondance entre la position spatiale d'un organe, le long d'une tige ou au sein d'une inflorescence, et son âge compté depuis son initiation.

Une représentation simple consiste à placer sur une échelle de temps le nombre d'organes (feuilles d'une tige, fleurs d'une inflorescence) ayant franchi des stades de développement

caractéristiques (initiation, fin de croissance, floraison, ..) (Fig.1). Une lecture horizontale de ce graphique indique les dates caractéristiques du développement de chaque organe en fonction de sa position le long de l'axe considéré (tige ou inflorescence). Une lecture verticale indique, à une date donnée, quel est l'âge ou le stade de développement de chacun des organes présents. Cette représentation s'applique aux organes successifs le long d'une tige (feuilles, inflorescences) mais aussi au sein d'inflorescences comme un épi de maïs ou un capitule de tournesol. Dans ce dernier cas, comme l'initiation des organes floraux est centripète, les organes sont ordonnés en âge décroissant depuis la périphérie vers le centre du capitule (Fig. 2, Art5).

### Représentation du développement reproducteur à l'échelle de la plante

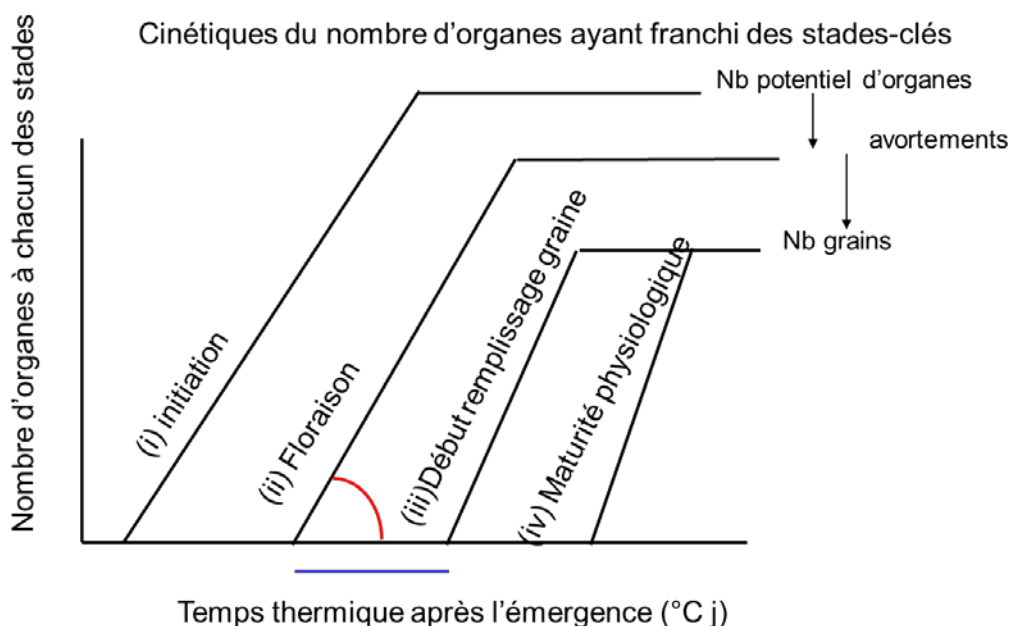


Figure 1. Modélisation du développement reproducteur chez le pois. Le nombre d'organes ayant franchi des stades-clés du développement reproducteur (initiation, floraison, début et fin du remplissage des grains) est représenté en fonction du temps écoulé depuis la levée des plantes. Il y a correspondance entre l'ordre d'initiation des organes par le méristème caulinaire et leur position spatiale le long de la tige. Une lecture horizontale du modèle délimite donc les phases successives de développement d'un organe en fonction de sa position le long de la tige (Art15 ; Art23 ; Chap2 ; Chap5 ; Chap6).

Ces modèles de développement ont été construits pour différentes espèces de plantes, d'une part comme objets d'études en tant que tels (description de la chronologie de mise en place de la surface foliaire et du rendement en graines ; définition de stades pertinents pour cette mise en place ; caractérisation des paramètres de ces modèles : vitesses et durées de développement, et leurs réponses à l'environnement et leur variabilité génétique), et d'autre part comme cadres d'analyse de la réponse des organes aux contraintes environnementales,

en termes de croissance, développement et processus sous-jacents, en mettant à profit les relations position-temps fournies par ces modèles. Repérer où se situent, et donc à quel stade sont, les organes qui sont impactés sur un processus donné par une contrainte environnementale se produisant à une date donnée s'est avéré un puissant outil pour analyser la réponse des plantes à l'environnement.

### *1.2 Mise en évidence de stades de développement caractéristiques*

- Exemple 1 : mise en place du rendement en grains chez le pois

Le développement d'un grain commence à la fécondation, qui suit de peu la pollinisation/floraison, et s'achève à la maturité physiologique lorsque l'accumulation de réserves dans le grain cesse suite à la rupture des relations vasculaires avec la plante mère. L'accumulation de biomasse dans le grain est souvent décrite par une courbe sigmoïde, présentant une phase de croissance lente au cours de laquelle se produisent de nombreuses divisions cellulaires dans l'embryon ou/et l'endosperme, suivie d'une phase de croissance rapide, parfois ajustée à une droite, correspondant au dépôt de réserves, puis d'un plateau après la maturité physiologique (Chap5). L'étude fine du devenir des grains a permis de montrer que les avortements se produisent pendant la première phase (Chap5). Tous les grains qui débutent la phase de remplissage rapide vont au bout de leur développement. La transition entre ces deux phases est appelée Stade Limite d'Avortement des grains (Final Stage in Seed Abortion). Ce stade a été caractérisé chez plusieurs légumineuses par une longueur de grain (Art20), le début du renflement des gousses ou par une teneur en eau caractéristique (Art15 ; Chap5). Ce stade permet de délimiter la période de formation du nombre de grains et la période de formation du poids des grains à l'échelle d'un phytomère, et sa progression le long de la tige délimite les périodes de formation de ces composantes à l'échelle de la plante entière. Cette formalisation du développement reproducteur met en évidence les périodes successives de l'élaboration du rendement, caractérisées par la nature des puits compétiteurs pour les assimilats (Art15 ; Chap5 ; Chap6). Pendant une première période, avant le début de la floraison, les organes en croissance sont les feuilles, les racines et les jeunes ébauches florales à l'intérieur du bourgeon apical. A partir du début de la floraison et jusqu'au début du remplissage (stade limite d'avortement) sur le premier phytomère reproducteur, s'y ajoutent les gousses et les jeunes grains en phase de divisions cellulaires actives. Pendant la troisième phase, la croissance végétative coexiste avec celle des jeunes gousses et grains sur les phytomères supérieurs et celle des graines en remplissage sur les phytomères inférieurs. La durée de cette phase, caractéristique des plantes à floraison étalée, est directement liée au nombre de phytomères reproducteurs, très sensible aux contraintes environnementales. Enfin, après le passage du stade limite d'avortement de la dernière graine formée, les graines en remplissage constituent le seul puits pour les assimilats. Ce découpage constitue le cadre sur lequel s'appuient les modèles de fonctionnement et les outils de diagnostic des cultures de pois (Chap3 ; Chap4) et d'autres légumineuses comme le pois chiche (Conf27).

Des modèles similaires ont été construits pour des plantes présentant des inflorescences avec des organogénèses totalement différentes. Ainsi, chez le tournesol, les organes reproducteurs sont initiés à partir d'un disque méristématique, à l'origine d'une inflorescence circulaire, le capitule. L'initiation des primordia floraux, ou fleurons, se produit en périphérie du méristème et progresse vers son centre. Les organes sont donc ordonnés selon leur âge décroissant depuis le bord du capitule jusqu'à son centre. (Fig. 2, Etu4). L'ordonnée des courbes du graphe représente à la fois le nombre d'organes ayant franchi le stade considéré à une date donnée, mais aussi la position spatiale (entre le bord et le centre du capitule) des organes atteignant ce stade à cette date.

### Mise en place des organes reproducteurs de tournesol

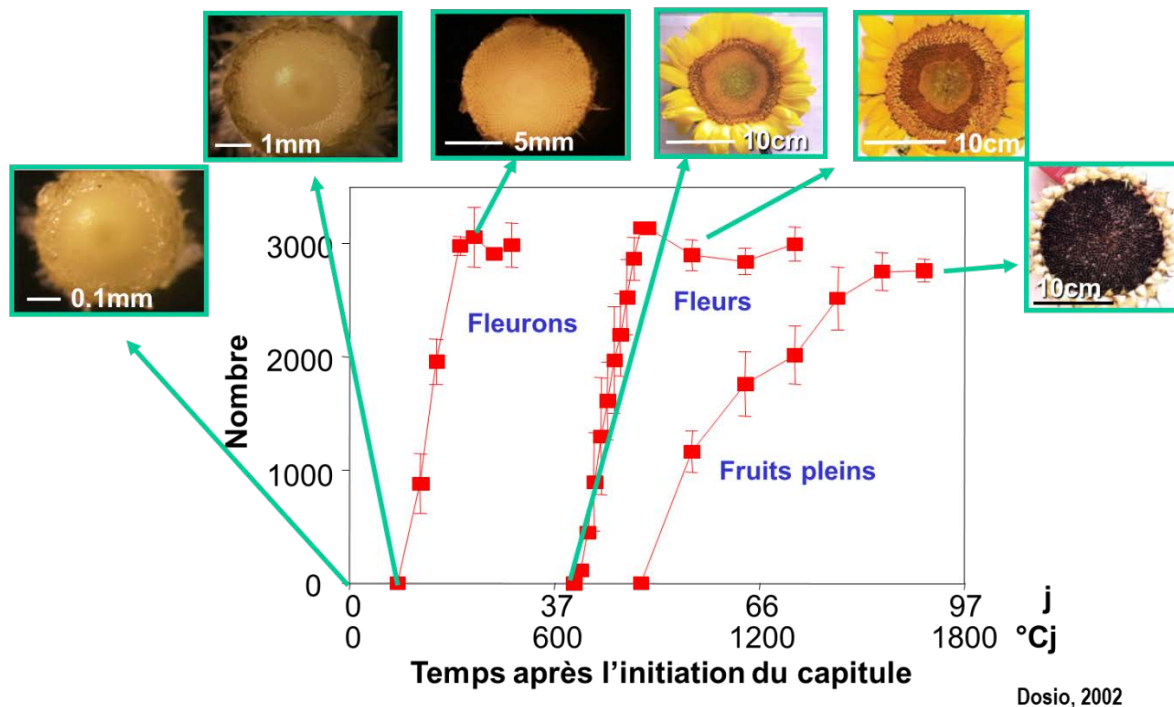


Figure 2. Modélisation du développement reproducteur du tournesol (Etu4). Le principe est le même que pour le pois (Fig. 1). Les stades-clés sont ici l'initiation des primordia floraux (fleurons), la floraison et la maturité des grains. Les organes sont ordonnés en âge décroissant depuis la périphérie vers le centre du capitule. La lecture horizontale du modèle indique ici le développement des organes selon leur position entre le bord et le centre du capitule.

Chez le maïs, il y a séparation spatiale entre l'inflorescence mâle, une panicule au sommet de la plante, et l'inflorescence femelle, un épi porté par une ramification latérale. Comme l'épi est enfermé à l'intérieur de bractées (les spathes), les styles et stigmates des fleurs femelles doivent croître de plusieurs dizaines de centimètres pour émerger des spathes et être exposées au pollen venant de la panicule pour assurer la fécondation des ovules de l'épi. Ces styles et stigmates très allongés spécifiques du maïs sont appelés les soies. Leur croissance

étant sensible aux contraintes environnementales, les stades clés de leur développement ont été inclus dans le modèle de développement mis au point pour le maïs (Fig. 3 ; Etu3). Là encore, l'ordonnée des courbes du graphe correspond à une position spatiale, dans ce cas entre le bas de l'épi, où se trouvent les organes les plus âgés, et le sommet de l'épi, qui porte les organes les plus jeunes.

### Cinétique de développement des organes reproducteurs de l'épi de maïs

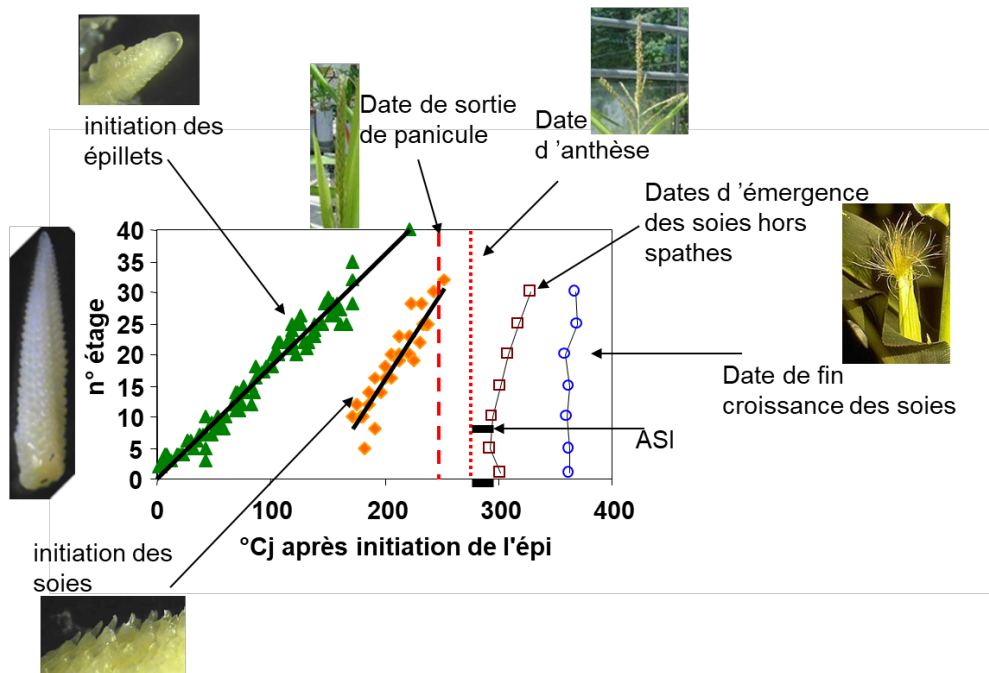


Figure 3. Modélisation du développement reproducteur du maïs (Etu3). Le modèle des stades-clés spécifiques au maïs concernant le développement des soies (les styles des fleurs femelles très allongés pour être accessibles au pollen) ainsi que les stades de l'inflorescence mâle (panicule au sommet de la plante). Le numéro d'étage (ou numéro de cohorte) en ordonnées est la position spatiale des ovaires comptée depuis la base de l'épi.

#### - Exemple 2 : Mise en place de la surface foliaire

La mise en place de la surface foliaire a été décrite selon le même principe. La progression du nombre de primordia initiés par le méristème caulinaire et celle du nombre de feuilles ayant achevé leur expansion définissent les périodes de croissance de chacune des feuilles le long de la tige (Fig. 4, tournesol, Art3).

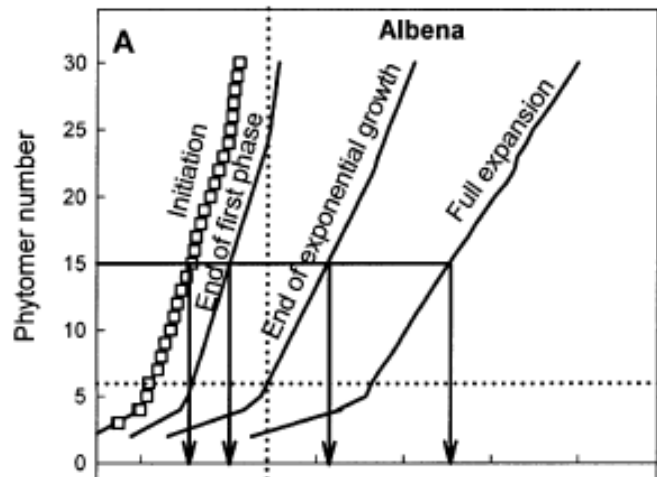


Figure 4. Modélisation du développement des feuilles de tournesol. Le principe est le même que pour le développement reproducteur du pois (Fig. 1). Les stades-clés sont ici l'initiation des primordia foliaires, la fin de la phase exponentielle (ou phase lente) de croissance et la fin de l'expansion foliaire. La lecture horizontale délimite les phases du développement de chaque feuille selon sa position le long de la tige (Art3).

L'étude de la cinétique de croissance des feuilles individuelles entre ces deux stades montre la succession de deux phases. Pendant la première, qui se déroule essentiellement alors que la feuille est à l'intérieur du bourgeon apical, la croissance est exponentielle, avec une vitesse relative de croissance stable et élevée et une vitesse absolue faible. Pendant la seconde phase la vitesse relative de croissance diminue rapidement, tandis que la vitesse absolue passe par son maximum avant de diminuer à son tour. Cette phase coïncide avec le déploiement de la feuille et sa croissance hors du bourgeon apical. La vitesse d'expansion des feuilles est affectée par un déficit en lumière seulement lorsque celui-ci intervient pendant la phase exponentielle (Fig. 5 ; Art4). Aucun impact n'est observé pour les feuilles ayant terminé la phase exponentielle avant le déficit en lumière. Ceci suggère que la transition entre ces deux phases correspond au passage à l'autotrophie : les feuilles ne dépendent plus alors de la photosynthèse des feuilles plus âgées. Il s'agit donc d'un stade critique pour la mise en place de la surface foliaire, intégré dans les modèles de développement foliaire chez différents espèces (tournesol, pois, arabidopsis. Art3 ; Art2 ; Art11).

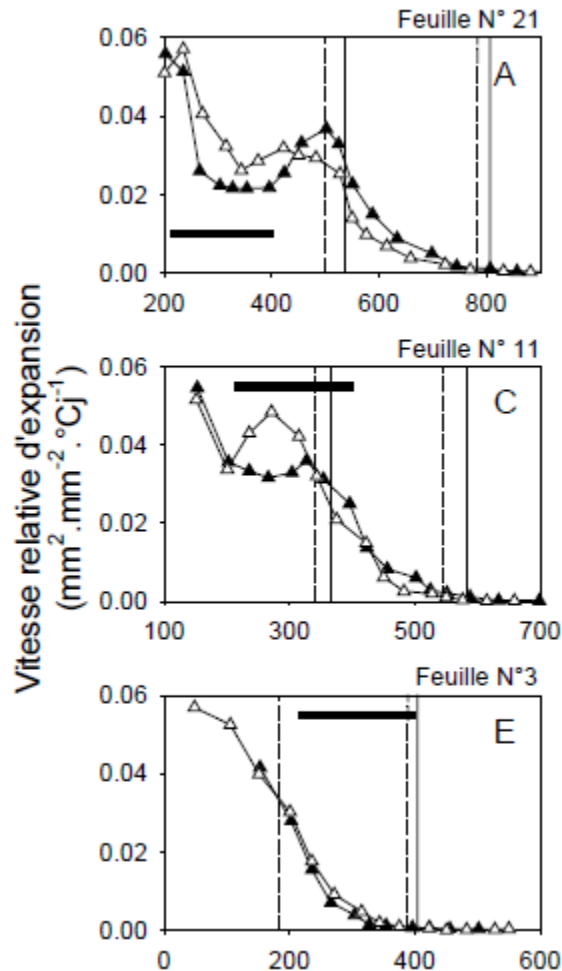


Figure 5. Effet d'un ombrage temporaire sur la vitesse relative de croissance des feuilles de tournesol (Art4). La période de contrainte lumineuse est indiquée par une barre horizontale. Selon la position de la feuille le long de la tige, la contrainte se produit entièrement (feuille 21) ou partiellement (feuille 11) pendant la phase de croissance exponentielle, ou bien après celle-ci (feuille 3). Les traits verticaux indiquent la fin de la phase exponentielle et la fin de croissance pour les feuilles des plantes ombrées (traits pleins) ou des plantes témoin (tirets).

### 1.3 Stabilité des modèles de développement sur une échelle de temps thermique

Les rythmes d'initiation des organes et leurs durées de développement sont stables lorsqu'on les exprime en temps thermique. Cela signifie que, quelles que soient les conditions de température, il y a une coordination entre le fonctionnement du méristème et le développement de chaque organe. Ceci s'explique par le fait que les deux processus, initiation des organes par le méristème et développement des organes initiés, présentent une réponse commune à la température (Fig. 6 ; Art23). Le temps thermique prend en compte la réponse à la température des processus de développement des plantes. Lorsqu'on considère une approximation linéaire de cette réponse (Fig. 6), on parle de degrés-jours ou de sommes de températures. La vitesse de développement est proportionnelle à la température dépassant un certain seuil, appelé température de base (abscisse à l'origine de la relation linéaire). Tous

les processus avec la même température de base sont coordonnés (Fig. 6). Cependant, l'approximation linéaire n'est valide que dans une certaine gamme de températures. Des formalismes plus complexes, fondés sur les réponses d'activités enzymatiques (lois d'Arrhenius) permettent d'étendre le concept à toute température (Fig. 7 ; Art18). Le temps thermique est alors exprimé en "durée équivalente" à une température de référence : jours à 20°C par exemple. Les processus présentant la même courbe de réponse, normalisée par la vitesse observée à 20 °C, sont coordonnés quelle que soit la température. On a ainsi montré que les réponses communes à la température concernent non seulement les rythmes de développement, mais aussi les processus de croissance (Fig. 7). Ces coordinations ont été montrées chez plusieurs espèces : pois, tournesol, arabidopsis, microvigne (Art23 ; Art9 ; Art8 ; Art12). Ainsi, les événements caractéristiques du développement de chaque organe se produisent à un temps thermique donné après la germination de la plante. Ce temps représente la somme de l'âge de la plante lors de l'initiation du phytomère et de la durée d'une phase donnée du développement de ce phytomère, tous deux stables en temps thermique. On peut donc représenter l'ensemble du développement de la plante dans un graphe présentant, en abscisse, le temps thermique après la germination (ou après la levée) et en ordonnée la position du phytomère sur la tige. Les dates clés du développement de chaque organe y apparaissent, avec des relations uniques dans une large gamme de situations.

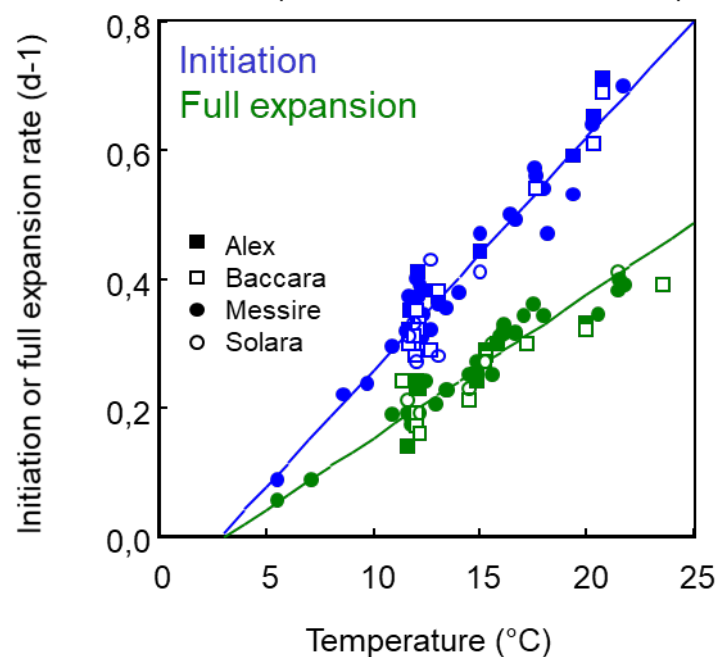


Figure 6. Réponse à la température du rythme d'initiation des primordia foliaires (courbe du haut) et de la vitesse de progression du stade fin expansion foliaire (courbe du bas) le long d'une tige de pois. Les deux processus répondent tous les deux à la température de façon linéaire et avec une même abscisse à l'origine (température de base pour le calcul du temps thermique). Ils sont donc coordonnés entre eux (même proportionnalité) quelle que soit la température (Art23).

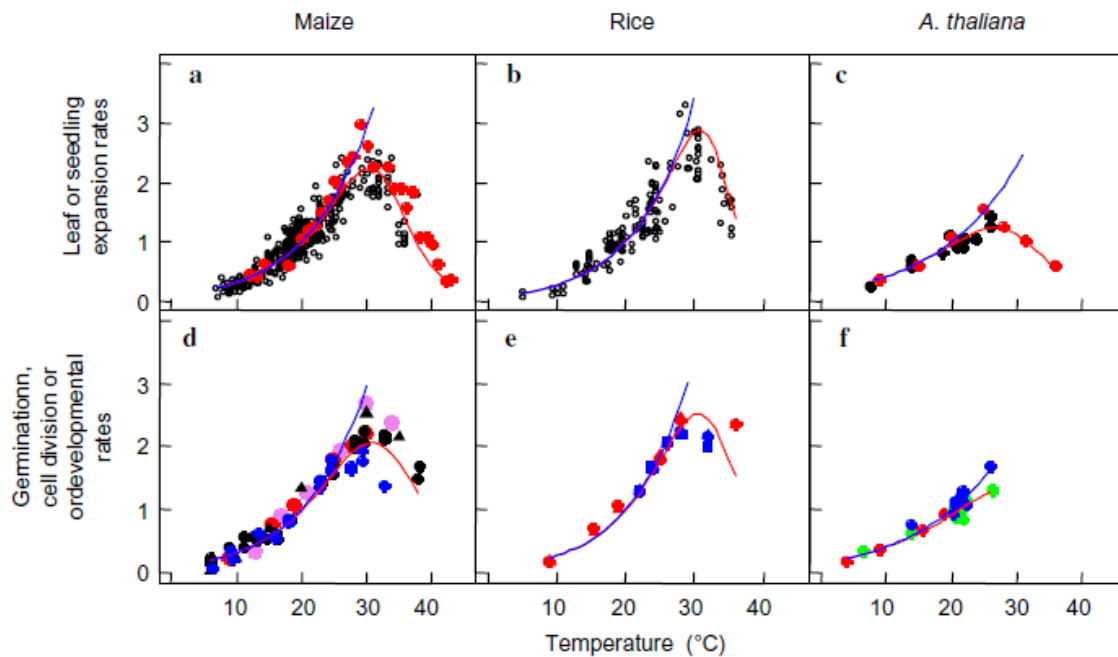


Figure 7. Réponse à la température de vitesses de croissance (graphes du haut) et de vitesses de développement (graphes du bas) chez 3 espèces (Art18). La courbe de réponse à la température est commune à tous les processus pour une espèce donnée, indiquant qu'ils sont coordonnés quelles que soient les conditions thermiques. La courbe varie d'une espèce à l'autre. Le formalisme adopté (lois d'Arrhenius) permet de prendre en compte toute la gamme de températures, et pas seulement la fenêtre correspondant à la phase croissante pseudo-linéaire (cf Fig. 6)

#### 1.4 Les modifications de développement en réponse au déficit hydrique

De façon générale, ni la date d'initiation des organes, ni la chronologie de leur apparition ne sont modifiées en cas de contrainte hydrique. Ceci concerne à la fois les feuilles et les organes reproducteurs, et a été montré chez plusieurs espèces (Art11 ; Art14 ; Chap8 ; Conf25 ; Etu4).

Les rythmes de développement des organes sont donc très peu sensibles au déficit hydrique.

En revanche, les durées de développement peuvent être impactées. Ainsi, chez le pois, la durée de remplissage des grains a tendance à diminuer en cas de déficit hydrique après la floraison (Art14).

La principale réponse du développement reproducteur du pois au déficit hydrique est une diminution du nombre de phytomères portant des fleurs (Fig. 8 ; Art14). Ceci correspond à un arrêt précoce de l'émission des organes (feuilles et fleurs) au niveau du bourgeon terminal. Il s'agit d'un blocage de toute l'extrémité apicale : l'ensemble des 10 phytomères qui la

constituent stoppent leur développement quasi-simultanément (Chap8). Ce phénomène se produit également, mais plus tard, lorsque les conditions hydriques sont favorables ou non.

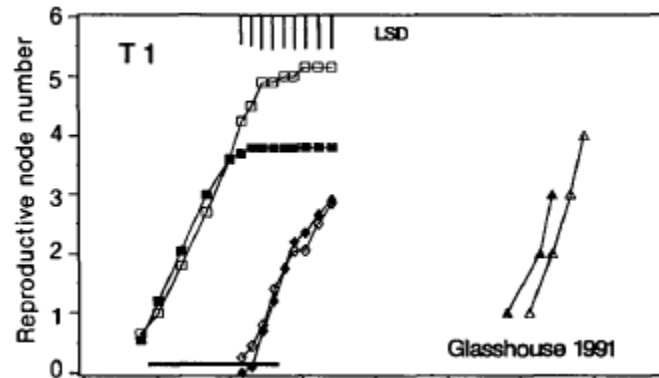


Figure 8. Effet d'un déficit hydrique pendant la floraison sur le développement reproducteur du pois. Les stades-clés successifs sont la floraison (carrés), le franchissement du stade limite d'avortement des grains (losanges) et la maturité physiologique (triangles). La barre horizontale indique la période de déficit hydrique. Symboles pleins : plantes en déficit hydrique ; symboles vides : plantes témoin (Art14).

La mise en place des graines sur les premiers étages est le facteur explicatif de ce blocage. Lorsque cette mise en place est empêchée par ablation continue des fleurs au stade fécondation, le blocage ne se produit pas et l'émission de nouveaux phytomères se poursuit indéfiniment (Art23 ; Art19).

La mise en place et le remplissage des graines sont accélérés en cas de stress hydrique. Une proportion plus élevée de graines se met en place sur les premiers phytomères (Chap8), et leur remplissage se produit plus tôt que chez les graines équivalentes des plantes non stressées (Conf25). Cette mise en place plus rapide semble à l'origine de l'arrêt précoce de l'extrémité apicale. Ces mêmes événements se produisent que la contrainte hydrique ait lieu avant ou pendant la mise en place des graines. Des résultats totalement concordants ont été obtenus chez le pois chiche.

La contrainte hydrique induit donc de façon précoce un changement d'aiguillage dans le fonctionnement de la plante, qui passe d'une phase de construction de nouveaux organes à une phase de remplissage des organes déjà en place. La contrainte a un effet direct sur la morphogenèse foliaire (divisions cellulaires et élongation) et sur le blocage du développement de jeunes organes reproducteurs.

## 2. Les modèles de développement des plantes, une plus-value pour analyser les réponses écophysiologicals à des contraintes environnementales

### *2.1 Analyse spatiale de la réponse de la croissance foliaire à une contrainte transitoire*

Le positionnement d'une contrainte sur le modèle de développement permet de déterminer à quels stades de développement se trouvaient les organes au moment de la contrainte.

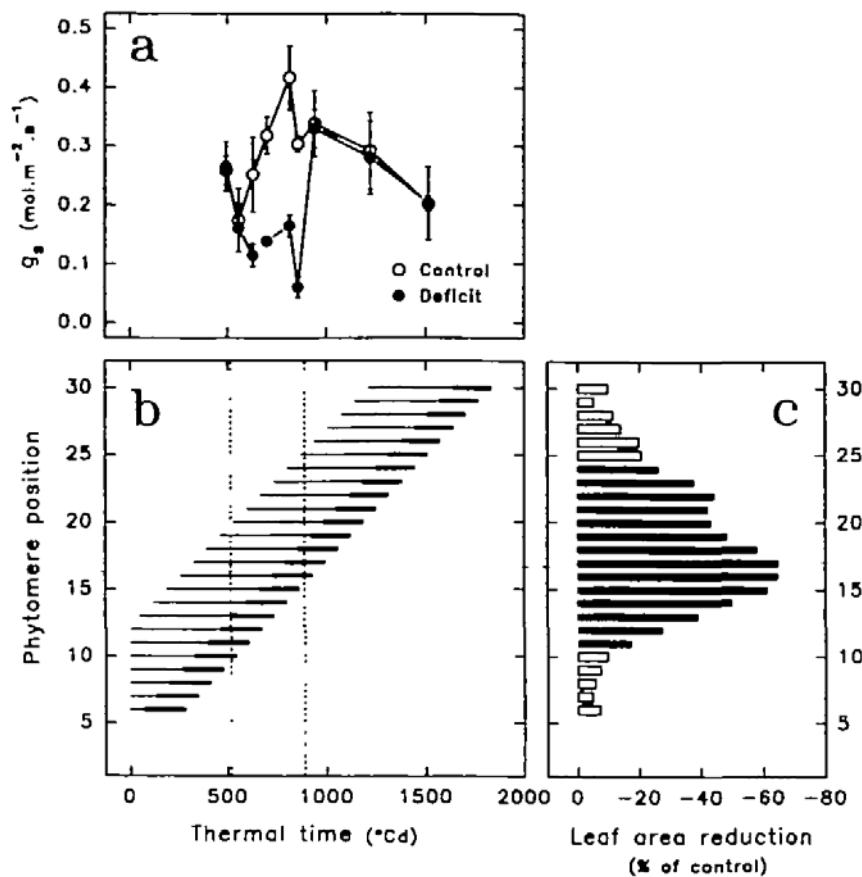


Figure 9. Réduction de la surface des feuilles de pois par un déficit hydrique selon leur position sur la tige. a, conductance stomatique. Symboles pleins : plantes en déficit hydrique ; symboles vides : plantes témoin. b, périodes de croissance lente (trait horizontal fin) et rapide (trait épais) pour chaque feuille le long de la tige. Les pointillés verticaux délimitent la période de déficit hydrique, durant laquelle la conductance stomatique est diminuée. c, réduction de surface foliaire en déficit hydrique (en % de la surface des plantes témoin). Les barres pleines indiquent les différences significatives. (Art11)

Ceci a été mis à profit chez le pois pour quantifier l'impact d'une contrainte hydrique sur les processus de division et d'expansion cellulaires dans les feuilles, selon le stade de développement auquel la contrainte se produit (Art11). La figure 9a compare, tout au long du cycle d'une culture de pois, la conductance stomatique de plantes bien alimentées en eau à

celle de plantes soumises à un déficit hydrique temporaire du sol. La période pendant laquelle la conductance stomatique est diminuée par rapport aux plantes contrôle délimite la phase du cycle où les plantes ont subi une contrainte hydrique. Celle-ci est reportée sur le calendrier de développement des feuilles (Fig. 9b), en distinguant, pour chaque feuille, la phase de croissance exponentielle (ou lente) et la phase de croissance quasi-linéaire (ou rapide). La réduction de surface foliaire finale due à la contrainte hydrique est indiquée pour chaque feuille sur la Fig. 9c. Toutes les feuilles s'étant développées pendant le déficit hydrique, et seulement ces feuilles-là, ont une surface finale diminuée par rapport aux plantes bien alimentées en eau. La réduction de surface est maximale pour les feuilles dont tout le développement, depuis l'initiation jusqu'à la fin de l'expansion, s'est déroulé pendant la contrainte. Elle est minimale pour les feuilles ayant achevé leur croissance juste après l'établissement de la contrainte, et pour les feuilles initiées juste avant la remise en eau. La mesure du nombre et de la dimension des cellules indique que la contrainte a affecté les divisions cellulaires des feuilles en phase de croissance lente, et l'expansion cellulaire des feuilles en phase de croissance rapide pendant la période de déficit hydrique. Ces résultats ont servi de base à l'établissement d'un modèle de simulation de la surface foliaire chez le pois (Art11) et à une revue sur les relations entre les processus de divisions cellulaires et d'expansion des tissus chez plusieurs espèces (Art9).

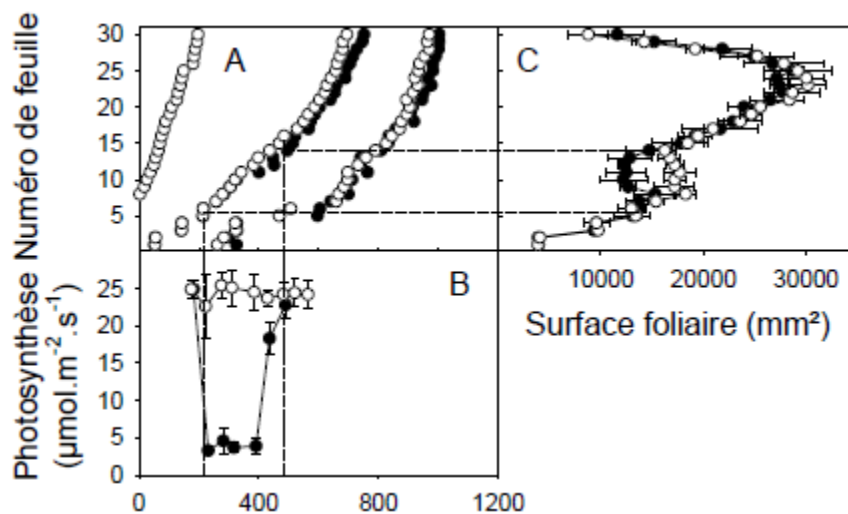


Figure 10. Réduction de la surface des feuilles de tournesol par un déficit en lumière selon leur position sur la tige. A, dates d'initiation, de fin de période exponentielle et de fin de croissance pour chaque feuille le long de la tige. B, photosynthèse. C, surface des feuilles selon leur position. Symboles pleins : plantes en déficit hydrique ; symboles vides : plantes témoin. Les tirets verticaux délimitent la période de déficit en lumière, durant laquelle la photosynthèse est diminuée. Les tirets horizontaux délimitent les feuilles pour lesquelles la réduction de surface est significative (Art4).

La même démarche a été mise à profit pour analyser l'effet de contraintes lumineuses sur la croissance foliaire du tournesol (Art4 ; Fig. 10). Dans ce cas, seules les feuilles ayant achevé

leur croissance exponentielle pendant la période d'ombrage ont eu une surface foliaire réduite par rapport aux plantes bien éclairées. L'analyse des cinétiques de croissance des feuilles (Fig. 5) montre que le déficit en lumière réduit la vitesse de croissance de toutes les feuilles en phase de croissance exponentielle pendant la contrainte. Lors de la remise en lumière, on observe une augmentation temporaire de la vitesse de croissance pour toutes les feuilles qui sont encore en phase exponentielle, ainsi qu'un allongement de la durée de cette phase pour ces mêmes feuilles. Ces deux phénomènes conjugués permettent une compensation totale de la surface foliaire finale pour toutes les feuilles en phase exponentielle lors du retour aux conditions lumineuses optimales. La croissance des feuilles en phase rapide (pseudo-linéaire) n'est affectée ni par la diminution, ni par l'augmentation de lumière.

## *2.2 Analyse du déroulement de la sénescence foliaire, utilisant conjointement le modèle de développement et des marqueurs moléculaires (Art19 ; Etu5).*

Les manifestations macroscopiques de la sénescence (baisse de photosynthèse, chutes des teneurs des feuilles en chlorophylle, en protéines totales et en RUBISCO) ont été placées dans le modèle de développement végétatif (Fig. 9b) et reproducteur (Fig. 1) du pois, et mises en relation avec l'accumulation d'ARNm et/ou de protéines choisis a priori pour leur lien avec la sénescence foliaire. Des feuilles situées à trois positions sur la tige ont été suivies chez des plantes irriguées, des plantes en déficit hydrique et des plantes dont la sénescence a été retardée par ablation des organes reproducteurs.

Les manifestations macroscopiques de la sénescence se sont produites plus tôt chez les plantes en déficit hydrique que chez les plantes irriguées. Elles étaient précédées dans les deux cas par une accumulation d'ARNm de cystéine protéinase (Fig. 11). Un comportement opposé a été observé chez les plantes dont les organes reproducteurs ont été excisés, avec un jaunissement retardé et une accumulation retardée d'ARNm de cystéine protéinase (Art19).

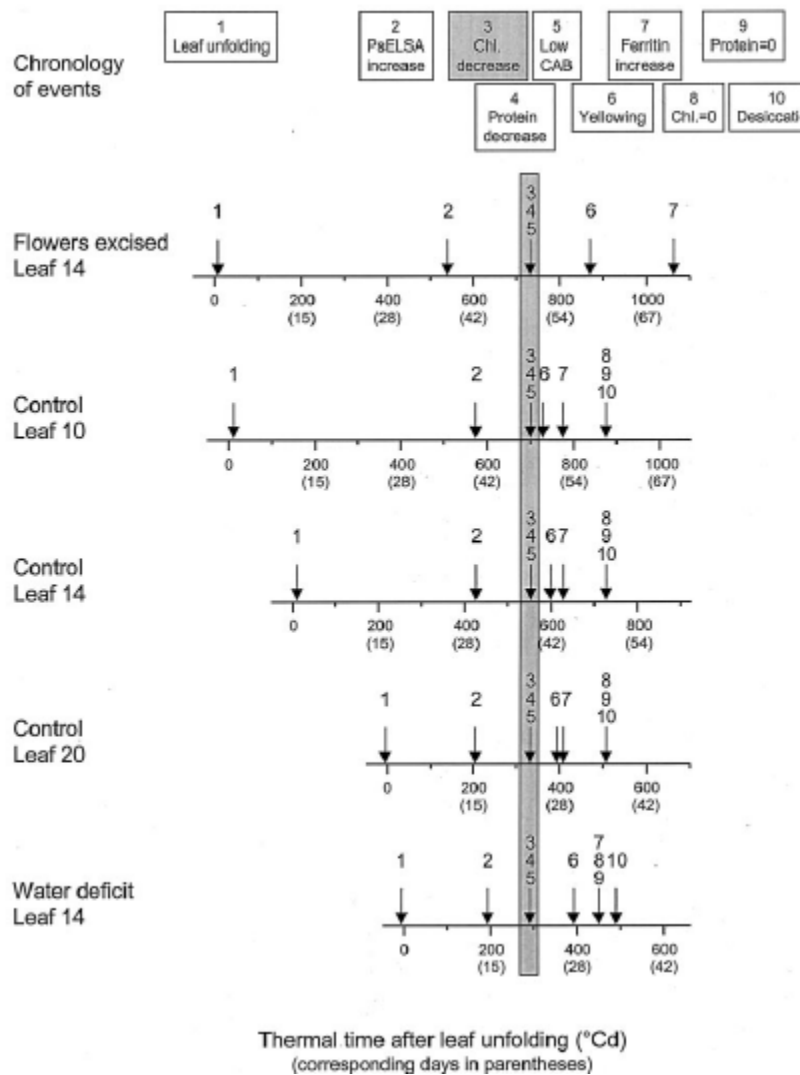


Figure 11. Confrontation des événements phénologiques, physiologiques et moléculaires associés à la sénescence des feuilles de pois. Trois feuilles d'âges différents (feuilles 10, 14 et 20) ont été étudiées chez des plantes témoin. La feuille 14 a également été suivie en situation de déficit hydrique et chez des plantes ayant subi l'ablation de leurs fleurs au fur et à mesure de leur émergence hors du bourgeon apical. Les calendriers de développement des feuilles ont été décalés de façon à aligner les événements biochimiques associés à l'entrée en sénescence. L'événement 2, qui précède la sénescence dans tous les cas correspond à l'accumulation d'ARNm d'une cystéine protéinase (Art19).

L'augmentation d'ARNm de cystéine protéinase par rapport aux ARN totaux a précédé de plusieurs semaines les manifestations macroscopiques de la sénescence dans toutes les feuilles analysées, quelles que soient leur position sur la tige et quel que soit le traitement. Ces deux expressions de la sénescence ont suivi des progressions similaires entre phytomères successifs de la plante avec des dates décalées d'environ 500°Cj. L'augmentation de teneur des ARNm de cystéine protéinase, comme le jaunissement des feuilles, se produit presque

simultanément sur les différents phytomères de la plante, alors que l'initiation de ces phytomères s'est étalée sur plus de 300°Cj. La sénescence est donc apparue à des âges différents pour chaque phytomère. Elle correspond vraisemblablement davantage à un événement à l'échelle de la plante entière qu'à un âge propre de la feuille. Cette augmentation coïncide avec la date où le nombre final de graines par plante est fixé (franchissement du stade limite d'avortement des graines, Art15).

### 2.3 Fonctionnement du méristème végétatif et reproducteur du tournesol

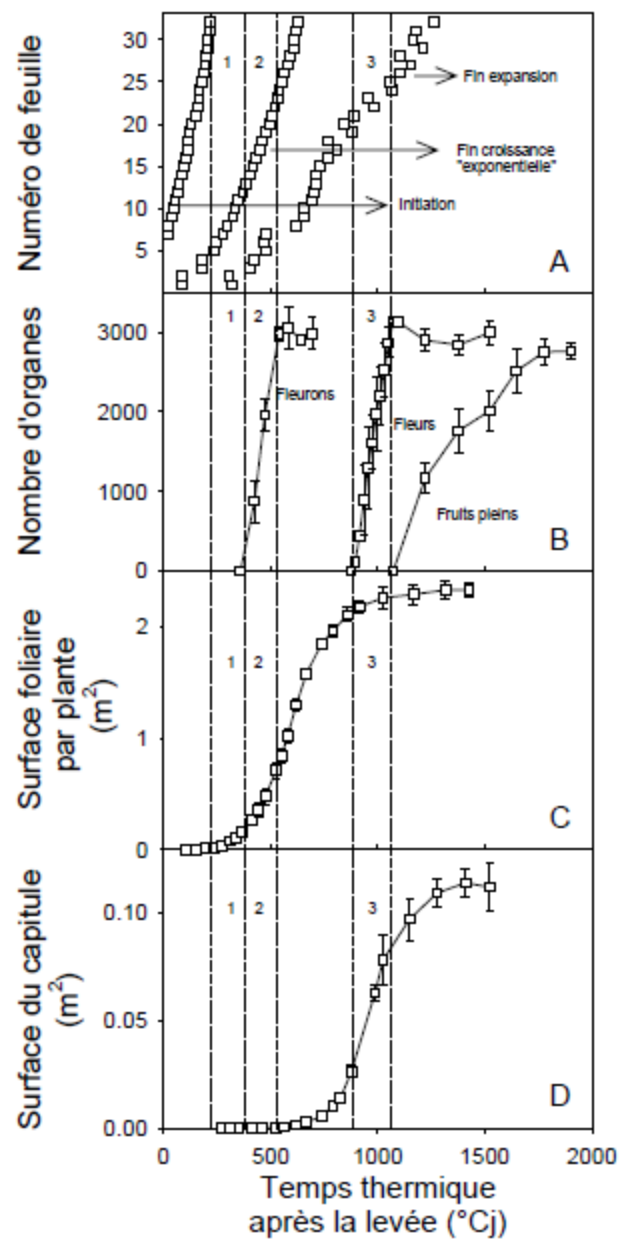


Figure 12. Confrontation des développements végétatif et reproducteur chez le tournesol. Les graphes A et B correspondent aux modèles de développement présentés Fig. 4 et Fig. 2 respectivement (Etu4).

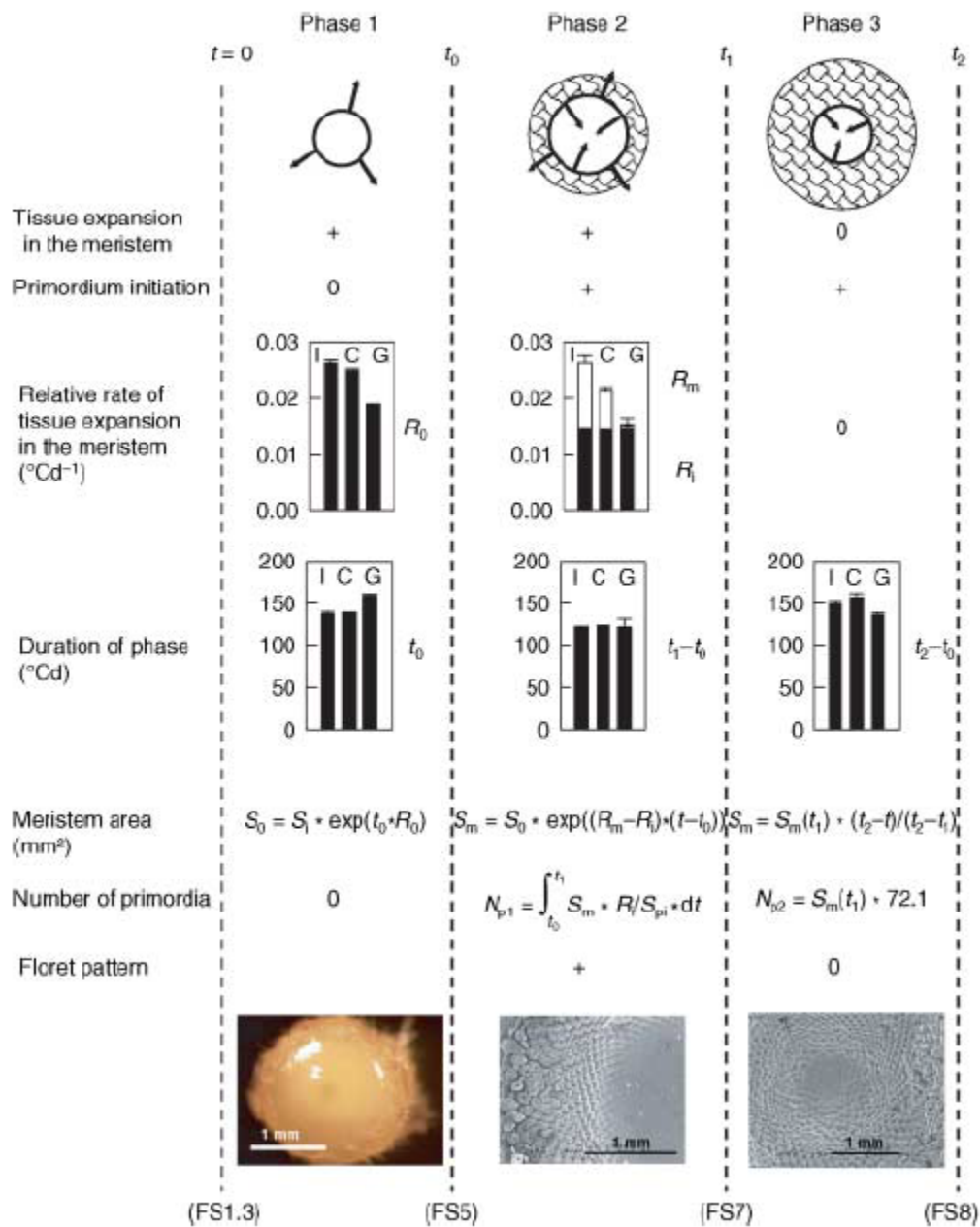


Figure 13. Les trois phases au cours de la mise en place du nombre de primordia initiés sur un capitule de tournesol. Les vitesses et durées des phases sont indiquées, ainsi que les équations pour le calcul de la surface du méristème et le nombre de primordia initiés (Art5).

La cinétique d'initiation des primordia floraux sur le capitule de tournesol a été modélisée en fonction du temps thermique (Art5). La confrontation des développements végétatif et reproducteur (Fig. 12) montre que l'initiation des primordia floraux sur le capitule de tournesol se produit pendant une période courte, au cours de laquelle les feuilles terminent séquentiellement (du bas vers le haut de la tige) la phase exponentielle de leur croissance ou phase hétérotrophe. Les feuilles les plus jeunes, qui acquièrent leur autotrophie carbonée tardivement, sont donc les plus exposées à une concurrence trophique avec le développement

du capitule. Ainsi, la vitesse relative d'expansion est plus faible sur les feuilles les plus jeunes que sur les plus âgées, en liaison avec l'avancement du développement reproducteur (Art3). Lors d'un déficit hydrique, la croissance de ces feuilles est plus affectée que celle du capitule, ce qui peut se traduire par un effet bénéfique d'une contrainte hydrique modérée sur le nombre de primordia initiés et le nombre de grains récoltés (Art6).

Les relations entre l'initiation des primordia et l'expansion du capitule ont été analysées, formalisées et mises en équations (Fig. 13 ; Art5). Trois phases distinctes ont été caractérisées pendant l'élaboration du nombre de primordia initiés (Fig. 13). Pendant la première, la surface du méristème croît de façon exponentielle, sans initiation de primordia. Pendant la seconde, la variation de surface du méristème est la résultante de l'expansion des tissus méristématiques, qui tend à augmenter la surface, et de l'initiation des primordia en périphérie du méristème, qui tend à diminuer sa surface (Fig. 13). Pendant la dernière phase, l'initiation des primordia se poursuit sans expansion des tissus méristématiques jusqu'à occuper tout l'espace central du capitule. Une analyse spatiale de la croissance du capitule a été conduite en mettant à profit l'arrangement spatial des boutons floraux en parastiques. Une méthode originale a été mise au point, en mettant à profit l'organisation spatiale des organes floraux qui s'alignent le long de parastiques. Le rang d'initiation des boutons floraux le long d'une parastique est un repère de position, et d'âge, sur le capitule. Des mesures de densités d'organes à différentes positions sur le capitule, échelonnées au cours du temps et sur des plantes soumises à différentes conditions environnementales ont ainsi mis en évidence des gradients de vitesse relative d'expansion entre la zone périphérique du capitule portant des primordia floraux et la zone centrale (méristème) qui n'en porte pas. En cas de contrainte, la vitesse relative d'expansion de la zone centrale est affectée alors que celle de la zone portant les boutons floraux initiés est stable et similaire dans toutes les conditions environnementales testées (Art6). La vitesse relative d'expansion du méristème est la variable explicative du nombre total de primordia initiés et de la croissance du capitule en conditions de déficits en eau ou en lumière (Fig. 14). Les autres variables du modèle (durée des phases, croissance des organes initiés, part du méristème allouée à l'initiation) n'ont pas été affectées par les contraintes environnementales testées (Art5).

Ces résultats soulignent le rôle central des processus d'expansion du méristème dans l'initiation des organes et dans la réponse aux contraintes en lumière et en eau.

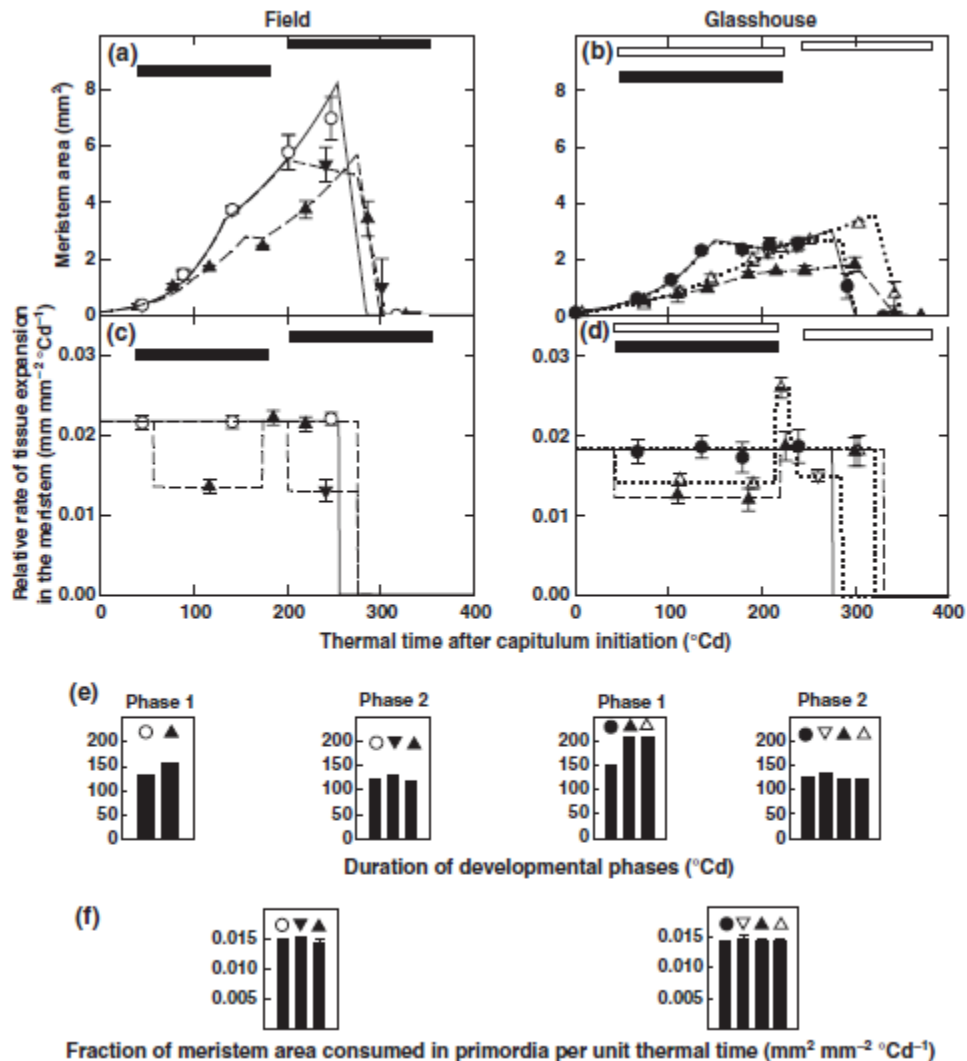


Figure 14. Croissance du méristème sur un capitule de tournesol chez des plantes soumises à des contraintes hydriques ou lumineuses. Les différences de croissance en surface du méristème et de nombre de primordia initiés sont expliquées par les variations de la vitesse relative d'expansion des tissus méristématiques. Les autres variables (durée des phase, fraction du méristème allouée à l'initiation) ne sont pas affectées. (Art6)

#### 2.4 Analyse spatiale de la croissance des soies de maïs : divisions cellulaires, expansion et lien avec le développement reproducteur (Art7)

Une analyse spatiale et temporelle de la croissance des soies a été menée afin de déterminer où et quand se produit l'extension des tissus dans les soies (Art7 ; Fig. 15). Cette analyse a mis à profit l'organisation spatiale des cellules de l'épiderme des soies en files cellulaires. L'analyse de la croissance des tissus et des cellules individuelles a permis de reconstruire les phases de développement dans toutes les zones des soies, depuis la base où se situent les cellules les plus jeunes jusqu'au sommet où se situent les âgées. Bien que les soies partagent des

caractéristiques morphologiques avec les racines et les feuilles de monocotylédones (croissance longitudinale, files cellulaires), la distribution spatiale et temporelle de leur croissance est plus proche de celle des feuilles de dicotylédones. Pendant une première phase, division et allongement cellulaires se produisent de façon uniforme tout le long de la soie. Ensuite, les divisions cellulaires cessent progressivement, du sommet vers la base de la soie, tandis que la vitesse relative d'extension des tissus est maintenue constante, quelle que soit la position le long de la soie. Quand le sommet de la soie émerge des spathes, la croissance cesse dans la partie émergée et diminue progressivement dans la portion incluse dans les spathes. Un déficit hydrique du sol ne modifie pas cette succession de phases, mais affecte les vitesses et durées des processus. Les vitesses de division et d'extension cellulaires sont d'autant plus affectées que le déficit est plus sévère, ce qui retarde l'émergence des soies. La durée des divisions cellulaires n'est pas affectée par le stress, et, dans toutes les situations observées, la fin des divisions cellulaires dans la soie coïncide avec la diffusion du pollen dans l'inflorescence male. Ainsi, l'intervalle anthèse – floraison femelle (sortie des soies), largement utilisé par les sélectionneurs pour caractériser la réponse des cultivars au déficit hydrique, correspond à une phase précise du développement des soies : entre la fin des divisions cellulaires, à la base de la soie, et l'arrêt de l'extension des cellules au sommet de la soie (Art7).

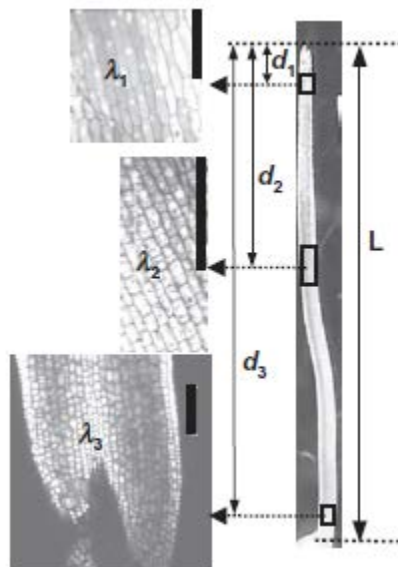


Figure 15. Analyse spatiale de la croissance dans les soies de maïs. La longueur des cellules épidermiques est mesurée à différentes positions le long de la soie, repérées par leur distance au sommet  $d_i$ . Les frontières entre les cellules constituent des marqueurs de position (Art7).

### 2.5 Réponse aux températures élevées chez la microvigne (Art12)

La microvigne est un mutant nain de vigne dont le méristème apical produit de façon continue de nouveaux phytomères portant à la fois une feuille et une grappe. Le fonctionnement du méristème se poursuit au-delà de la date de maturité des premières grappes du bas de la tige (Figure 16).

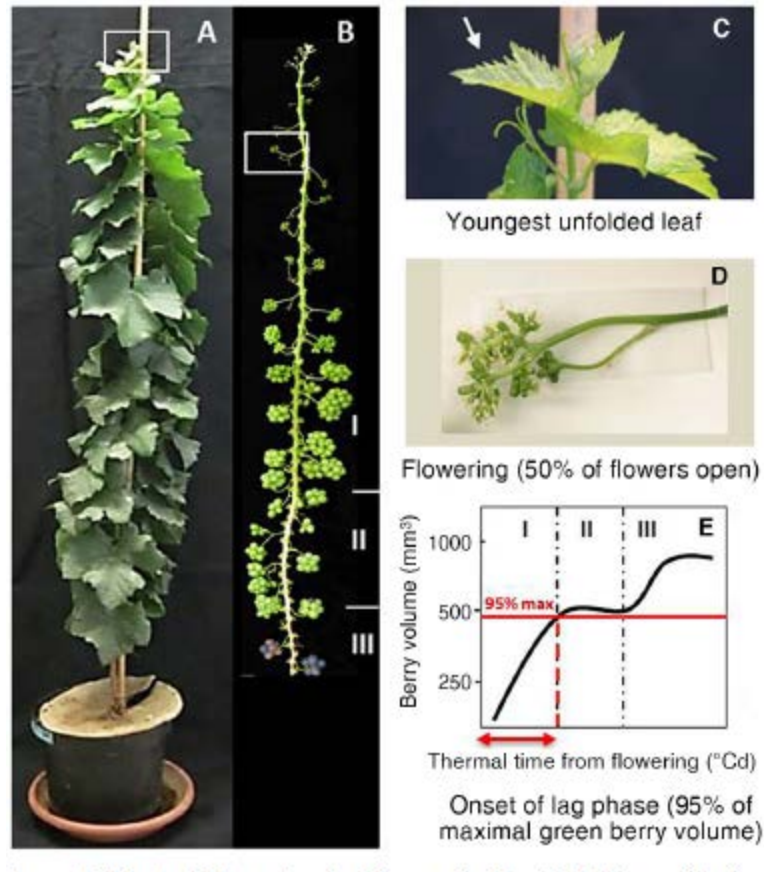


Figure 16. A, plant de microvigne au stade 45 feuilles visibles. B, le même plant sans ses feuilles montre la présence d'une grappe à chaque phytomère. Les grappes les plus âgées sont au stade véraison (phase III de la croissance des baies) et les plus jeunes n'ont pas fleuri. C et D, détail des stades feuille déployée et floraison, dont la position sur la tige est indiquée par un rectangle blanc en A et B respectivement. E, les 3 phases (I, II et III) du développement des baies dont la position sur la tige est indiquée en B (Art12).

Ainsi, tous les stades de développement des feuilles et des grappes sont présents simultanément le long de la tige, depuis l'initiation des primordia au niveau de l'apex jusqu'aux stades matures en bas de la tige. Les caractéristiques du modèle de développement (vitesse d'initiation des organes, durée de développement de chacun d'eux, stables en temps thermique) permettent de calculer, à une date donnée, l'âge des organes (feuille ou grappe) à chacun des phytomères en temps thermique depuis l'initiation ou la floraison. Ceci permet, à partir de données spatiales obtenues à une seule date, de reconstituer des évolutions temporelles. Ceci a été appliqué pour étudier l'impact d'une élévation de température de 8°C (30/20°C jour/nuit vs 22/12°C) sur la croissance des organes végétatifs et reproducteurs et leur contenu en glucides (sucres solubles et amidon). L'étude montre que les fortes

températures affectent de façon différentielle les organes végétatifs et reproducteurs. Les durées de développement des feuilles et entrenœuds sont inchangées en temps thermique, alors que le développement des organes reproducteurs (floraison, accumulation de sucres, maturation) est nettement ralenti. La croissance des organes végétatifs est accélérée, et celle des organes reproducteurs est ralentie. L'utilisation du modèle de développement permet à moindre coût, en une seule récolte, de construire des cinétiques selon une échelle de temps pertinente. La comparaison des deux traitements phytomère par phytomère aurait conduit à interprétation difficile et peut-être erronée.

### 3. L'impact du déficit hydrique sur les organes reproducteurs s'explique-t-il par leur statut carboné ?

#### *3.1 Le déficit hydrique s'accompagne d'une accumulation de sucres dans les organes reproducteurs en croissance*

Chez le tournesol, pendant l'initiation des primordia floraux, la vitesse relative d'expansion du méristème est corrélée à la teneur en sucres solubles dans le capitule, pour des plantes bien alimentées en eau présentant des quantités de rayonnement intercepté contrastées (Fig. 17 ; Art6 ; Art13). La corrélation disparaît chez les plantes soumises à un déficit hydrique, pour lesquelles on observe une accumulation de sucres et une diminution de la vitesse d'expansion. Lors de la ré-irrigation de plantes stressées, une augmentation transitoire de la vitesse relative d'expansion du capitule est observée. On retrouve alors la corrélation entre vitesse d'expansion et disponibilité en sucres (Art6 ; Art13).

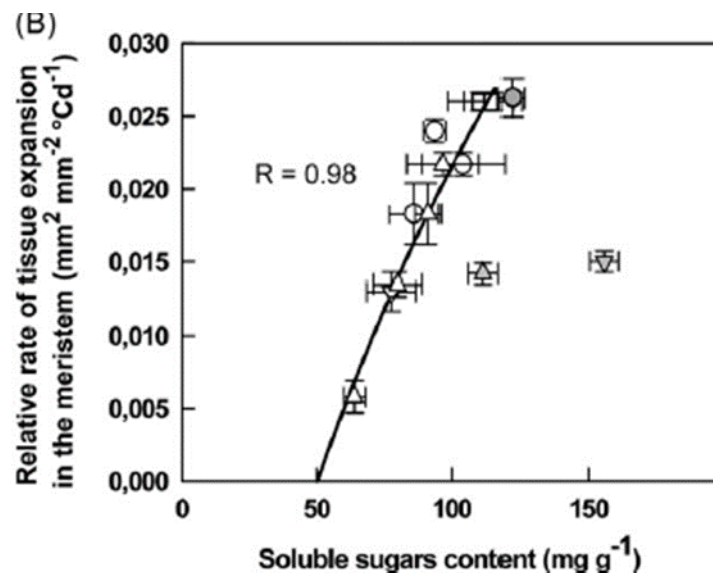


Figure 17. Relation entre la vitesse relative d'expansion des tissus méristématiques et la teneur en sucres solubles de capitules de tournesol pendant la période d'initiation des primordia floraux. Chaque symbole correspond à un traitement expérimental. Les points obtenus en conditions hydriques favorables, mais dans des conditions lumineuses variées,

sont étroitement corrélés. Les points correspondants à des déficits hydriques (triangles grisés) présentent une forte accumulation de sucres solubles et s'écartent nettement de la relation commune (Art6 ; Art13).

Chez le maïs, on observe également une accumulation de sucres dans les ovaires et dans les soies de plantes soumises à un déficit hydrique modéré (Fig. 18 ; Art16). Cette accumulation concerne surtout les sucres solubles, et en particulier le saccharose, dont la concentration est significativement supérieure chez les plantes en déficit hydrique, que ce soit dans les ovaires de la base de l'épi, qui vont aller au bout de leur développement, ou les ovaires situés vers l'apex de l'épi, qui vont avorter en situation de déficit hydrique. Ceci est également observé dans les soies correspondantes et pendant toute la durée de l'application du déficit hydrique (Fig. 18). Les concentrations en amidon sont au moins égales et parfois supérieures en déficit hydrique.

Les organes reproducteurs en phase de croissance ont donc un statut carboné au moins préservé, et souvent amélioré, chez des plantes soumises à un déficit hydrique. La limitation de leur croissance n'est donc pas due à un défaut d'approvisionnement en assimilats carbonés, mais plutôt à un effet direct du déficit hydrique sur les transferts d'eau dans la plante qui pilotent l'expansion des tissus. Comme le déficit hydrique affecte plus les processus d'expansion que la photosynthèse, cela se traduit par une accumulation de sucres dans les organes dont la croissance est limitée (Art13).

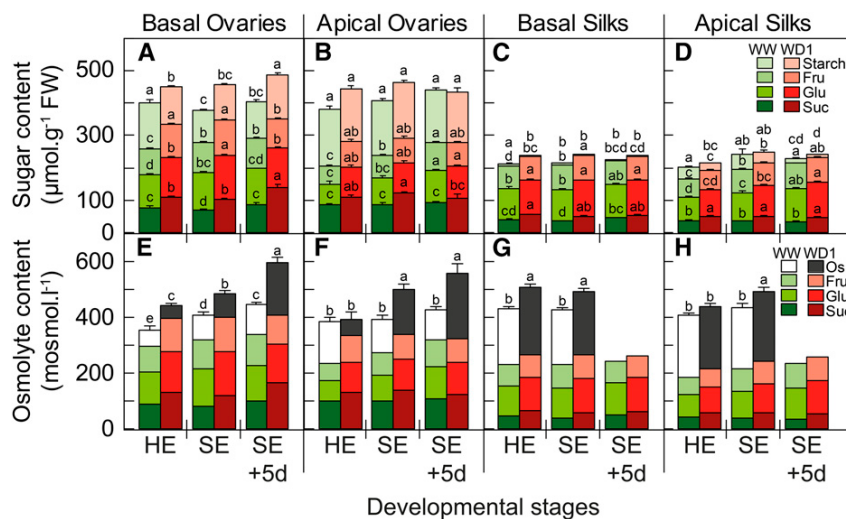


Figure 18. Accumulation de sucres et d'osmolytes dans les organes reproducteurs de maïs au cours d'un déficit hydrique modéré. Les échantillons ont été prélevés à 3 stades : émergence des spathes (HE), émergence des premières soies (SE) et 5 jours plus tard (SE +5d) juste avant la remise en eau des plantes en déficit hydrique. Les dosages sont faits dans les organes de la base (A, ovaire ; C, soies) et du sommet de l'épi (B, ovaire ; D, soies). Pour chaque date, la colonne de gauche représente les plantes bien irriguées (WW) et celle de droite les plantes en déficit hydrique (WD1). De haut en bas de chaque colonne sont indiquées les teneurs en

amidon, fructose, glucose et saccharose. Les différences significatives sont indiquées par des lettres différentes. (Art16)

### 3.2 Séquence d'événements conduisant à l'avortement des ovaires de maïs en déficit hydrique

La croissance, le développement et le devenir (avortement ou non) des ovaires de maïs ont été suivis en fonction de leur position spatiale le long de l'épi (cf Fig. 3) pour des plantes subissant ou non une contrainte hydrique modérée autour de la floraison (- 3 jours à + 5 jours) (Art17). La morphogenèse de l'épi produit des cohortes d'organes de développement synchrone disposées sous forme de couronnes du bas de l'épi (cohortes âgées) vers l'apex (cohortes les plus jeunes). La répartition spatiale des avortements en déficit hydrique n'est pas aléatoire (Fig. 19) : la probabilité d'avortement est maximale pour les cohortes les plus jeunes, et elle est reliée au retard de pollinisation de la cohorte considérée par rapport aux premières pollinisations (Fig. 20A).



Figure 19. Le déficit hydrique provoque des avortements au sommet de l'épi, d'autant plus marqués que le déficit est sévère. WW, plantes bien irriguées ; WD, plantes en déficit hydrique (Art17).

Le déficit hydrique réduit fortement le retard de pollinisation à partir duquel l'avortement se produit (Fig. 20A). Pour obtenir une relation commune aux différentes situations entre le taux d'avortement et le stade de développement des cohortes (Fig. 20B), il faut tenir compte de la date d'arrêt de la croissance des soies. Lors d'un déficit hydrique toutes les soies cessent leur croissance de façon synchrone de 1 à 3 jours après l'émergence des premières soies (= premières pollinisations), alors que cet événement se produit 6 à 8 jours plus tard pour les plantes bien irriguées (Art17). Aucun avortement ne se produit pour les cohortes d'ovaires dont les soies ont été pollinisées plus de 2 jours avant l'arrêt de croissance des soies, tandis que l'avortement est total pour les cohortes pollinisées moins d'un jour avant cette date, avec des valeurs intermédiaires pour les cohortes situées entre ces deux bornes, selon une relation commune à différents génotypes et scénarios (Fig. 20B). L'avortement associé au déficit hydrique est donc déterminé moins de 3 jours après l'émergence des premières soies via le nombre de soies émergées à la date d'arrêt de croissance des soies (Fig. 21). Ces deux causes développementales (retard de pollinisation et arrêt de croissance des soies) expliquent plus

de 90 % des avortements associés au déficit hydrique (Fig. 21). L'hypothèse explicative est que l'arrêt de croissance des soies, induite par le déficit hydrique, s'accompagne d'une rigidification des tissus de la soie qui bloque la progression des tubes polliniques, empêchant la fécondation des ovules. L'avortement concerne tous les ovaires non fécondés à cette date (Art17).

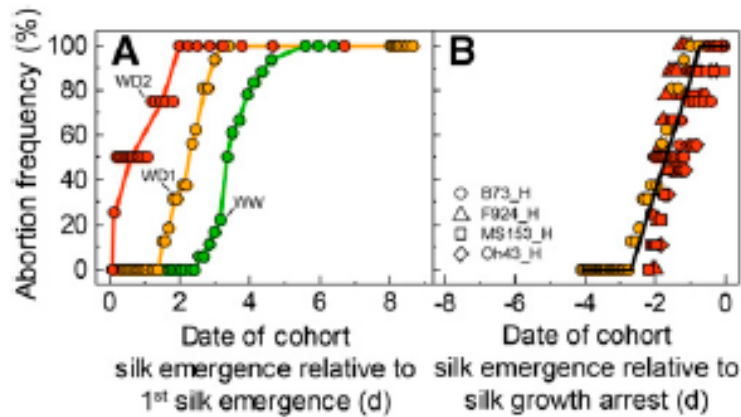


Figure 20. A, Relation entre la probabilité d'avortement des cohortes d'organes le long d'un épi de maïs et leur retard de pollinisation sur les premières cohortes pollinisées. WW, plantes bien irriguées ; WD1, déficit hydrique modéré ; WD2, déficit hydrique sévère. B, la probabilité d'avortement d'une cohorte est corrélée à l'écart entre la date d'émergence des soies de la cohorte et la date d'arrêt de la croissance de l'ensemble des soies de l'épi. La relation est commune à 4 génotypes et 3 modalités de contrainte hydrique (Art17).

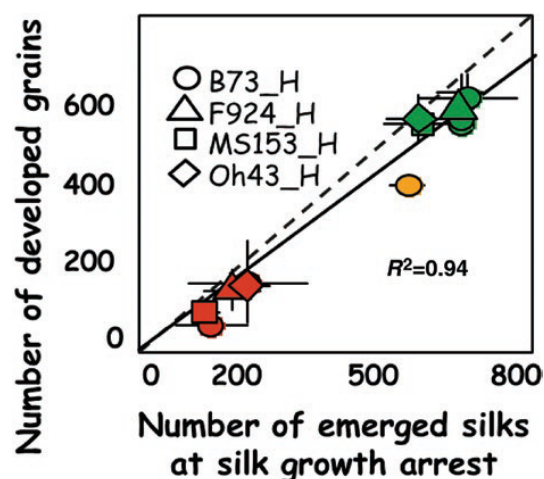


Figure 21. Le nombre de grains pleins par épi à la récolte est corrélé au nombre de soies émergées au moment de l'arrêt de croissance simultanée des soies de l'épi (Art17).

### 3.3 Analyse des événements moléculaires associés à l'avortement des ovaires

L'analyse des activités enzymatiques et des gènes exprimés dans les ovaires et dans les soies a été menée pour des plantes bien irriguées et des plantes subissant un déficit hydrique modéré autour de la floraison (Art16). Les gènes dont l'activité est réprimée par le déficit hydrique concernent essentiellement les processus de croissance, et très peu le métabolisme carboné (Fig. 22). Ils apparaissent d'abord dans les soies, puis dans les ovaires. Les activités enzymatiques et les gènes qui contrôlent le métabolisme carboné sont affectés par le déficit hydrique seulement 5 jours après l'émergence des premières soies, c'est-à-dire après le déclenchement du processus d'avortement associé à l'arrêt de croissance des soies. La restriction du flux de carbone vers les ovaires apicaux semble donc être la conséquence et non la cause de l'avortement (Art16)

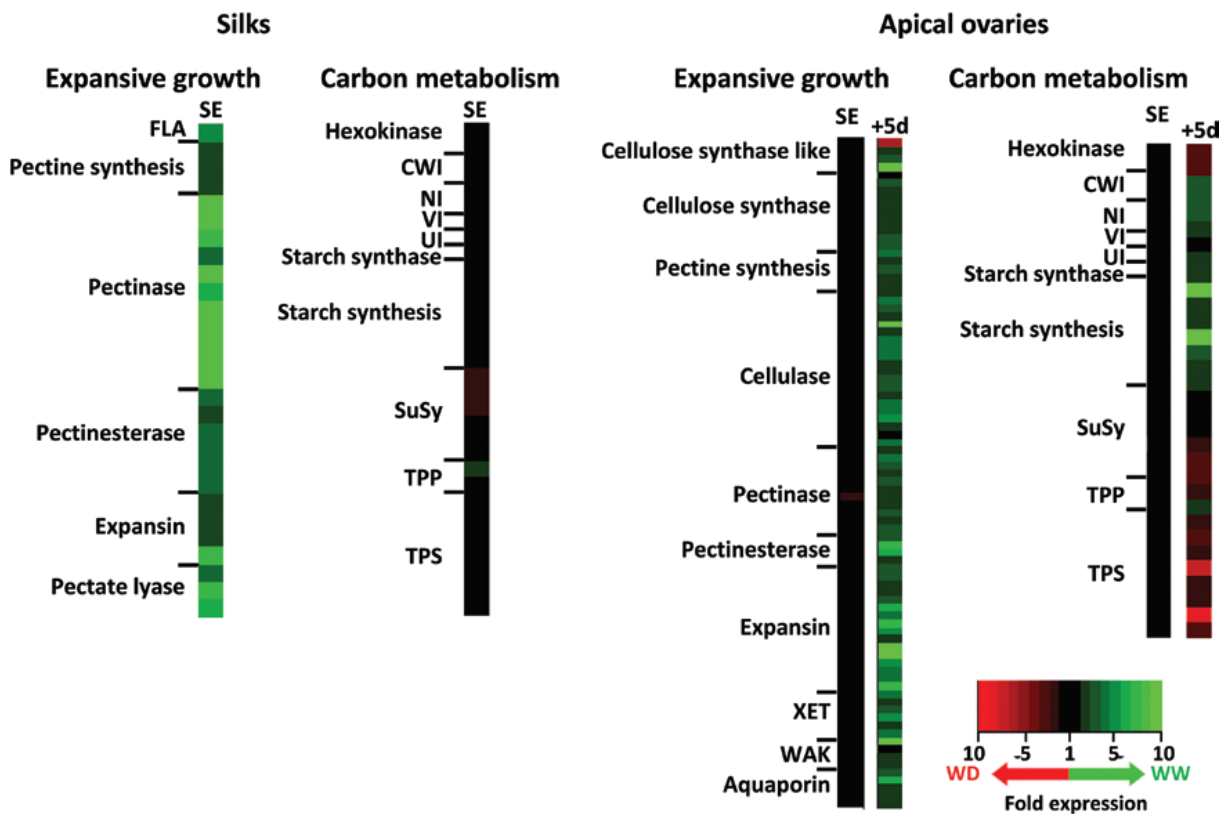


Figure 22. Analyse des transcrits dans les soies et les ovaires de maïs à l'émergence des premières soies (SE) et 5 jours plus tard (+5d). Les gènes sont classés selon leur implication dans les processus d'expansion des tissus ou dans le métabolisme carboné. La couleur verte indique une répression des gènes par le déficit hydrique, le rouge une surexpression, et le noir l'absence d'effet significatif. (Art16)

### 3.4 Un contrôle hydraulique de la croissance des soies, similaire à celui des feuilles (Art22)

Les expérimentations sur le développement reproducteur du maïs ont bénéficié de la mise au point, au sein de l'équipe, d'un dispositif de mesure à haut débit de la croissance et de la transpiration de monocotylédones. Ce dispositif, initialement conçu pour des feuilles de maïs, a été adapté pour suivre la croissance des soies (Art22). Il permet la mesure simultanée, au pas de temps de 15 minutes (i) de la croissance des organes de 360 plantes en serre et de 60 plantes en chambre de culture, (ii) de l'état hydrique du sol et de la transpiration des plantes par pesée automatique des pots et (iii) du microclimat au voisinage des plantes (éclairage, température de l'air et du méristème des plantes, demande évaporative)

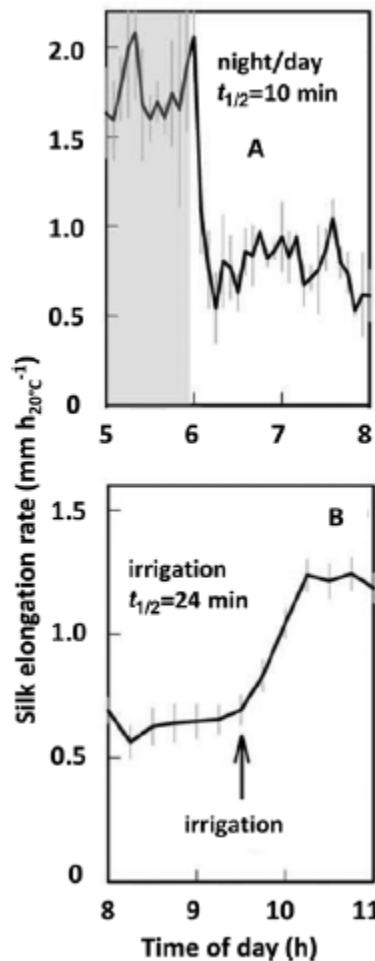


Figure 23. Effet de la transition nuit/jour (A) et de la ré-irrigation de plantes en déficit hydrique (B) sur la vitesse d'allongement des soies. Les temps de réponses de l'ordre de la dizaine de minutes sont compatibles avec un contrôle hydraulique. (Art22)

Les cinétiques de croissance des soies et des feuilles en réponse au déficit hydrique du sol et de l'air présentent des similitudes, qui vont toutes dans le sens d'une limitation hydraulique de la croissance. (i) La vitesse de croissance des soies est affectée par un déficit hydrique atmosphérique. La croissance diurne est inférieure à la croissance nocturne, même chez les plantes bien irriguées. Ceci est observé sur des plantes en transpiration, même en l'absence

d'évaporation directe des soies. (ii) Lors d'un déficit hydrique du sol, la croissance diurne des feuilles et des soies s'annule rapidement, alors que la croissance nocturne est encore active (iii) Lors d'une ré-irrigation, la croissance des soies et des feuilles est restaurée au même niveau que chez les plantes n'ayant pas subi de dessèchement du sol avec un temps de réponse rapide comparable avec celui observé sur les feuilles (Fig. 23). Dans tous les cas, les cinétiques de croissance des soies sont compatibles avec un contrôle via le potentiel hydrique du xylème, comme pour les feuilles, indépendamment de la demande climatique au voisinage des soies ou de la photosynthèse instantanée.

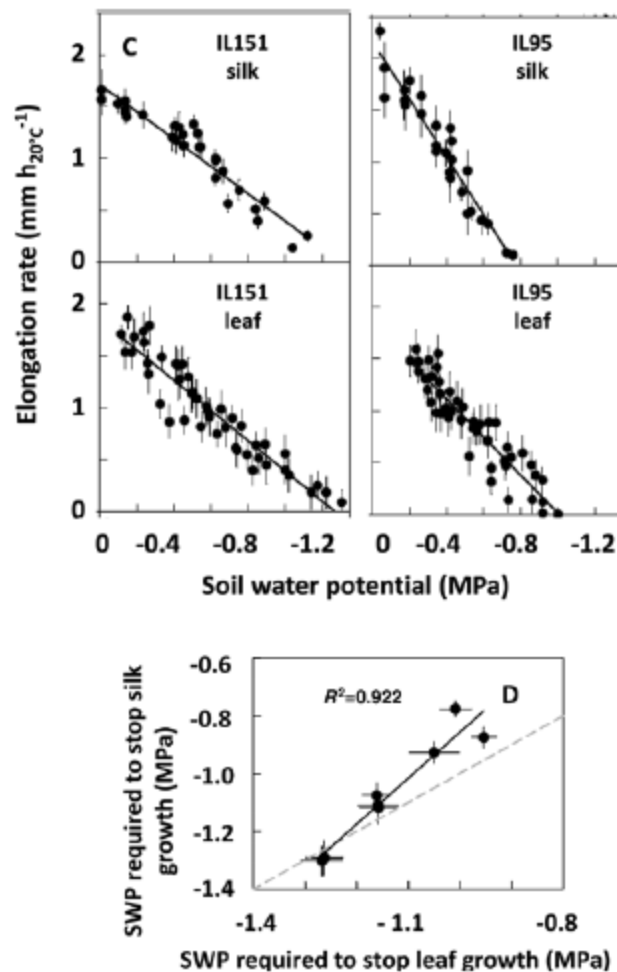


Figure 24. C, courbes de réponse au potentiel hydrique du sol de la croissance des soies (silk) et des feuilles (leaf) pour 2 lignées contrastées (IL151 et IL95). D, relation entre la sensibilité des soies au potentiel hydrique du sol et celle des feuilles. Les sensibilités correspondent au potentiel hydrique pour lequel la croissance s'annule (abscisse à l'origine des courbes de réponse présentées en C). (Art22)

Le comportement de quelques lignées contrastées est cohérent avec l'hypothèse de déterminisme génétique commun pour la réponse des feuilles et des soies chez le maïs (Art22). Les lignées qui maintiennent la croissance de leurs feuilles en situation de déficit

hydrique, maintiennent également la croissance de leurs soies (Fig. 24). Dans les 2 cas, les processus hydrauliques semblent prépondérants dans le contrôle de l'expansion des organes.

### 3.5 Avortement d'organes reproducteurs et processus d'expansion

La répartition spatiale des avortements le long d'une tige de pois, et sa modification lors d'un déficit hydrique (Art24), présentent des similitudes avec ce qui a été décrit plus haut pour l'épi de maïs. L'avortement provoqué par le déficit hydrique concerne les organes les plus jeunes, situés vers l'apex de la tige (Fig. 25A et B). Comme pour le maïs, la probabilité d'avortement d'un organe dépend de son âge, exprimé en jours depuis la pollinisation, au moment d'un événement critique (Fig. 25C). Dans le cas du pois, cet événement critique est l'arrêt de croissance de l'ensemble du bourgeon apical, qui provoque l'arrêt de la production de nouvelles feuilles et de nouvelles inflorescences. Cet arrêt est plus précoce en déficit hydrique, ce qui diminue le nombre de phytomères reproducteurs et décale les avortements vers le bas de la tige (Fig. 25A et B). Cependant, la relation est conservée pour toutes les situations entre la probabilité d'avorter et l'âge des organes à cette date (Fig. 25C). Comme pour le maïs, l'événement de développement explicatif des avortements est un blocage des processus d'expansion des tissus qui simultanément tous les phytomères. Le nombre de primordia initiés sur un capitule de tournesol dépend lui aussi de processus d'expansion dans le méristème et de la date d'arrêt de croissance de celui-ci (Fig. 13 et 14).

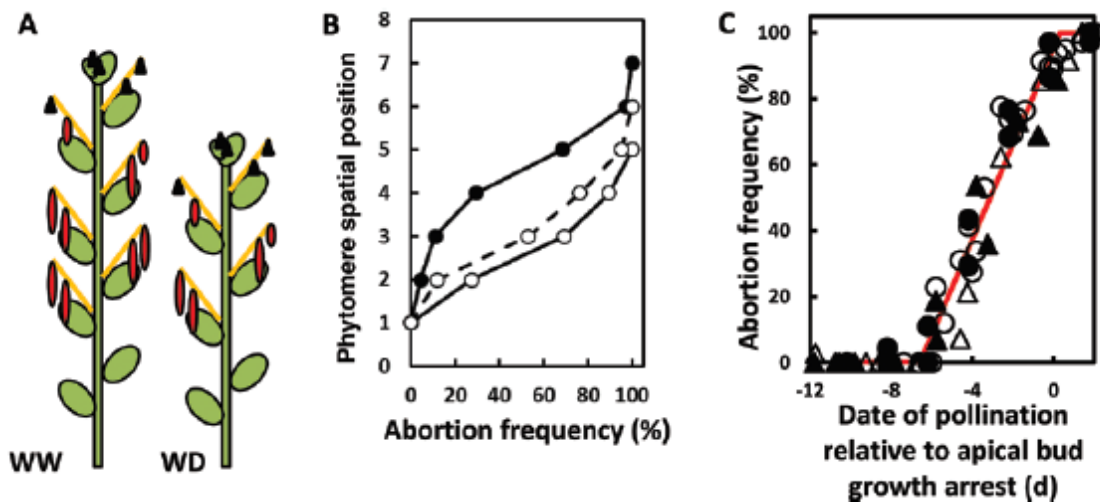


Figure 25. Effet d'un déficit hydrique pendant la floraison sur la distribution spatiale des avortements de grains chez le pois. A, le déficit hydrique réduit le nombre de phytomères reproducteurs en raison d'un arrêt précoce de la croissance de l'ensemble du bourgeon apical. B, les avortements sont décalés vers le bas de la tige. C, la fréquence des avortements à une position sur la tige est liée à l'âge des organes, en jours depuis la pollinisation, au moment du blocage du bourgeon apical. (Art24)

Les relations entre l'avortement des organes reproducteurs et les processus d'expansion des tissus et de transfert d'eau dans la plante sont donc communs à différentes espèces végétales, et peuvent être vues comme un mécanisme adaptatif qui permet, en cas de limitation des ressources, d'éliminer les organes les moins développés pour assurer la production de graines viables avec les organes les plus avancés, et ce, avant même que le statut carboné soit affecté (Art24). Ce contrôle par des processus hydrauliques concerne les avortements précoces, autour de la floraison, lorsqu'il y a encore continuité vasculaire entre la plante mère et les organes floraux. Pour les avortements plus tardifs, lorsqu'il y a discontinuité vasculaire entre la plante mère et le grain, la disponibilité en carbone devient probablement prépondérante dans le contrôle des avortements.

#### 4. Projet de recherche

L'ensemble des résultats obtenus concourt à démontrer et quantifier l'implication des processus d'extension des tissus dans la réponse du développement reproducteur aux contraintes environnementales. La principale cause de l'avortement des ovaires et jeunes grains de maïs, qui se produit au sommet de l'épi lors d'un déficit hydrique pendant la floraison, est développementale (Art17). L'avortement résulte du retard de pollinisation de ces ovaires, conséquence de la réduction de croissance des soies, et se produit alors que le statut carboné des ovaires concernés est favorable (Art16). L'analyse de la réponse de la croissance des soies au déficit hydrique montre que cette réponse partage des mécanismes de contrôle communs avec la réponse de l'expansion des tissus, qu'elle présente une variabilité génétique, et qu'elle est corrélée génétiquement à la réponse de la croissance foliaire (Art22).

Ces résultats obtenus sur le maïs structurent le projet de recherche pour les années à venir. Il s'agira dans un premier temps de conforter notre hypothèse que la croissance des soies est au cœur de la réponse du rendement en grain du maïs au déficit hydrique, en analysant si le progrès génétique pour le rendement va de pair avec des modifications de traits liés à la croissance des soies (projet 1). D'autre part, nous explorerons les déterminants physiologiques (projet 2) et génétiques (projet 3) de la réponse de la croissance des jeunes organes reproducteurs aux contraintes environnementales, afin de simuler et prévoir le comportement de génotypes, et leur rendement en grain, en fonction des scénarios climatiques (projet 4). Le projet s'appuiera sur les plateformes de phénotypage du LEPSE qui permettent de suivre la croissance et le développement de plus de 1600 plantes en pilotant leur état hydrique. Cette étude nécessite la mise au point de nouvelles méthodes afin de mesurer de façon automatisée les traits associés au développement reproducteur (projet 4a).

#### *4.1 Projet 1 : analyse rétrospective du progrès génétique chez le maïs*

Il s'agit ici de conforter notre hypothèse que la croissance des soies est au cœur de la réponse du rendement en grain du maïs au déficit hydrique, en analysant si le progrès génétique pour le rendement va de pair avec des modifications de traits liés à la croissance des soies.

Les études rétrospectives du progrès génétique permettent d'identifier les caractères phénotypiques ayant permis l'augmentation du rendement au cours des générations de sélection. Le principe consiste à étudier, en général au champ, les performances de variétés commerciales qui ont été mises sur le marché à des dates différentes, par exemple sur une période de 50 ans, et à analyser quels sont les traits qui sont associés avec les gains de rendement (via une corrélation, positive ou négative, année de mise sur le marché). Les expérimentations en conditions optimales renseignent sur les traits associés à l'augmentation tendancielle des performances potentielles au cours de la sélection variétale. Inclure à l'étude des expérimentations en conditions de stress, bien caractérisées, permet d'analyser si le progrès génétique s'accompagne ou non d'une meilleure tolérance aux conditions contraignantes, et quels sont, le cas échéant, les traits associés.

Aucune étude de ce type sur le maïs n'a été conduite en France depuis 30 ans. Le développement récent de plateformes de phénotypage, en particulier au LEPSE, fournit une opportunité pour identifier les caractères phénotypiques associés au progrès génétique chez le maïs. En effet, les caractères associés à la mise en place du rendement et à la réponse aux stress abiotiques (mise en place des appareils végétatifs et reproducteurs) sont accessibles sur ces plateformes sur des centaines de plantes, et de façon automatisée pour certains (mise en place de l'architecture de la plante par exemple). L'accès automatisé à des traits pertinents pour caractériser la croissance des soies nécessite des mises au point méthodologiques qui font l'objet du projet 4a.

Une telle étude est en cours sur les plateformes du LEPSE dans le cadre d'une action du projet d'investissement d'avenir Amaizing. Elle comporte 60 hybrides commerciaux mis sur le marché entre 1950 et 2015, ayant tous été des succès dans la zone Europe. Elle inclut plusieurs traitements expérimentaux : des conditions optimales témoin ainsi que différents scénarios de contraintes hydriques ou thermiques autour de la floraison. La caractérisation des plantes concerne la mise en place de la surface foliaire (cinétique du nombre et de la surface des feuilles), les dates de floraison mâle et femelle, la croissance des inflorescences mâles (panicule) et femelle (épi) et la croissance des soies. Ces traits seront rapprochés des performances en terme de rendement et de ses composantes observées pour les mêmes 60 hybrides dans un réseau d'essais au champ couvrant la diversité des situations de la zone de culture du maïs en Europe et comprenant différents scénarios d'alimentation hydrique.

#### 4.2 Projet 2 : Déterminants physiologiques : visualisation des flux d'eau (IRM)

Il s'agit ici de tester l'hypothèse que le développement des jeunes organes reproducteurs est limité par des processus de transfert d'eau, avant toute limitation de leur statut carboné, lors de déficits hydriques intervenant autour de la floraison.

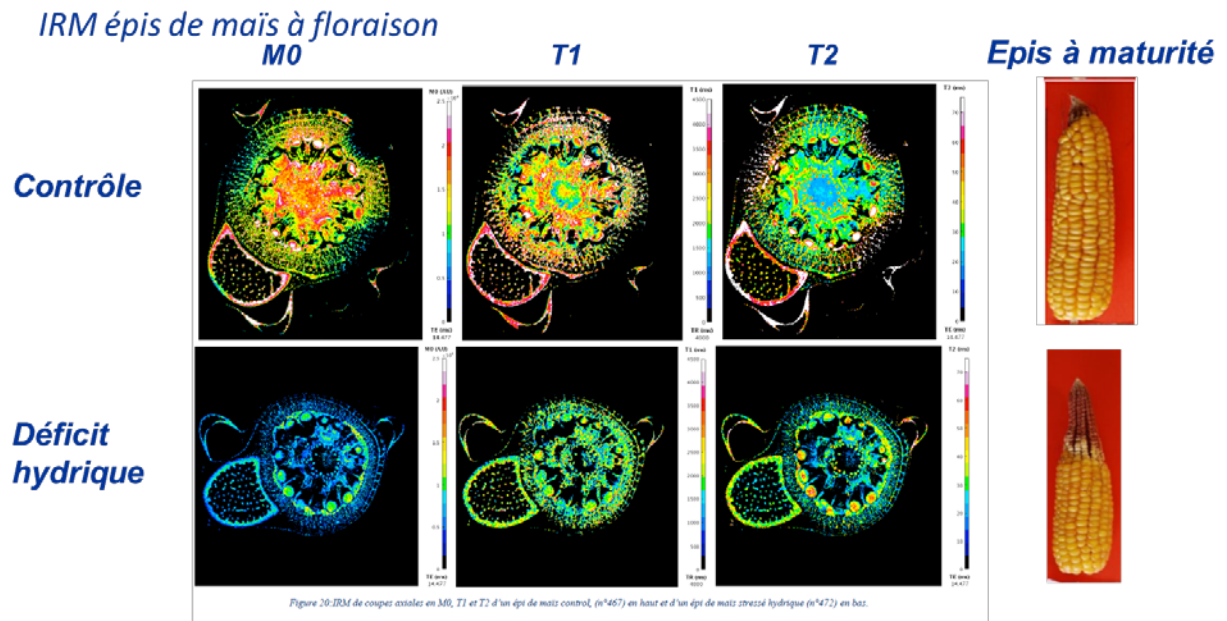
La compréhension de l'avortement précoce des organes reproducteurs bute aujourd'hui sur des verrous expérimentaux concernant l'accès en dynamique et in situ à des variables intrinsèques telles que l'état hydrique ou carboné des organes ainsi que leur anatomie pendant les phases précoces de développement. Les techniques non invasives issues du monde médical, comme la spectroscopie et l'imagerie par résonance magnétique nucléaire (RMN) pourraient permettre, grâce à une approche quantitative, dynamique et locale, de lever ces blocages méthodologiques, ouvrant ainsi de nouvelles perspectives pour la compréhension et la modélisation de l'organogénèse et du fonctionnement des plantes en conditions de stress.

Le projet repose sur une collaboration entre PSH, le LEPSE, la plateforme PHIV-MRI et la plateforme BioNanoMRI et bénéficie du projet APLIM, soutenu par la fondation Agropolis, qui vise à répondre à la demande des sciences du végétal pour l'application des techniques d'IRM et de RMN à l'étude des plantes. Il utilisera les derniers développements de la plateforme BioNanoMRI de Montpellier (capteurs RMN, chambre climatique dédiée aux mesures RMN) mais pourra également orienter le développement de nouveaux capteurs ou dispositifs plus adaptés.

Les mesures RMN et IRM à proprement parler sont de courte durée (quelques heures à plusieurs jours). Les plantes seront préalablement élevées en condition témoin, en condition de stress hydrique ou en condition de stress thermique (plateforme LEPSE) et déplacées pour les mesures de RMN-IRM (plateforme BNIF). Une enceinte climatique non magnétique dédiée est en cours de développement pour permettre de réaliser les expérimentations RMN et IRM dans des conditions contrôlées (température, humidité et rayonnement) les plus proches possibles des conditions d'élevage.

Les inflorescences *in planta* seront placées directement dans le scanner IRM et les variations de volume ainsi que les flux d'eau et de carbone à l'entrée des jeunes organes seront mesurés par segmentation automatique sur des périodes de 5 jours pendant les phases sensibles de développement. Une cartographie des sucres et de l'eau sera réalisée à l'échelle de l'ovaire au cours de la nouaison. Des expérimentations sur inflorescences détachées et mises sur des milieux de culture enrichis avec des nanoparticules (agents de contraste) seront réalisées en parallèle, afin de quantifier et visualiser par des modifications des temps de relaxation RMN (T1 et T2), l'évolution des flux en fonction de la composition en sucres du milieu nutritif. Sur ces inflorescences détachées, l'analyse IRM sera réalisée sur des périodes de 5 jours pendant les phases sensibles de développement. Les données seront confrontées aux observations *in planta* afin d'appréhender la réponse à la disponibilité locale en sucre dans une large gamme de concentration. Des séquences d'acquisition et les méthodes de segmentation des images

ont déjà été mises au point sur différents tissus végétaux (tomate, riz, sorgho, vigne). Ces méthodes seront affinées si nécessaire.



**Les quantités et mouvements d'eau dans les ovaires au moment de la fécondation sont réduits par le déficit hydrique, ce qui se traduit par des avortements de grains. Idem pour un stress thermique à floraison**

Figure 26. IRM de coupes transversales d'épis de plantes bien irriguées ou soumises à une contrainte hydrique pendant la floraison. L'observation des mêmes épis à maturité indique les zones présentant de l'avortement. Les coupes présentées ici ont été réalisées 2 jours après l'émergence des premières soies et correspondent à la zone médiane de l'épi, avec des grains pleins à maturité pour les plantes contrôle et des grains avortés pour les plantes en déficit hydrique.

Le développement de l'inflorescence sera observé pendant quelques jours une fois la plante sortie du scanner IRM pour évaluer l'évolution de l'ovaire, puis les organes seront prélevés et leur composition (eau et carbone) analysée. En parallèle, les phénomènes d'avortement et de nouaison seront observés dans les différentes conditions d'élevage afin de relier les flux mesurés dans chaque condition à la probabilité d'avortement. Des ovaires seront prélevés à 5 stades pendant les phases sensibles de développement pour des analyses de l'état hydrique et carboné (potentiel hydrique, teneur en eau, sucres et amidon) dans chaque condition. Les cinétiques du nombre et de la taille des cellules des jeunes organes seront mesurées sur des coupes d'organes réalisées à ces 5 stades.

Ainsi le projet va s'appuyer sur ces méthodes d'imagerie et de spectroscopie non invasives par RMN afin d'identifier les événements morphogénétiques pendant la phase de développement précoce des organes reproducteurs et de quantifier l'implication des flux d'eau et de carbone

à l'échelle locale sur l'avortement, notamment en réponse aux stress hydrique et thermique. Un premier exemple de résultat d'IRM est présenté Fig. 26.

#### *4.3 Projet 3 : Exploration des déterminants génétiques*

Le projet d'investissement d'avenir *AMAIZING* conjugue des approches génotypiques et phénotypiques mettant en œuvre des techniques d'analyses haut débit afin d'identifier les facteurs génétiques impliqués dans les caractères d'intérêt agronomique tels que le rendement, la qualité et la tolérance aux stress abiotiques

Dans le cadre de ce programme, du matériel génétique dédié a été produit et en particulier des lignées quasi-isogéniques sont maintenant disponibles (collaboration LEPSE – UMR GQE Le Moulon). Les allèles introgressés couvrent une large part de la variabilité à l'intérieur de l'espèce maïs. Sur la base des données des marqueurs génétiques, des lignées ont été sélectionnées pour leur introgression située dans des zones du génome (QTL) identifiées comme impliquées dans la réponse du rendement en graines au déficit hydrique, et des zones impliquées dans l'expansion des tissus (vitesse d'élongation des feuilles et sa réponse au potentiel hydrique du sol).

La dynamique de croissance des soies de ces lignées sera analysée en plateforme dans différents scénarios de disponibilité en eau. Comme dans l'étude du progrès génétique, des expérimentations au champ viendront compléter le dispositif en fournissant des données sur le rendement en grains et ses composantes dans différentes situations environnementales. Ces études permettront de tester le lien génétique entre la croissance des soies et celle des feuilles, et entre la croissance des soies et l'avortement de grains en déficit hydrique. Elles permettront d'établir s'il y a une base génétique aux corrélations détectées dans les études physiologiques (articles 2016). D'autre part, ces études permettront de disséquer les zones du génome impliquées en réduisant la taille des QTL, jusqu'à la recherche de gènes candidats présents dans la zone d'intérêt.

#### *4.4 Projet 4 : phénotypage de la croissance des soies et modélisation de l'élaboration du rendement en grains*

- Projet 4a : comment mettre à profit la plateforme d'imagerie pour faire du phénotypage pertinent du développement reproducteur ?

Une méthode permettant de détecter les soies et de suivre leur croissance de façon automatisée a été mise au point sur la plateforme de phénotypage PhénoArch (Art1). Plusieurs centaines de plantes peuvent ainsi être caractérisées de façon quotidienne, voire biquotidienne. La position de l'épi est repérée avant même l'émergence des premières soies en détectant le renflement de la tige causé par l'épi par analyse d'image en temps réel des photographies de la plante entière prises dans la première cabine d'imagerie du dispositif. Les coordonnées x, y, z de cette zone permettent de piloter une deuxième caméra, portée par un bras mobile, qui vient pointer sur la zone de l'épi pour prendre un cliché en haute définition.

Les pixels correspondant aux soies sont repérés grâce à leur texture différente. L'évolution de leur nombre au cours du temps fournit une cinétique de croissance du massif de soie pour chaque plante analysée (Fig. 27). On obtient donc des caractéristiques de l'émergence des soies pour différents génotypes et différentes conditions.

L'étape suivante de ce travail consiste à tester la pertinence de cette méthode en tant qu'outil de phénotypage à haut-débit pour des analyses génétiques (cf projets 1 et 3). Il s'agit tout d'abord de vérifier que ces mesures sont pertinentes vis-à-vis des traits mesurés de façon manuelle : sont-elles de bons estimateurs de la vitesse et de la durée d'émergence, et reflètent-elles bien la variabilité génétique et environnementale des traits réels ? Il faut également s'assurer qu'elles ont du sens pour l'élaboration du rendement : rendent-elles compte de la variabilité des réponses observées pour la mise place du nombre de grains selon les génotypes et les conditions environnementales ? L'expérimentation sur l'analyse rétrospective du progrès génétique décrite plus haut (projet 1) servira de support à ce test.

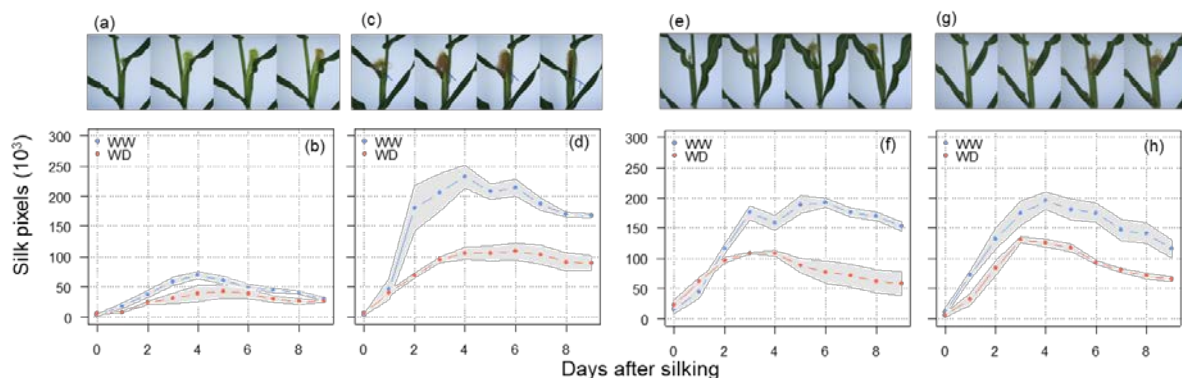


Figure 27. Cinétiques du nombre de pixels de soies (b, d, f, h) détectés automatiquement à partir d'images (a, c, e, g) obtenues sur la plateforme PhenoArch pour 4 hybrides soumis (WD) ou non (WW) à un déficit hydrique pendant la floraison. (Art1)

- Projet 4b : vers un modèle de simulation de la culture de maïs intégrant des formalismes issus de ces travaux pour rendre compte de la réponse au déficit hydrique.

Les résultats décrits dans ce mémoire ont des conséquences fortes pour la modélisation de l'élaboration du nombre de grains en situation de déficit hydrique, car tous les modèles actuels relient le nombre de grains au flux de carbone vers l'épi pendant une période critique. Le cadre conceptuel du module de simulation du nombre de grains dans le modèle de culture APSIM est proche du nôtre puisqu'il prend en considération des cohortes d'organes d'âges différents fondées sur leur date de pollinisation (idem Oury 2016b). L'âge de ces cohortes définit un ordre de priorité pour l'allocation des assimilats carbonés, ainsi que le niveau des besoins en carbone de chaque cohorte. Chaque jour, l'offre en carbone est estimée, et distribuée selon l'ordre de priorité des cohortes. L'avortement intervient pour les cohortes les

plus jeunes dont les besoins ne peuvent être assurés une fois les organes prioritaires servis. Dans ce modèle, le déficit hydrique est pris en compte via son effet sur la photosynthèse qui diminue l'offre en carbone et augmente donc le nombre de cohortes dont les besoins en carbone ne sont pas assurés, ce qui provoque leur avortement. Or nos résultats indiquent que l'avortement intervient avant même que le statut carboné des organes soit affecté, notamment parce que l'impact du déficit hydrique est plus fort sur les processus de croissance que sur la photosynthèse. Une collaboration est en cours (Univ. Queensland, Australie ; Pioneer, USA ; Messina et al., 2015 (*Conf16*)) pour intégrer dans le modèle de culture APSIM un module de simulation du nombre de grains fondé sur des formalismes issus de ces résultats. Ceci implique notamment d'introduire un module de croissance et d'émergence des soies, incluant des sensibilités au déficit hydrique du sol variables selon les géotypes. Ainsi, l'impact du déficit hydrique sur les processus d'expansion serait directement pris en compte. Il rendrait alors compte de la dynamique d'émergence des soies qui est le facteur explicatif de plus de 90 % des avortements précoces en cas de déficit hydrique modéré à la floraison dans nos études (Oury, 2016b). Les expérimentations décrites dans le projet 1 constitueront le support pour calibrer le modèle. La combinaison des caractéristiques d'émergence des soies obtenues en plateforme pour 60 hybrides et différents scénarios hydriques et des données du réseau d'essais champ permettront d'aller jusqu'au rendement. L'objectif à moyen terme est une prise en main du modèle au niveau de l'équipe, comme c'est déjà le cas pour le module de simulation du développement végétatif, largement remanié et maintenant fondé sur les concepts issus des travaux de l'équipe sur la croissance foliaire.

## Liste des publications

Articles de revues internationales. Facteur d'impact moyen : 4,9

- Art1. **Brichet N, Fournier C, Turc O, Strauss O, Artzet S, Pradal C, Welcker C, Tardieu F, Cabrera-Bosquet L** (2017) A robot-assisted imaging pipeline for tracking the growths of maize ear and silks in a high-throughput phenotyping platform. *Plant Methods* **13**: 96.
- Art2. **Cookson SJ, Turc O, Massonnet C, Granier C** (2010) Phenotyping the development of leaf area in *Arabidopsis thaliana*. *Methods in Molecular Biology* **655**: 89-103.
- Art3. **Dosio GAA, Rey H, Lecoeur J, Izquierdo NG, Aguirrezabal LAN, Tardieu F, Turc O** (2003) A whole-plant analysis of the dynamics of expansion of individual leaves of two sunflower hybrids. *Journal of Experimental Botany* **54**: 2541-2552.
- Art4. **Dosio GAA, Rey H, Lecoeur J, Turc O** (2003) La radiación solar durante etapas tempranas del desarrollo afecta al área foliar del girasol. *Revista Argentina de Agrometeorología* **2**: 113-118.
- Art5. **Dosio GAA, Tardieu F, Turc O** (2006) How does the meristem of sunflower capitulum cope with tissue expansion and floret initiation? A quantitative analysis. *New Phytologist* **170**: 711-722.
- Art6. **Dosio GAA, Tardieu F, Turc O** (2011) Floret initiation, tissue expansion and carbon availability at the meristem of the sunflower capitulum as affected by water or light deficits. *New Phytologist* **189**: 94-105.
- Art7. **Fuad-Hassan A, Tardieu F, Turc O** (2008) Drought-induced changes in anthesis-silking interval are related to silk expansion: a spatio-temporal growth analysis in maize plants subjected to soil water deficit. *Plant Cell and Environment* **31**: 1349-1360.
- Art8. **Granier C, Massonnet C, Turc O, Muller B, Chenu K, Tardieu F** (2002) Individual leaf development in *Arabidopsis thaliana*: a stable thermal-time-based programme. *Annals of Botany* **89**: 595-604.
- Art9. **Granier C, Turc O, Tardieu F** (2000) Co-ordination of cell division and tissue expansion in sunflower, tobacco, and pea leaves: Dependence or independence of both processes? *Journal of Plant Growth Regulation* **19**: 45-54.
- Art10. **Lecoeur J, Wery J, Turc O** (1992) Osmotic Adjustment as a Mechanism of Dehydration Postponement in Chickpea (*Cicer-Arietinum* L) Leaves. *Plant and Soil* **144**: 177-189.
- Art11. **Lecoeur J, Wery J, Turc O, Tardieu F** (1995) Expansion of Pea Leaves Subjected to Short Water-Deficit - Cell Number and Cell-Size Are Sensitive to Stress at Different Periods of Leaf Development. *Journal of Experimental Botany* **46**: 1093-1101.
- Art12. **Luchaire N, Rienth M, Romieu C, Nehe A, Chatbanyong R, Houel C, Ageorges A, Gibon Y, Turc O, Muller B, Torregrosa L, Pellegrino A** (2017) Microvine: A New Model to Study Grapevine Growth and Developmental Patterns and their Responses to Elevated Temperature. *American Journal of Enology and Viticulture* **68**: 283-292.
- Art13. **Muller B, Pantin F, Génard M, Turc O, Freixes S, Piques M, Gibon Y** (2011) Water deficits uncouple growth from photosynthesis, increase C content, and modify the relationships between C and growth in sink organs. *Journal of Experimental Botany* **62**: 1715-1729.

- Art14. **Ney B, Duthion C, Turc O** (1994) Phenological Response of Pea to Water-Stress During Reproductive Development. *Crop Science* **34**: 141-146.
- Art15. **Ney B, Turc O** (1993) Heat-Unit-Based Description of the Reproductive Development of Pea. *Crop Science* **33**: 510-514.
- Art16. **Oury V, Caldeira CF, Prodhomme D, Pichon J-P, Gibon Y, Tardieu F, Turc O** (2016) Is change in ovary carbon status a cause or a consequence of maize ovary abortion in water deficit during flowering? *Plant Physiology* **171**: 997-1008.
- Art17. **Oury V, Tardieu F, Turc O** (2016) Ovary apical abortion under water deficit is caused by changes in sequential development of ovaries and in silk growth rate in maize. *Plant Physiology* **171**: 986-996.
- Art18. **Parent B, Turc O, Gibon Y, Stitt M, Tardieu F** (2010) Modelling temperature-compensated physiological rates, based on the coordination of responses to temperature of developmental processes. *Journal of Experimental Botany* **61**: 2057-2069.
- Art19. **Pic E, Teysseidier de la Serve B, Tardieu F, Turc O** (2002) Leaf senescence induced by mild water deficit follows the same sequence of macroscopic, biochemical, and molecular events as monocarpic senescence in pea. *Plant Physiology* **128**: 236-246.
- Art20. **Pigeaire A, Duthion C, Turc O** (1986) Characterization of the final stage in seed abortion in indeterminate soybean, white lupin and pea. *Agronomie* **6**: 371-378.
- Art21. **Tardieu F, Parent B, Simonneau T, Turc O, Welcker C** (2008) Tailoring plants to environmental constraints by scaling up from molecular biology to crop physiology. *Italian Journal of Agronomy* **3**: 569-570.
- Art22. **Turc O, Bouteillé M, Fuad-Hassan A, Welcker C, Tardieu F** (2016) The growth of vegetative and reproductive structures (leaves and silks) respond similarly to hydraulic cues in maize. *New Phytologist* **212**: 377-388.
- Art23. **Turc O, Lecoeur J** (1997) Leaf primordium initiation and expanded leaf production are co-ordinated through similar response to air temperature in pea (*Pisum sativum* L.). *Annals of Botany* **80**: 265-273.
- Art24. **Turc O, Tardieu F** (2018) Drought affects abortion of reproductive organs by exacerbating developmentally-driven processes, via expansive growth and hydraulics. *Journal of Experimental Botany* **69**:3245-3254.
- Art25. **Wery J, Turc O, Salsac L** (1986) Relationship between growth, nitrogen fixation and assimilation in a legume (*Medicago sativa* L.). *Plant and Soil* **96**: 17-29.

#### Chapitres d'ouvrages

- Chap1. **Cookson SJ, Turc O, Massonnet C, Granier C** (2010) Phenotyping the development of leaf area in *Arabidopsis thaliana*. In JM Walker, ed, *Plant Developmental Biology*. Humana Press Inc., Totowa, NJ, USA., pp 89-103.
- Chap2. **Lecoeur J, Turc O** (1994) Initiation et chronologie d'apparition des organes sur une tige de pois. In *Agrophysiologie du pois protéagineux*. UNIP-ITCF-INRA, pp 13-20.

- Chap3. Munier-Jolain N, Turc O, Ney B* (2005) Développement reproducteur. In N Munier-Jolain, V Biarnes, I Chaillet, J Lecoeur, MH Jeuffroy, eds, *Agrophysiologie du pois proteagineux*. INRA Editions, Paris, France, pp 45-51.
- Chap4. Munier-Jolain N, Turc O, Ney B* (2010) Reproductive development. In N Munier-Jolain, V Biarnes, I Chaillet, J Lecoeur, MH Jeuffroy, eds, *Physiology of the pea crop*. Science Publishers and CRC Press, Boca Raton, FL, USA, pp 23-29.
- Chap5. Ney B, Turc O* (1994) Modélisation du développement reproducteur du pois en conditions non limitantes. In *Agrophysiologie du pois protéagineux*. UNIP-ITCF-INRA, pp 27-34.
- Chap6. Turc O* (1994) Construction d'un schéma d'élaboration de rendement pour le pois proteagineux. In L Combe, D Picard, eds, *L'élaboration du rendement des principales cultures annuelles*. INRA Editions, pp 113-121.
- Chap7. Turc O, Granier C, Lecoeur J* (2000) Models of development to analyse and predict plant responses to drought. In L Ayerbe, JL Tenorio, EF de Andrés, FJ Sanchez Jimenez, D Sanz Frutos, eds, *Simposium Hispano-Portugués de Relaciones Hidricas en las Plantas Vol 5*. Universidad de Alcala, Alcala de Henares, Spain, pp 48-54.
- Chap8. Turc O, Ney B* (1994) Déficit hydrique et mise en place des graines chez le pois. In *Agrophysiologie du pois protéagineux*. UNIP-ITCF-INRA, pp 171-178.
- Chap9. Wery J, Turc O, Lecoeur J* (1993) Mechanisms of resistance to cold, heat and drought in cool-season legumes, with special reference to chickpea and pea. In KB Singh, MC Saxena, eds, *Breeding for stress tolerance in cool-season food legumes*. John Wiley and Sons, Chichester, UK, pp 271-291.

#### *Compte-rendus de conférences*

- Conf1. Aguirrezabal LAN, Tardieu F, Turc O* (1994) Modelling the effects of intercepted PPFD and temperature on elongation of the root system of sunflower (*Helianthus annuus* L.). In M Borin, M Sattin, eds, *3rd Congress of the European Society for Agronomy*, Abano-Padova, Italy
- Conf2. Berthezene S, Brichet N, Negre V, Parent B, Suard B, Tireau A, Turc O, Tardieu F, Welcker C* (2015) PHENODYN: a high throughput platform for measurement of organ elongation rate and plant transpiration with high temporal resolution. In C Welcker, R Tuberosa, F Tardieu, eds, *Recent progress in drought tolerance: from genetics to modelling*. DROPS and Eucarpia, Montpellier, France. p 80.
- Conf3. Berthezene S, Brichet N, Nègre V, Parent B, Suard B, Tireau A, Turc O, Tardieu F, Welcker C* (2015) PHENODYN: A high throughput platform for measurement of organ elongation rate and plant transpiration with high temporal resolution. In *EPPN Plant Phenotyping Symposium*, Barcelona, p 40.
- Conf4. Brichet N, Cabrera Bosquet L, Turc O, Welcker C, Tardieu F* (2017) An image-based automated pipeline for maize ear and silk detection in a highthroughput phenotyping platform. In ICRISAT, ed, *Interdrought V*, Hyderabad, India, pp P-055.

- Conf5. **Combaud S, Turc O** (1995) Prediction of leaf area at different water conditions. *In 2. European conference on grain legumes*. European Association for Grain Legume Research, Copenhagen, pp 110-111.
- Conf6. **Dosio G, Lefeuvre T, Suard B, Izquierdo N, Aguirrezabal L, Turc O** (2000) Stability of sunflower leaf development in France and Argentina. *In Proceedings of the 15<sup>th</sup> International Sunflower Conference*. International Sunflower Association, Toulouse, France. pp D47-51.
- Conf7. **Dosio GAA, Turc O** (2002) Efecto de una disminución temprana de la radiación solar incidente sobre el área foliar en girasol. *In Asociación Argentina de Agrometeorología, ed, Agrometeorología y agricultura sustentable en el nuevo milenio*, Vaquerías, Valle Hermoso, Córdoba, Argentina.
- Conf8. **Fuad-Hassan A, Tardieu F, Turc O** (2005) Analysis of maize silk growth during water stress. *In Comparative Biochemistry and Physiology a-Molecular & Integrative Physiology*, Vol 141 pp S310-S310.
- Conf9. **Fuad-Hassan A, Tardieu F, Turc O** (2007) Spatial and temporal analysis of cell division and tissue elongation in silks of maize plants subjected to soil water deficit. *In Workshop on Growth Phenotyping and Imaging in Plants*, Montpellier, France. p 25.
- Conf10. **Fuad-Hassan A, Turc O** (2004) A framework of analysis of the response of maize silk elongation to soil water deficits. *In Workshop of the Challenge Program Generation*. Agropolis International, Montpellier, France.
- Conf11. **Fuad-Hassan A, Turc O** (2005) A model to predict anthesis silking interval in maize : analysis of differential responses to water deficit of ear-axis organs. *In A Blum, R Tuberosa, eds, Proceedings of the 2nd International Conference on Integrated Approaches to Sustain and Improve Plant Production Under Drought Stress Interdrought II*, Roma, Italy.
- Conf12. **Joets J, Coursol S, Turc O, Cabrera-Bosquet L, Martin-Magnette M-L, Salvi S, Venon A, Chaignon S, Laplaige J, Gendrot G, Palaffre C, Castel S, Pateyron S, Brunaud V, Soubigou-Taconnat L, Dumas F, Marande W, Rousselet A, Belcram H, Charcosset A, Tardieu F, Welcker C, Rogowsky P, Vitte C** (2018) Molecular origin and functional impact of structural variation in maize *In Maize Genetics Conference*, Saint-Malo, France
- Conf13. **Lecoœur J, Wery J, Turc O** (1992) Characterization of the various types of mechanisms of adaptation to drought in field grown chickpeas (*Cicer arietinum*). *In A Scaife, ed, 2nd Congress of the European Society for Agronomy*, Warwick University, UK.
- Conf14. **Luchaire N, Rienth M, Romieu C, Torregrosa L, Gibon Y, Turc O, Muller B, Pellegrino A** (2015) Role of plant carbon status in yield components responses to elevated temperatures in microvine. *In 19. Journées Internationales de Viticulture GiESCO*, Gruissan, France. pp 66-70.
- Conf15. **Luchaire N, Torregrosa L, Gibon Y, Rienth M, Romieu C, Turc O, Pellegrino A** (2016) Yield reduction under high temperature is paired with a low carbon status in microvine. *In 10. International Symposium on Grapevine Physiology and Biotechnology*, Verone, Italy

- Conf16. **Messina C, Hammer G, Tardieu F, McLean G, Chapman S, van Oosterom E, Schussler J, Cooper M** (2015) Modeling kernel abortion in maize. In C Welcker, R Tuberosa, F Tardieu, eds, *Recent progress in drought tolerance: from genetics to modelling*. Drops and Eucarpia, Montpellier, France. p 25.
- Conf17. **Ney B, Turc O, Duthion C** (1990) A model for describing reproductive development of a pea crop. In A Scaife, ed, *1st Congress of the European Society of Agronomy*. European Society of Agronomy, Paris, France, p 218.
- Conf18. **Oury V, Prodhomme D, Gibon Y, Tardieu F, Turc O** (2013) Seed abortion of maize under water deficit is linked to a developmental process and not to carbon deprivation. In *Proceedings of Interdrought IV Conference*, Perth, Australia. p 361.
- Conf19. **Pic E, Turc O, Teyssendier de la Serve B, Tardieu F** (1998) Analyse de la sénescence foliaire du pois (*Pisum sativum* L., cv Messire) : utilisation conjointe d'un modèle de développement et de marqueurs moléculaires. In *Actes du 5ème Forum des Jeunes Chercheurs de la Société Française de Physiologie Végétale.*, Montpellier, France.
- Conf20. **Salifou I, Wery J, Turc O, Salsac L** (1988) Relation between growth, nitrogen fixation and assimilation in a legume (*Medicago sativa* L.). In *Colloque*. INRA, Toulouse, p 138.
- Conf21. **Tardieu F, Caldeira CF, Oury V, Cabrera-Bosquet L, Turc O, Welcker C** (2013) Dissection of drought tolerance; vegetative and reproductive growths in water deficit. In *Interdrought IV Conference*, Perth, Australia.
- Conf22. **Tardieu F, Ehlert C, Parent B, Simonneau T, Turc O, Welcker C** (2008) An integrated approach of tolerance to water deficit involving precise phenotyping and modelling. In *4th EPSO Conference "Plants for Life"*, Toulon, France.
- Conf23. **Tardieu F, Parent B, Simonneau T, Turc O, Welcker C** (2008) Tailoring plants to environmental constraints by scaling up from molecular biology to crop physiology. In *10th Congress of the European Society for Agronomy "Multi-functional Agriculture - Agriculture as a Resource for Energy and Environmental Preservation"*, Bologna, Italy.
- Conf24. **Tardieu F, Welcker C, Turc O** (2007) Growth maintenances of maize leaves and silks under water deficit : Genetic variability of dynamic responses. In *Australian Centre for Plant Functional Genomics (ACPGF) Genomics Symposium The Genomics of Drought*, Adelaide, Australia.
- Conf25. **Turc O** (1995) Drought stress accelerates seed growth and development in pea. In *2nd European conference on grain legumes*. European Association for Grain Legume Research, Copenhagen, Denmark, pp 106-107.
- Conf26. **Turc O** (2013) Seed abortion and yield stability: a key role for growth processes of reproductive organs. In *Genomic, physiological and breeding approaches for enhancing drought resistance in crops*, Baeza, Spain.
- Conf27. **Turc O, Farinha NC, Sousa CJF, Ney B** (1994) A characterization of seed growth and water content to describe the development of chickpeas seeds. In M Borin, M Sattin, eds, *3rd Congress of the European Society for Agronomy*, Abano-Padova, Italy, p 161.

- Conf28. **Turc O, Ney B, Wery J** (1990) Effect of drought stress on reproductive development and seed production in pea and chickpea. *In* ASA, CSSA, SSSA, eds, *Agronomy Abstracts 1990*, San Antonio, Texas, USA, p 161.
- Conf29. **Turc O, Oury V** (2011) Abortion and water deficit in maize : sugars or not sugars ? *In* *2nd DROPS modelling meeting*, Montpellier, France.
- Conf30. **Turc O, Oury V, Gibon Y, Prodhomme D, Tardieu F** (2017) Yield maintenance under drought: expansive growth and hydraulics also matter in reproductive organs. *In* ICRISAT, ed, *Interdrought V*, Hyderabad, India, pp P-076.
- Conf31. **Turc O, Oury V, Gibon Y, Prodhomme D, Tardieu F, Welcker C** (2018) Grain abortion under drought in maize: expansive growth and hydraulics also matter. *In* *Maize Genetics Conference*, Saint-Malo, France
- Conf32. **Turc O, Oury V, Tardieu F** (2012) A central role for silking dynamics in maize ovary abortion. *In* *2nd annual meeting Drought-tolerant yielding plants*, Sabanci University, Istanbul, Turkey.
- Conf33. **Turc O, Oury V, Tardieu F** (2012) Ovary or kernel abortion and water deficit: a central role for silking dynamics. *In* *3rd DROPS modelling meeting*, Des Moines, USA.
- Conf34. **Turc O, Roumet P, Desclaux D** (1995) Contrainte hydrique et développement chez les plantes à floraison indéterminée. *In* *Rencontres*, Bordeaux, p 2 p.
- Conf35. **Turc O, Tardieu F, Oury V** (2015) Grain abortion and yield stability under drought: a key role for growth processes in reproductive organs. *In* C Welcker, R Tuberosa, F Tardieu, eds, *Recent progress in drought tolerance: from genetics to modelling*. Drops and Eucarpia, Montpellier, France. p 26.
- Conf36. **Turc O, Wery J, Lecœur J** (1992) Drought stress and development of reproductive organs in pea (*Pisum sativum* L.). *In* *1. Conference europeenne sur les proteagineux*. Editions Soft Publicite, Angers, pp 209-210.
- Conf37. **Turc O, Wery J, Sao Chan Cheong G** (1990) A limited drought stress as a tool for the management of the balance between vegetative and reproductive components of peas (*Pisum sativum* L.). *In* A Scaife, ed, *1st Congress of the European Society of Agronomy*. European Society of Agronomy, Paris, France, p 113.
- Conf38. **Welcker C, Boussuge B, Tireau A, Naudin P, Neveu P, Sadok W, Parent B, Turc O, Hilgert N, Tardieu F** (2007) A phenotyping platform and an information system to dissect the genetic variability for growth and transpiration rates in response to water deficit. *In* *The genomics of drought*, Adelaide, Australia.
- Conf39. **Welcker C, Boussuge B, Tireau A, Naudin P, Neveu P, Sadok W, Parent B, Turc O, Hilgert N, Tardieu F** (2007) A phenotyping platform and an information system to dissect the genetic variability for growth and transpiration rates in response to water deficit. *In* *Challenge Programme Generation, Breeding application*, Johannesburg, South Africa.
- Conf40. **Welcker C, Turc O, Boussuge B, Bencivenni C, Fuad-Hassan A, Ribaut JM, Tardieu F** (2007) Is there a common genetic determinism between source and sink strengths in maize subjected to water deficit ? *In* *Challenge Programme Generation, Genomic resources and gene/pathway discovery*, Johannesburg, South Africa.

- Conf41. Welcker C, Turc O, Fournier C, Tardieu F (2009) Modelling the genetic variability of growth under water deficit and its impact on grain yield. In 21st International Conference EUCARPIA, Maize and Sorghum breeding in the genomics era, Bergamo, Italy.*
- Conf42. Wery J, Turc O, Soussana J-F (1986) Utilisation de mesures enzymatiques pour l'étude de la fixation et de l'assimilation de l'azote chez la luzerne. In INRA, ed, Actes du VI<sup>e</sup> Colloque International pour l'Optimisation de la Nutrition des Plantes, Vol 4. INRA, Versailles, France, pp 1413-1428.*

#### Transfert de connaissances

- Trans1 Berthézène S, Brichet N, Hamard P, Nègre V, Domerg C, Welcker C, Suard B, Bousuge B, Tireau A, Naudin P, Neveu P, Sadok W, Parent B, Turc O, Tardieu F (2010) PHENODYN : une plateforme de phénoypage à définition temporelle fine. In Journées de la mesure et de la Métrologie INRA, Nouan-le-Fuzelier, France.*
- Trans2 Tardieu F, Belaygue C, Ben Haj Salah H, Lecoeur J, Turc O, Wery J (1997) Croissance de la surface foliaire sous déficit hydrique. In Inra - Secteur Environnement Physique et Agronomique, ed, Le programme valorisation et protection des ressources en eau 1992-1995. 1. Valorisation des ressources en eau : Résultats. INRA Editions, 8 p.*
- Trans3 Turc O (2012) Préserver les ressources en eau. In Agronomie - Plantes cultivées et systèmes de culture, Vol 12 Les Dossiers - Agropolis. Agropolis International, Montpellier, France, pp 39-41.*
- Trans4 Turc O (2012) Preserving water resources. In Agronomy - Crops and cropping systems, Vol 12 Les Dossiers - Agropolis. Agropolis International, Montpellier, France, pp 39-41.*
- Trans5 Turc O (2015) Réponses physiologiques des plantes à la sécheresse et aux fortes températures : identifier les variétés adaptées face au changement climatique. Les Dossiers - Agropolis 20: 80.*
- Trans6 Turc O, Lecoeur J, Combaud S, Wery J (1995) Déficit hydrique et architecture du pois. Perspectives Agricoles 203: 98-104.*
- Trans7 Turc O, Lecoeur J, Combaud S, Wery J (1996) Les stress hydriques précoces, un puissant modulateur de l'architecture du pois. In Rencontre nationale recherche-développement sur le pois protéagineux. UNIP, Paris, pp 16-17.*
- Trans8 Turc O, Roumet P, Desclaux D (1995) Contrainte hydrique et développement chez les plantes à floraison indéterminée. In Rencontres, Bordeaux, p 2 p.*
- Trans9 Wery J, Turc O (1990) Veut-on produire des protéagineux dans la zone méditerranéenne ? Progrès Agricole et Viticole 105: 123-124.*
- Trans10 Wery J, Turc O (1990) Les besoins en eau des productions de semences de légumineuses. Bulletin FNAMS Semences 111: 22-25.*

# Annexe

## Publications choisies





REVIEW PAPER

# Drought affects abortion of reproductive organs by exacerbating developmentally driven processes via expansive growth and hydraulics

Olivier Turc\* and François Tardieu

LEPSE, INRA, Montpellier SupAgro, Univ Montpellier, Montpellier, France

\* Correspondence: [olivier.turc@inra.fr](mailto:olivier.turc@inra.fr)

Received 1 November 2017; Editorial decision 21 February 2018; Accepted 21 February 2018

Editor: Jianhua Zhang, Hong Kong Baptist University, Hong Kong

## Abstract

Abortion of reproductive organs is a major limiting factor of yield under water deficit, but is also a trait selected for by evolutionary processes. The youngest reproductive organs must be prone to abortion so older organs can finish their development in case of limited resources. Water deficit increases natural abortion via two developmentally driven processes, namely a signal from the first fertilized ovaries and a simultaneous arrest of the expansive growth of all ovaries at a precise stage. In maize (*Zea mays*) subjected to water deficits typically encountered in dryland agriculture, these developmental mechanisms account for 90% of drought-associated abortion and are irreversible 3 d after silk emergence. Consistently, transcripts and enzyme activities suggest that the molecular events associated with abortion affect expansive growth in silks whereas ovaries maintain a favourable carbon status. Abortion due to carbon starvation is only observed for severe drought scenarios occurring after silking. Both kinetic and genetic evidence indicates that vegetative and reproductive structures share a partly common hydraulic control of expansive growth. Hence, the control of expansive growth of reproductive structures probably has a prominent effect on abortion for mild water deficits occurring at flowering time, while carbon starvation dominates in severe post-flowering drought scenarios.

**Keywords:** Carbon status, expansive growth, grain abortion, grain set, hydraulics, maize, ovary abortion, water deficit.

## Introduction

The development of reproductive organs (fruits, seeds and their precursors, ovaries, and ovules) plays a dominant role in global crop production (Liu *et al.*, 2013). Among the top 15 major crops worldwide, 10 are consumed as fruit or grain (Ross-Ibarra *et al.*, 2007) and 75% of the total worldwide crop yield comes from fruit and grain crops (Ruan *et al.*, 2010). Fruit and grain abortion under water deficit is a major limiting factor for achieving crop yield potential (Boyer and McLaughlin, 2007; Patrick and Stoddard, 2010; Ruan *et al.*, 2010). Indeed, abiotic stresses during early reproductive

stages often result in failure of fertilization or abortion of fruits and seeds (Thakur *et al.*, 2010), thereby dramatically decreasing crop yield (Setter *et al.*, 2011; Kakumanu *et al.*, 2012). For example, drought at the flowering stage causes severe grain abortion in maize (*Zea mays*; McLaughlin and Boyer, 2004) and heat stress can cause up to 80% flower abortion in tomato (*Solanum lycopersicum*; Ruan *et al.*, 2010). Hence, reducing the sensitivity of fruit and seed set to abiotic stresses is a viable option for sustaining crop yield in the face of climate change.

In the plant life cycle, the early stages of fruit and grain development are the most sensitive to abiotic stresses such as heat, drought, or cold (Barnabás *et al.*, 2008; Hedhly *et al.*, 2009; Thakur *et al.*, 2010). The period with maximum risk of abortion extends, in most species, from the beginning of flowering time to the end of cell division in the embryo or endosperm (Hedley and Ambrose, 1980; Ney *et al.*, 1993; Patrick and Stoddard, 2010). No further abortion occurs after the latter stage so the risk of abortion occurs during a very limited period of time in a wide range of species including crops and non-cultivated trees or herbs (Stephenson, 1981). The failure of reproductive organs during this period can occur before or after fertilization and is termed ‘abortion’ here for simplicity. Recent reviews on this topic have focused on the importance of hormones (Sotelo-Silveira *et al.*, 2014) or of carbon metabolism (Ruan *et al.*, 2010; Liu *et al.*, 2013) during this short period of time. The present paper examines the role of developmental processes, in particular the interaction between reproductive organs of different ages in the same plant and the role of the superposition of controls at organ and at plant level. This involves mechanisms such as expansive growth, hydraulics, and carbon metabolism at the reproductive organ and whole-plant levels.

From an evolutionary point of view, the youngest reproductive organs should be the most prone to abortion to ensure that older reproductive organs that are already developing have access to sufficient resources and can produce viable seeds. Indeed, reproductive organs of different ages usually coexist in a plant or an inflorescence (Stephenson, 1981), suggesting that interactions between them may act as feedbacks that result in a developmental control of abortion. Even in crop plants, grain abortion can be favourable in very dry climates by securing full development of a limited number of grains. In wheat (*Triticum aestivum*), an allele causing reduction in grain number has a highly positive effect on yield under severe water deficit but not in milder scenarios in which

yield is associated with high grain number (Parent *et al.*, 2017). The hypothesis proposed in this paper is that, whereas the evolutionary trend to favour abortion in dry conditions is observed in most species, carbon availability to developing ovaries is not always the triggering mechanism of abortion. We present evidence from previously published studies for a role of developmental processes, which can avoid carbon shortage in reproductive processes, by ‘mimicking’ carbon-starvation-driven abortion before any carbon stress occurs at the plant or ovary level.

## Developmental control of abortion

*Abortion occurs at preferential locations within or among inflorescences*

In pea (*Pisum sativum*), a steep developmental gradient exists within a single plant: the oldest basal pods begin seed filling when apical reproductive organs are still at early stages in the shoot apex, with all intermediate stages between them (Fig. 1A; Ney and Turc, 1993). The same occurs in the maize ear, in which basal ovaries are older than apical ovaries (Kieselbach, 1949), and in the sunflower (*Helianthus annuus*) capitulum, in which central akenes are the youngest because of centripetal initiation of floret primordia (Palmer and Steer, 1985; Dosio *et al.*, 2006). In these three cases, a clear localization of aborted ovaries is observed in regions carrying the youngest ovaries, i.e. at the shoot apex in pea (Fig. 1A), at the ear apex in maize (Fig. 2A) and at the capitulum centre in sunflower (Connor and Sadras, 1992; Sinsawat and Steer, 1993; Alkio *et al.*, 2003). Water deficit does not change this pattern, but essentially extends the region of shoot/inflorescence in which ovaries abort (Figs 1, 2). This suggests that a link may exist between position, age, water deficit, and abortion frequency. This link is also observed in other species in which the spatial gradients of

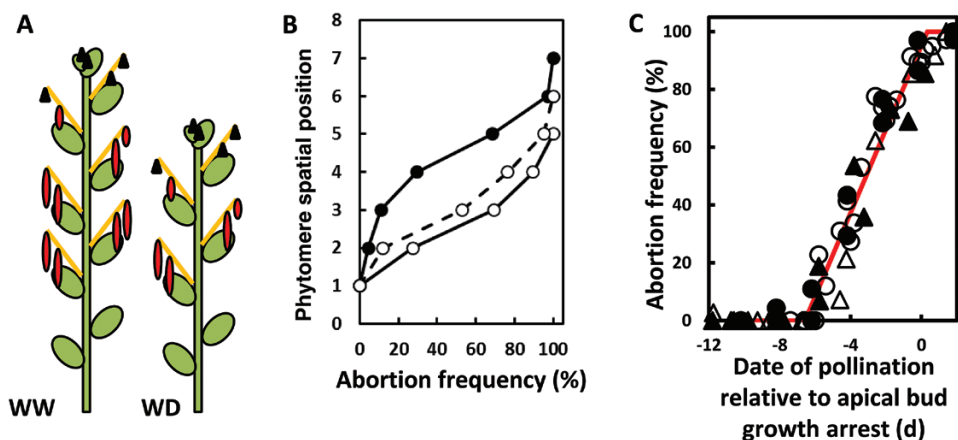


**Fig. 1.** Abortion occurs in youngest apical ovaries in pea (*Pisum sativum* L.), and water deficits reduce the number of fertile phytomeres. (A) Schematic representation of pea plants during seed filling. The stem is made of successive phytomeres with an internode, a leaf and an inflorescence. Youngest phytomeres are located in the apical bud at the top of the plant. WW, well-watered plant; WD, plant subjected to a moderate soil water deficit at flowering. Pods at later stages are represented as vertical ovals, and the triangles represent aborted reproductive organs. (B) Abortion frequency is related to the spatial position of reproductive organs along the stem. It is calculated as  $(SN_i - SN_{max}) / SN_{max}$ , where  $SN_i$  and  $SN_{max}$  are the number of seeds counted, respectively, at the position  $i$  and at the oldest reproductive phytomere. WW, closed symbols; WD, open symbols. Two water deficits were applied during flowering. (Data from Ney *et al.*, 1994.) (C) Abortion frequency is related to the time elapsed between the growth arrest of the apical bud and the stage ‘open flower’ (pollination) of the considered organ. (Data from Ney *et al.* (1994): circles; and Guillioni *et al.* (2003): triangles.)

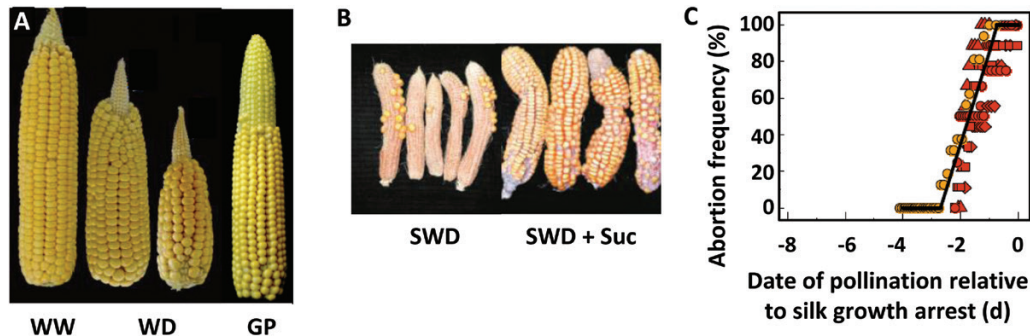


**Fig. 2.** (A) Abortion is predominantly apical in maize (*Zea mays* L.) ears, with an aborted region that increases in length in plants subjected to a moderate water deficit (WD) or to asynchronous pollination (GP). WW, well-watered plants. (B) A severe water deficit after silking (SWD) induces a randomly distributed abortion that is partly reversed by sucrose (Suc) feeding (Adapted from McLaughlin JE, Boyer JS. 2004. Sugar-responsive gene expression, invertase activity, and senescence in aborting maize ovaries at low water potentials. *Annals of Botany* 94, 675–689, by permission of Oxford University Press). (C) The abortion frequency of each ovary cohort is related to the time elapsed between silk growth arrest and silk emergence of the considered cohort. The relationship is common to four hybrids and three levels of soil water deficit at flowering. (A, C) Adapted from Oury *et al.*, 2016b. Ovary apical abortion under water deficit is caused by changes in sequential development of ovaries and in silk growth rate in maize. *Plant Physiology* 171, 986–996, ([www.plantphysiol.org](http://www.plantphysiol.org)), 'Copyright American Society of Plant Biologists'.

abortion frequency coincide with an opposite gradient of pollination or fertilization (see review by Stephenson, 1981), for ovaries located within a fruit (Rocha and Stephenson, 1991; Susko, 2006), in different fruits of an inflorescence (Cawoy *et al.*, 2007), or in different inflorescences of a plant (Ney *et al.*, 1994; Egli and Bruening, 2006).

#### *Spatial gradients of ovary abortion as a result of developmental sequences in maize and pea*

The maize ear is a coalesced inflorescence composed of spikelet pairs arranged in rings sequentially initiated at the ear apex (Bonnett, 1940; Kiesselbach, 1949). These rings are therefore cohorts of ovaries that are initiated simultaneously. Styles and stigma of female flowers, called silks, must rapidly elongate at flowering time to emerge from bracts and collect pollen originating from the apical male inflorescences (or tassels) (Weatherwax, 1916; Kiesselbach, 1949). The first silks to emerge originate from basal spikelets and the last ones from apical spikelets. Two mechanisms account for early ovary abortion and result in the typical distribution of aborted ovaries at the ear tip (Fig. 2A), which contrasts with the random distribution observed with later carbon-starvation-based grain abortion under severe drought (Fig. 2B).

First, the fertilization of basal, oldest, ovaries is sufficient to stop the development of younger, apical, ovaries and cause their abortion. This happens, for example, when fertilization occurs at two different dates, either naturally or via an artificial asynchronous pollination (Freier *et al.*, 1984; Cárcova and Otegui, 2001). In this case, young ovaries located at the tip of the ear abort, even in the absence of carbon deficiency or water deficit (Fig. 2A, 'GP'). This suggests that ovaries progressively lose competence to develop into grains after the fertilization of the first older ovaries, probably because of a signalling process. This explains why aborting ovaries are located at the ear tip, where the youngest ovaries are located, but probably not the increased abortion in cases of water deficit. The nature of the signal remains unknown but may involve cytokinins synthesized during the early development

of grains needed for the development of starchy endosperm (Brugière *et al.*, 2003). Other hormones have been hypothesized to contribute to this systemic signal, such as ABA (Wang *et al.*, 2002; Setter and Parra, 2010; Setter *et al.*, 2011) or ethylene (Cheng and Lur, 1996; Habben *et al.*, 2014).

Second, the temporal pattern of ear development can also cause abortion of ovaries located close to the ear tip. In our analysis, abortion rate is accounted for by the superposition of (i) the sequential emergence of silks originating from ovaries of different cohorts along the ear with (ii) one event occurring on a single day for the whole ear, namely the simultaneous arrest of the growth of silks originating from all ovary cohorts. Abortion occurs in all ovaries that are not pollinated 2 d before silk growth arrest (Fig. 2C). This superposition of events explains why aborting ovaries are located at the ear tip; they cannot be pollinated before silk growth arrest because they are younger than basal ovaries. In contrast with the signalling process presented above, this temporal process also explains why the aborted region of the ear increases in size when silk growth rate decreases with water deficit (Fig. 2A, 'WD'). Indeed, the decreased silk growth rate due to water deficit delays silk emergence so the time from silk emergence to silk growth arrest is shorter in water deficit (typically 2–3 d) than in well-watered plants (typically 7–8 d; Oury *et al.*, 2016b). A greater number of ovary cohorts therefore cannot be pollinated before silk growth arrest and eventually abort. The link between silk growth arrest and abortion may be due to the ability of pollen tubes to grow into the silks. Indeed, during the normal pollination process, tissue stiffening occurs along the silk after the passage of the first pollen tube, thereby blocking the progression of additional pollen tubes (Kapu and Cosgrove, 2010). If tissue stiffening accompanies the early arrest of silk growth in water deficit, as it does in growing leaves (Chazen and Neumann, 1994; Vincent *et al.*, 2005) or roots (Zhu *et al.*, 2007), it may block the progression of the first pollen tube, thereby impeding fertilization. The limit of 2 d before silk growth arrest might be linked to the necessary time for a pollen tube to reach the ovule through the silk (Miller, 1919). Alternatively, it could correspond to

the end of the period of sensitivity of ovaries to plant water status that occurs when ovary tissues become hydraulically isolated from the mother tissues a few days after fertilization (Westgate and Grant, 1989; Bradford, 1994). Overall, 90% of drought-associated abortion was already irreversible 3 d after the emergence of the first silk when silk emergence stopped in plants subjected to water deficit (Fig. 3; Oury *et al.*, 2016b).

Pea is a species with indeterminate flowering in which each phytomere, from the first reproductive phytomere and above, carries an inflorescence originating from an axillary bud (Fig. 1A). The stage ‘open flower’, synchronous with pollination, occurs first at the most basal reproductive phytomere and then progresses sequentially towards apical positions. The duration of flowering, and therefore the developmental lag time between the fertilization of basal and apical organs, is typically 12–20 d in well-watered plants (Ney and Turc, 1993; Ney *et al.*, 1994; Guilioni *et al.*, 2003), i.e. much longer compared with maize. As in the case of maize, abortion occurs in the youngest organs: abortion frequency is 100% in the most apical reproductive organ regardless of watering treatments (Fig. 1B). When plants are subjected to soil water deficit during flowering, abortion occurs at more basal positions than in well-watered plants (Ney *et al.*, 1994; Guilioni *et al.*, 2003; Fig. 1). The final number of reproductive phytomeres that emerge from the apical bud is also reduced by water deficit due to an early arrest of phytomere initiation (Ney *et al.*, 1994; Guilioni *et al.*, 2003). This event is synchronous with a simultaneous cessation of growth and development of all the phytomeres located in the apical bud (Kelly and Davies, 1988; Roche *et al.*, 1998). Leaf emergence and flowering therefore stop simultaneously, 4–10 d (2–5 phyllochrons) earlier in plants subjected to soil water deficit compared to well-watered plants (Ney *et al.*, 1994; Guilioni *et al.*, 2003). As in the case of maize, the abortion frequency of the reproductive organs is explained by the organ age (days from pollination) at this

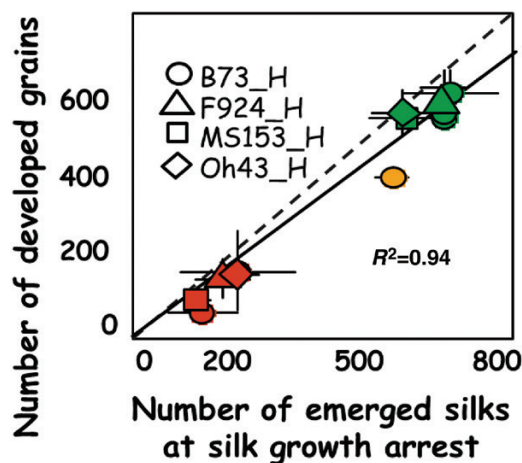


**Fig. 3.** More than 90% of drought-associated abortion is already irreversible at silk growth arrest, i.e. 2–3 d after the emergence of the first silk in water deficit. The relationship is common to four hybrids and three levels of soil water deficit at flowering (Adapted from Oury *et al.*, 2016b). Ovary apical abortion under water deficit is caused by changes in sequential development of ovaries and in silk growth rate in maize. Plant Physiology 171, 986–996, ([www.plantphysiol.org](http://www.plantphysiol.org)), ‘Copyright American Society of Plant Biologists’. (This figure is available in colour at JXB online.)

critical stage (Fig. 1C). Abortion occurs in all reproductive organs that are pollinated less than 1 d before apex growth arrest, whereas all reproductive organs that have been pollinated more than 7 d before that date complete their development (Fig. 1C). A common relationship between organ age and abortion rate was observed for various levels of soil water deficit and different genotypes (Fig. 1C, data from Ney *et al.* (1994) and Guilioni *et al.* (2003)).

Abortions occurring in pea and maize therefore present striking similarities, shared with other species: (i) the presence of fertilized reproductive organs affects the development of young, non-fertilized ovaries in maize, pea (Guilioni *et al.*, 1997) and other species (Stephenson, 1981), even in the absence of any carbon limitation or abiotic stress; and (ii) the distribution of abortion frequency in the youngest ovaries under water deficit is associated with an early arrest of growth that occurs simultaneously for all the silks of the maize ear or for all the phytomeres in the pea apical bud. A similar situation is observed in sunflower, in which one observes a synchronous cessation of the development of all youngest organs located in the centre of the capitulum, due to the arrest of capitulum meristem growth (Dosio *et al.*, 2006). In these three species, a gradient of reproductive organ age in the shoot or inflorescence results in abortion for organs younger than a threshold at a given date, associated with cessation of growth. The effect of water deficit is mainly to amplify these effects, in relation with the expansive growth of silks, capitulum, or shoot apex.

### Is ovary/grain abortion in water deficit caused by carbon starvation or by developmental processes?

The mechanisms presented above at first sight contradict the well-accepted theory that abortion in maize is linked to carbon starvation in young ovaries, based on a series of experiments showing that sucrose feeding can partly reverse the effect of water deficit on abortion (Boyle *et al.*, 1991; Zinselmeier *et al.*, 1995a; Zinselmeier *et al.*, 1999; McLaughlin and Boyer, 2004). In these experiments, the sucrose flux to ovaries decreases to near-zero but is partly restored upon sucrose feeding (Mäkelä *et al.*, 2005). Enzyme activity and gene expression of cell wall invertases increases 5–8 d after silking in ovaries of well-watered plants, whereas they remain low under water deficit (Zinselmeier *et al.*, 1995b; Zinselmeier *et al.*, 1999; McLaughlin and Boyer, 2004). This has led several authors to consider cell wall invertases, in particular *INCW2*, as a causal link between water deficit, sugar availability to ovaries and ovary abortion (Boyer and McLaughlin, 2007; Ruan *et al.*, 2010). It was recently demonstrated that the targeted overexpression in developing maize ovaries of a gene involved in sugar signalling improves maize yield under water deficit by reducing grain abortion (Nuccio *et al.*, 2015). This was interpreted as evidence for the central role of sucrose sensing and carbon metabolism in grain set and abortion (Smeekens, 2015; Griffiths and Paul, 2017).

Several arguments lead us to consider that ‘developmental’ and ‘carbon-starvation-based’ abortion might correspond to events occurring at two separate phenological stages during maize reproductive development. First, it is important to note that all experiments with sucrose perfusion reported in the previous paragraph follow a common protocol, in which a water deficit is imposed for 6 d following silk emergence (Zinselmeier *et al.*, 1999). As a consequence, mechanisms occurring earlier, such as silk growth arrest, cannot be observed in the protocol followed by Boyle *et al.* (1991) and in further studies. Secondly, this protocol causes a drastic reduction in photosynthesis, which is not the case in natural drought scenarios in which photosynthesis is in most cases at least partially maintained. Finally, this protocol involves artificial synchronous pollination 5–7 d after silk emergence, so the consequences of asynchronous pollination cannot be observed. The protocol of Boyle *et al.* (1991) and further studies is, therefore, appropriate to characterize carbon-starvation-associated processes leading to abortion but, by its characteristics, cannot account for other causes. It is noteworthy that this protocol results in a random abortion in the ear (Fig. 2B), whereas water deficits in natural conditions result in abortion at the ear tip, in both field and controlled conditions (Fig. 2A). This reinforces the possibility that carbon-starvation-based and development-based abortion may coexist.

In the experiments reported in Fig. 4 (Oury *et al.*, 2016a) where plants were subjected to a moderate water deficit (soil water potential between  $-0.25$  and  $0.30$  MPa), the analysis of transcript abundance suggests no carbon deficiency in either ovaries or silks. The amount of sugars and starch in ovaries even tended to be higher in water deficit than in

well-watered plants (Oury *et al.*, 2016a), as it did in other experiments including soil water shortage (Andersen *et al.*, 2002; Nuccio *et al.*, 2015) or osmotic stress due to salt (Henry *et al.*, 2015). The most striking changes in gene expression were observed in silks rather than ovaries, and were related to genes involved in cell wall mechanical properties, such as expansins, pectinases, pectinesterases, cellulases or wall-associated kinases. A counter example could be the higher vacuolar acid invertase activity in well-watered than in droughted plants. However, the latter was probably associated with high tissue expansion rate, as it is in several studies involving pea epicotyl, maize roots and silks, Arabidopsis roots, and cotton (*Gossypium hirsutum*) fibres (Morris and Arthur, 1984; Sturm and Tang, 1999; Tang *et al.*, 1999; Kohorn *et al.*, 2006; Wang *et al.*, 2010). A favourable carbon status of ovaries and silks in droughted plants is also suggested by the level of trehalose-6-phosphate (T6P), which acts as a signalling intermediate for reporting the cellular sucrose status (Lunn *et al.*, 2006; Yadav *et al.*, 2014). T6P content is increased in maize ovaries during salt stress (Henry *et al.*, 2015) and water deficit (Nuccio *et al.*, 2015). The reduction of transcript abundance of trehalose-6-phosphate phosphatase, the enzyme converting T6P to trehalose, observed in silks of plants subjected to a moderate water deficit (Oury *et al.*, 2016a) suggests an increased level of T6P in silks.

In ovaries, the main changes in carbon-related transcript amounts and enzyme activities occur only 5–8 d after silk emergence (e.g. Andersen *et al.*, 2002; Oury *et al.*, 2016a), i.e. when ovaries had already engaged in the abortion process for several days (Fig. 3). The same conclusion applies to changes in concentrations and amounts of sugars in ovaries. Hence, it has been proposed that these late changes in carbon

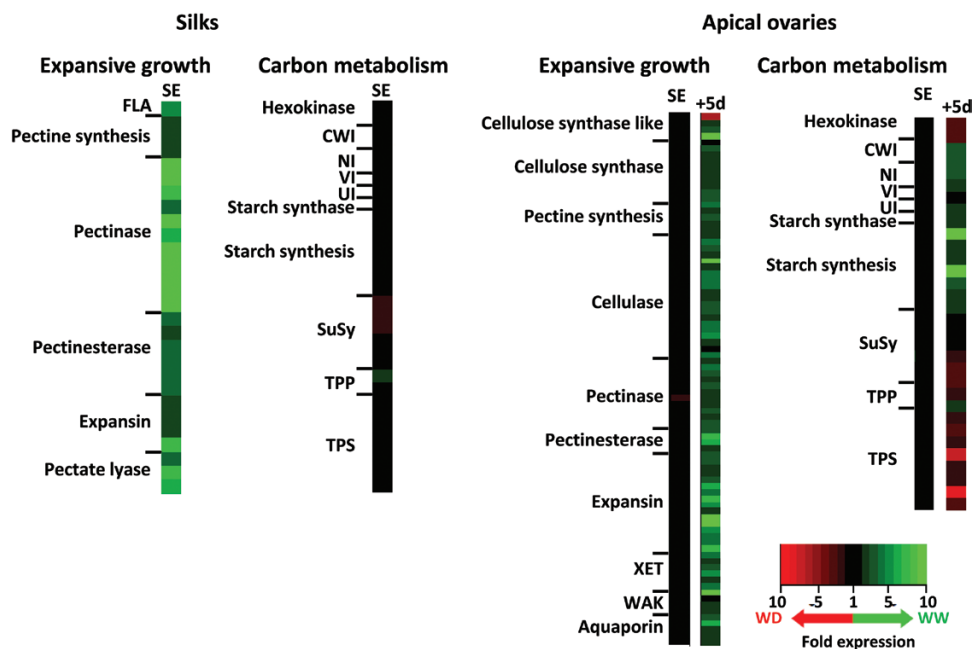


**Fig. 4.** The first molecular events associated with water deficit in reproductive organs occur in silks rather than in ovaries, and involve genes affecting expansive growth rather than sugar metabolism. SE, first silk emergence; +5d: 5 d later; WD, moderate water deficit at flowering; WW, well-watered plants. Colours represent the ratio of expression between WW and WD plants. Adapted from Oury *et al.*, 2016. Is change in ovary carbon status a cause or a consequence of maize ovary abortion in water deficit during flowering? *Plant Physiology* 171, 997–1008, ([www.plantphysiol.org](http://www.plantphysiol.org)), ‘Copyright American Society of Plant Biologists’.

metabolism of ovaries are a consequence rather than a cause of the beginning of ovary abortion (Oury *et al.*, 2016a). The absence of an appreciable effect of moderate water deficit on carbon status is consistent with studies indicating that moderate water deficits induce a carbon satiation because expansive growth of sink organs, including peach (*Prunus persica*) and tomato fruit, sunflower capitulum, and Arabidopsis expanding leaves, is more affected than photosynthesis (Hummel *et al.*, 2010; Dosio *et al.*, 2011; Muller *et al.*, 2011; Pantin *et al.*, 2013). Hence, plants subjected to moderate water deficit show ovary abortion that is probably not linked to carbon deprivation, in opposition to the later and intense water deficit imposed in the protocol of Boyle *et al.* (1991) and further studies of Boyer's group.

The above paragraphs suggest that two successive periods of sensitivity of reproductive organs coexist in maize. The first period is associated with developmental processes (arrest of silk growth and first fertilization), characterized by abortion located near the ear tip (Fig. 2A). The second period, linked to carbon deprivation, occurs after fertilization, is only observed under severe water deficit that drastically decreases photosynthesis, and results in a random distribution of abortion on the ear (Fig. 2B).

### Vegetative and reproductive structures share a partly common hydraulic control of expansive growth

The developmental controls presented above suggest a major role for expansive growth in grain abortion in maize, pea, and sunflower. In maize, the control of silk elongation might be key for grain abortion, consistent with the fact that the anthesis–silking interval is closely correlated with yield in water deficit, both phenotypically and genotypically (Bolaños and Edmeades, 1996; Ribaut *et al.*, 1997; Bruce *et al.*, 2002). In drought the anthesis–silking interval is linked to silk growth because the rates of both silk elongation and cell division are reduced by water deficit, resulting in a delayed silk emergence, whereas anthesis is essentially unaffected by water deficit (Fuad-Hassan *et al.*, 2008). Expansive growth, defined as an increase in organ volume via water entry into growing cells, depends on the interplay of cell wall extensibility and of gradients of water potential and hydraulic conductance on the water pathway from the xylem to cells (Lockhart, 1965). It is loosely coordinated with carbon accumulation, in particular via the contribution of sugars to osmotic adjustment (Hummel *et al.*, 2010). However, a limited contribution of carbon supply to expansive growth is usually observed under water deficit (Hummel *et al.*, 2010; Muller *et al.*, 2011; Tardieu *et al.*, 2011; Fatichi *et al.*, 2014).

Diel kinetics of silk elongation rate strongly suggest a hydraulic control for silk elongation (Turc *et al.*, 2016): (i) the half-time of change in silk elongation rate is about 30 min upon changes in soil water potential (Fig. 5B) or evaporative demand (Fig. 5A); (ii) maximum silk elongation rate is observed during the dark period when photosynthesis is arrested but plant water status is most

favourable because of a low evaporative demand (Fig. 5A); and (iii) silk elongation rate largely decreases with evaporative demand, even when ear and silk transpiration is impeded, so it is the whole-plant water status that affects silk growth (Turc *et al.*, 2016). These characteristics are similar to those in leaves, in which the half-times of changes in elongation rate are 20–30 min upon changes in soil water potential or evaporative demand, the elongation rate is maximum during nights, and the day-time elongation rate is closely related to evaporative demand (Caldeira *et al.*, 2014). Consistently, both leaves and silks are maternal tissues directly connected to the xylem (Heslop-Harrison *et al.*, 1984; Tao *et al.*, 2006), whereas the embryo is largely isolated hydraulically from maternal tissues (Felker and Shannon, 1980; Miller and Chourey, 1992). The genetic variability of the sensitivity of silk elongation rate to water deficit is related to that of leaves. It was estimated in eight maize inbred lines carrying quantitative trait locus alleles for contrasting sensitivity of leaf elongation rate to soil water potential (Fig. 5C). This has allowed identification of the soil water potential that stops elongation of both silks and leaves of each line (Fig. 5C). Strikingly, the values corresponding to silks were closely related to those in leaves in this set of lines (Fig. 5D), thereby suggesting that alleles affecting leaf elongation also affect silk elongation. Consistent with Westgate and Boyer (1985), silks were more sensitive than leaves because the regression line was above the 1:1 line meaning that, for a given maize line, silks stopped elongation at soil water potentials higher than those of leaves (Fig. 5D).

Taken together these elements suggest a commonality of mechanisms controlling the response of elongation in leaves and silks. This conclusion cannot be extended to the growth of the endosperm and of the embryo (which are weakly connected hydraulically to the stem) with a disruption of vascular elements in the ovary pedicel (Kiesselbach, 1949; Felker and Shannon, 1980; Miller and Chourey, 1992), resulting in lower symptoms of water deficit than in maternal tissues (Yu and Setter, 2003).

Recent studies propose that the diurnal time courses of leaf elongation rate closely follows that of xylem water potential over changes in evaporative demand (Caldeira *et al.*, 2014; Tardieu *et al.*, 2015). The response curve of leaf and silk elongation rates to soil water potential during the night can be interpreted as a response to xylem water potential because water potentials equilibrate in silks, leaves, in the xylem, and in the soil during the night, in the absence of transpiration. The model of Tardieu *et al.* (2015) uses this relationship to simulate the time course of leaf elongation rate during the day, in such a way that diurnal variations in elongation rate reflect those of xylem water potential following changes in evaporative demand and soil water potential. This conclusion can probably be extended to silks, which are also directly connected to the stem xylem. The similarity of time courses of silk and leaf elongation rates, but also the genetic correlation between them, leads us to propose that silk elongation rate also follows xylem water potential, in spite of the fact that these are two different

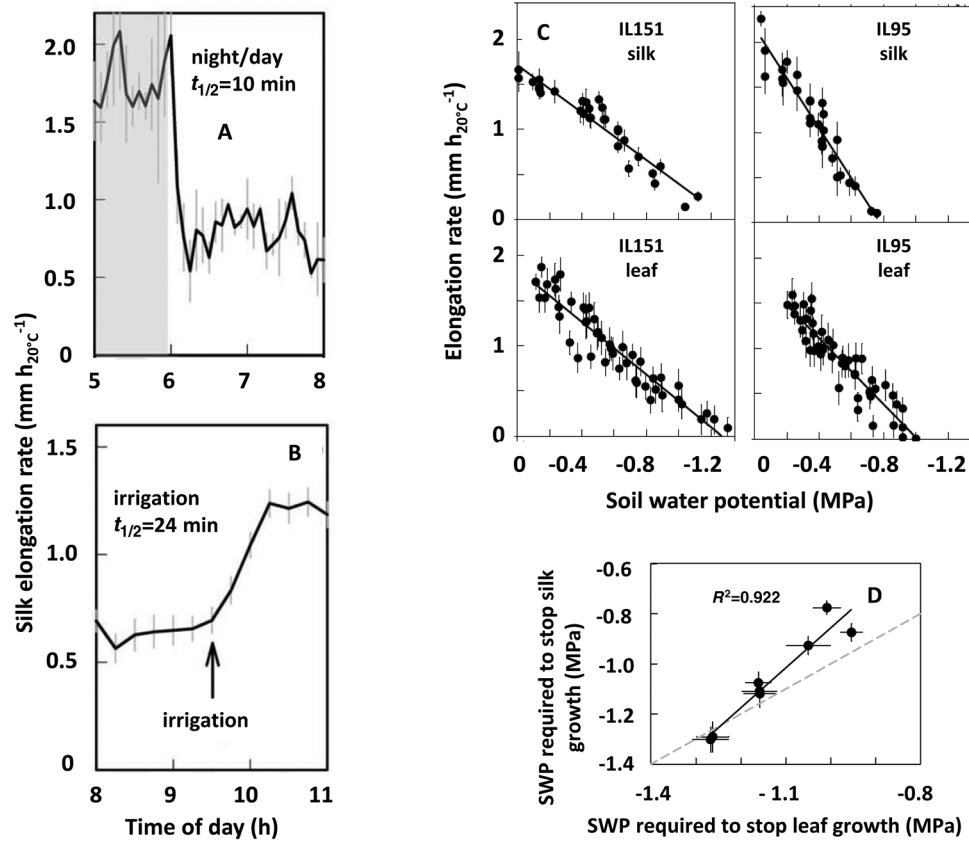


**Fig. 5.** Hydraulic control of expansive growth in maize silks and leaves. (A) Silk elongation rate is more rapid during nights than days, with a rapid transition ( $t_{1/2}$ , half-time). (B) Recovery of silk elongation rate is also rapid upon soil rehydration. (C) The relationship between elongation rate and soil water potential is linear in both leaves and silks in two maize lines introgressed with alleles conferring contrasting sensitivities. (D) Leaf and silk sensitivities are closely correlated in a panel of eight lines. They are estimated by the soil water potential (SWP) causing growth arrest (x-intercept of response curves in (C)). Adapted from Turc *et al.*, 2016. The growth of vegetative and reproductive structures (leaves and silks) respond similarly to hydraulic cues in maize. *New Phytologist* 212, 377–388. Courtesy of the New Phytologist Trust and John Wiley & Sons.

organs carried by plants at different phenological stages. The expansive growth of leaves and silks may therefore be governed by common alleles that control cell wall mechanical properties (Cosgrove, 2005) or the water entry into growing cells via changes in hydraulic conductance as modelled in Tardieu *et al.* (2015). Expansins may be involved in the common control, via their effect on cell wall properties (Zhang *et al.*, 2014). This is consistent with the fact that transcript amounts of genes involved in water movements (aquaporins) and in cell wall properties (expansins, xyloglucan endotransglycosylase) are more expressed in silks of well-watered than of droughted plants (Oury *et al.*, 2016a).

The link between the sensitivities of leaf elongation rate and silk elongation rate via hydraulic processes probably explains the common genetic control observed between leaf elongation and anthesis–silking interval (Welcker *et al.*, 2007). Anthesis–silking interval has long been considered as a trait associated with maintenance of maize yield in water deficit, so hydraulic processes may eventually have a role on grain abortion via silk elongation. This may explain the unexpected result that the sensitivity of grain number to water deficit in the field has a high genetic correlation with the sensitivity of leaf growth to water deficit in young plants assessed in a phenotyping platform (Chapuis *et al.*, 2012).

## Concluding remarks

Grain or ovary abortion is, from an evolutionary point of view, a feedback mechanism that allows plants to produce at least a few viable seeds, whereas there would be a risk that no seed is viable if all ovaries continued development after flowering time under unfavourable conditions. Plants carrying such alleles have therefore not been able to reproduce during very dry years. In agronomic conditions, a favourable effect of abortion on yield can be observed in extreme drought scenarios by ensuring adequate grain filling in spite of limited resources (Parent *et al.*, 2017). However, a maximum grain number, involving minimum abortion rate, is a favourable trait in most drought scenarios (Millet *et al.*, 2016; Parent *et al.*, 2017), so breeding for limited abortion under water deficit is needed.

In this context it would be tempting to consider that carbon availability to ovaries is the triggering mechanism causing abortion, whereas it is proposed here that developmental mechanisms ‘mimic’ an effect of carbon supply before any carbon starvation is sensed in reproductive organs. These mechanisms involve the effect of fertilized reproductive organs on the development of younger organs, the superposition of a gradient of ovary development with a ‘stop’ signal occurring on a given day, and, in maize, hydraulic processes that

affect silk elongation rate. However, carbon-starvation-based and water-fluxes-based abortion are not mutually exclusive, and probably correspond to different phenological stages in maize. Early developmental abortion is prominent when the water deficit is moderate during flowering time, as it is in more than 40% of drought scenarios in Europe (Harrison *et al.*, 2014). Carbon-starvation-based abortion occurs later, in particular when a severe water deficit at flowering time causes a drastic reduction in photosynthesis. This case is estimated as 18% of drought scenarios in Europe (Harrison *et al.*, 2014).

The results reviewed here have two major consequences for both modelling and breeding. First, the timing and preferential location of abortion can be accounted for by models of reproductive organogenesis, which simulate the distribution and hierarchy of organs at any time of the reproductive period (e.g. Ney and Turc, 1993; Moreau *et al.*, 2007; Chenu *et al.*, 2009). Coupled with rules of assimilate partitioning, these models allow one to account for spatial and temporal distribution of abortion in inflorescences (Mathieu *et al.*, 2009; Egli, 2010; Jullien *et al.*, 2011).

Second, alleles related to the maintenance of processes of tissue expansion in both vegetative and reproductive organs may have a direct effect on yield maintenance under drought. Genetic variability exists in maize for this maintenance. Phenotyping silk elongation rate is a difficult task at a throughput compatible with genetic analyses, i.e. hundreds of genotypes, but is feasible *in situ* via a combination of robot-assisted image analysis and machine learning (Bricchet *et al.*, 2017). The commonality of mechanisms controlling the responses of expansive growth to environmental constraints in both vegetative and reproductive structures, centred on hydraulic processes, has therefore potentially large consequences in breeding for plants adapted to changing environments, but also in understanding plant adaptive traits and in modelling plant–water interactions from the cell to the global scale. This is consistent with recent studies addressing the modelling and prediction of terrestrial carbon and water dynamics, which suggest revising the hierarchy of plant growth control in the vegetation models (Fatichi *et al.*, 2014) by giving a pivotal role to plant hydraulics (Fatichi *et al.*, 2015; Pappas *et al.*, 2016).

## Acknowledgements

This review is based on works supported by the European project FP7-244374 (DROPS) and the Agence Nationale de la Recherche project ANR-10-BTBR-01 (Amaizing), and is indebted to Vincent Oury and Yves Gibon for their fruitful collaboration during those projects.

## References

- Alkio M, Schubert A, Diepenbrock W, Grimm E. 2003. Effect of source-sink ratio on seed set and filling in sunflower (*Helianthus annuus* L.). *Plant, Cell & Environment* **26**, 1609–1619.
- Andersen MN, Asch F, Wu Y, Jensen CR, Naested H, Mogensen VO, Koch KE. 2002. Soluble invertase expression is an early target of drought stress during the critical, abortion-sensitive phase of young ovary development in maize. *Plant Physiology* **130**, 591–604.
- Barnabás B, Jäger K, Fehér A. 2008. The effect of drought and heat stress on reproductive processes in cereals. *Plant, Cell & Environment* **31**, 11–38.
- Bolaños J, Edmeades GO. 1996. The importance of the anthesis-silking interval in breeding for drought tolerance in tropical maize. *Field Crops Research* **48**, 65–80.
- Bonnett OT. 1940. Development of the staminate and pistillate inflorescence of sweet corn. *Journal of Agricultural Research* **60**, 25–37.
- Boyer JS, McLaughlin JE. 2007. Functional reversion to identify controlling genes in multigenic responses: analysis of floral abortion. *Journal of Experimental Botany* **58**, 267–277.
- Boyle MG, Boyer JS, Morgan PW. 1991. Stem infusion of liquid culture medium prevents reproductive failure of maize at low water potential. *Crop Science* **31**, 1246–1252.
- Bradford KJ. 1994. Water stress and the water relations of seed development: a critical review. *Crop Science* **34**, 1–11.
- Bricchet N, Fournier C, Turc O, Strauss O, Artzet S, Pradal C, Welcker C, Tardieu F, Cabrera-Bosquet L. 2017. A robot-assisted imaging pipeline for tracking the growths of maize ear and silks in a high-throughput phenotyping platform. *Plant Methods* **13**, 96.
- Bruce WB, Edmeades GO, Barker TC. 2002. Molecular and physiological approaches to maize improvement for drought tolerance. *Journal of Experimental Botany* **53**, 13–25.
- Bругière N, Jiao S, Hantke S, Zinselmeier C, Roessler JA, Niu X, Jones RJ, Habben JE. 2003. Cytokinin oxidase gene expression in maize is localized to the vasculature, and is induced by cytokinins, abscisic acid, and abiotic stress. *Plant Physiology* **132**, 1228–1240.
- Caldeira CF, Bosio M, Parent B, Jeanguenin L, Chaumont F, Tardieu F. 2014. A hydraulic model is compatible with rapid changes in leaf elongation under fluctuating evaporative demand and soil water status. *Plant Physiology* **164**, 1718–1730.
- Cárcova J, Otegui ME. 2001. Ear temperature and pollination timing effects on maize kernel set. *Crop Science* **41**, 1809–1815.
- Cawoy V, Lutts S, Ledent JF, Kinet JM. 2007. Resource availability regulates reproductive meristem activity, development of reproductive structures and seed set in buckwheat (*Fagopyrum esculentum*). *Physiologia Plantarum* **131**, 341–353.
- Chapuis R, Delluc C, Debeuf R, Tardieu F, Welcker C. 2012. Resilience to water deficit in a phenotyping platform and in the field: how related are they in maize? *European Journal of Agronomy* **42**, 59–67.
- Chazen O, Neumann PM. 1994. Hydraulic signals from the roots and rapid cell-wall hardening in growing maize (*Zea mays* L.) leaves are primary responses to polyethylene glycol-induced water deficits. *Plant Physiology* **104**, 1385–1392.
- Cheng CY, Lur HS. 1996. Ethylene may be involved in abortion of the maize caryopsis. *Physiologia Plantarum* **98**, 245–252.
- Chenu K, Chapman SC, Tardieu F, McLean G, Welcker C, Hammer GL. 2009. Simulating the yield impacts of organ-level quantitative trait loci associated with drought response in maize: a 'gene-to-phenotype' modeling approach. *Genetics* **183**, 1507–1523.
- Connor DJ, Sadras VO. 1992. Physiology of yield expression in sunflower. *Field Crops Research* **30**, 333–389.
- Cosgrove DJ. 2005. Growth of the plant cell wall. *Nature Reviews. Molecular Cell Biology* **6**, 850–861.
- Dosio GA, Tardieu F, Turc O. 2006. How does the meristem of sunflower capitulum cope with tissue expansion and floret initiation? A quantitative analysis. *New Phytologist* **170**, 711–722.
- Dosio GA, Tardieu F, Turc O. 2011. Floret initiation, tissue expansion and carbon availability at the meristem of the sunflower capitulum as affected by water or light deficits. *New Phytologist* **189**, 94–105.
- Egli DB. 2010. SOYPOD: a model of fruit set in soybean. *Agronomy Journal* **102**, 39–47.
- Egli DB, Bruening WP. 2006. Fruit development and reproductive survival in soybean: position and age effects. *Field Crops Research* **98**, 195–202.
- Fatichi S, Leuzinger S, Körner C. 2014. Moving beyond photosynthesis: from carbon source to sink-driven vegetation modeling. *New Phytologist* **201**, 1086–1095.
- Fatichi S, Pappas C, Ivanov VY. 2015. Modeling plant–water interactions: an ecohydrological overview from the cell to the global scale. *Wiley Interdisciplinary Reviews* **3**, 327–368.
- Felker FC, Shannon JC. 1980. Movement of C-labeled assimilates into kernels of *Zea mays* L: III. An anatomical examination and

- microautoradiographic study of assimilate transfer. *Plant Physiology* **65**, 864–870.
- Freier G, Vilella F, Hall AJ.** 1984. Within-ear pollination synchrony and kernel set in maize. *Maydica* **29**, 317–324.
- Fuad-Hassan A, Tardieu F, Turc O.** 2008. Drought-induced changes in anthesis-silking interval are related to silk expansion: a spatio-temporal growth analysis in maize plants subjected to soil water deficit. *Plant, Cell & Environment* **31**, 1349–1360.
- Griffiths CA, Paul MJ.** 2017. Targeting carbon for crop yield and drought resilience. *Journal of the Science of Food and Agriculture* **97**, 4663–4671.
- Guilioni L, Wery J, Lecoœur J.** 2003. High temperature and water deficit may reduce seed number in field pea purely by decreasing plant growth rate. *Functional Plant Biology* **30**, 1151–1164.
- Guilioni L, Wery J, Tardieu F.** 1997. Heat stress-induced abortion of buds and flowers in pea: is sensitivity linked to organ age or to relations between reproductive organs? *Annals of Botany* **80**, 159–168.
- Habben JE, Bao X, Bate NJ, et al.** 2014. Transgenic alteration of ethylene biosynthesis increases grain yield in maize under field drought-stress conditions. *Plant Biotechnology Journal* **12**, 685–693.
- Harrison MT, Tardieu F, Dong Z, Messina CD, Hammer GL.** 2014. Characterizing drought stress and trait influence on maize yield under current and future conditions. *Global Change Biology* **20**, 867–878.
- Hedhly A, Hormaza JI, Herrero M.** 2009. Global warming and sexual plant reproduction. *Trends in Plant Science* **14**, 30–36.
- Hedley CL, Ambrose MJ.** 1980. An analysis of seed development in *Pisum sativum* L. *Annals of Botany* **46**, 89–105.
- Henry C, Bledsoe SW, Griffiths CA, Kollman A, Paul MJ, Sakr S, Lagrimini LM.** 2015. Differential role for trehalose metabolism in salt-stressed maize. *Plant Physiology* **169**, 1072–1089.
- Hummel I, Pantin F, Sulpice R, et al.** 2010. Arabidopsis plants acclimate to water deficit at low cost through changes of carbon usage: an integrated perspective using growth, metabolite, enzyme, and gene expression analysis. *Plant Physiology* **154**, 357–372.
- Jullien A, Mathieu A, Allirand JM, Pinet A, de Reffye P, Cournède PH, Ney B.** 2011. Characterization of the interactions between architecture and source-sink relationships in winter oilseed rape (*Brassica napus*) using the GreenLab model. *Annals of Botany* **107**, 765–779.
- Kakumanu A, Ambavaram MM, Klumas C, Krishnan A, Batlang U, Myers E, Grene R, Pereira A.** 2012. Effects of drought on gene expression in maize reproductive and leaf meristem tissue revealed by RNA-Seq. *Plant Physiology* **160**, 846–867.
- Kapu NU, Cosgrove DJ.** 2010. Changes in growth and cell wall extensibility of maize silks following pollination. *Journal of Experimental Botany* **61**, 4097–4107.
- Kelly MO, Davies PJ.** 1988. Photoperiodic and genetic control of carbon partitioning in peas and its relationship to apical senescence. *Plant Physiology* **86**, 978–982.
- Kiesselbach TA.** 1949. The structure and reproduction of corn. Lincoln, NE, USA: University of Nebraska.
- Kohorn BD, Kobayashi M, Johansen S, Riese J, Huang LF, Koch K, Fu S, Dotson A, Byers N.** 2006. An Arabidopsis cell wall-associated kinase required for invertase activity and cell growth. *The Plant Journal* **46**, 307–316.
- Liu YH, Offler CE, Ruan YL.** 2013. Regulation of fruit and seed response to heat and drought by sugars as nutrients and signals. *Frontiers in Plant Science* **4**, 282.
- Lockhart JA.** 1965. An analysis of irreversible plant cell elongation. *Journal of Theoretical Biology* **8**, 264–275.
- Lunn JE, Feil R, Hendriks JH, Gibon Y, Morcuende R, Osuna D, Scheible WR, Carillo P, Hajirezaei MR, Stitt M.** 2006. Sugar-induced increases in trehalose 6-phosphate are correlated with redox activation of ADP-glucose pyrophosphorylase and higher rates of starch synthesis in *Arabidopsis thaliana*. *The Biochemical Journal* **397**, 139–148.
- Heslop-Harrison Y, Reger BJ, Heslop-Harrison J.** 1984. The pollen-stigma interaction in the grasses. 5. Tissue organization and cytochemistry of the stigma ('silk') of *Zea mays* L. *Acta Botanica Neerlandica* **33**, 81–99.
- Mäkelä P, McLaughlin JE, Boyer JS.** 2005. Imaging and quantifying carbohydrate transport to the developing ovaries of maize. *Annals of Botany* **96**, 939–949.
- Mathieu A, Cournède PH, Letort V, Barthélémy D, de Reffye P.** 2009. A dynamic model of plant growth with interactions between development and functional mechanisms to study plant structural plasticity related to trophic competition. *Annals of Botany* **103**, 1173–1186.
- McLaughlin JE, Boyer JS.** 2004. Sugar-responsive gene expression, invertase activity, and senescence in aborting maize ovaries at low water potentials. *Annals of Botany* **94**, 675–689.
- Miller EC.** 1919. Development of the pistillate spikelet and fertilization in *Zea mays* L. *Journal of Agricultural Research* **18**, 881–916.
- Miller ME, Chourey PS.** 1992. The maize invertase-deficient miniature-1 seed mutation is associated with aberrant pedicel and endosperm development. *The Plant Cell* **4**, 297–305.
- Millet EJ, Welcker C, Kruijer W, et al.** 2016. Genome-wide analysis of yield in Europe: allelic effects vary with drought and heat scenarios. *Plant Physiology* **172**, 749–764.
- Moreau D, Salon C, Munier-Jolain N.** 2007. A model-based framework for the phenotypic characterization of the flowering of *Medicago truncatula*. *Plant, Cell & Environment* **30**, 213–224.
- Morris DA, Arthur ED.** 1984. Invertase activity in sinks undergoing cell expansion. *Plant Growth Regulation* **2**, 327–337.
- Muller B, Pantin F, Génard M, Turc O, Freixes S, Piques M, Gibon Y.** 2011. Water deficits uncouple growth from photosynthesis, increase C content, and modify the relationships between C and growth in sink organs. *Journal of Experimental Botany* **62**, 1715–1729.
- Ney B, Duthion C, Fontaine E.** 1993. Timing of reproductive abortions in relation to cell division, water content, and growth of pea seeds. *Crop Science* **33**, 267–270.
- Ney B, Duthion C, Turc O.** 1994. Phenological response of pea to water-stress during reproductive development. *Crop Science* **34**, 141–146.
- Ney B, Turc O.** 1993. Heat-unit-based description of the reproductive development of pea. *Crop Science* **33**, 510–514.
- Nuccio ML, Wu J, Mowers R, et al.** 2015. Expression of trehalose-6-phosphate phosphatase in maize ears improves yield in well-watered and drought conditions. *Nature Biotechnology* **33**, 862–869.
- Oury V, Caldeira CF, Prodhomme D, Pichon JP, Gibon Y, Tardieu F, Turc O.** 2016a. Is change in ovary carbon status a cause or a consequence of maize ovary abortion in water deficit during flowering? *Plant Physiology* **171**, 997–1008.
- Oury V, Tardieu F, Turc O.** 2016b. Ovary apical abortion under water deficit is caused by changes in sequential development of ovaries and in silk growth rate in maize. *Plant Physiology* **171**, 986–996.
- Palmer JH, Steer BT.** 1985. The generative area as the site of floret initiation in the sunflower capitulum and its integration to predict floret number. *Field Crops Research* **11**, 1–12.
- Pantin F, Fanciullino AL, Massonnet C, Dauzat M, Simonneau T, Muller B.** 2013. Buffering growth variations against water deficits through timely carbon usage. *Frontiers in Plant Science* **4**, 483.
- Pappas C, Fatichi S, Burlando P.** 2016. Modeling terrestrial carbon and water dynamics across climatic gradients: does plant trait diversity matter? *New Phytologist* **209**, 137–151.
- Parent B, Bonneau J, Maphosa L, Kovalchuk A, Langridge P, Fleury D.** 2017. Quantifying wheat sensitivities to environmental constraints to dissect genotype × environment interactions in the field. *Plant Physiology* **174**, 1669–1682.
- Patrick JW, Stoddard FL.** 2010. Physiology of flowering and grain filling in faba bean. *Field Crops Research* **115**, 234–242.
- Ribaut JM, Jiang C, Gonzalez-de-Leon D, Edmeades GO, Hoisington DA.** 1997. Identification of quantitative trait loci under drought conditions in tropical maize. 2. Yield components and marker-assisted selection strategies. *Theoretical and Applied Genetics* **94**, 887–896.
- Rocha OJ, Stephenson AG.** 1991. Order of fertilization within the ovary of *Phaseolus coccineus* L. *Sexual Plant Reproduction* **4**, 126–131.
- Roche R, Jeuffroy M-H, Ney B.** 1998. A model to simulate the final number of reproductive nodes in pea (*Pisum sativum* L.). *Annals of Botany* **81**, 545–555.
- Ross-Ibarra J, Morrell PL, Gaut BS.** 2007. Plant domestication, a unique opportunity to identify the genetic basis of adaptation. *Proceedings of the National Academy of Sciences, USA* **104**, 8641–8648.

- Ruan YL, Jin Y, Yang YJ, Li GJ, Boyer JS.** 2010. Sugar input, metabolism, and signaling mediated by invertase: roles in development, yield potential, and response to drought and heat. *Molecular Plant* **3**, 942–955.
- Setter TL, Parra R.** 2010. Relationship of carbohydrate and abscisic acid levels to kernel set in maize under postpollination water deficit. *Crop Science* **50**, 980–988.
- Setter TL, Yan J, Warburton M, Ribaut JM, Xu Y, Sawkins M, Buckler ES, Zhang Z, Gore MA.** 2011. Genetic association mapping identifies single nucleotide polymorphisms in genes that affect abscisic acid levels in maize floral tissues during drought. *Journal of Experimental Botany* **62**, 701–716.
- Sinsawat V, Steer BT.** 1993. Growth of florets of sunflower (*Helianthus annuus* L.) in relation to their position in the capitulum, shading and nitrogen supply. *Field Crops Research* **34**, 83–100.
- Smeeckens S.** 2015. From leaf to kernel: trehalose-6-phosphate signaling moves carbon in the field. *Plant Physiology* **169**, 912–913.
- Sotelo-Silveira M, Marsch-Martínez N, de Folter S.** 2014. Unraveling the signal scenario of fruit set. *Planta* **239**, 1147–1158.
- Stephenson AG.** 1981. Flower and fruit abortion: proximate causes and ultimate functions. *Annual Review of Ecology and Systematics* **12**, 253–279.
- Sturm A, Tang GQ.** 1999. The sucrose-cleaving enzymes of plants are crucial for development, growth and carbon partitioning. *Trends in Plant Science* **4**, 401–407.
- Susko DJ.** 2006. Effect of ovule position on patterns of seed maturation and abortion in *Robinia pseudoacacia* (Fabaceae). *Canadian Journal of Botany—Revue Canadienne De Botanique* **84**, 1259–1265.
- Tang GQ, Lüscher M, Sturm A.** 1999. Antisense repression of vacuolar and cell wall invertase in transgenic carrot alters early plant development and sucrose partitioning. *The Plant Cell* **11**, 177–189.
- Tao TY, Ouellet T, Dadej K, Miller SS, Johnson DA, Singh J.** 2006. Characterization of a novel glycine-rich protein from the cell wall of maize silk tissues. *Plant Cell Reports* **25**, 848–858.
- Tardieu F, Granier C, Muller B.** 2011. Water deficit and growth. Co-ordinating processes without an orchestrator? *Current Opinion in Plant Biology* **14**, 283–289.
- Tardieu F, Simonneau T, Parent B.** 2015. Modelling the coordination of the controls of stomatal aperture, transpiration, leaf growth, and abscisic acid: update and extension of the Tardieu-Davies model. *Journal of Experimental Botany* **66**, 2227–2237.
- Thakur P, Kumar S, Malik JA, Berger JD, Nayyar H.** 2010. Cold stress effects on reproductive development in grain crops: an overview. *Environmental and Experimental Botany* **67**, 429–443.
- Turc O, Bouteillé M, Fuad-Hassan A, Welcker C, Tardieu F.** 2016. The growth of vegetative and reproductive structures (leaves and silks) respond similarly to hydraulic cues in maize. *New Phytologist* **212**, 377–388.
- Vincent D, Lapierre C, Pollet B, Cornic G, Negroni L, Zivy M.** 2005. Water deficits affect caffeate *O*-methyltransferase, lignification, and related enzymes in maize leaves. A proteomic investigation. *Plant Physiology* **137**, 949–960.
- Wang L, Li XR, Lian H, Ni DA, He YK, Chen XY, Ruan YL.** 2010. Evidence that high activity of vacuolar invertase is required for cotton fiber and Arabidopsis root elongation through osmotic dependent and independent pathways, respectively. *Plant Physiology* **154**, 744–756.
- Wang Z, Mambelli S, Setter TL.** 2002. Abscisic acid catabolism in maize kernels in response to water deficit at early endosperm development. *Annals of Botany* **90**, 623–630.
- Weatherwax P.** 1916. Morphology of the flowers of *Zea mays*. *Bulletin of the Torrey Botanical Club* **43**, 127–144.
- Welcker C, Boussuge B, Bencivenni C, Ribaut JM, Tardieu F.** 2007. Are source and sink strengths genetically linked in maize plants subjected to water deficit? A QTL study of the responses of leaf growth and of anthesis-silking interval to water deficit. *Journal of Experimental Botany* **58**, 339–349.
- Westgate ME, Boyer JS.** 1985. Osmotic adjustment and the inhibition of leaf, root, stem and silk growth at low water potentials in maize. *Planta* **164**, 540–549.
- Westgate ME, Grant DL.** 1989. Water deficits and reproduction in maize: response of the reproductive tissue to water deficits at anthesis and mid-grain fill. *Plant Physiology* **91**, 862–867.
- Yadav UP, Ivakov A, Feil R, et al.** 2014. The sucrose-trehalose 6-phosphate (Tre6P) nexus: specificity and mechanisms of sucrose signalling by Tre6P. *Journal of Experimental Botany* **65**, 1051–1068.
- Yu LX, Setter TL.** 2003. Comparative transcriptional profiling of placenta and endosperm in developing maize kernels in response to water deficit. *Plant Physiology* **131**, 568–582.
- Zhang W, Yan H, Chen W, Liu J, Jiang C, Jiang H, Zhu S, Cheng B.** 2014. Genome-wide identification and characterization of maize expansin genes expressed in endosperm. *Molecular Genetics and Genomics* **289**, 1061–1074.
- Zhu J, Alvarez S, Marsh EL, et al.** 2007. Cell wall proteome in the maize primary root elongation zone. II. Region-specific changes in water soluble and lightly ionically bound proteins under water deficit. *Plant Physiology* **145**, 1533–1548.
- Zinselmeier C, Jeong BR, Boyer JS.** 1999. Starch and the control of kernel number in maize at low water potentials. *Plant Physiology* **121**, 25–36.
- Zinselmeier C, Lauer MJ, Boyer JS.** 1995a. Reversing drought-induced losses in grain-yield: sucrose maintains embryo growth in maize. *Crop Science* **35**, 1390–1400.
- Zinselmeier C, Westgate ME, Schussler JR, Jones RJ.** 1995b. Low water potential disrupts carbohydrate metabolism in maize (*Zea mays* L.) ovaries. *Plant Physiology* **107**, 385–391.

# The growth of vegetative and reproductive structures (leaves and silks) respond similarly to hydraulic cues in maize

Olivier Turc, Marie Bouteillé, Avan Fuad-Hassan, Claude Welcker and François Tardieu

UMR LEPSE, INRA, Montpellier SupAgro, 34000 Montpellier, France

Author for correspondence:

Olivier Turc

Tel: +33 499 612 633

Email: [olivier.turc@supagro.inra.fr](mailto:olivier.turc@supagro.inra.fr)

Received: 19 January 2016

Accepted: 6 May 2016

*New Phytologist* (2016) **212**: 377–388

doi: 10.1111/nph.14053

**Key words:** evaporative demand, hydraulics, leaf growth, silk growth, tissue expansive growth, water deficit, *Zea mays* (maize).

## Summary

- The elongation of styles and stigma (silks) of maize (*Zea mays*) flowers is rapid ( $1\text{--}3\text{ mm h}^{-1}$ ), occurs over a short period and plays a pivotal role in reproductive success in adverse environments.

- Silk elongation rate was measured using displacement transducers in 350 plants of eight genotypes during eight experiments with varying evaporative demand and soil water status.

- Measured time courses revealed that silk elongation rate closely followed changes in soil water status and evaporative demand, with day–night alternations similar to those in leaves. Day–night alternations were steeper with high than with low plant transpiration rate, manipulated via evaporative demand or by covering part of the leaf area. Half times of changes in silk elongation rate upon changes in evaporative demand or soil water status were 10–30 min, similar to those in leaves. The sensitivity of silk elongation rate to xylem water potential was genetically linked to that of leaf elongation rate. Lines greatly differed for these sensitivities.

- These results are consistent with a common hydraulic control of expansive growth in vegetative and reproductive structures upon changes in environmental conditions via a close connection with the xylem water potential. They have important implications for breeding, modelling and phenotyping.

## Introduction

Processes governing tissue expansion are the first to be impacted when plants face soil water depletion (Boyer, 1970; Muller *et al.*, 2011). Expansive growth, defined as an increase in organ volume via water entry into growing cells, depends on the interplay of the effects of cell wall extensibility of growing cells and of gradients of water potential and hydraulic conductance from the xylem to cells (Lockhart, 1965). It is loosely coordinated with carbon accumulation, which may have limited direct effects on expansive growth under water deficit (Muller *et al.*, 2011; Tardieu *et al.*, 2011; Fatichi *et al.*, 2014). We have recently proposed that the response of leaf growth rate to water deficit and evaporative demand is essentially controlled by hydraulic mechanisms (Tardieu *et al.*, 2014), with (1) half times shorter than 30 min for changes in leaf elongation rate following changes in soil water potential or evaporative demand (Caldeira *et al.*, 2014) or the inhibition of Plasma membrane Intrinsic Proteins (PIP) aquaporins (Ehlert *et al.*, 2009), (2) a central role of plant hydraulic conductance in an aquaporin and abscisic acid (ABA)-dependent manner (Ehlert *et al.*, 2009; Parent *et al.*, 2009), even in continuous light in which oscillations of leaf elongation rate are synchronous with those of plant hydraulic conductance and of aquaporin PIP transcripts (Caldeira *et al.*, 2014), (3) a close correspondence between the time courses of xylem water potential and leaf elongation rate upon changes in evaporative demand,

soil water status or circadian oscillations (Tardieu *et al.*, 2015), (4) a largely common genetic control of the responses of leaf elongation rate to water deficit and evaporative demand (Welcker *et al.*, 2011).

The styles and stigma of female maize (*Zea mays*) flowers, usually designated ‘silks’, must rapidly elongate at flowering time to emerge from bracts (or husks) and collect pollen originating from the apical male inflorescences (or tassels) (Weatherwax, 1916; Kiesselbach, 1949). They show mono-dimensional development that has similarities with that of the leaves of monocotyledons, although there are also marked differences (Fuad-Hassan *et al.*, 2008): (1) cell division and tissue expansion occur uniformly all along the silk at the beginning of silk development (versus growth and division occurring in the basal region of monocot leaves; Tardieu *et al.*, 2000); (2) then, cell division progressively ceases from tip to base, while elongation remains spatially uniform until silk tips emerge from the bracts; (3) after silk emergence, elongation is restricted to the basal region enclosed in bracts while it stops in emerged apical silk tissues, probably as a result of direct evaporative demand. The rates of tissue elongation and cell division are both reduced by water deficit, resulting in delayed silk emergence. The date of silk emergence plays a pivotal role in the control of reproductive success in adverse environments (Lemcoff & Loomis, 1994; Edmeades *et al.*, 2000; Bruce *et al.*, 2002). We have recently shown a causal link between silk growth and floret abortion (Oury *et al.*, 2016b), an original example of coupling

between expansive growth and developmental processes. Silk elongation stops 2–3 d after the first silk emergence in plants subjected to water deficit, synchronously for all silks, although florets are initiated sequentially on the ear with a base–apex gradient. Growth arrest occurs in well-watered plants after 7–8 d. Abortion occurs in the youngest ovaries whose silks do not emerge at least 2 d before silk growth arrest, irrespective of plant water status, ovary volume, growth rate or sugar status (Oury *et al.*, 2016a,b). This developmental mechanism linked to silk growth accounted for 90% of drought-related abortion in a series of experiments with contrasting water deficits and genotypes (Oury *et al.*, 2016a, b). It resembles the control in other species in which abortion follows the reciprocal of the pollination/fertilization gradient for ovaries within a fruit (Rocha & Stephenson, 1991; Susko, 2006), for fruits within an inflorescence (Cawoy *et al.*, 2007) or for inflorescences within a plant (Ney *et al.*, 1994; Egli & Bruening, 2006).

The objective of the present study was to take advantage of recent advances in our understanding of the mechanisms controlling growth in vegetative organs to investigate the control of growth in reproductive tissues. Silk elongation is particularly sensitive to water deficit compared with roots, stems and leaves (Westgate & Boyer, 1985). Silks are part of the maternal tissues. They have direct connections with the stem xylem (Kiesselbach, 1949; Heslop-Harrison *et al.*, 1984; Tao *et al.*, 2006), whereas inner ovary tissues, such as nucellus, endosperm and embryo, are not directly connected to the xylem because of a disruption of vascular elements in the ovary pedicel (Kiesselbach, 1949; Felker & Shannon, 1980; Miller & Chourey, 1992). The direct connection of silks with the plant xylem suggests that the control of silk elongation in conditions of water deficit might have common features with that of leaf elongation, in particular with high sensitivity to evaporative demand even in the absence of soil water deficit, and with a short time constant of silk elongation rate upon changes in evaporative demand. Hence, we aimed to test the hypothesis that silks and leaves share part of their environmental and genetic controls, by comparing the time courses of their responses to soil water deficit and evaporative demand, in particular half times of response, and by examining genetic correlations between the sensitivities of silk and leaf growth to evaporative demand. An original automated method was designed for measuring silk growth with a temporal definition of minutes.

## Materials and Methods

### Plants and growing conditions

Experiments were carried out in the glasshouse and in the growth chamber in the phenotyping platform Phenodyn (<http://bioweb.supagro.inra.fr/phenodyn/>; Sadok *et al.*, 2007). The experimental set-up consists of scales that continuously measure changes in soil water status, displacement transducers that measure organ elongation and a set of environmental sensors.

Experiments are summarized in Supporting Information Table S1. Expt 1 aimed to test the method for measuring silk

elongation rate in the glasshouse, over a series of successive growing periods, in the maize (*Zea mays* L.) inbred line F252, an early dent line. Expts 2–7 were designed to quantify the effect of temperature and evaporative demand on silk elongation rate under stable environmental conditions in a growth chamber. Expt 8 was performed in the glasshouse to compare eight maize lines in terms of their responses of silk elongation rate to soil water deficit: F252, CML444, a tropical drought-tolerant line developed at the International Maize and Wheat Improvement Center (CIMMYT), the tropical lines P1 and P2 belonging to the Tuxpeño germplasm and contrasting in anthesis–silking interval (Ribaut *et al.*, 1996, 1997), and four inbred lines from a P1 × P2 cross (IL86, IL95, IL129 and IL151) with contrasted responses of leaf growth and anthesis–silking interval to soil water deficit (Welcker *et al.*, 2007).

Three seeds were sown in 12-l polyvinyl chloride (PVC) pots containing a mixture of loamy soil (aggregate diameter ranging from 0.1 to 4.0 mm) and organic compost in volumes of 0.4:0.6. Two plants per pot were kept after thinning when plants had four visible leaves. Pots were watered daily with a modified tenth-strength Hoagland solution supplemented with minor nutrients.

Air temperature and relative humidity were measured every 1 min at plant level (HMP35A; Vaisala Oy, Helsinki, Finland). The temperature of the growing ear of 12 plants per experiment was measured with a fine copper-constantan thermocouple (0.2 mm diameter) located inside the ear-leaf sheath or inside the husks when they became visible. Light was measured every 1 min using two photosynthetic photon flux density (PPFD) sensors (LI-190SB; Li-Cor Inc., Lincoln, NE, USA). All data for temperature, PPFD and relative humidity were averaged and stored every 15 min in a data logger (LTD-CR10X wiring panel; Campbell Scientific, Shepshed, UK). Ear temperature in each experimental treatment was used to express time in equivalent hours or days at 20°C (Parent *et al.*, 2010).

Day temperature ranged from 20 to 25°C and night temperature from 16 to 20°C in the glasshouse (Expts 1 and 8). Vapour pressure deficit (VPD) never exceeded 1.5 kPa during plant growth. Additional light was provided by a bank of sodium lamps that maintained PPFD above 200  $\mu\text{mol m}^{-2} \text{s}^{-1}$  for 12 h d<sup>-1</sup>. In Expts 2–7, plants were transferred just before silk emergence to a growth chamber where stable environmental conditions were maintained until completion of silk growth with a photoperiod of 12 h, a PPFD of 500  $\mu\text{mol m}^{-2} \text{s}^{-1}$  at ear level and, depending on treatment, day/night temperatures of 22:20°C or 28:25°C, and day:night VPD of 0.8:0.6 kPa or 2.4:2.0 kPa (Table S1). A photoperiod of 12 h was chosen because it is appropriate for tropical lines which show very late flowering times in the photoperiods of 14–16 h to which temperate lines are typically adapted. Evaporative demands experienced by silks or whole plants were distinguished in Expt 6 by wrapping either both ears and silks (direct effect of VPD on silks) or 30% of the leaf area (whole plant effect) in aluminium foil during the period of silk growth (Table S1). Soil water content was measured by weighing columns every 15 min. It was first measured directly in three soil samples before sowing in order to estimate the amounts of dry

soil and water in each pot. Subsequent changes in pot weight were attributed to changes in soil water status, after correction for plant weight (root + shoot fresh weight) measured on frequently harvested plants for each genotype. A water-release curve for the soil (Fig. S1) was obtained by measuring the soil water potential of soil samples with different water contents, in the range 0.45–0.13 g g<sup>-1</sup> (WP4-T Dewpoint Meters; Decagon Devices, Pullman, WA, USA). This allowed calculation and adjustment of soil water content to target values corresponding to the desired soil water potential. In well-watered (WW) treatments (Table S1) all pots were maintained at a soil water potential of  $-0.07 \pm 0.02$  MPa throughout the experiment. This soil water potential was also maintained in other treatments until the initiation of the first silks on the developing florets. Pots were then distributed in groups with four levels of soil water potential, namely  $-0.07 \pm 0.02$  MPa (WW),  $-0.4 \pm 0.1$  MPa (WD1, mild deficit),  $-0.7 \pm 0.1$  MPa (WD2, medium deficit) and  $-0.9 \pm 0.1$  MPa (WD3, severe deficit). In the three water deficit treatments, irrigation was withheld until the soil water content reached the target value, which was then maintained by controlling the pot weight daily before and after irrigation (Fig. S2). Two irrigations per day were often necessary during the period of silk growth to maintain soil water potential in the desired range over the day. Expts 1, 3–5 and 7 included WW, WD1 and WD2 treatments; Expt 8 included the four treatments. Because the aim of Expt 7 was to establish the relationships between soil water potential and silk elongation rate during both day and night, WD1 plants were watered at the end of the day (18:00 h) while WD2 plants were watered at dawn (06:00 h), so the soil water content differed between treatments during the night but not at the beginning of the day.

### Observations and manual measurements

The dates of the reproductive stages (tassel emergence, anthesis and silk emergence) were recorded through daily observations of individual plants. Male inflorescences (tassels) were excised just before pollen shedding to avoid an early arrest of silk growth as a result of ovule fertilization (Kiesselbach, 1949). Ear development was monitored on plants that were sampled twice a week from the appearance of the 6th leaf to silk initiation, by dissecting the developing ears of two plants per genotype under a binocular microscope (Leica MZ75; Leica Microsystems GmbH, Wetzlar, Germany) in Expts 1 and 8. Husks were gently removed with a fine scalpel blade to allow a clear view of successive flowers along the ear. A silk was considered as initiated when it reached 0.1 mm long.

In Expt 1, two plants per treatment were sampled daily from silk initiation to silk emergence, and every second day thereafter. The lengths of four to six silks per ovary cohort and the distance from ear axis base to silk insertion point were measured in cohorts located at the 1<sup>st</sup>, 5<sup>th</sup>, 10<sup>th</sup>, 15<sup>th</sup>, 20<sup>th</sup>, 25<sup>th</sup> and 30<sup>th</sup> positions counted from the ear base, using an interactive image analysis system (OPTIMAS 6.5; Media Cybernetics Inc., Bethesda, MD, USA) coupled to the binocular microscope. At latest stages, when silk length exceeded the field of the microscope (25 mm),

silks were carefully excised, and lengths and distances were measured with a ruler.

Predawn leaf water potential was measured in the ear leaf  $\pm 2$  positions on the stem with a pressure chamber (3000 Plant Water Status Console; Soil Moisture Equipment Corp., Goleta, CA, USA) at the end of the dark period in plants of the eight inbred lines in Expt 8. Plants were placed for 16 h in a dark growth chamber with water-saturated air to prevent any transpiration. In the absence of transpiration, leaf water potential, xylem water potential and soil water potential equilibrate so leaf water potential can be considered a proxy of xylem water potential. Predawn leaf water potential was closely related to soil water content via a water release curve (Fig. S1). As observed in previous studies (Reymond *et al.*, 2003, 2004) this curve did not differ between lines and matched the water-release curve obtained with direct measurements on soil samples (Fig. S1).

### Automated measurement of silk and leaf elongation rates

Silk elongation rate was measured on six to 12 plants per treatment with rotational displacement transducers (RDTs; 601-1045 Full 360° Smart Position Sensor; Spectrol Electronics Ltd, Swindon, UK). The sensor was attached to a pulley which carried a linen thread fixed to silk tips and to a 20-g counterweight. Five to 20 silks that emerged on the same day were fixed with a medical silicone adhesive (Telesis 5; Premiere Products Inc., Pacoima, CA, USA) to the linen thread. The transducers were fixed to a metal frame placed above the plants, and were connected to a data logger (LTD-CR10X wiring panel; Campbell Scientific) that recorded the transducer signal every 15 min (Fig. 1a). Leaf elongation rates of the same eight genotypes in response to soil water deficit were measured with the same equipment in separate experiments presented elsewhere (Sadok *et al.*, 2007; Welcker *et al.*, 2007, 2011). Briefly, plants at the 6th leaf stage were subjected to contrasting soil water potentials from 0 to  $-1.3$  MPa and then re-watered for a second drying cycle. Measurements began when the tip of the 6th leaf appeared above the whorl and lasted until the appearance of leaf 8. This period corresponds to a plateau during which the leaf elongation rate is stable (Sadok *et al.*, 2007). In this case, the linen thread was clipped to the tip of the 6th leaf.

## Results

### A reliable method for *in situ* measurement of silk elongation rate

Transducers attached to silks (Fig. 1a) measured the displacement of silk tips, with large day–night oscillations and a maximum displacement rate of 3 mm h<sup>-1</sup> (Fig. 1d). In addition to silk elongation rate, this displacement included the elongations of all tissues supporting silks, namely stem, ear shank and the ear portion supporting silks. Because the growth of the leaf carrying the ear was already completed at silk emergence, attaching the sheath of this leaf to the transducer (Fig. 1c) allowed measurement of the cumulated elongation of the stem from its base to the ear

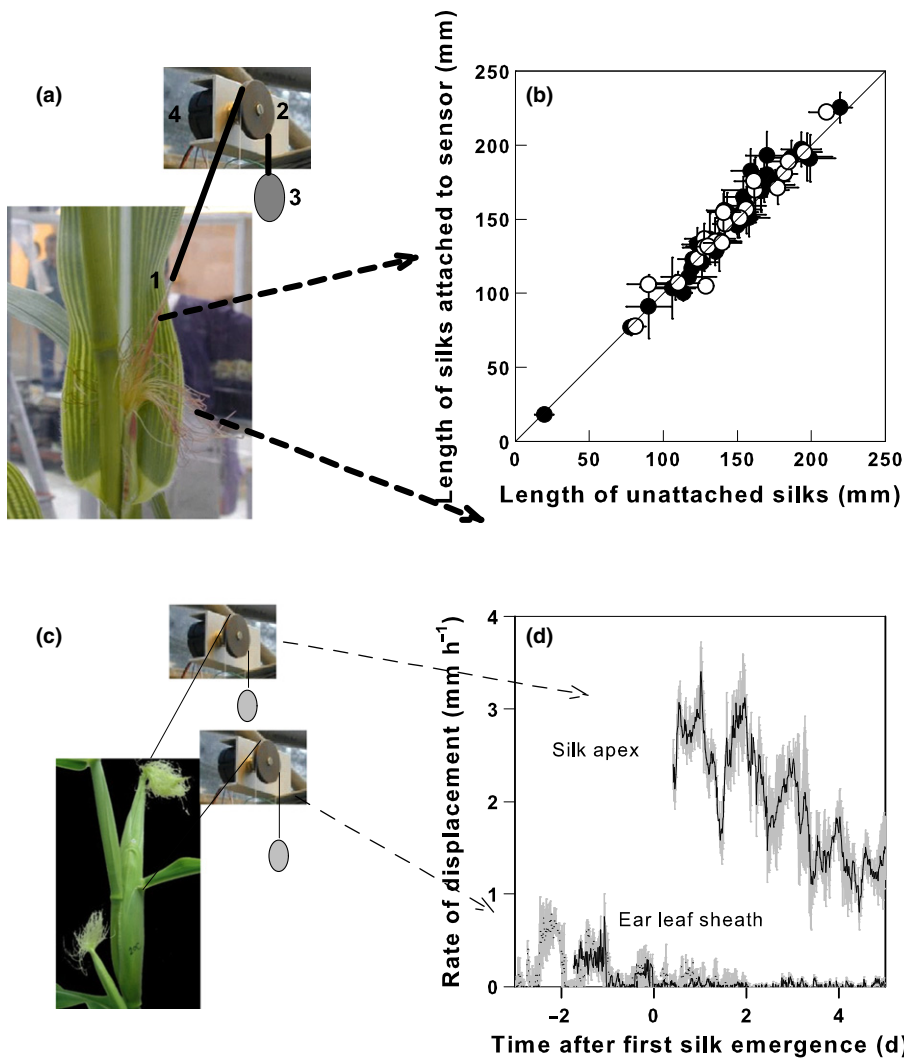


**Fig. 1** Method of continuous measurement of silk elongation rate in maize (*Zea mays*). (a) Five to 20 silks were fixed together with a medical silicone adhesive to a linen thread (1) connected to a pulley (2) with a counterweight (3). Silk elongation was transmitted to a rotating displacement transducer (4) whose signal was recorded every 15 min by a data logger. (b) Final length of attached silks plotted against that of unattached silks inserted at the same position on the ear. Attached and unattached silks originated either from the same ear (closed circles) or from different plants in the same treatment (open circles). (d) Contribution of stem elongation rate, measured via the displacement of the leaf sheath inserted at the ear node (c), to the displacement of silk apices. Dotted line, F252; solid line, IL151. Error bars (b, d) denote two confidence intervals ( $P = 0.05$ ;  $n = 5-8$ ).

position. This elongation was appreciable for the 2–3 d preceding silk emergence (Fig. 1d), and was then negligible compared with displacement of silk tips in both lines F252 and IL151 (<3%; Fig. 1c,d).

The respective contributions of other supporting tissues (ear shank and the ear portion lower than the silk insertion point) were estimated via daily destructive measurements, for silks inserted at seven positions on the ear (Fig. 2c). We measured in this way the silk length (Fig. 2a) and the distance from the base of the peduncle carrying the ear to the silk insertion point (Fig. 2b,c). All silks showed sigmoidal growth (Fig. 2a) with a maximum rate at the time of silk emergence (Fig. 2d), while supporting tissues grew linearly with lower rates. Silks located at positions 1, 5 and 10 emerged almost simultaneously on the first day of silking (see detailed analysis in Oury *et al.*, 2016b) and grew at similar rates (Fig. 2d), so the elongation of a bundle of silks attached to the transducers on the first day of silking was consistent with measurements by destructive sampling on individual silks. The growth of underlying tissues represented <10% of total growth during 2–3 d (Fig. 2d). Attaching silks later than 3 d after the emergence of the first silk had two disadvantages.

First, bundles of silks with different growth rates were attached to the transducer (Fig. 2d), so the signal corresponded to the slowest silk and not to mean silk elongation rate. Second, a high proportion of recorded growth corresponded to nonsilk tissues. Hence, silk elongation rates presented below were collected during the first 3 d after the emergence of the first silk, on bundles attached to the transducer on the first day of silking, and were corrected by a factor of 8%, representing the proportion of the signal corresponding to the growth of nonsilk tissues. The cumulated elongation rate of attached silks was indistinguishable from the final length of unattached silks originating from the same positions on the ear (Fig. 1b), indicating that the calculation was correct, that the weight attached to silks did not cause extra elongation as a result of plastic deformation of tissues, and that the glue had no toxic effect on silk cell growth.

An oscillating pattern of silk elongation rate with a temperature effect that was accounted for by thermal time

The typical time courses of silk elongation rate are presented in Fig. 3(a) for two experiments with contrasting temperatures.

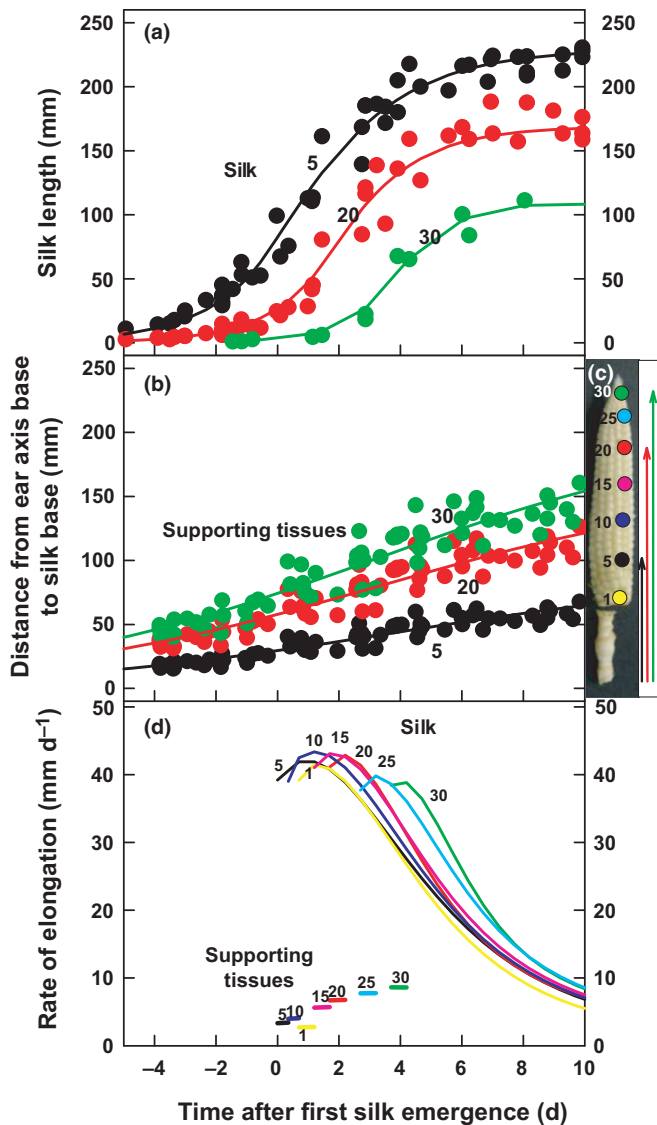


**Fig. 2** Components of the vertical displacement of the silk apex for silks inserted at different positions along the ear in maize (*Zea mays*). (a) Silk length, (b) distance from the base of the ear shank to the silk insertion point, measured as indicated in (c). (d) Time courses of the elongation rate of silks originating from seven positions on the ear (coloured lines), and of the elongation rate of supporting tissues (ear shank + ear portion below the silk insertion point; arrows in c) on the day of silk emergence (horizontal bars). In (a) and (b), data were obtained by daily dissecting sampled plants. Each point corresponds to a single plant. Colours respectively indicate the 1<sup>st</sup> (yellow), 5<sup>th</sup> (black), 10<sup>th</sup> (dark blue), 15<sup>th</sup> (pink), 20<sup>th</sup> (red), 25<sup>th</sup> (light blue) or 30<sup>th</sup> (green) position from the ear base, as illustrated in (c). In (d), elongation rates were deduced from curve fits in (a) and (b). Only positions 5, 20 and 30 are represented in (a) and (b) for clarity.

Over successive days, the silk elongation rate decreased during the day and increased during the night, with a general tendency to a decrease with silk aging from day 2 onwards, consistent with the destructive measurements presented in Fig. 2(d). This pattern was common to the two experiments shown in Fig. 3(a) and to all further experiments (Fig. 3c,d). Expression of elongation rate per unit thermal time (equivalent hours at 20°C) resulted in a

common time course for experiments at two temperatures (Fig. 3b). This allowed us to perform joint analyses of different experiments carried out at different temperatures. In particular, the same day–night pattern was observed for plants growing either with stable temperature in the growth chamber (Figs 3, 4a–d, 5) or in fluctuating temperatures under various values of soil water status in the glasshouse (Fig. 6), for eight maize lines representing a total of > 350 plants (Table S1).

Silk elongation rate responded to changes in transpiration rate and soil water status with short half times similar to those in leaves

The decrease in silk elongation rate during the day was steeper at high than at low VPD (2.4 vs 0.6 kPa, respectively), without an appreciable effect of VPD during the night (Fig. 3c), thereby suggesting that the day effect was linked to transpiration, which was 70% higher at high vs low VPD during the day (17 vs 10 g h<sup>-1</sup> per plant, respectively) and indistinguishable during the night (1 g h<sup>-1</sup> per plant in both cases). The half time of the decrease in silk elongation rate in the early morning ranged from 10 to 30 min (Fig. 4a,c,e), similar to half times observed for leaves (Caldeira *et al.*, 2014). Similar half times were observed for the increase in silk elongation rate at nightfall (Fig. 4b,d,f). The half time of growth recovery upon soil rehydration was 20 min (Fig. 4g,h), again similar to that in leaves. This suggests that similar hydraulic processes occurred in both leaves and silks, possibly linked to their direct connection with the xylem.

The depressive effect of VPD was associated with whole-plant transpiration and not with a local effect of evaporative demand on silk growth. Indeed, the time course of silk elongation rate at 2.4 kPa was similar whether silks were fully transpiring or silk transpiration was impeded by wrapping ears in aluminium foil (Fig. 5a). Limiting plant transpiration rate under high VPD by covering 30% of the leaf area with aluminium foil caused an increase in silk elongation rate during the day, thereby mimicking the effect of a low VPD and suggesting that whole-plant transpiration is the causal link between evaporative demand and silk elongation rate (Fig. 5c,d). This increase occurred although photosynthesis per plant decreased by 30%, in direct proportion to the covered leaf area as photosynthesis rate per unit leaf area was unchanged (Fig. 5d, inset). This suggests that carbon availability did not limit silk elongation rate in this experiment, consistent with measurements of transcripts, sugar contents and enzyme activities in silks (Oury *et al.*, 2016a).

Soil water deficit amplified the rapid decrease in silk elongation rate during the day (Fig. 3d), without changing half times compared with well-watered situations (Fig. 4c–f). Night-time silk elongation rate decreased with soil water potential (Figs 3d, 5e) and did not depend on photosynthesis or transpiration rate during the day (Fig. 5e,f). This was confirmed in an experiment in which plants were watered either at the end of the night or at the end of the day, so that they all experienced the same soil water status in the morning. Transpiration rate was similar in the two treatments (Fig. 5f), indicating that all plants effectively experienced the same soil water deficit during the day. Consistently,

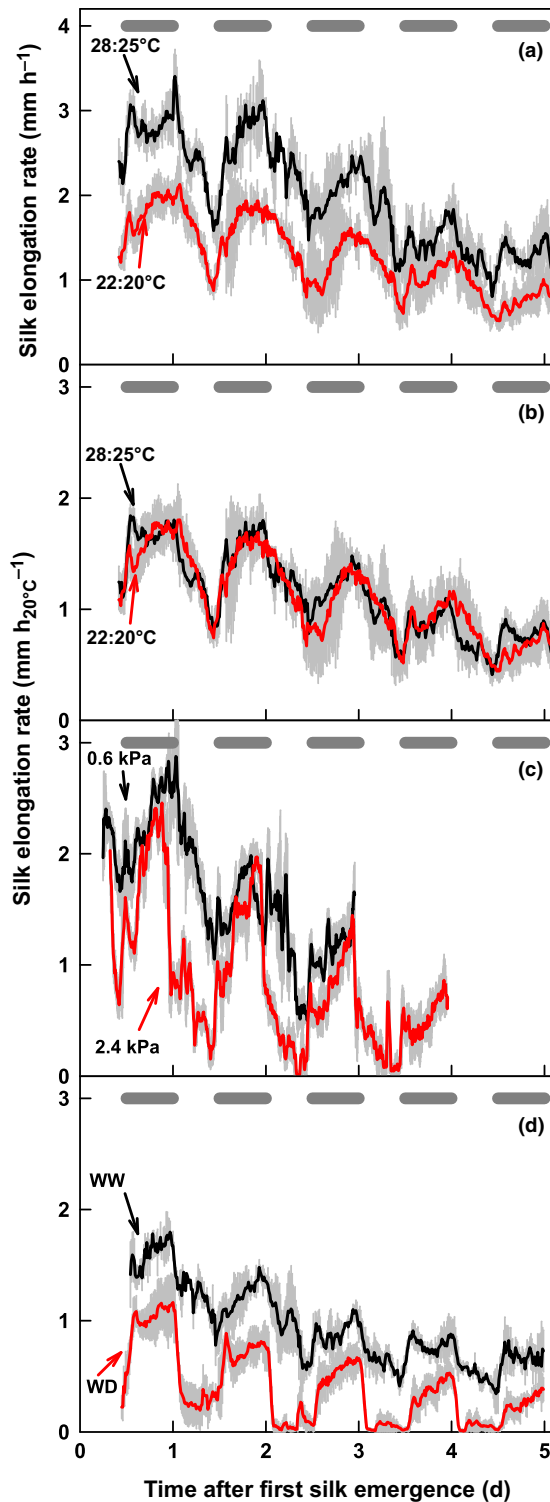


**Fig. 3** Time course of silk elongation rate under various air temperatures (a, b), evaporative demands (c) and soil water potentials (d) in maize (*Zea mays*). (a, b) Well-watered plants were grown at either 28°C : 25°C (black) or 22°C : 20°C (red) day : night temperatures. In (a), rates are expressed in mm h<sup>-1</sup>; they are expressed per unit thermal time (mm h<sub>20°C</sub><sup>-1</sup>) in (b–d). (c) Well-watered plants subjected to vapour pressure deficit (VPD) of 0.6 kPa (black) or 2.4 kPa (red), (d) well-watered plants (WW; black) and plants subjected to mild soil water deficit (WD; red). Vertical grey bars denote two confidence intervals ( $P = 0.05$ ;  $n = 6–8$ ). Horizontal grey bars, night periods.

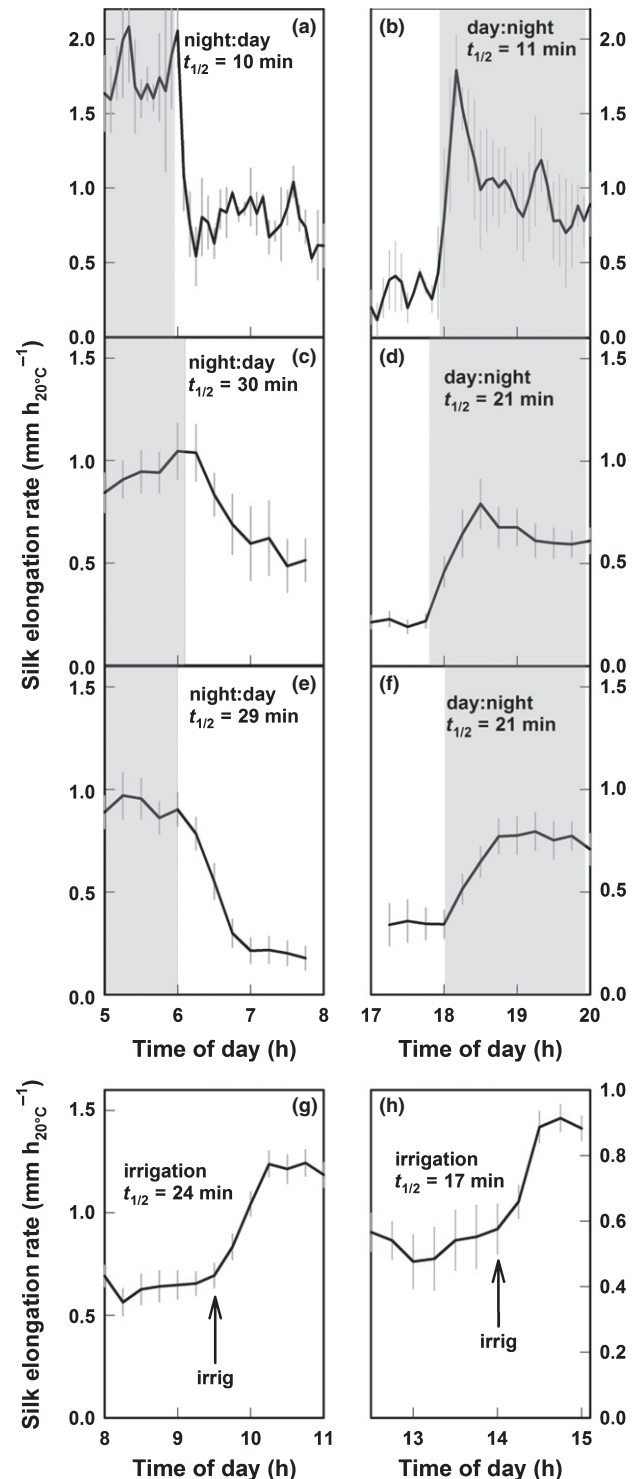


**Fig. 4** Changes in silk elongation rate over short time periods at the transition between night and day (a, c, e), at the transition between day and night (b, d, f) and upon rapid soil rehydration (g, h) in maize (*Zea mays*). Corresponding half times are indicated ( $t_{1/2}$ ). (a–d) Well-watered plants subjected to vapour pressure deficit (VPD) of 2.4 kPa. (e, f) Plants subjected to a moderate water deficit and a VPD of 0.6 kPa. (g, h) Plants subjected to a moderate water deficit and a VPD of 1.5 kPa and irrigated twice a day, at 09:00 and 14:00 h. Elongation rates are expressed per unit thermal time (mm h<sub>20°C</sub><sup>-1</sup>). Temporal definition of silk elongation rate was 5 min in (a, b) and 15 min elsewhere. Vertical grey bars denote two confidence intervals ( $P = 0.05$ ;  $n = 10–18$ ).

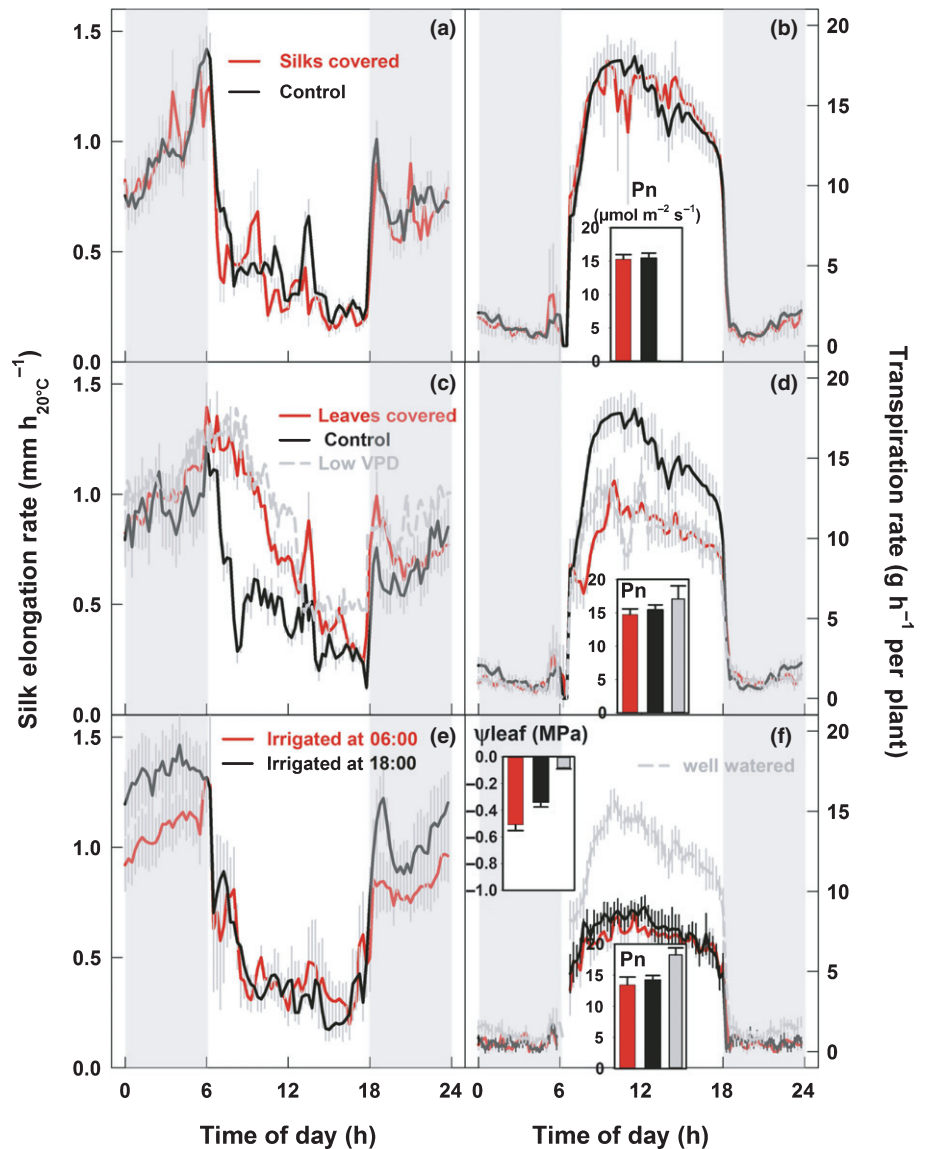


**Fig. 5** Silk elongation rate (a, c, e) and transpiration rate (b, d, f) of maize (*Zea mays*) plants subjected to various evaporative demands or soil water potentials. (a, b) Well-watered plants subjected to vapour pressure deficit (VPD) of 2.4 kPa. Plants had silks either directly exposed to air (black) or covered with aluminium foil (red). (c, d) Well-watered plants subjected to VPD of 2.4 kPa. Leaf area was either fully exposed to air (black) or 30% of it was covered with aluminium foil (red); grey lines represent plants with a VPD of 0.6 kPa. (e, f) Plants were watered either at dawn (06:00 h; red) or at the end of the day (18:00 h; black), so that soil water content was similar in the two treatments at the beginning of the day, but differed during the night. Well-watered plants are represented in grey. Elongation rates are expressed per unit thermal time ( $\text{mm h}_{20^\circ\text{C}}^{-1}$ ). Insets in (b, d, f), photosynthesis rate (Pn) in corresponding treatments. Inset in (f), pre-dawn leaf water potential ( $\Psi_{\text{leaf}}$ ). Error bars denote two confidence intervals ( $P = 0.05$ ;  $n = 15\text{--}24$ ).

neither daytime silk elongation rate (Fig. 5e) nor photosynthesis (Fig. 5f, inset) differed among treatments. By contrast, compared with plants watered at dawn, the night-time silk elongation rate was higher in plants watered at dusk (Fig. 5e), which were subjected to a more favourable soil water status during the night, as indicated by the predawn leaf water potential ( $-0.34 \pm 0.04$  MPa vs  $-0.51 \pm 0.04$  MPa, respectively; Fig. 5f, inset).

#### A genetic correlation between the sensitivities of leaf and silk elongation rates to soil water potential

The silk elongation rate was measured in eight maize lines at four soil water potentials (Figs 6, S2). The day–night pattern was conserved in all lines and soil water potentials, and the maximum elongation rate, measured during the second half of the dark period, decreased with soil water potential as it does in leaves (Tardieu *et al.*, 2010). This decrease in night-time elongation rate with soil water potential was more pronounced for IL95

(Fig. 6e–h) compared with IL151 (Fig. 6a–d). At soil water potentials below  $-0.8$  MPa, silk elongation was nearly stopped for IL95 (Fig. 6h), while it was maintained at  $0.5 \text{ mm h}_{20^\circ\text{C}}^{-1}$  for IL151 (Fig. 6d). Elongation rate measured during the second half of the dark period was plotted against soil water potential measured during the same time interval to obtain the response curve of silk elongation rate to soil water potential for the eight lines studied (Fig. 7). Because water potentials equilibrated at that time in the plant and in the soil, these curves can also be interpreted as the curves of the response of silk elongation rate to xylem water potential. Genotypes greatly differed both for the slope of the linear regression and for the soil water potential that stopped silk elongation. IL86 and IL95 stopped silk elongation at soil water potentials of  $\approx -0.8$  MPa, while CML444 and IL151 continued silk elongation at soil water potentials  $< -1.2$  MPa.

Curves of the response of silk elongation rate to soil water potential were compared with those of leaf elongation rate in the same eight lines (Fig. 7). A clear genetic correlation ( $r^2 = 0.92$ )

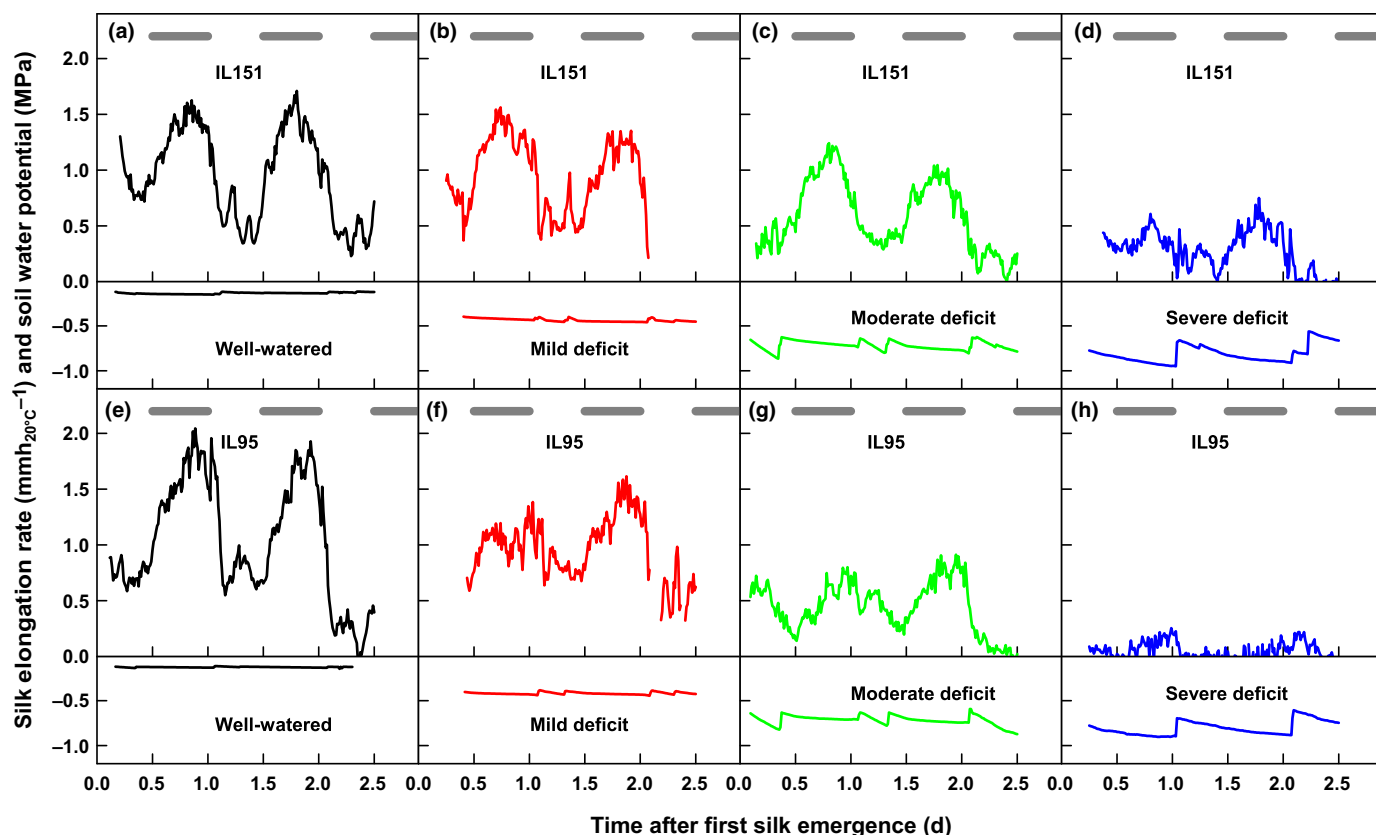


**Fig. 6** Time course of silk elongation rate (upper panel in each graph) and of soil water potential (lower panel) in maize (*Zea mays*) lines IL151 (a–d) and IL95 (e–h) subjected to four soil water status treatments. (a, e) Well-watered plants, (b, f) mild water deficit, (c, g) moderate water deficit, and (d, h) severe water deficit. Elongation rates are expressed per unit thermal time ( $\text{mm h}_{20}^{\circ\text{C}^{-1}}$ ). Horizontal grey bars, dark periods.

was observed between the sensitivities of silk and leaf elongation rates to soil water potential, estimated as the soil water potential that stops elongation (Fig. 8). In silks as well as in leaves, IL95 and IL86 were the most sensitive, and CML444 and IL151 the least sensitive. Overall, silks tended to be more sensitive than leaves to soil water potential, as the water potential that stopped growth was in most cases higher for silks than for leaves.

## Discussion

A common hydraulic control for leaf and silk elongation rates via a close connection with xylem water potential?

The diel kinetics of silk elongation rate shared common features with those of leaves: a maximum elongation rate observed during the dark period, a decrease during the day in response to evaporative demand, and a negative impact of reduced soil water potential, more pronounced during the day than during the night (Ben Haj Salah & Tardieu, 1997; Reymond *et al.*, 2003; Sadok *et al.*, 2007). The steep responses of silk elongation rate to evaporative demand and soil rehydration, with short half times of *c.* 30 min, resembled those of leaves (Caldeira *et al.*, 2014). The curves of the response of silk elongation rate to environmental variables (temperature and soil water potential) were also similar to those of leaves (Reymond

*et al.*, 2003; Sadok *et al.*, 2007; Welcker *et al.*, 2011), and the sensitivities of the elongation rates of silks and leaves to water deficit were closely correlated. Taken together, these elements suggest a commonality of mechanisms controlling the response of elongation in the two organs.

Recent studies proposed that the diurnal time courses of measured leaf elongation rate closely follow that of simulated xylem water potential over changes in evaporative demand (Caldeira *et al.*, 2014; Tardieu *et al.*, 2015). The curve of the response of leaf and silk elongation rates to soil water potential during the night can be interpreted as a response to xylem water potential because water potentials equilibrate in the leaves, in the xylem and in the soil during the night, in the absence of transpiration. The model of Tardieu *et al.* (2015) uses this relationship to simulate the time course of leaf elongation rate during the day, in such a way that diurnal variations in elongation rate reflect those of xylem water potential following changes in evaporative demand and soil water potential. Because the same patterns of time courses were observed here for silk elongation rate in terms of time constants and responses to VPD, we propose to extend this conclusion to silks, consistent with the fact that both leaves and silks are directly connected to the stem xylem. The similarity of time courses of silk and leaf elongation rates, but also the genetic correlation between them, lead us to propose that the silk elongation rate also follows xylem water potential, in spite of the fact

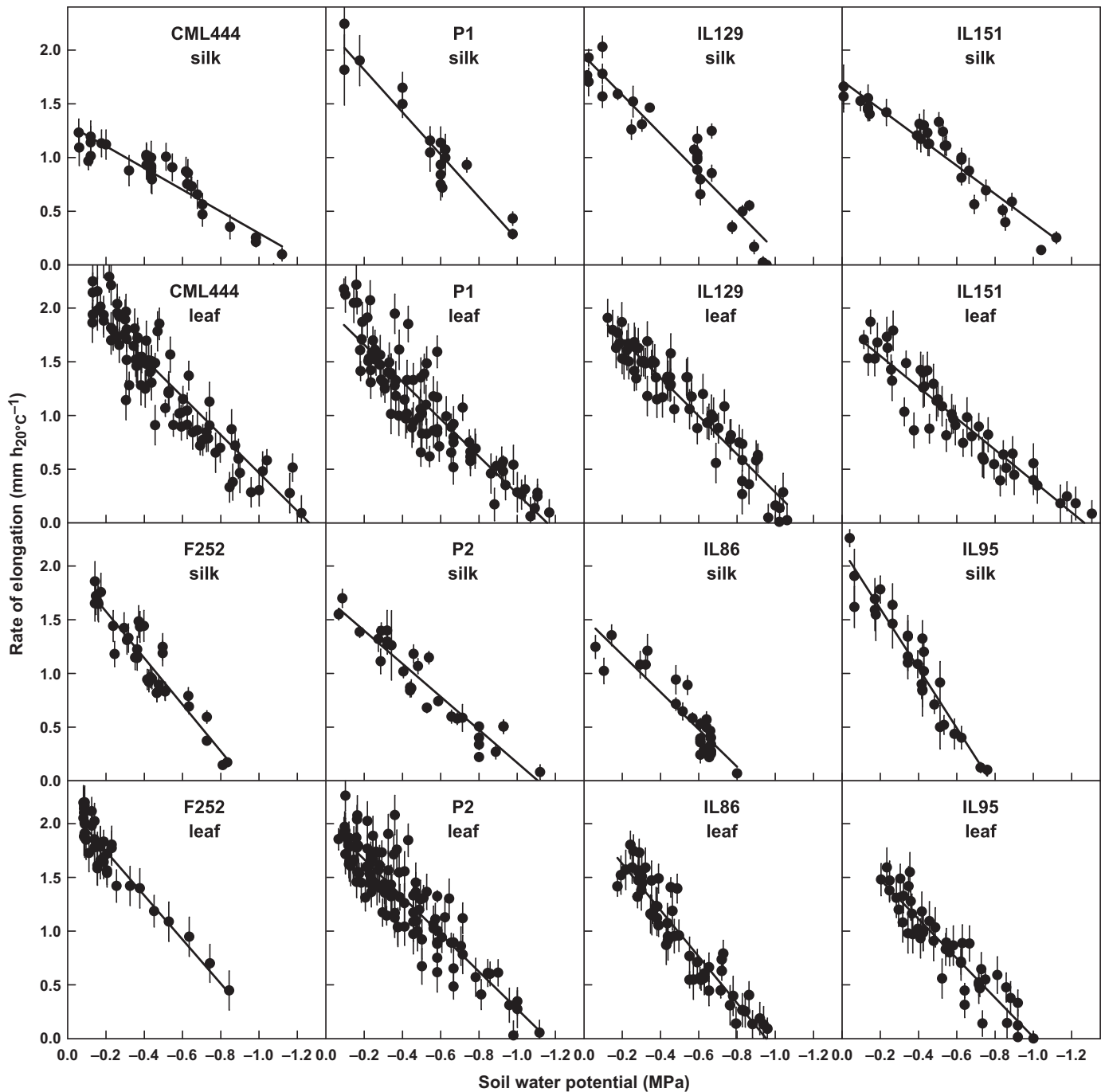


**Fig. 7** Response of silk and leaf elongation rates to soil water potential for eight inbred maize (*Zea mays*) lines. Each point represents the rate of elongation in one plant, averaged over the last 6 h of one night, plotted against the soil water potential measured at the same time in the corresponding pot. Elongation rates are expressed per unit thermal time ( $\text{mm h}_{20^{\circ}\text{C}}^{-1}$ ). Data were restricted to the first two nights following the first silk emergence for silk elongation rate and to the period from leaf stage 6.2 to 8.0 for leaf elongation rate. Error bars denote two confidence intervals ( $P = 0.05$ ;  $n = 24$ ).

that these are two different organs carried by plants at different phenological stages.

The silk elongation rate fluctuated in accordance with whole-plant transpiration, but not with local evaporative demand around silk tips emerged from bracts. This is probably attributable to the fact that expansive growth is restricted to the part of silks enclosed by bracts, while the emerged part does not grow (Fuad-Hassan *et al.*, 2008). Hence, the

elongation of the growing part, well connected with the xylem, responded to whole-plant transpiration and was recorded by the transducers attached to the silk tip. Because the emerged part did not grow, it could not be sensitive to local VPD. The fact that local VPD did not affect the nonemerged parts of silks suggests a hydraulic discontinuity between emerged and nonemerged tissues, possibly because of xylem embolism in emerged tips.

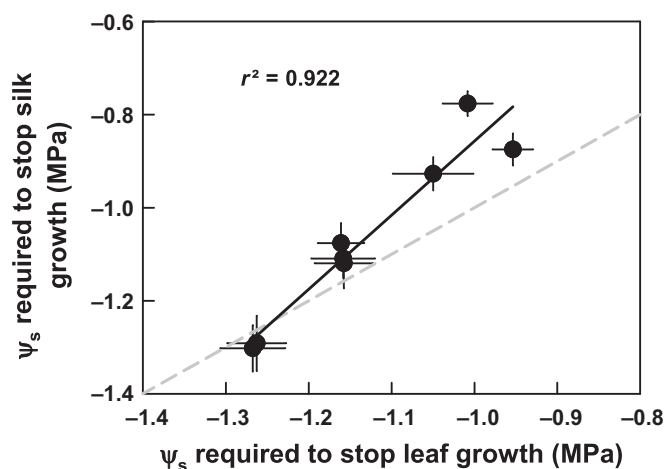


**Fig. 8** Comparison of silk and leaf sensitivities to soil dehydration for eight maize (*Zea mays*) inbred lines. For both organs, sensitivity is represented by the soil water potential ( $\Psi_s$ ) required to stop organ growth (x-intercept of linear fit in Fig. 7). Dashed line:  $y = x$ . Error bars,  $\pm 2$  SE.

The expansive growth of leaves and silks may therefore be governed by common mechanisms that control cell wall mechanical properties (Cosgrove, 2005) or water entry into growing cells via changes in hydraulic conductance as modelled in Tardieu *et al.* (2015). Expansins may be involved in the common control, via their effect on cell wall properties (Zhang *et al.*, 2014). This conclusion is reinforced by the findings of a recent study showing that genes involved in expansive growth show differential expression in silks of plants that are either well watered or water stressed, whereas this is not the case for genes involved in carbon metabolism (Oury *et al.*, 2016a). By contrast, we probably cannot extend our conclusions to the growth of the endosperm and of the embryo which are weakly connected hydraulically to the stem, with a disruption of vascular elements in the ovary pedicel (Kiesselbach, 1949; Felker & Shannon, 1980; Miller & Chourey, 1992), resulting in weaker effects of water deficit than in maternal tissues (Yu & Setter, 2003).

#### A reliable method for analysing differences among genotypes in the response of silk growth to environment

The method proposed here allows continuous analysis of silk elongation rate in tens of plants simultaneously. Classical methods for directly measuring silk length with a ruler are time consuming and only provide one measurement per day (Bassetti & Westgate, 1993; Anderson *et al.*, 2004) against one every 5 min in our system. The literature mentions few examples of the use of displacement transducers to measure silk elongation (Herrero & Johnson, 1981; Westgate & Boyer, 1985), with the number of devices limited to one or two, against hundreds at the Phenodyn platform. We have checked the reliability and the reproducibility of our method, and shown that it allows the determination of time courses of silk elongation rate and analysis of their relationships with current environmental conditions. The response to water deficit of silk elongation rate of each genotype was characterized via the parameters of these relationships. Necessary precautions are to attach the silks to the device on the first day after

first silk emergence, and to limit the analysis to 2–3 d, because of artefacts resulting from the growth of underlying tissues that occurs later in silk development.

#### Genotypic variability of silk growth responses to drought

The values of water potential required to stop silk growth varied among genotypes from  $-0.8$  to  $-1.2$  MPa in our study (Fig. 8), and were close to  $-0.8$  MPa for hybrid B73xMo17 in the study of Westgate & Boyer (1985). Water potentials were measured at the end of the dark period (predawn) in both cases and can therefore be analysed jointly. Other studies mention genotypic variability for turgor maintenance in silks (Schoper *et al.*, 1987). Higher sensitivities were observed in the dent North-American hybrid B73xMo17 and dent European line F252 than in the tropical lines CML444, IL151, P1 and P2, thereby suggesting that sources of tolerance may exist for silk growth in tropical germplasm.

The genetic link observed in this study between the sensitivities of leaf and silk elongation rates to water deficit is consistent with the results of earlier studies carried out by our group. In particular, common quantitative trait loci (QTLs) were found for leaf elongation rate and the anthesis–silking interval, an indicator of silk growth (Fuad-Hassan *et al.*, 2008), in both well-watered and drought conditions (Welcker *et al.*, 2007). In the same way, common QTLs for leaf elongation rate and silk biomass were observed by Dignat *et al.* (2013).

#### Consequences for phenotyping and modelling

The above-mentioned results suggest that drought tolerance in maize could partly rely on the maintenance of processes of tissue expansion in both vegetative and reproductive organs. Genetic variability exists for this maintenance and has to be characterized through phenotyping. Even with the method presented here, phenotyping silk elongation rate is a difficult task at a throughput compatible with genetic analyses, that is, hundreds of genotypes instead of eight in the present study. High-throughput phenotyping for silk growth might be feasible using image analysis. An alternative might emerge from the above-proposed hypothesis of common mechanisms controlling expansive growth in leaves and silks, resulting in a genetic correlation between silk growth and leaf growth under drought. Phenotyping for silk growth could therefore be at least partly deduced from that of leaf growth under water deficit. Another possibility would be to use the anthesis–silking interval as a predictor of silk elongation rate, as proposed by Fuad-Hassan *et al.* (2008) and confirmed by a close correlation between anthesis–silking interval and silk elongation rate in the present study (data not shown).

The genetic link between the sensitivities of leaf elongation rate and silk elongation rate (this study), of leaf elongation and anthesis–silking interval (Welcker *et al.*, 2007) and of silk elongation and floret abortion rate (Oury *et al.*, 2016b) may explain the unexpected result that the sensitivity of grain number to water deficit in the field has a high genetic correlation with the sensitivity of leaf growth to water deficit in young plants assessed in a

phenotyping platform (Chapuis *et al.*, 2012). The commonality of mechanisms controlling the responses of expansive growth to environmental constraints in both vegetative and reproductive structures, centred on hydraulic processes as underlined in the present study, has therefore potentially large consequences in breeding for plants adapted to changing environments, but also in understanding plant adaptive traits and in modelling plant–water interactions from the cell to the global scale. This is consistent with recent studies addressing the modelling and prediction of terrestrial carbon and water dynamics, which suggest revision of the hierarchy of plant growth control in the vegetation models (Fatichi *et al.*, 2014) by giving a pivotal role to plant hydraulics (Fatichi *et al.*, 2015; Pappas *et al.*, 2016).

## Acknowledgements

This work was supported by the French Agence Nationale de la Recherche (project ANR-08-GENM-003) and by the EU project FP7-244374 (DROPS). We thank Stéphane Berthézène and Benoît Suard for their help during experiments in the phenotyping platform Phenodyn.

## Author contributions

O.T. conceived, designed and performed the research, and performed data analysis and interpretation; A.F.-H. and M.B. performed the experiments and collected data; C.W. supervised the experiments and data analyses on leaf growth; F.T. supervised the research; O.T. and F.T. wrote the paper.

## References

- Anderson SR, Lauer MJ, Schoper JB, Shibles RM. 2004. Pollination timing effects on kernel set and silk receptivity in four maize hybrids. *Crop Science* **44**: 464–473.
- Bassetti P, Westgate ME. 1993. Emergence, elongation, and senescence of maize silks. *Crop Science* **33**: 271–275.
- Ben Haj Salah H, Tardieu F. 1997. Control of leaf expansion rate of droughted maize plants under fluctuating evaporative demand – a superposition of hydraulic and chemical messages? *Plant Physiology* **114**: 893–900.
- Boyer JS. 1970. Leaf enlargement and metabolic rates in corn, soybean, and sunflower at various leaf water potentials. *Plant Physiology* **46**: 233–235.
- Bruce WB, Edmeades GO, Barker TC. 2002. Molecular and physiological approaches to maize improvement for drought tolerance. *Journal of Experimental Botany* **53**: 13–25.
- Caldeira CF, Bosio M, Parent B, Jeanguenin L, Chaumont F, Tardieu F. 2014. A hydraulic model is compatible with rapid changes in leaf elongation under fluctuating evaporative demand and soil water status. *Plant Physiology* **164**: 1718–1730.
- Cawoy V, Lutts S, Ledent JF, Kinet JM. 2007. Resource availability regulates reproductive meristem activity, development of reproductive structures and seed set in buckwheat (*Fagopyrum esculentum*). *Physiologia Plantarum* **131**: 341–353.
- Chapuis R, Delluc C, Debeuf R, Tardieu F, Welcker C. 2012. Resilience to water deficit in a phenotyping platform and in the field: how related are they in maize? *European Journal of Agronomy* **42**: 59–67.
- Cosgrove DJ. 2005. Growth of the plant cell wall. *Nature Reviews Molecular Cell Biology* **6**: 850–861.
- Dignat G, Welcker C, Sawkins M, Ribaut JM, Tardieu F. 2013. The growths of leaves, shoots, roots and reproductive organs partly share their genetic control in maize plants. *Plant, Cell & Environment* **36**: 1105–1119.
- Edmeades GO, Bolaños J, Elings A, Ribaut JM, Banziger M, Westgate ME. 2000. The role and regulation of the anthesis-silking interval in maize. In: Westgate ME, Boote K, eds. *Physiology and modeling kernel set in maize*. Madison, WI, USA: Crop Science Society of America, 43–73.
- Egli DB, Bruening WP. 2006. Fruit development and reproductive survival in soybean: position and age effects. *Field Crops Research* **98**: 195–202.
- Ehler C, Maurel C, Tardieu F, Simonneau T. 2009. Aquaporin-mediated reduction in maize root hydraulic conductivity impacts cell turgor and leaf elongation even without changing transpiration. *Plant Physiology* **150**: 1093–1104.
- Fatichi S, Leuzinger S, Korner C. 2014. Moving beyond photosynthesis: from carbon source to sink-driven vegetation modeling. *New Phytologist* **201**: 1086–1095.
- Fatichi S, Pappas C, Ivanov VY. 2015. Modeling plant–water interactions: an ecohydrological overview from the cell to the global scale. *Wiley Interdisciplinary Reviews: Water* **3**: 327–368.
- Felker FC, Shannon JC. 1980. Movement of <sup>14</sup>C-labeled assimilates into kernels of *Zea mays* L. III. An anatomical examination and microautoradiographic study of assimilate transfer. *Plant Physiology* **65**: 864–870.
- Fuad-Hassan A, Tardieu F, Turc O. 2008. Drought-induced changes in anthesis-silking interval are related to silk expansion: a spatio-temporal growth analysis in maize plants subjected to soil water deficit. *Plant, Cell & Environment* **31**: 1349–1360.
- Herrero MP, Johnson RR. 1981. Drought stress and its effects on maize reproductive systems. *Crop Science* **21**: 105–110.
- Heslop-Harrison Y, Reger BJ, Heslop-Harrison J. 1984. The pollen-stigma interaction in the grasses. 5. Tissue organization and cytochemistry of the stigma (“silk”) of *Zea mays* L. *Acta Botanica Neerlandica* **33**: 81–99.
- Kiesselbach TA. 1949. *The structure and reproduction of corn*. Lincoln, NE, USA: University of Nebraska.
- Lemcoff JH, Loomis RS. 1994. Nitrogen and density influences on silk emergence, endosperm development, and grain-yield in maize (*Zea mays* L). *Field Crops Research* **38**: 63–72.
- Lockhart JA. 1965. An analysis of irreversible plant cell elongation. *Journal of Theoretical Biology* **8**: 264–275.
- Miller ME, Chourey PS. 1992. The maize Invertase-Deficient miniature-1 Seed mutation Is associated with aberrant pedicel and endosperm development. *Plant Cell* **4**: 297–305.
- Muller B, Pantin F, Génard M, Turc O, Freixes S, Piques M, Gibon Y. 2011. Water deficits uncouple growth from photosynthesis, increase C content, and modify the relationships between C and growth in sink organs. *Journal of Experimental Botany* **62**: 1715–1729.
- Ney B, Duthion C, Turc O. 1994. Phenological response of pea to water-stress during reproductive development. *Crop Science* **34**: 141–146.
- Oury V, Caldeira CF, Prodhomme D, Pichon J-P, Gibon Y, Tardieu F, Turc O. 2016a. Is change in ovary carbon status a cause or a consequence of maize ovary abortion in water deficit during flowering? *Plant Physiology* **171**: 997–1008.
- Oury V, Tardieu F, Turc O. 2016b. Ovary apical abortion under water deficit is caused by changes in sequential development of ovaries and in silk growth rate in maize. *Plant Physiology* **171**: 986–996.
- Pappas C, Fatichi S, Burlando P. 2016. Modeling terrestrial carbon and water dynamics across climatic gradients: does plant trait diversity matter? *New Phytologist* **209**: 137–151.
- Parent B, Hachez C, Redondo E, Simonneau T, Chaumont F, Tardieu F. 2009. Drought and ABA effects on aquaporin content translate into changes in hydraulic conductivity and leaf growth rate: a trans-scale approach. *Plant Physiology* **149**: 2000–2012.
- Parent B, Turc O, Gibon Y, Stitt M, Tardieu F. 2010. Modelling temperature-compensated physiological rates, based on the coordination of responses to temperature of developmental processes. *Journal of Experimental Botany* **61**: 2057–2069.
- Reymond M, Muller B, Leonardi A, Charcosset A, Tardieu F. 2003. Combining quantitative trait loci analysis and an ecophysiological model to analyze the genetic variability of the responses of maize leaf growth to temperature and water deficit. *Plant Physiology* **131**: 664–675.
- Reymond M, Muller B, Tardieu F. 2004. Dealing with the genotype × environment interaction via a modelling approach: a comparison of

- QTLs of maize leaf length or width with QTLs of model parameters. *Journal of Experimental Botany* 55: 2461–2472.
- Ribaut JM, Hoisington DA, Deutsch JA, Jiang C, GonzalezdeLeon D. 1996. Identification of quantitative trait loci under drought conditions in tropical maize. 1. Flowering parameters and the anthesis-silking interval. *Theoretical and Applied Genetics* 92: 905–914.
- Ribaut JM, Jiang C, Gonzalez-de-Leon D, Edmeades GO, Hoisington DA. 1997. Identification of quantitative trait loci under drought conditions in tropical maize. 2. Yield components and marker-assisted selection strategies. *Theoretical and Applied Genetics* 94: 887–896.
- Rocha OJ, Stephenson AG. 1991. Order of fertilization within the ovary of *Phaseolus coccineus* L. *Sexual Plant Reproduction* 4: 126–131.
- Sadok W, Naudin P, Boussuge B, Muller B, Welcker C, Tardieu F. 2007. Leaf growth rate per unit thermal time follows QTL-dependent daily patterns in hundreds of maize lines under naturally fluctuating conditions. *Plant, Cell & Environment* 30: 135–146.
- Schoper JB, Lambert RJ, Vasilas BL, Westgate ME. 1987. Plant factors controlling seed set in maize. The influence of silk, pollen, and ear-leaf water status and tassel heat treatment at pollination. *Plant Physiology* 83: 121–125.
- Susko DJ. 2006. Effect of ovule position on patterns of seed maturation and abortion in *Robinia pseudoacacia* (Fabaceae). *Canadian Journal of Botany—Revue Canadienne De Botanique* 84: 1259–1265.
- Tao TY, Ouellet T, Dadej K, Miller SS, Johnson DA, Singh J. 2006. Characterization of a novel glycine-rich protein from the cell wall of maize silk tissues. *Plant Cell Reports* 25: 848–858.
- Tardieu F, Granier C, Muller B. 2011. Water deficit and growth. Co-ordinating processes without an orchestrator? *Current Opinion in Plant Biology* 14: 283–289.
- Tardieu F, Parent B, Caldeira CF, Welcker C. 2014. Genetic and physiological controls of growth under water deficit. *Plant Physiology* 164: 1628–1635.
- Tardieu F, Parent B, Simonneau T. 2010. Control of leaf growth by abscisic acid: hydraulic or non-hydraulic processes? *Plant, Cell & Environment* 33: 636–647.
- Tardieu F, Reymond M, Hamard P, Granier C, Muller B. 2000. Spatial distributions of expansion rate, cell division rate and cell size in maize leaves: a synthesis of the effects of soil water status, evaporative demand and temperature. *Journal of Experimental Botany* 51: 1505–1514.
- Tardieu F, Simonneau T, Parent B. 2015. Modelling the coordination of the controls of stomatal aperture, transpiration, leaf growth, and abscisic acid: update and extension of the Tardieu-Davies model. *Journal of Experimental Botany* 66: 2227–2237.
- Weatherwax P. 1916. Morphology of the flowers of *Zea mays*. *Bulletin of the Torrey Botanical Club* 43: 127–144.
- Welcker C, Boussuge B, Bencivenni C, Ribaut JM, Tardieu F. 2007. Are source and sink strengths genetically linked in maize plants subjected to water deficit? A QTL study of the responses of leaf growth and of Anthesis-Silking Interval to water deficit. *Journal of Experimental Botany* 58: 339–349.
- Welcker C, Sadok W, Dignat G, Renault M, Salvi S, Charcosset A, Tardieu F. 2011. A common genetic determinism for sensitivities to soil water deficit and evaporative demand: meta-analysis of quantitative trait loci and introgression lines of maize. *Plant Physiology* 157: 718–729.
- Westgate ME, Boyer JS. 1985. Osmotic adjustment and the inhibition of leaf, root, stem and silk growth at low water potentials in maize. *Planta* 164: 540–549.
- Yu L-X, Setter TL. 2003. Comparative transcriptional profiling of placenta and endosperm in developing maize kernels in response to water deficit. *Plant Physiology* 131: 568–582.
- Zhang W, Yan H, Chen W, Liu J, Jiang C, Jiang H, Zhu S, Cheng B. 2014. Genome-wide identification and characterization of maize expansin genes expressed in endosperm. *Molecular Genetics and Genomics* 289: 1061–1074.

## Supporting Information

Additional Supporting Information may be found online in the Supporting Information tab for this article:

**Fig. S1** Water-release curve of the soil used in the eight experiments.

**Fig. S2** Time-course of pre-dawn soil water potential in the four treatments in Expt 8.

**Table S1** List of experiments, treatments and growing conditions

Please note: Wiley Blackwell are not responsible for the content or functionality of any supporting information supplied by the authors. Any queries (other than missing material) should be directed to the *New Phytologist* Central Office.

# Ovary Apical Abortion under Water Deficit Is Caused by Changes in Sequential Development of Ovaries and in Silk Growth Rate in Maize<sup>1</sup>[OPEN]

Vincent Oury, François Tardieu, and Olivier Turc\*

INRA, UMR 759 Laboratoire d'Ecophysiologie des Plantes sous Stress Environnementaux, F-34060 Montpellier, France

ORCID IDs: 0000-0003-2994-0111 (V.O.); 0000-0003-0659-1406 (O.T.).

Grain abortion allows the production of at least a few viable seeds under water deficit but causes major yield loss. It is maximum for water deficits occurring during flowering in maize (*Zea mays*). We have tested the hypothesis that abortion is linked to the differential development of ovary cohorts along the ear and to the timing of silk emergence. Ovary volume and silk growth were followed over 25 to 30 d under four levels of water deficit and in four hybrids in two experiments. A position-time model allowed characterizing the development of ovary cohorts and their silk emergence. Silk growth rate decreased in water deficit and stopped 2 to 3 d after first silk emergence, simultaneously for all ovary cohorts, versus 7 to 8 d in well-watered plants. Abortion rate in different treatments and positions on the ear was not associated with ovary growth rate. It was accounted for by the superposition of (1) the sequential emergence of silks originating from ovaries of different cohorts along the ear with (2) one event occurring on a single day, the simultaneous silk growth arrest. Abortion occurred in the youngest ovaries whose silks did not emerge 2 d before silk arrest. This mechanism accounted for more than 90% of drought-related abortion in our experiments. It resembles the control of abortion in a large range of species and inflorescence architectures. This finding has large consequences for breeding drought-tolerant maize and for modeling grain yields in water deficit.

Breeding has led to a massive increase in maize (*Zea mays*) yield under water deficit over the last 50 years (Cooper et al., 2014; Lobell et al., 2014), in good part associated with the fine-tuning of the coordination of the developments of the ear and the whole plant. This coordination is currently approached by breeders via the anthesis-silking interval (ASI), which has decreased markedly with genetic progress (Bolaños and Edmeades, 1996; Duvick, 2005). ASI is the time elapsing from male flowering to the emergence of styles (silks) over the modified leaf sheaths (husks) that enclose the ear and is the phenological stage with a maximum sensitivity to water deficit (Denmead and Shaw, 1960; Grant et al., 1989). An irreversible switch in ear development is observed when water deficit is imposed at this time, resulting in ovary/grain abortion, even when viable

pollen is provided to silks (Boyer and Westgate, 2004). The causal link between the timing of silk emergence and ovary abortion is not clearly understood. It has been proposed that increase in ASI is a symptom rather than a mechanism causing abortion and that both would be due to a decreased assimilate flux toward the ear (Edmeades et al., 1993, 2000). This would be in line with studies suggesting that sugar deprivation is a major cause of ovary abortion (Boyle et al., 1991; Zinselmeier et al., 1995a, 1995b, 1995c, 1999; McLaughlin and Boyer, 2004). However, water deficit can cause ovary abortion even when ovary sugars are not depleted (Schussler and Westgate, 1995; Andersen et al., 2002) and has a larger effect on ovary abortion than a low-light treatment that causes a similar decrease in photosynthesis (Schussler and Westgate, 1991). This suggests that part of ovary abortion under water deficit is due to a direct effect of low water potential ( $\Psi_p$ ), independently of assimilate supply.

The development of inflorescences is involved in the control of ovary abortion in several species such as trees (Cawoy et al., 2007) or indeterminate legumes (Ney et al., 1994; Egli and Bruening, 2006). In these species, abortion occurs in youngest ovaries that do not reach a critical stage at a given date (Ney et al., 1994; Egli and Bruening, 2006). The maize ear can be analyzed as a coalesced inflorescence because it is composed of spikelet pairs arranged in rings sequentially initiated at the ear apex (Bonnett, 1940; Kiesselbach, 1949), thereby suggesting that the above mechanism may apply to maize. Furthermore, the fertilization of basal, oldest ovaries can

<sup>1</sup> This work was supported by the European Union (project no. FP7-244374, Drought-Tolerant Yielding Plants) and the Agence Nationale de la Recherche (project no. ANR-08-GENM-003).

\* Address correspondence to olivier.turc@supagro.inra.fr.

The author responsible for distribution of materials integral to the findings presented in this article in accordance with the policy described in the Instructions for Authors ([www.plantphysiol.org](http://www.plantphysiol.org)) is: Olivier Turc ([olivier.turc@supagro.inra.fr](mailto:olivier.turc@supagro.inra.fr)).

O.T. conceived the research plan and supervised the experiments; V.O. designed and performed the experiments and analyzed the data; F.T. supervised the project and the writing; V.O., F.T., and O.T. wrote the article.

[OPEN] Articles can be viewed without a subscription.

[www.plantphysiol.org/cgi/doi/10.1104/pp.15.00268](http://www.plantphysiol.org/cgi/doi/10.1104/pp.15.00268)

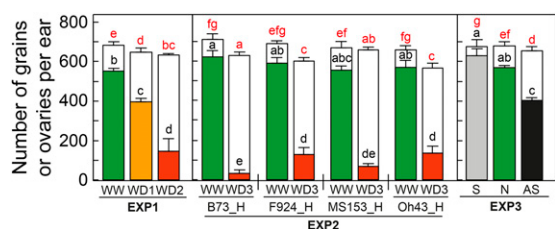


**Figure 1.** Grain number per ear (colored bars) and number of aborted ovaries per ear (white bars) in all treatments, experiments, and genotypes in Exp1, experiment 2 (Exp2), and experiment 3 (Exp3). Green, WW and normal pollination (N); yellow, mild water deficit (WD1); red, moderate water deficit (WD2) and severe water deficit (WD3) in Exp1 and Exp2, respectively; gray, synchronous pollination (S); black, asynchronous pollination (AS). Plants were hand-pollinated daily with fresh pollen from well-watered plants. Error bars indicate SE ( $n \geq 3$ ). Different letters indicate significant differences in a Kruskal-Wallis test ( $P < 0.05$ ); black letters are for grain number and red letters are for number of aborted ovaries.

stop the development of younger, apical ovaries and cause their abortion, in particular when fertilization occurs at two different dates via an artificial asynchronous pollination (Freier et al., 1984; Cárcova and Otegui, 2001). Water deficit might reproduce such a sequence of events because water deficit strongly decreases silk growth (Fuad-Hassan et al., 2008), thereby generating a delay in silk emergence from the basal to the apical ovary cohorts followed by a naturally occurring asynchronous fertilization.

We have tested if a mechanism linked to the sequential development of ovaries and to the timing of silk emergence could be a major cause of ovary abortion under water deficit. For that, we have explored a range of abortion rates caused by various degrees of water deficit in different genotypes and by the timing of pollination in well-watered (WW) plants. In all treatments, we measured the growths of ovaries and silks as a function of time and position on the ear. A novel position-time model allowed us to interpolate temporal patterns of growth from the spatial position of ovaries along the ear. This model is equivalent to those based on the plastochron index for leaf development (Erickson and Michelini, 1957; Meicenheimer, 2014), in which organs of different generations are analyzed as having common growth rates with delayed development stages according to their spatial positions. We could analyze in this way the links between the abortion frequency of apical ovaries, the temporal patterns of ovary and silk growth, and the base-to-apex gradient of development.

The involvement of carbon metabolism in those processes is analyzed in a companion article in a series of experiments with the same protocol as that of this study (Oury et al., 2016).

## RESULTS

### A Range of Abortion Rates Was Caused by Water Deficits with Limited Effects on Photosynthesis and Transpiration

Drought treatments in experiment 1 (Exp1) caused massive abortion rates, from 29% to 77% (Fig. 1; Table I), resulting in decreased grain numbers, 394 and 146 grains, respectively, in WD1 (soil  $\Psi_p = -0.22$  MPa; Fig. 2A) and WD2 ( $\Psi_p = -0.48$  MPa). WD3 in Exp2 ( $\Psi_p = -0.6$  MPa; Fig. 2D) resulted in higher abortion rates with large differences between hybrids (Fig. 1). Abortion occurred in spite of the fact that treatments had a limited effect on transpiration rate (32% and 54% in Exp1; Fig. 2, B and D) and photosynthesis (26% and 42% in Exp1; Fig. 2C). The number of ovaries per ear was similar in WW and water deficit plants at the onset of water deficit, close to the final number of ovaries 23 d after silk emergence in WW plants. This indicates that water deficit acted on grain number via ovary/grain abortion. The slight decrease in ovary number observed in the severe water deficit treatment of Exp2 (Fig. 1) probably reflected the difficulty of quantifying at that stage the number of very small aborted ovaries at apical positions of the ear. It is worth mentioning that silks were hand-pollinated every day with fresh pollen of WW plants, so observed abortions were not a consequence of a lack of pollen availability or viability.

The abortion frequency increased with ovary position on the ear in all treatments. It became appreciable beyond the sixth, 20th, and 31st ovary positions in WD2, WD1, and WW treatments, respectively, and reached 100% at the 20th, 32nd, and 44th ovary positions in the same treatments (Fig. 3, A and B). This was also the case in the treatment with an asynchronous pollination in WW plants (Fig. 3, C and D), which had a spatial pattern of abortion frequency similar to that in WD1, although with larger aborted ovules, suggesting that the mechanism of abortion was partly common. Hence, we have considered the possibility that this spatial gradient was due to a difference in history of ovaries along the ear, thereby requiring a position-time model to establish correspondences between spatial positions and the time course of ovary growth and development.

**Table I.** Environmental conditions during the three experiments in growth chamber (GC) or greenhouse (GH)

T, Temperature ( $^{\circ}\text{C}$ ); VPD, vapor pressure deficit (kPa); PPFD, photosynthetic photon flux density ( $\text{mol m}^{-2} \text{d}^{-1}$ ). Photoperiod is in hours. Mean values (sd) from tassel emergence to 7 d after silk emergence are shown.

Experiment	Growth Conditions	T Day	T Night	VPD Day	VPD Night	Photoperiod	PPFD
Exp1	GC	25.69 (1.02)	25.53 (0.80)	0.82 (0.18)	0.82 (0.10)	16	23.47 (3.48)
Exp2	GH	23.30 (1.96)	20.06 (1.16)	1.64 (0.43)	1.22 (0.23)	14	9.55 (1.18)
Exp3	GH	24.04 (1.58)	20.91 (1.30)	1.88 (0.48)	1.19 (0.33)	14	10.09 (0.19)

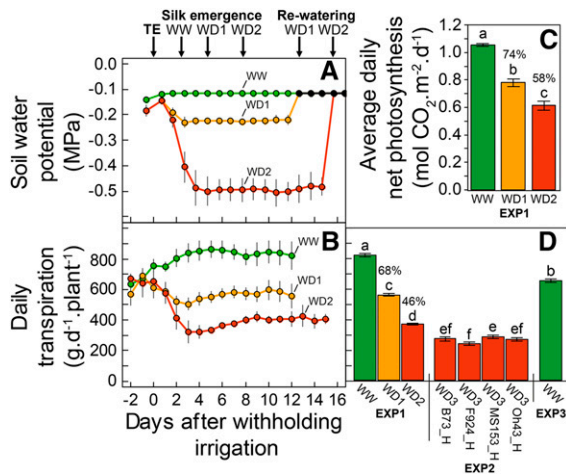


**Figure 2.** A and B, Time courses of soil  $\Psi_p$  (A) and daily transpiration (B) during the period of water deficit in the three treatments in Exp1. C, Net photosynthesis in Exp1. Mean values from 3 d after the beginning of water deficit to rewatering time (four, 19, and five replicates in WW treatment, WD1, and WD2 respectively) are shown. D, Mean daily transpiration from day 3 of water depletion to rewatering in Exp1 (WW, WD1, and WD2 treatments), Exp2 (water deficit in four maize hybrids), and Exp3 (WW treatments). Green, WW treatment; yellow, WD1; red, WD2 and WD3 in Exp1 and Exp2, respectively. Tassel emergence (TE) in A is synchronous with the beginning of water deficit; black points indicate soil  $\Psi_p$  after rewatering. Error bars in A and B represent 95% confidence intervals ( $n \geq 4$ ). Error bars in C and D are SE values ( $n \geq 3$ ). Different letters indicate significant differences in a Kruskal-Wallis test ( $P < 0.05$ ). Percentages represent transpiration or net photosynthesis in water deficit compared with WW treatment. The transpiration of control plants in the WW treatment in Exp2, not represented here, was close to 700 g d<sup>-1</sup>.

**A Common Position-Time Model Applied to Ovaries and Silks Regardless of Plant Water Status**

The first silks to emerge originated from ovaries at positions 5 to 8 from the ear base in WW plants (Fig. 4B, rankings closest to 1). The spatial origin of newly emerged silks was then checked every day. Ovaries located at positions higher than 8 carried silks that emerged sequentially, with a linear correspondence between ovary position and ranking of silk emergence (Fig. 4B). Ovaries located at positions 1 to 4 carried silks that also emerged sequentially, but in inverse order of position (position 4 first and position 1 last). Hence, the number of ovary positions carrying emerged silks first increased rapidly with time, when newly appeared silks originated sequentially from both sides of positions 5 to 8 (Fig. 5C). This rate decreased after the silks from position 1 emerged, so that the only silks to emerge were those at positions higher than 13 (Fig. 5C). Overall, nearly all silks had emerged 7 d after the first silk. The position-time pattern presented above for WW plants also applied to plants subjected to WD1 and WD2 (Fig. 4B). In particular, silks emerged sequentially with the same ranking in all three watering treatments, with the first emerged silks at positions 5 to 8 from the ear base (Fig. 4B). The main difference between treatments was the highest ovary position that carried an emerged silk.

The same typical V-shaped distribution also applied to ovary volume along the ear at all sampling dates (Fig. 4C; Supplemental Fig. S1). In WW plants, the largest ovaries (ranking closest to 1) were located at positions 5 to 8 regardless of sampling date. Ovary volume decreased with position at both sides of positions 5 to 8 (Fig. 4D). This unchanged ranking of volume with time was due to the fact that relative expansion rates were uniform (0.43 mm<sup>3</sup> mm<sup>-3</sup> d<sup>-1</sup>) at all positions of the ear from 2.5 d before silk emergence until 7 d after it (Figs. 6A and 7). As a consequence, the curves representing time courses of ovary volumes were all parallel if expressed on a log scale, with different initial volumes on day 2.5 before silk emergence (Fig. 6A). Hence, the large difference in volume between ovaries at any time reflected a temporal pattern. Plants under water deficit followed the same pattern as WW plants for ovary growth during the period from tassel emergence to silk emergence (Figs. 6, B and C, and 7A), with a nearly uniform relative expansion rate in the whole ear but with lower values than in WW plants (0.27 and 0.13 mm<sup>3</sup> mm<sup>-3</sup> d<sup>-1</sup>).

Overall, the correspondence between position and time of emergence defines a position-time model by identifying cohorts of ovaries emerging and growing sequentially, each characterized by a common position on the ear (ring of ovaries on the ear; Figs. 3A and 4A) and a synchronous development (growth and silk emergence).

**The Duration of Silk Growth and Emergence Was Largely Reduced by Water Deficit and Accounted for the Differences in the Final Number of Ovaries Developing to Grains**

Tassel emergence was synchronous in the three watering treatments, followed by silk emergence after 2 to 3 d in WW plants regardless of experiments and

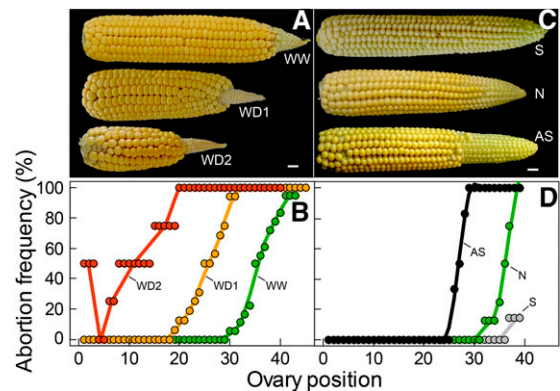


**Figure 3.** Abortion frequency of ovary cohorts as a function of ovary spatial position along the ear, with abortions due to water deficit in Exp1 (B) or to the timing of pollination in Exp3 (D). A and C show images of ears 23 d (A) and 15 d (C) after pollination. In B, green, WW treatment; yellow, WD1; red, WD2. In D, green, WW normal pollination (N); gray, synchronous pollination (S); black, asynchronous pollination (AS). Note that the scales differ between A and C (bars = 1 cm) and B and D because of the varying sizes of ovaries along the ear.

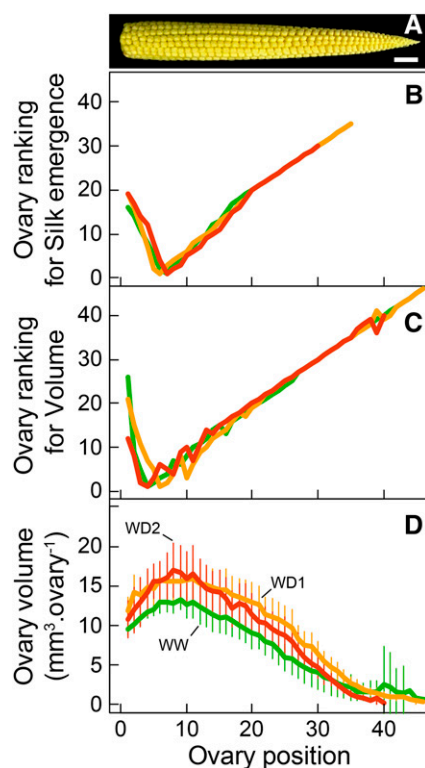


**Figure 4.** Ovary ranking for silk emergence (B), ovary ranking for volume (C), and ovary volume at silk emergence (D) as a function of ovary spatial position along the ear from base to apex in Exp1. A shows an image of an ear at silk emergence. Green, WW treatment; yellow, WD1; red, WD2. Error bars in D represent 90% confidence intervals ( $n \geq 4$ ). Bar in A = 1 cm.

genotypes and with a delay of 2.3 and 5.3 d, respectively, in WD1 and WD2 (Table II). Silk fresh weight was reduced significantly in WD1 and WD2 treatments on the first day of silk emergence and 7 d after it (Fig. 5A), in accordance with a reduced silk length (Supplemental Video S1). Silk dry weight was reduced to a lesser extent (data not shown).

Silk emergence occurred over the 7 to 8 d following the emergence of the first silk in WW plants of both Exp1 and Exp2 (Fig. 5, B and C). It stopped when nearly all ovaries of the ear (about 700; Fig. 1) carried an emerged silk (Fig. 5, B and C; i.e. when the silks of the most apical [youngest] cohort emerged from the husks). In WD2, silk emergence occurred for 2 d and stopped when 147 to 294 silks had emerged (Fig. 5C; Supplemental Video S1; i.e. less than half of ovary number). This duration was slightly longer in WD1 (Fig. 5B). All silks stopped growth simultaneously in a given plant, causing the end of silk emergence (arrows in Fig. 5A; Supplemental Video S1), probably including nonemerged silks whose apex was close to husk aperture at that time (data not shown). Furthermore, the arrest of silk growth under water deficit was independent of ovule fertilization because it occurred in extreme cases before the emergence of any silk. This was the case for 40% of plants of

hybrid B73\_H in Exp2, whose silks stopped growth inside the husks, without any pollination or fertilization.

The position-time model derived from the observed patterns (Fig. 4B), together with the time course of the number of emerged silks (Fig. 5, B and C), allows establishing a correspondence between the timing of silk emergence and ovary positions on the ear. At the time of emergence of cohort  $i$ , the accumulated number of emerged silks equals  $i \times r$ , where  $r$  is the number of silks per cohort (i.e. the number of ovaries per ring [16 for hybrid B73\_H]). This time  $t_i$  was calculated for each cohort by solving Equation 3 (see “Materials and Methods”) for  $SN_{t_i} = i \times r$ . Abortion frequencies of cohorts in the different treatments of Exp1 are presented in Figure 8A as a function of  $t_i$ . In WW plants of Exp1, all ovary cohorts carrying silks that emerged later than 4 d after the first silk finally aborted (Fig. 8A). The same applied to plants with water deficit but with shorter delays. Ovary cohorts carrying silks that emerged later than 2 d (respectively 1 d) after the first silk aborted in WD1 (respectively WD2) treatment. This switch to abortion was closely linked to the respective timings of silk emergence (that differed between cohorts) and of silk growth arrest (that was common to all cohorts). All basal cohorts that emerged

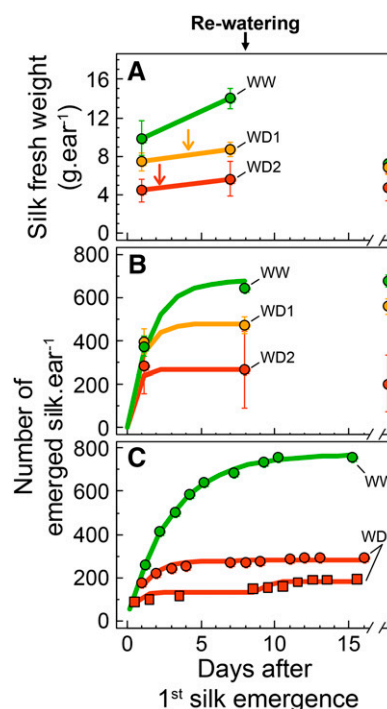


**Figure 5.** Time courses of silk fresh weight (A) and silk emergence in Exp1 (B) and Exp2 (C). Green, WW treatment; yellow, WD1; red, WD2 and WD3 in Exp1 and Exp2, respectively. Error bars represent 90% confidence intervals ( $n \geq 4$ ). Arrows in A indicate the date of silk growth arrest determined with time-lapse videos (Supplemental Video S1). Solid lines indicate regressions with a negative exponential equation. In C, a second equation was fitted after day 8 in one case.

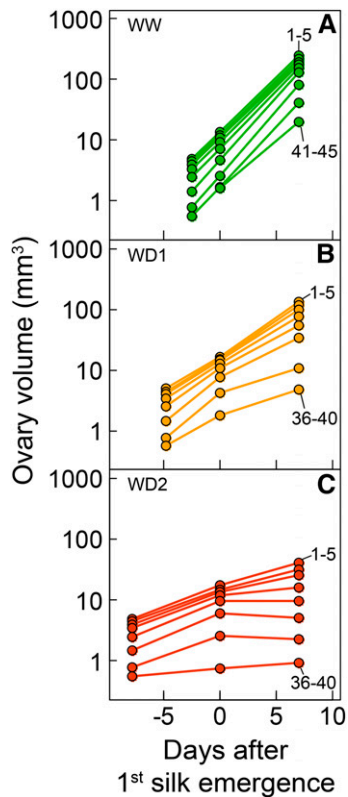


**Figure 6.** Time courses of the volume of ovary cohorts in WW (A), WD1 (B), and WD2 (C) treatments of Exp1. Ovary volumes are plotted in logarithmic scale against time after first silk emergence. Each point is the mean of five successive cohorts (1–5, 6–10, etc.) from first to 45th. Rewatering occurred 8 d after first silk emergence.

at least 2 d before silk growth arrest developed into grains, all (younger) apical cohorts that emerged on the day of silk growth arrest aborted, and cohorts with intermediate silk emergence had intermediate frequency of abortion (Fig. 8B). This rule proved valid for all studied hybrids subjected to WD1, WD2, or WD3, although the spatial position of the youngest aborted ovaries changed with hybrids and treatments (Fig. 3). Hence, the switch to abortion was probably (1) related to the timing of silk emergence rather than to spatial positions of ovaries and (2) already determined at the end of silk emergence (i.e. 2–3 d after the emergence of the first silk in plants subjected to water deficit).

#### Changes in Ovary Growth Rate Probably Occurred Later Than the Switch to Abortion

Most of the changes in abortion rate between treatments and between hybrids were already irreversible 2 to 3 d after the first silk emergence in water deficit. Indeed, the final number of emerged silks, fixed at silk growth arrest, largely accounted for differences in grain number between individual plants of Exp1 (Fig. 9A;  $r^2 = 0.75$ ). It also accounted for differences between

treatments and hybrids (Fig. 9B;  $r^2 = 0.94$ ). The 1:1 line in Figure 9A indicates situations in which all ovaries bearing emerged silks would develop into grains. The vertical distance to this line (i.e. the number of ovaries that aborted although their silks had emerged and were pollinated) corresponds to the silks emerging later than 4, 2, and 1 d after first silk emergence in WW, WD1, and WD2 treatments (Fig. 8A; i.e. the silks emerging during the last few days of the period of silk emergence).

The base-to-apex gradient of abortion frequency was not associated with ovary growth rate at pollination, because the relative expansion rates of apical ovaries did not differ significantly from those of basal ovaries in any treatment (Fig. 7A). It also was not linked to ovary volume at silk emergence, which did not differ significantly between treatments at this stage at any position along the ear (Fig. 4D). The reduction in ovary growth rate (Fig. 7A) was compensated for by the delay in silk emergence in water deficit plants (Table II). For example, ovary volume at the 23rd position from the ear base was close to 10 mm<sup>3</sup> in all treatments (Fig. 4D), whereas the abortion frequency for these ovaries was 0%, 25%, and 100% in WW, WD1, and WD2 treatments, respectively (Fig. 3B).

Appreciable gradients of relative expansion rate in the ear occurred after silk emergence (Fig. 7B). In both WD1 and WD2, basal (oldest) cohorts of ovaries continued growth with an unchanged relative expansion rate, whereas ovaries with more apical positions had a decreased rate. These changes were only appreciable 7 d after first silk emergence, suggesting that the decrease of ovary growth was a consequence of the switch to ovary abortion that occurred several days earlier, at the date of silk growth arrest.

#### A Second Cause for Ovary Abortion Is Linked to the Timing of Pollination

Asynchronous pollination resulted in total abortion of cohorts at the 24th to 30th ovary positions, where

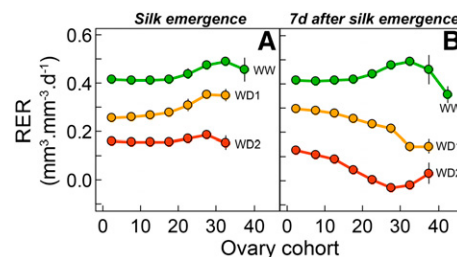


**Figure 7.** Relative expansion rate (RER) of ovary cohorts calculated from tassel emergence to first silk emergence (A) and from first silk emergence to 7 d after it (B). Each point is the mean of five successive cohorts from first to 45th. Green, WW treatment; yellow, WD1; red, WD2. Error bars are SE values ( $n = 5$ ).

**Table II.** Time interval between tassel emergence (TE) and first silk emergence (SE), and ASI in the three experiments

Water deficits were performed by reducing water supply from tassel emergence to 8 d after silk emergence. N, Normal pollination; S, synchronous pollination; AS, asynchronous pollination. All plants except in S and AS treatments were hand-pollinated daily with fresh pollen. Mean values (confidence interval  $P = 0.1$ ) of at least three plants are shown.

Experiment	Genotype	Treatment	TE to SE	ASI
<i>d</i>				
Exp1	B73_H	WW	2.45 (0.45)	-1.71 (0.32)
		WD1	4.74 (0.66)	0.65 (0.45)
		WD2	7.77 (1.82)	3.17 (1.42)
Exp2	B73_H	WW	2.67 (1.95)	0.33 (1.95)
		WD3	6.75 (3.66)	5.13 (3.59)
	F924_H	WW	1.67 (0.97)	0.33 (1.95)
		WD3	3.67 (3.07)	2.22 (3.26)
	MS153_H	WW	3.33 (1.95)	0.67 (2.57)
		WD3	7.13 (4.17)	5.38 (3.95)
Oh43_H	WW	2.00 (0.00)	0.50 (0.68)	
	WD3	5.11 (3.79)	3.78 (3.52)	
Exp3	B73_H	N	2.38 (0.61)	-2.12 (0.66)
		S	2.29 (0.55)	-2.57 (0.39)
		AS	2.50 (1.25)	-2.66 (0.85)

abortion did not occur under normal pollination (Fig. 3, C and D). The use of the position-time model showed that aborted cohorts were those with silk emergence occurring 2 to 4 d after first emergence. Synchronous pollination resulted in a near-zero abortion, including the most delayed ovary cohorts (more than 4-d delay). Aborted ovules were larger in plants with asynchronous pollination than in droughted plants (Fig. 3, A and C), consistent with the fact that abortion occurred later in the first case.

A common relationship between cohort age and abortion frequency was obtained for all treatments when considering the time of silk exposure to pollen relative to the time of first pollination (Fig. 10C) rather than the time after the first silk emergence (Fig. 10B). This suggests a role for the development of fertilized embryos at ear basal positions on the abortion of ovaries at apical positions. A natural split pollination occurred in WD1 in Exp1 (Fig. 5B), because of the second period of silk emergence that occurred after rewatering. Indeed, the number of emerged silks increased between the last two sampling dates (Fig. 5B). This was also observed on some plants in Exp2 (Fig. 5C). The newly emerged silks corresponded to silks that previously stopped growth inside the husks during the period of water deficit and recovered afterward, thereby reproducing a second period of pollination. Hence, split pollination changed the relationship between abortion frequency and date of silk emergence of the ovary cohorts (Fig. 10B). The increased vertical distance to the line 1:1 in Figure 9 in both artificial and natural (WD1) split pollination treatments corresponded to the abortion of late pollinated ovaries.

## DISCUSSION

### A First Switch to Abortion Linked to the Arrest of Silk Growth in Drought-Stressed Plants

In our analysis, the first switch to abortion results from the superposition of one event that occurs sequentially on the ear, namely silk emergence, and one event that occurs at a given time, namely silk growth arrest. Abortion was observed in those ovaries carrying silks that did not emerge at least 2 d before silk growth arrest, so the shorter duration of silk growth after emergence caused the increased abortion rate. This was observed here, with increasing abortion frequencies from plants with 8-d duration in WW conditions to 2- to 3-d duration in WD3. In one hybrid (B73\_H), silk growth even stopped before emergence in an appreciable proportion of plants, so this arrest was independent of ovule fertilization.

Abortion associated with water deficit during flowering time was already irreversible when silk emergence stopped, so 94% of drought-associated abortion was determined 2 to 3 d after the emergence of the first silk. The shorter duration of silk growth after silk emergence is probably the consequence of a slower silk elongation rate before emergence. The results of Fuad-Hassan et al. (2008) suggest that the duration from silk initiation to the end of growth is constant. The delay of silk emergence due to slower elongation rate, therefore, would result in a shorter duration of silk growth outside of the husks. Ultimately, silk elongation rate as affected by water deficit would be the cause of drought-related abortion, consistent with the fact that changes in the expression of genes associated with cell wall mechanical properties in silks were the first molecular events associated with drought in reproductive organs that eventually abort in the companion study (Oury et al., 2016).

The link between silk growth arrest and abortion could be due to the requirement of active silk growth to allow pollen tube progression along the silk. Indeed, tissue stiffening occurs after the end of silk growth, thereby blocking the progression of pollen tubes

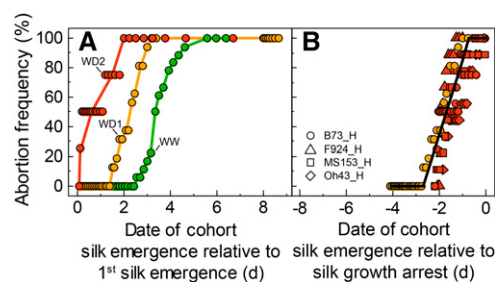


**Figure 8.** Abortion frequency of each ovary cohort as a function of the date of cohort silk emergence relative to the first silk emergence (A) or relative to the date of silk growth arrest (B). A, WW and water deficit plants in Exp1. B, water deficit plants in Exp1 and Exp2. Green, WW treatment; yellow WD1; red WD2 and WD3 in Exp1 and Exp2, respectively.

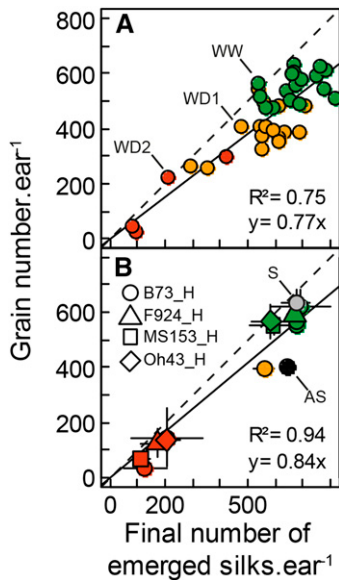


**Figure 9.** Grain number as a function of the final number of emerged silks. In A, each symbol represents a plant of Exp1. In B, each symbol represents mean values corresponding to one experimental treatment in Exp1 to Exp3. Green, WW and natural pollination; yellow, WD1; red, WD2 and WD3 in Exp1 and Exp2, respectively; gray, synchronous pollination (S); black, asynchronous pollination (AS). Solid lines indicate linear regression, and dashed lines indicate 1:1. Error bars represent 90% confidence intervals ( $n \geq 3$ ). All plants were hand-pollinated daily with fresh pollen except in treatments S and AS.

(Kapu and Cosgrove, 2010). The limit of 1 to 2 d before silk growth arrest might be linked to the necessary time for a pollen tube to reach the ovary through the silk (Miller, 1919). Alternatively, this limit of 1 to 2 d could correspond to the end of the period of sensitivity of ovaries to plant water status, which would occur when ovule tissues become hydraulically isolated from the mother tissues a few days after fertilization (Westgate and Grant, 1989; Bradford, 1994). In that case, abortion would include embryos just after fertilization (Westgate and Boyer, 1986).

The spatial gradients of abortion frequency, resulting from the difference in timing for silk growth and emergence across water deficit treatments and genotypes, share similarities with those observed in other species for which abortion follows the reciprocal of the pollination/fertilization gradient for ovaries within a fruit (Rocha and Stephenson, 1991; Susko, 2006), between fruits within an inflorescence (Cawoy et al., 2007), or between inflorescences within a plant (Ney et al., 1994; Egli and Bruening, 2006).

In our analysis, ovary abortion was not linked directly to ovary growth itself, which appeared as largely unrelated to abortion both temporally and spatially in the ear. In particular, the relative expansion rate of ovaries was affected at pollination by the same ratio in basal ovaries that will develop into grains and in apical ovaries that will abort later on. Accordingly, the decreased growth rate observed 7 d later for ovaries

prone to abort could be the consequence and not the cause of an abortion that had already been induced several days before. Carbon availability was probably not involved either, consistent with an analysis of sugar content and activities of enzymes related to carbon metabolism, which showed no link with abortion rate at this stage in a companion study (Oury et al., 2016). Processes controlling water movements toward ovaries and silks are more likely to explain the synchronous silk growth arrest across all ovaries under water deficit. This would be consistent with studies indicating that moderate water deficits affect growth processes while organ and plant carbon status is preserved or even improved (Hummel et al., 2010; Muller et al., 2011).

### A Second Switch to Abortion Linked to the Timing of Fertilization of Emerged Silks

This second switch had a small effect on abortion in water deficit, in which fertilization was almost synchronous for all ovaries because of the short window of time from silk emergence to the end of silk growth. It caused appreciable abortion in WW plants (up to 20%), with differences between hybrids, or when plant rehydration allowed silks to resume growth. Consistent with previous studies (Cárcova et al., 2000; Cárcova and Otegui, 2007; Uribebarrea et al., 2008), this second switch to abortion had a large effect when a delay of fertilization was caused by the artificial asynchrony of silk emergence or by rewatering plants with arrested silks. This caused abortion of the last cohorts of ovaries with a postponed silk exposure. This second switch was suppressed when all silks were fertilized synchronously in WW plants.

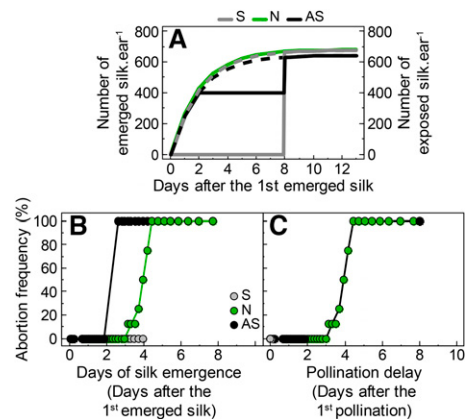


**Figure 10.** A, Time course of silk emergence and silk exposure to pollen. B and C, Abortion frequency of each ovary cohort as a function of the time of silk emergence (B) or silk exposure to pollen (C) relative to first silk emergence (B) or first silk exposure (C) in Exp3. Solid lines in A represent the number of exposed silks, which differed from the number of emerged silks (dashed line) during the time ears were covered in synchronous pollination (S) and asynchronous pollination (AS) treatments. Green, WW and normal pollination (N); gray, synchronous pollination; black, asynchronous pollination.

This suggests that ovaries progressively lose competence to develop into grains after the first fertilization, so a delay in pollination would cause abortion. This abortion mechanism could be that fertilization of the oldest ovules causes a whole-ear signaling process that provokes abortion of the youngest ovaries after a given time, as is the case in pea (*Pisum sativum*; Guillioni et al., 1997). This signal remains unknown in maize but may imply cytokinins synthesized during the early development of grains (Brugière et al., 2003), abscisic acid (Wang et al., 2002; Setter and Parra, 2010; Setter et al., 2011), or ethylene (Cheng and Lur, 1996; Habben et al., 2014).

### The Events Described Here Occurred Earlier Than Those Classically Considered to Cause Abortion

The view presented above differs appreciably from that proposed by Boyer and coworkers (Boyle et al., 1991; Zinselmeier et al., 1995a, 1995b, 1995c, 1999; McLaughlin and Boyer, 2004). The experimental protocol common to these studies avoided the interaction between water deficit and silk growth occurring in natural field conditions and the two switches to abortion presented above. Indeed, in these studies, water deficit only became noticeable 2 d after silk emergence. This avoided the first switch involving silk arrest, which, according to our study, would essentially occur from 8 d before to 2 d after silk emergence. Additionally, silks were prevented from pollination after silk emergence and fertilized synchronously 5 or 6 d after it (Zinselmeier et al., 1995a, 1995b, 1995c, 1999; McLaughlin and Boyer, 2004), thereby avoiding the switch associated with pollination delay, as in the treatment with synchronous pollination in our study.

It is logical, therefore, that the series of studies by Boyer and coworkers pointed out a third switch, different from those of our study, namely carbon limitation during the postsilking period. A companion to our study (Oury et al., 2016) shows that the first signs of carbon starvation occurred 5 d after silk emergence in a series of experiments with the same protocol as that of this study. The expression of invertase genes increased in ovaries developing into grains but not in ovaries that eventually abort, consistent with previous studies (Andersen et al., 2002; McLaughlin and Boyer, 2004; Qin et al., 2004). The mechanisms associated with this period of time are unlikely to have contributed appreciably to ovary abortion in our study, given the timing of abortion, which ended 2 to 3 d after silk emergence in water deficit.

### Consequences for Breeding for a Reduced Abortion Rate, for Phenotyping, and for Modeling

Reducing seed number under water deficit is an evolutionary process allowing plants to produce at least a few viable seeds so their alleles are not lost during dry years (Tardieu et al., 2014). Farmers and breeders most often wish to reduce these protections, because allele

viability is usually not a major issue in agronomic conditions in which seeds can be produced in dedicated fields with favorable conditions. Farmers also wish to reduce abortion because they usually do not place plants in very dry scenarios involving a risk of total plant failure, so tolerance to mild or moderate drought scenarios is the main issue for agriculture in drought-prone environments (Tardieu, 2012; Harrison et al., 2014; Gaffney et al., 2015). Therefore, we propose that silk growth and emergence are crucial processes to take into account in breeding because they occur in moderate stresses, whereas a maintained carbon supply to ovaries in water deficit might be less crucial because this maintenance is preserved in mild or moderate water deficits observed in the field. The comparison between four hybrids suggests that an appreciable genetic variability in silk growth and emergence may exist, with a larger sensitivity for the hybrid B73\_H than for the other three studied hybrids.

Phenotyping silk growth and expansion is a difficult task at least at a throughput compatible with genetic analyses. Direct phenotyping of grain number is not fully satisfactory, because grain number per unit area involves earlier events such as plant emergence and early vigor and other traits such as the number of rows per ear and of ovaries per row. High-throughput phenotyping for silk growth might be feasible via image analysis. An alternative might emerge from the genetic correlation between silk growth and leaf growth proposed by our group. In particular, the quantitative trait loci for silk weight and leaf elongation rate largely collocate in maize (Dignat et al., 2013). Those for ASI, which reflect silk growth rate (Fuad-Hassan et al., 2008), also largely collocate with quantitative trait loci of leaf elongation rate in plants subjected to water deficit (Welcker et al., 2007). This results in the unexpected fact that the sensitivity of grain number to water deficit in the field has a high genetic correlation with the sensitivity of leaf growth to water deficit measured in a phenotyping platform (Chapuis et al., 2012). If this is confirmed by further studies, phenotyping for silk growth could be at least partly deduced from that of leaf growth under water deficit (Sadok et al., 2007).

Finally, the results presented here bring elements in the current debate on plant growth drivers (carbon source versus sink-driven processes) into crop or vegetation models (Fatichi et al., 2014). They potentially have a large impact on the modeling of grain abortion and grain set, most often unsatisfactory in crop models (Boote et al., 2013). Instead of simulating them as a result of plant carbon status, it would be possible to consider the silk growth of ovary cohorts in a model, which is currently under way (C. Messina and G. Hammer, personal communication).

## MATERIALS AND METHODS

### Plant Material, Growing Conditions, and Pollination

Three experiments were carried out (Table I). Maize (*Zea mays*) plants were grown in a greenhouse in cylindrical plastic pots (12 L for Exp1 and Exp3 and

9 L for Exp2) at a plant density of three plants  $m^{-2}$ . The genetic material included four maize hybrids obtained from the cross of the flint line UH007 with the dent lines B73, F924, MS153, and Oh43. Three seeds per pot were sown in compost composed of clay and peat 30:70 (v/v) enriched in minerals. Plants were thinned to one per pot at the two-leaf stage. Each pot was placed on a balance that allowed calculating soil water content from pot weight, corrected for plant weight estimated by regularly sampling plants (Caldeira et al., 2014). All plants were maintained at a soil  $\Psi_p$  above  $-0.12$  MPa by daily irrigation, except for a short period around flowering for plants in water deficit treatments (Fig. 2A).

At tassel emergence, recorded individually in each plant, water was withheld until soil water content reached the desired soil  $\Psi_p$  (Fig. 2A). Pots were then watered at the end of each day to restore the desired soil  $\Psi_p$ , namely  $-0.22$  and  $-0.48$  MPa for WD1 and WD2 treatments of Exp1 and  $-0.6$  MPa in the water deficit of Exp2 (for details, see Caldeira et al., 2014). Soil  $\Psi_p$  decreased during the day and reached  $-0.44$  MPa in WD1 and  $-0.98$  MPa in WD2 and WD3 (Fig. 2; Supplemental Fig. S2).

Plants were transferred into a growth chamber from tassel emergence to 7 d after silk emergence in Exp1, while they remained in the greenhouse in Exp2 (Table 1). All plants were hand-pollinated twice a day with fresh pollen originating from WW plants distributed in the greenhouse or in the growth chamber until the last emerged silks became senescent. Exp3, involving pollination treatments, was carried out in the greenhouse in WW conditions similar to those in the other two experiments. Two pollination treatments were carried out in addition to the pollination technique presented above. Synchronous pollination was obtained by enclosing ears in bags from silk emergence to 8 d after it and then pollinating all silks with fresh pollen. An asynchronous pollination was obtained by pollinating silks for the 2 d following silk emergence, then enclosing ears in bags for 6 d, and finally pollinating all silks. Plants with silks cut every day in Exp2 (see below) were hand-pollinated 1 h after silks were cut, without any decrease in pollination success and grain set.

## Photosynthesis Measurement

Plant photosynthesis was followed in Exp1 from 3 d after tassel emergence until 7 d after silk emergence on the ear leaf (leaf number 10 or 11) using the CIRAS-2 portable gas-exchange system (PP Systems) with a  $2.5\text{-cm}^2$  leaf chamber and an air flow rate of  $300\text{ cm}^3\text{ s}^{-1}$ . Light intensity was  $425\text{ }\mu\text{mol m}^{-2}\text{ s}^{-1}$  both in the growth chamber at leaf level and in the gas-exchange system. Air temperature and vapor pressure deficit in the chamber of CIRAS-2 also mimicked the environmental conditions in the growth chamber (i.e.  $25^\circ\text{C}$  and  $1\text{--}1.5$  kPa). Measurements were carried out for the whole photoperiod (16 h) of four, 19, and five plants in WW, WD1, and WD2 treatments, respectively (Supplemental Fig. S2).

## Plant Sampling, Ovary Volume, and Relative Expansion Rate

Ears were sampled 1 d after tassel emergence, at silk emergence, and then 7 and 23 d after silk emergence in each treatment of Exp1. The first sampling was common to all treatments because it occurred before any water deficit. Ears were sampled 23 and 15 d after silk emergence in Exp2 and Exp3, respectively. Hence, sampling dates followed individual developmental stages of individual plants. Samples were collected at the end of the day, and fresh weights of ear and silks were measured immediately. Ears were photographed, and ovary or grain number and dimensions were measured with the software ImageJ. The width ( $W_o$ ) and height ( $H_o$ ) of each ovary were measured at each position along the row counted from the ear base. The ratio of cob diameter to ear diameter ( $R_{c/e}$ ) was measured on ear cross sections across sampling dates, positions along the ear, and genotypes. Considering that ovary rows are contiguous without space between them and that ear cross sections are circular, ovary cross sections occupy the external ring of a circle of circumference  $N_o \times W_o$ , where  $N_o$  is the number of rows and  $W_o$  is the mean ovary width at the considered position. Ovary volume ( $V$ ) was calculated at each position along the rows as the product of cross-sectional ovary area and ovary height according to the following equation:

$$V = \frac{H_o N_o W_o^2 (1 - R_{c/e}^2)}{4\pi}$$

Because ovary growth was essentially exponential during the period studied, we characterized it with the rate of the exponential curve of ovary volume against time:

$$V = V_0 \exp(RER \times t)$$

The ovary relative expansion rate ( $RER$ ) between two sampling times,  $t_1$  and  $t_2$ , was calculated at each position along the ear from the average volume measured at  $t_1$  ( $V_1$ ) and  $t_2$  ( $V_2$ ):

$$RER = \ln(V_2/V_1)/(t_2 - t_1)$$

## Silk Emergence Dynamics and Grain Number

The number of emerged silks was determined daily in Exp3 on three plants per treatment with the method described by Cárcova et al. (2000). Exposed sections of silks were cut from the apical ear of the same plants. All newly exposed silks, characterized by their bisected apical end, were manually counted to develop a cumulative curve of silk emergence. Sampled silk sections were stored in 90% (v/v) ethanol solution at  $4^\circ\text{C}$  before counting. The number of exposed silks was counted in the same way at three developmental stages in Exp1. It was counted every day in Exp2. The number of emerged silks  $SN_t$  against time  $t$  was fitted to a negative exponential equation:

$$SN_t = SN_f(1 - \exp(-a(t - t_0)))$$

where  $SN_f$  was the final number of emerged silks and  $t_0$  was the time of first silk emergence.

In addition, silk apices emerging out of the husks were marked with black ink in 24 plants per treatment of Exp2. Husk tissues were gently removed with a fine scalpel blade, taking care to avoid breaking the ovary-silk junctions, to allow a clear view of successive flowers and silks along the ear. The number of emerged silks inserted at each spatial position was counted to calculate the frequency of each flower position among the emerged silks. Furthermore, time-lapse videos were performed on 12 ears. Image capture was performed with an automaton, based on a Raspberry Pi (model B revision 2, Farnell element 14), which controlled image capture every 5 min of several USB cameras (C920; Logitech) and triggered additional lighting during the night at the moment of capture (approximately 4 s). Time-lapse videos are available as Supplemental Videos S1 and S2. The number of aborted ovaries was estimated at the last sampling date (15, 20, and 23 d after silk emergence in Exp3, Exp2, and Exp1, respectively).

## Statistical Analyses

Comparisons of mean values between treatments, experiments, and genotypes were performed using Kruskal-Wallis nonparametric tests. All analyses were performed using R (R Core Team, 2013). The parameters of Equations 2 and 4 were estimated for each plant or treatment by least-squares fitting, using an algorithm of generalized reduced gradient (Marquardt-Levenberg algorithm in the software Sigma Plot 2004 version 9.0; SPSS Science).  $\text{SE}$  values on parameters were provided by the software.

## Supplemental Data

The following supplemental materials are available.

**Supplemental Figure S1.** Ovary ranking for volume as a function of ovary spatial position along the ear.

**Supplemental Figure S2.** Daily course of soil water potential, plant transpiration, and net photosynthesis in Exp1.

**Supplemental Video S1.** Time-lapse video of silk emergence in a maize plant under water deficit.

**Supplemental Video S2.** Time-lapse video of silk emergence in a well-watered maize plant.

## ACKNOWLEDGMENTS

We thank Benoît Suard, Stéphane Berthézène, Ivan Peironnenche, Célia Pequignot, and Julia Soewarto for technical support, Cloé Check and David Verney for silk counting, and Vincent Nègre for the video automaton.

Received February 20, 2015; accepted November 21, 2015; published November 23, 2015.

## LITERATURE CITED

- Andersen MN, Asch F, Wu Y, Jensen CR, Naested H, Mogensen VO, Koch KE (2002) Soluble invertase expression is an early target of drought stress during the critical, abortion-sensitive phase of young ovary development in maize. *Plant Physiol* **130**: 591–604
- Bolaños J, Edmeades GO (1996) The importance of the anthesis-silking interval in breeding for drought tolerance in tropical maize. *Field Crops Res* **48**: 65–80
- Bonnett OT (1940) Development of the staminate and pistillate inflorescence of sweet corn. *J Agric Res* **60**: 25–37
- Boote KJ, Jones JW, White JW, Asseng S, Lizaso JI (2013) Putting mechanisms into crop production models. *Plant Cell Environ* **36**: 1658–1672
- Boyer JS, Westgate ME (2004) Grain yields with limited water. *J Exp Bot* **55**: 2385–2394
- Boyle MG, Boyer JS, Morgan PW (1991) Stem infusion of liquid culture medium prevents reproductive failure of maize at low water potential. *Crop Sci* **31**: 1246–1252
- Bradford KJ (1994) Water stress and the water relations of seed development: a critical review. *Crop Sci* **34**: 1–11
- Brugière N, Jiao S, Hantke S, Zinselmeier C, Roessler JA, Niu X, Jones RJ, Habben JE (2003) Cytokinin oxidase gene expression in maize is localized to the vasculature, and is induced by cytokinins, abscisic acid, and abiotic stress. *Plant Physiol* **132**: 1228–1240
- Caldeira CF, Bosio M, Parent B, Jeanguenin L, Chaumont F, Tardieu F (2014) A hydraulic model is compatible with rapid changes in leaf elongation under fluctuating evaporative demand and soil water status. *Plant Physiol* **164**: 1718–1730
- Cárcova J, Otegui ME (2001) Ear temperature and pollination timing effects on maize kernel set. *Crop Sci* **41**: 1809–1815
- Cárcova J, Otegui ME (2007) Ovary growth and maize kernel set. *Crop Sci* **47**: 1104–1110
- Cárcova J, Uribelarrea M, Borrás L, Otegui ME, Westgate ME (2000) Synchronous pollination within and between ears improves kernel set in maize. *Crop Sci* **40**: 1056–1061
- Cawoy V, Lutts S, Ledent JF, Kinet JM (2007) Resource availability regulates reproductive meristem activity, development of reproductive structures and seed set in buckwheat (*Fagopyrum esculentum*). *Physiol Plant* **131**: 341–353
- Chapuis R, Delluc C, Debeuf R, Tardieu F, Welcker C (2012) Resilience to water deficit in a phenotyping platform and in the field: how related are they in maize? *Eur J Agron* **42**: 59–67
- Cheng CY, Lur HS (1996) Ethylene may be involved in abortion of the maize caryopsis. *Physiol Plant* **98**: 245–252
- Cooper M, Ghossein C, Leafgren R, Tang T, Messina C (2014) Breeding drought-tolerant maize hybrids for the US corn-belt: discovery to product. *J Exp Bot* **65**: 6191–6204
- Denmead OT, Shaw RH (1960) The effects of soil moisture stress at different stages of growth on the development and yield of corn. *Agron J* **52**: 272–274
- Dignat G, Welcker C, Sawkins M, Ribaut JM, Tardieu F (2013) The growths of leaves, shoots, roots and reproductive organs partly share their genetic control in maize plants. *Plant Cell Environ* **36**: 1105–1119
- Duvick DN (2005) The contribution of breeding to yield advances in maize (*Zea mays* L.). *Adv Agron* **86**: 83–145
- Edmeades GO, Bolaños J, Elings A, Ribaut JM, Banziger M, Westgate ME (2000) The role and regulation of the anthesis-silking interval in maize. In: Edmeades GO, Bänziger M, Edmeades GO, eds. *Physiology and Modeling Kernel Set in Maize*, Vol. 29. Crop Science Society of America, Madison, WI, pp 43–73
- Edmeades GO, Bolaños J, Hernandez M, Bello S (1993) Causes for silk delay in a lowland tropical maize population. *Crop Sci* **33**: 1029–1035
- Egli DB, Bruening WP (2006) Fruit development and reproductive survival in soybean: position and age effects. *Field Crops Res* **98**: 195–202
- Erickson RO, Michelini FJ (1957) The plastochron index. *Am J Bot* **44**: 297–305
- Fatichi S, Leuzinger S, Körner C (2014) Moving beyond photosynthesis: from carbon source to sink-driven vegetation modeling. *New Phytol* **201**: 1086–1095
- Freier G, Vilella F, Hall AJ (1984) Within-ear pollination synchrony and kernel set in maize. *Maydica* **29**: 317–324
- Fuad-Hassan A, Tardieu F, Turc O (2008) Drought-induced changes in anthesis-silking interval are related to silk expansion: a spatio-temporal growth analysis in maize plants subjected to soil water deficit. *Plant Cell Environ* **31**: 1349–1360
- Gaffney J, Schussler JR, Löffler C, Cai W, Paszkiewicz S, Messina C, Groeteke J, Keaschall J, Cooper M (2015) Industry scale evaluation of maize hybrids selected for increased yield in drought stress conditions of the U.S. Corn Belt. *Crop Sci* **55**: 1608–1618
- Grant RF, Jackson BS, Kiniry JR, Arkin GF (1989) Water deficit timing effects on yield components in maize. *Agron J* **81**: 61–65
- Guilioni L, Wery J, Tardieu F (1997) Heat stress-induced abortion of buds and flowers in pea: is sensitivity linked to organ age or to relations between reproductive organs? *Ann Bot (Lond)* **80**: 159–168
- Habben JE, Bao X, Bate NJ, DeBruin JL, Dolan D, Hasegawa D, Helentjaris TG, Lafitte RH, Lovan N, Mo H, et al (2014) Transgenic alteration of ethylene biosynthesis increases grain yield in maize under field drought-stress conditions. *Plant Biotechnol J* **12**: 685–693
- Harrison MT, Tardieu F, Dong Z, Messina CD, Hammer GL (2014) Characterizing drought stress and trait influence on maize yield under current and future conditions. *Glob Change Biol* **20**: 867–878
- Hummel I, Pantin F, Sulpice R, Piques M, Rolland G, Dauzat M, Christophe A, Pervent M, Bouteillé M, Stitt M, et al (2010) *Arabidopsis* plants acclimate to water deficit at low cost through changes of carbon usage: an integrated perspective using growth, metabolite, enzyme, and gene expression analysis. *Plant Physiol* **154**: 357–372
- Kapu NUS, Cosgrove DJ (2010) Changes in growth and cell wall extensibility of maize silks following pollination. *J Exp Bot* **61**: 4097–4107
- Kiesselbach TA (1949) The structure and reproduction of corn. *Research Bulletin* 161. University of Nebraska, Lincoln, NE
- Lobell DB, Roberts MJ, Schlenker W, Braun N, Little BB, Rejesus RM, Hammer GL (2014) Greater sensitivity to drought accompanies maize yield increase in the U.S. Midwest. *Science* **344**: 516–519
- McLaughlin JE, Boyer JS (2004) Sugar-responsive gene expression, invertase activity, and senescence in aborting maize ovaries at low water potentials. *Ann Bot (Lond)* **94**: 675–689
- Meicenheimer RD (2014) The plastochron index: still useful after nearly six decades. *Am J Bot* **101**: 1821–1835
- Miller EC (1919) Development of the pistillate spikelet and fertilization in *Zea mays* L. *J Agric Res* **18**: 881–916
- Muller B, Pantin F, Génard M, Turc O, Freixes S, Piques M, Gibon Y (2011) Water deficits uncouple growth from photosynthesis, increase C content, and modify the relationships between C and growth in sink organs. *J Exp Bot* **62**: 1715–1729
- Ney B, Duthion C, Turc O (1994) Phenological response of pea to water-stress during reproductive development. *Crop Sci* **34**: 141–146
- Oury V, Caldeira CF, Prodhomme D, Pichon JP, Gibon Y, Tardieu F, Turc O (2016) Is change in ovary carbon status a cause or a consequence of maize ovary abortion in water deficit during flowering? *Plant Physiol* **171**: 997–1008
- Qin LX, Trouverie J, Chateau-Joubert S, Simond-Cote E, Thevenot C, Prioul JL (2004) Involvement of the *Ivr2*-invertase in the perianth during maize kernel development under water stress. *Plant Sci* **166**: 371–379
- R Core Team (2013) R: A Language and Environment for Statistical Computing. R Foundation for Statistical Computing, Vienna
- Rocha OJ, Stephenson AG (1991) Order of fertilization within the ovary of *Phaseolus coccineus* L. *Sex Plant Reprod* **4**: 126–131
- Sadok W, Naudin P, Boussuge B, Muller B, Welcker C, Tardieu F (2007) Leaf growth rate per unit thermal time follows QTL-dependent daily patterns in hundreds of maize lines under naturally fluctuating conditions. *Plant Cell Environ* **30**: 135–146
- Schussler JR, Westgate ME (1991) Maize kernel set at low water potential. II. Sensitivity to reduced assimilates at pollination. *Crop Sci* **31**: 1196–1203
- Schussler JR, Westgate ME (1995) Assimilate flux determines kernel set at low water potential in maize. *Crop Sci* **35**: 1074–1080
- Setter TL, Parra R (2010) Relationship of carbohydrate and abscisic acid levels to kernel set in maize under postpollination water deficit. *Crop Sci* **50**: 980–988
- Setter TL, Yan J, Warburton M, Ribaut JM, Xu Y, Sawkins M, Buckler ES, Zhang Z, Gore MA (2011) Genetic association mapping identifies single nucleotide polymorphisms in genes that affect abscisic acid levels in maize floral tissues during drought. *J Exp Bot* **62**: 701–716
- Susko DJ (2006) Effect of ovule position on patterns of seed maturation and abortion in *Robinia pseudoacacia* (Fabaceae). *Can J Bot* **84**: 1259–1265

- Tardieu F** (2012) Any trait or trait-related allele can confer drought tolerance: just design the right drought scenario. *J Exp Bot* **63**: 25–31
- Tardieu F, Parent B, Caldeira CF, Welcker C** (2014) Genetic and physiological controls of growth under water deficit. *Plant Physiol* **164**: 1628–1635
- Uribelarrea M, Cárcova J, Borrás L, Otegui ME** (2008) Enhanced kernel set promoted by synchronous pollination determines a tradeoff between kernel number and kernel weight in temperate maize hybrids. *Field Crops Res* **105**: 172–181
- Wang Z, Mambelli S, Setter TL** (2002) Abscisic acid catabolism in maize kernels in response to water deficit at early endosperm development. *Ann Bot (Lond)* **90**: 623–630
- Welcker C, Boussuge B, Bencivenni C, Ribaut JM, Tardieu F** (2007) Are source and sink strengths genetically linked in maize plants subjected to water deficit? A QTL study of the responses of leaf growth and of anthesis-silking interval to water deficit. *J Exp Bot* **58**: 339–349
- Westgate ME, Boyer JS** (1986) Reproduction at low silk and pollen water potentials in maize. *Crop Sci* **26**: 951–956
- Westgate ME, Grant DL** (1989) Water deficits and reproduction in maize: response of the reproductive tissue to water deficits at anthesis and mid-grain fill. *Plant Physiol* **91**: 862–867
- Zinselmeier C, Jeong BR, Boyer JS** (1999) Starch and the control of kernel number in maize at low water potentials. *Plant Physiol* **121**: 25–36
- Zinselmeier C, Lauer MJ, Boyer JS** (1995a) Reversing drought-induced losses in grain-yield: sucrose maintains embryo growth in maize. *Crop Sci* **35**: 1390–1400
- Zinselmeier C, Westgate ME, Jones RJ** (1995b) Kernel set at low water potential does not vary with source/sink ratio in maize. *Crop Sci* **35**: 158–163
- Zinselmeier C, Westgate ME, Schussler JR, Jones RJ** (1995c) Low water potential disrupts carbohydrate metabolism in maize (*Zea mays* L.) ovaries. *Plant Physiol* **107**: 385–391



# Is Change in Ovary Carbon Status a Cause or a Consequence of Maize Ovary Abortion in Water Deficit during Flowering?<sup>1</sup>[OPEN]

Vincent Oury, Cecilio F. Caldeira<sup>2</sup>, Dyuên Prodhomme, Jean-Philippe Pichon, Yves Gibon, François Tardieu, and Olivier Turc\*

INRA, UMR 759 LEPSE, 34060 Montpellier, France (V.O., C.F.C., F.T., O.T.); INRA, UMR Biologie du Fruit et Pathologie, 33883 Villenave d'Ornon, France (D.P., Y.G.); INRA, Plateforme Métabolome Bordeaux, 33883 Villenave d'Ornon, France (D.P.); and Biogemma, Centre de Recherche de Chappes, 63720 Chappes, France (J.-P.P.)

ORCID IDs: 0000-0003-2994-0111 (V.O.); 0000-0003-4762-3515 (C.F.C.); 0000-0002-4220-1404 (J.-P.P.); 0000-0003-0659-1406 (O.T.).

Flower or grain abortion causes large yield losses under water deficit. In maize (*Zea mays*), it is often attributed to a carbon limitation via the disruption of sucrose cleavage by cell wall invertases in developing ovaries. We have tested this hypothesis versus another linked to the expansive growth of ovaries and silks. We have measured, in silks and ovaries of well-watered or moderately droughted plants, the transcript abundances of genes involved in either tissue expansion or sugar metabolism, together with the concentrations and amounts of sugars, and with the activities of major enzymes of carbon metabolism. Photosynthesis and indicators of sugar export, measured during water deprivation, suggested sugar export maintained by the leaf. The first molecular changes occurred in silks rather than in ovaries and involved genes affecting expansive growth rather than sugar metabolism. Changes in the concentrations and amounts of sugars and in the activities of enzymes of sugar metabolism occurred in apical ovaries that eventually aborted, but probably after the switch to abortion of these ovaries. Hence, we propose that, under moderate water deficits corresponding to most European drought scenarios, changes in carbon metabolism during flowering time are a consequence rather than a cause of the beginning of ovary abortion. A carbon-driven ovary abortion may occur later in the cycle in the case of carbon shortage or under very severe water deficits. These findings support the view that, until the end of silking, expansive growth of reproductive organs is the primary event leading to abortion, rather than a disruption of carbon metabolism.

Water deficit (WD) largely decreases yield, with a maximum effect during flowering time in several species (Lilley and Fukai, 1994; Saini and Westgate, 2000; Rapoport et al., 2012). In maize (*Zea mays*), ovary development is highly drought sensitive (Boyer and

Westgate, 2004) while pollen viability is not (Herrero and Johnson, 1981; Schoper et al., 1986, 1987). A disruption of carbon metabolism in ovaries has been suggested to be the main cause of abortion, based on a series of experiments showing that Suc feeding can partly reverse the effect of WD on abortion (Boyle et al., 1991; Zinselmeier et al., 1995a, 1999; McLaughlin and Boyer, 2004). These experiments had a common protocol in which a WD was imposed for 6 d following silk emergence (SE) and caused a drastic reduction in photosynthesis and starch content in ovaries (Zinselmeier et al., 1999). The Suc flux to ovaries decreased to near zero but was partly restored upon Suc feeding (Mäkelä et al., 2005). Enzyme activities and gene expression of cell wall invertases increased 5 to 8 d after silking in ovaries of well-watered (WW) plants, whereas they remained low under WD (Zinselmeier et al., 1995b, 1999; McLaughlin and Boyer, 2004). This led several authors to consider cell wall invertases, in particular *INCW2*, as a causal link between WD, sugar availability to ovaries, and ovary abortion (Boyer and McLaughlin, 2007; Ruan et al., 2012). We use the term abortion here in its broad sense: arrest of development of an organ (flower, ovary, grain, etc.). Therefore, it is not restricted to the failure of zygotic development after fertilization

<sup>1</sup> This work was supported by the European Union (grant no. FP7–244374) and the Agence Nationale de la Recherche (grant no. ANR–08–GENM–003).

<sup>2</sup> Present address: Vale Institute of Technology Sustainable Development, Rua Boaventura da Silva, 955 Nazaré, 66055–090 Belém, Pará, Brazil.

\* Address correspondence to [olivier.turc@supagro.inra.fr](mailto:olivier.turc@supagro.inra.fr).

The author responsible for distribution of materials integral to the findings presented in this article in accordance with the policy described in the Instructions for Authors ([www.plantphysiol.org](http://www.plantphysiol.org)) is: Olivier Turc ([olivier.turc@supagro.inra.fr](mailto:olivier.turc@supagro.inra.fr)).

O.T. conceived the research and supervised the experiments and the data analysis; V.O. designed and performed the experiments and analyzed the data; D.P. performed the biochemical analyses under the supervision of Y.G.; J.-P.P. supervised transcript analyses; V.O. and C.F.C. performed analysis and interpretation of transcript data; F.T. supervised the research; O.T. and F.T. wrote the article with contributions of all the authors.

[OPEN] Articles can be viewed without a subscription.

[www.plantphysiol.org/cgi/doi/10.1104/pp.15.01130](http://www.plantphysiol.org/cgi/doi/10.1104/pp.15.01130)

but also includes the developmental arrest of ovary (or floret) occurring earlier.

Several arguments have led us to question the generality of the link between carbon metabolism and ovary abortion under WD.

(1) A decreased photosynthesis at flowering time has a lesser effect on ovary abortion if caused by low light rather than by WD (Schussler and Westgate, 1991; Hiyane et al., 2010), whereas drought-caused abortion can occur without appreciable depletion of ovary sugar content (Schussler and Westgate, 1995; Andersen et al., 2002). This suggests a direct effect of low water potential, independent of assimilate supply (Schussler and Westgate, 1991).

(2) Several studies indicate that carbon availability to growing organs is increased by moderate WDs in different species because growth processes are more affected than carbon assimilation (Hummel et al., 2010; Muller et al., 2011; Pantin et al., 2013). The dependency of ovary abortion upon carbon supply, therefore, might be lower under moderate drought scenarios representative of European field conditions (Harrison et al., 2014) than under the severe drought stress occurring in the studies mentioned by Boyer and McLaughlin (2007) and Ruan et al. (2012).

(3) We show in a companion article that the causal link between WD at flowering time and ovary abortion involves the growth arrest of silks 2 to 3 d after first SE (Oury et al., 2016). In this case, abortion concerns the youngest apical ovaries whose silks did not emerge 2 d before silk arrest, irrespective of ovary growth rate (Oury et al., 2016). This suggests that the carbon supply to ovaries would not be involved directly, and one could expect that the earliest molecular events associated with abortion should occur in silks rather than in ovaries. Furthermore, the changes in ovary sugar content and enzyme activities, measured in several studies 5 to 8 d after SE (Zinselmeier et al., 1995b; Andersen et al., 2002), would occur when ovaries were already engaged in the abortion process for several days.

We have tested with a molecular approach the hypothesis proposed in a companion article (Oury et al., 2016) that ovary abortion under WD is caused by silk growth arrest 2 to 3 d after first visible silk and not by carbon availability. For that, we have measured the transcript abundances of genes involved in tissue expansion or in sugar metabolism, together with the concentrations and amounts of sugars and enzyme activities in silks and ovaries at several phenological stages encompassing SE. The resulting analysis supports the view that the first molecular events associated with WD in reproductive organs occur in silks rather than in ovaries and involve genes affecting expansive growth rather than sugar metabolism. Hence, we propose that changes in the transcript amounts and activities of enzymes involved in ovary sugar metabolism, and changes in the concentrations and amounts of sugars 5 d after SE, could be a consequence rather than a cause of the beginning of ovary abortion.

## RESULTS

### Transient WDs during Flowering Time Affected Ovary Abortion, Silk and Ovary Growth, and Sugar Content in the Same Manner in Hybrid B73xUH007 and Inbred Line B73

WD was imposed on plants of the B73xUH007 hybrid (experiment 1) or of the B73 inbred line (experiment 2). In both experiments, a common treatment with moderate water deficit (WD1) was imposed for 10 d, from tassel emergence to 6 d after SE, with a soil water potential of  $-0.3$  MPa (Fig. 1). Transpiration was reduced in WD1 to 74% and 67% and photosynthesis to 71% and 74% of their values in WW plants in experiments 1 and 2, respectively (Table I). Abortion occurred at the ear tip in both experiments (Fig. 2B), as it does in field studies (Supplemental Fig. S2A). WD had no significant effect on the number of initiated ovaries (Fig. 2A), so the reduction in grain number was not due to a lack of floret initiation but to ovary (before fertilization) or grain (after fertilization) abortion. Pollen sterility was not involved in abortion because hand pollination was performed every day until the end of SE with fresh pollen of WW plants.

Responses to soil WD shared common features in the experiments with either the hybrid B73xUH007 or the inbred line B73 (Table I). First, total silk fresh weight was already reduced significantly when the first silk emerged, while ovary fresh weight was not yet affected. Second, soluble sugars accumulated during WD in silks and ovaries, suggesting that expansive growth was more affected than carbon availability in both organs. Third, silk growth and SE stopped 1 to 3 d after first SE in WD plants versus 6 to 7 d in WW plants. Finally, WD caused losses of grain number by 36% to 77% depending on the severity of the WD (Table I), with 98% of ovary abortion related to the number of emerged silks at the date of silk growth arrest (Fig. 2C). Indeed, a common relationship was observed between final grain number and silk number on the day of silk growth arrest, suggesting that the switch to abortion in apical ovaries of WD plants was triggered 1 to 3 d after SE and was associated with silk growth arrest. Hence, abortion in WD plants concerned both florets with nonexposed silks and, to a lesser extent, ovaries whose silks emerged less than 2 d before silk growth arrest and, therefore, were in contact with pollen. This relationship applied indifferently to the hybrid in WW and WD1 treatments of experiment 1, to line B73 in the four treatments of experiment 2, and to four hybrids and three treatments analyzed by Oury et al. (2016).

As a consequence, common causes of abortion and, probably, common mechanisms operated in the whole data set in both the B73 line and the hybrid. All results presented hereafter involve the hybrid, except for the transcriptome analysis that was performed in the inbred line for a better matching of probes that were specific of the B73 line (experiment 2, WD1).

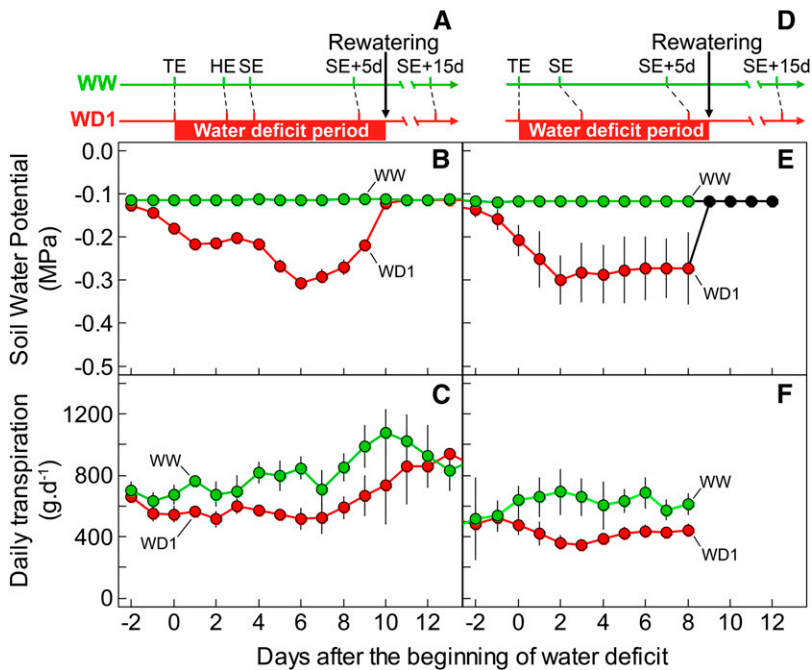


**Figure 1.** Time course of sampling dates (A and D), soil water potential (B and E), and daily transpiration (C and F) during the period of WD in hybrid B73xUH007 (left column; experiment 1) and line B73 (right column; experiment 2). HE, Husk emergence; SE+5d and SE+15d, 5 and 15 d after SE, respectively; TE, tassel emergence (beginning of WD). Green, WW; red, WD1. Error bars represent 95% confidence intervals ( $n \geq 3$ ).

### The Growth of All Reproductive Organs Was Affected, with an Irreversible Effect on Ovaries Located at the Ear Tip

Ovary fresh weight was maintained in WD1 plants at all positions of the ear until SE (Fig. 3, D and E). Over the following 5 d, it was affected by WD with similar effects in both basal and apical ovaries (Fig. 3, D and E). Ovary volume (linearly related to fresh weight; Supplemental Fig. S3) had no straightforward relation with abortion frequency (Supplemental Fig. S1). In contrast, silks and husks were already affected from SE onward (Fig. 3, A and F), and the peduncle was affected even earlier (Fig. 3B). The growth of all organs of WD1 plants resumed after rewatering, including basal ovaries that recovered rapidly, with the exception of apical ovaries that did not grow over 9 d after rewatering and, therefore, were irreversibly arrested.

### The Carbon Export from Source Leaves Was Maintained in WD1 Plants

No clear temporal tendency was observed for photosynthesis, metabolite contents, and enzyme activities in leaves of WD1 plants during the period from husk emergence to 5 d after SE, so results are presented in Figure 4 as means over the whole period (four sampling dates). Suc content in leaves and activities of Suc phosphate synthase (SPS; EC 2.4.1.14) and cytosolic Fru-1,6-bisphosphatase (FBPase; EC 3.1.3.11), both involved in Suc synthesis for export, were maintained in WD1 plants at the same level as in WW plants (Fig. 4, C–E). Hexose contents tended to be higher in WD1 than in WW leaves: differences were significant for Glc content (11.1 versus  $2.5 \mu\text{mol g}^{-1}$ ) but not for Fru content (7.4 versus  $5.1 \mu\text{mol g}^{-1}$ ; Fig. 4C). Leaf starch content did not differ significantly between WD1 and WW plants, with a tendency to a reduction by 20% at

**Table 1.** Effect of soil WD on grain loss, photosynthesis, transpiration, date of silk growth arrest, fresh weight in silks and ovaries, and soluble sugar content in silks and ovaries at SE

GC, Growth chamber; GH, greenhouse. WD1, WD2, and WD3 represent soil WDs imposed from tasseling to 5 d after SE. Different letters within a column indicate significant differences in a Kruskal-Wallis test ( $P < 0.05$ ).

Experiment	Location	Genotype	Treatment	Soil	Grain	Photosynthesis	Transpiration	Date of	Silk Fresh	Ovary	Silk	Ovary
				Water				Loss		Growth	Weight	Fresh
				Potential	% WW			Arrest	at SE	at SE	Sugar	Sugar
				MPa				d after SE	% WW		Content	Content
Experiment 1	GH	B73xUH007	WW	-0.08a	0 a	100 a	100 a	6.5 a	100 a	100 a	100 a	100 a
			WD1	-0.28b	49 b	71 b	74 b	3.2 b	72 b	92 a	113 a,b	130 b
Experiment 2	GC	B73	WW	-0.08a	0 a	100 a	100 a	5.7 a	100 a	100 a	100 a	100 a
			WD1	-0.30b	42 b	74 b	67 b	2.4 b,c	60 b	95 a	129 b	129 b
			WD2	-0.50c	64 c	59 c	49 c	1.9 c	33 c	104 a	153 c	128 b
			WD3	-0.60d	77 d	45 d	40 d	1.3 d	20 d	103 a	-	127 b

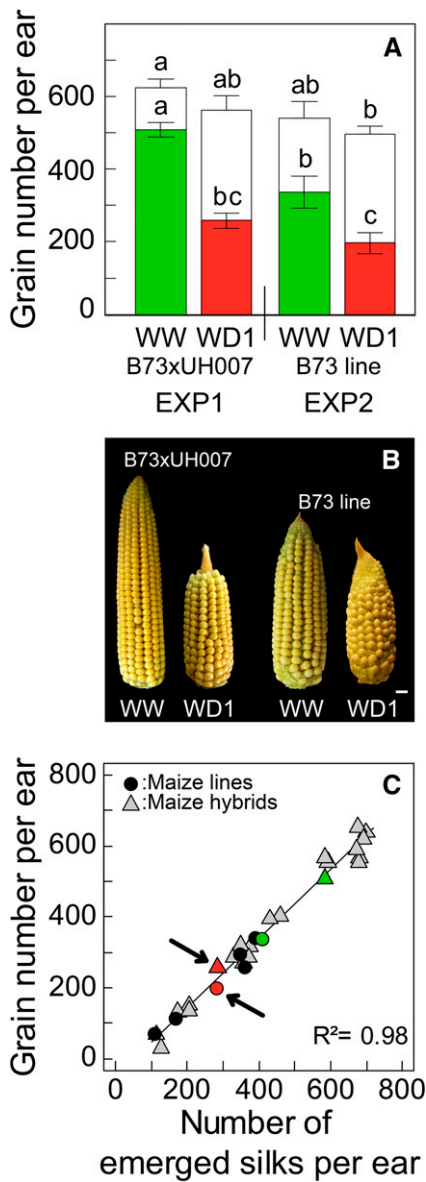


**Figure 2.** A, Grain number per ear (colored bars) and number of initiated ovaries per ear (white bars) in experiments 1 and 2. Error bars represent  $SE$  ( $n \geq 3$ ). Different letters indicate significant differences in a Kruskal-Wallis test ( $P < 0.05$ ). B, Ears 15 d after SE in experiments 1 and 2. Bar = 1 cm. C, Grain number as a function of the number of emerged silks at the date of silk growth arrest. Green, WW; red, WD1. Each point represents the mean value in one experimental treatment from experiment 1 (hybrid B73xUH007; colored triangles), experiment 2 (line B73; circles), and Oury et al. (2016; four hybrids; gray triangles). Arrows indicate the WD1 treatments, in which the characterization of metabolite content and enzyme activities (experiment 1; red triangle) or of transcript levels (experiment 2; red circle) was performed.

the end of the light period and by 30% at the end of the dark period (Fig. 4B). This suggests that starch might be metabolized more rapidly in WD1 plants, thereby contributing to maintain Suc and hexose concentrations. A higher mobilization of starch reserves in WD1 plants during the night, when plant water status partly

recovered, could sustain Suc export to sink reproductive organs (Fig. 4B). Overall, these results show that Suc export from source leaves was probably not appreciably affected by WD. This, coupled with the unaffected ovary growth in WD1 plants until SE and lower sink strength of peduncles (lower growth rate), suggests that the flux of Suc to ovaries was maintained until SE.

**The Changes in Transcript Abundance in Ovaries and Silks Involved Genes Related to Expansive Growth Rather Than to Carbon Metabolism**

In silks sampled at SE, genes involved in tissue expansion were much more expressed in WW than in WD1 plants (Fig. 5A). This was the case for genes involved in cell wall mechanical properties that drive expansive growth (Cosgrove, 2005; Babu et al., 2013; Xiao et al., 2014), namely four expansins and pectinases (exopolysaccharuronase). Conversely, the transcripts of genes involved in carbon metabolism showed small differences in expression between WW and WD1 plants (Fig. 5B). Only two genes (four probes) out of 67 (92 probes) representing major gene families involved in sugar metabolism showed small but significant differences in transcript amounts, namely one Suc synthase and one TPP. Because TPP expression is increased by carbon deprivation (Yadav et al., 2014), the decrease observed in WD1 plants (Fig. 5B) suggests that their silks did not lack carbon.

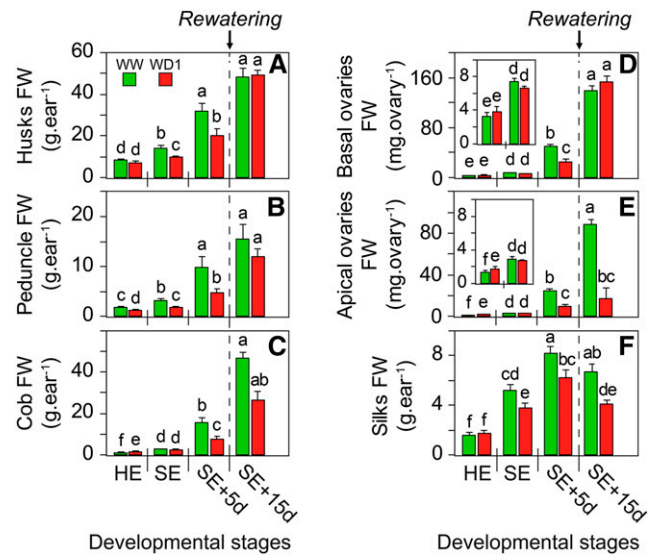


**Figure 3.** Fresh weight (FW) of husks (A), peduncle (B), cob (C), basal ovaries (D), apical ovaries (E), and silks (F) as a function of developmental stages in hybrid B73xUH007 in experiment 1. Green, WW; red, WD1. HE, Husk emergence; SE+5d and SE+15d, 5 and 15 d after SE, respectively. Error bars represent  $SE$  ( $n \geq 6$  at HE, SE, and SE+5d;  $n \geq 3$  at SE+15d). Different letters indicate significant differences in a Kruskal-Wallis test ( $P < 0.05$ ).

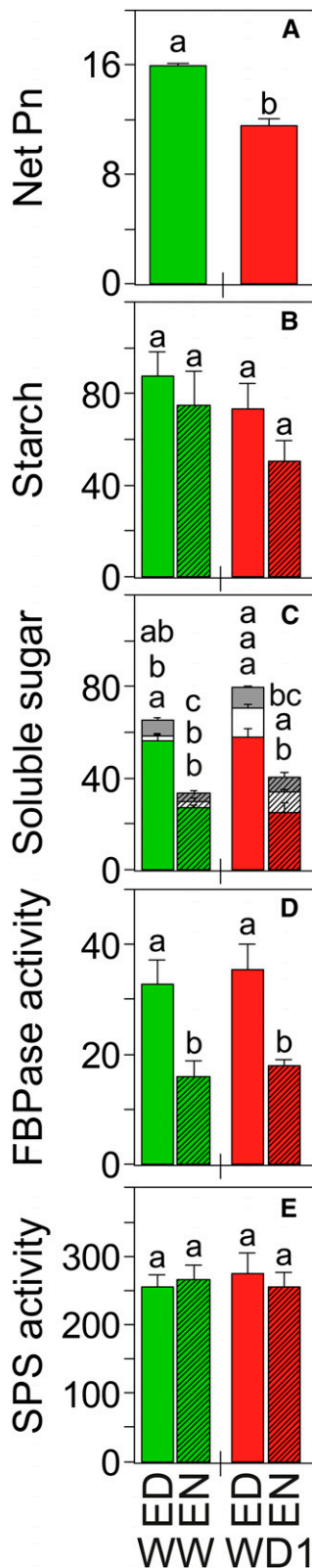


**Figure 4.** A, Net photosynthesis (Pn;  $\mu\text{mol CO}_2 \text{ m}^{-2} \text{ s}^{-1}$ ), in mean values from 3 d after the beginning of WD to rewatering time. B and C, Starch in  $\mu\text{mol Glc equivalent g}^{-1}$  fresh weight (B) and soluble sugar content, Suc (green or red), Glc (white), and Fru (gray), in  $\mu\text{mol g}^{-1}$  fresh weight (C).

In ovaries sampled at SE, differences in transcript abundance were very small between WW and WD1 plants in both basal and apical regions of the ear, for genes involved in either carbon metabolism or expansive growth (Fig. 6, A and B). Only one gene (the Suc synthase *SHRUNKEN1*), out of 67 (92 probes) tested for their role in carbon metabolism, showed a small significant difference. In particular, the transcript abundances of cell wall invertases, neutral invertases, and vacuolar invertases were not affected significantly by WD at this stage (Supplemental Table S1). Five days later, a clear difference appeared between basal and apical ovaries. The strongest differences were observed for genes involved in water transfer, such as aquaporins, and in cell wall mechanical properties, such as expansins, XET, cellulase, and pectin esterase, which were significantly and considerably more expressed in WW than in WD1 plants in apical but not in basal ovaries. The same applied, to a lesser extent, to genes involved in carbon metabolism (Fig. 6B; Supplemental Table S1). Several enzymes involved in starch metabolism, such as one starch synthase, one isoamylase, and several Glc-6-P/phosphate translocators, were more expressed in apical ovaries of WW than of WD1 plants, suggesting that apical ovaries of WW plants were beginning starch accumulation while those in WD1 were blocked. Several genes involved in sugar sensing, such as hexokinases (Granot et al., 2013) or trehalose 6-phosphate synthase (Yadav et al., 2014), were more expressed in WD1 than in WW plants, suggesting that starch accumulation in apical ovaries of WD1 plants was not restricted by Suc availability. Finally, several invertases were overexpressed in apical ovaries of WW compared with WD1 plants, in particular one cell wall invertase (*INCW1*) and to lesser extent neutral invertases (Fig. 6B; Supplemental Table S1). Differences were not significant in basal ovaries, except for one vacuolar invertase (*INV2*).

Taken together, these results do not indicate a clear disruption of carbon metabolism in either silks or ovaries at SE. Differences in transcripts of genes involved in carbon metabolism were only observed in apical ovaries 5 d after SE, a date by which the switch to abortion had already been triggered. Hence, observed differences in the expression of genes involved in starch metabolism and those of invertase in apical ovaries may be seen as a consequence of the switch to abortion that stopped ovary growth, starch accumulation, and the cleavage of Suc. These results are consistent with the time sequence leading to abortion in both the B73xUH007 hybrid and the B73 inbred line (Fig. 2; Table I; Oury et al., 2016).

D and E, FBPase (D) and SPS (E) activities ( $\text{nmol min}^{-1} \text{ mg}^{-1} \text{ protein}$ ) in hybrid B73xUH007 in experiment 1. Green, WW; red, WD1. Metabolite content and enzyme activities were measured at the end of the day (ED) and 10 to 11 h later at the end of the night (EN). Error bars represent se ( $n \geq 4$ ). Different letters indicate significant differences between the four modalities (period of the day × water treatment) in a Kruskal-Wallis test ( $P < 0.05$ ).

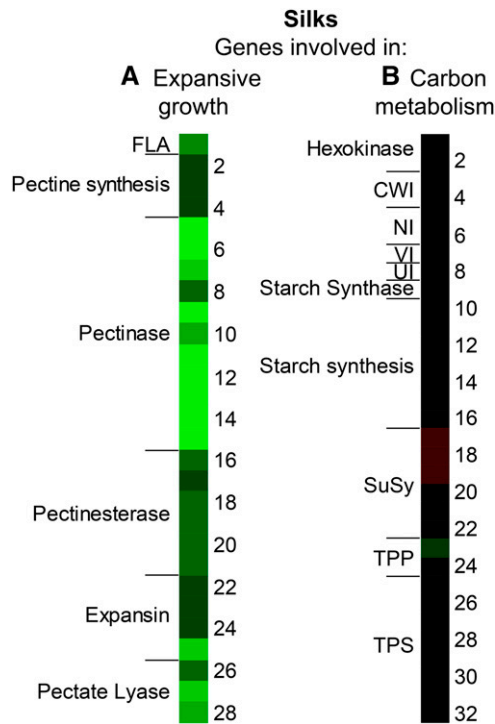


**Figure 5.** Transcriptome analysis at SE in silks in inbred line B73 in experiment 2. A, Genes involved in expansive growth and/or in cell walls. B, Genes involved in carbon metabolism. Colors represent the ratio of expression between WW and WD1 plants (see chart in Fig. 6C): green, higher expression in WW; red, higher expression in WD1. The details corresponding to each probe, identified with the numbers at right, are presented in Supplemental Table S1 (carbon metabolism) and Supplemental Table S2 (expansive growth). The criterion for selecting probes was a significant difference coupled with a ratio greater than 2 between the water treatments. Probes were selected when the criterion was fulfilled in silks (A; expansive growth) or in either silks or ovaries at least at one sampling date (B; carbon metabolism), so the list of probes involved in carbon metabolism (Supplemental Table S1) was common for both organs. No significant differences (Student's *t* test,  $P > 0.05$ ;  $n \geq 4$ ) and differences less than 2-fold are represented as black rectangles. CWI, Cell wall invertase; FLA, fasciclin-like arabinogalactan protein; NI, neutral invertase; SuSy, Suc synthase; TPP, trehalose 6-phosphate phosphatase; TPS, trehalose 6-phosphate phosphatase; UI, uncharacterized invertase; VI, vacuolar invertase.

**The Concentrations of Sugars Were Maintained or Increased in Reproductive Organs of WD Plants**

The concentrations of starch, Suc, Glc, and Fru were measured in basal and apical ovaries, basal and apical silks, and cobs (Fig. 7, A–D) at husk emergence, at SE, and 5 d after SE. The total osmolyte content, calculated from the osmotic potential, increased with WD plants in all studied organs (Fig. 7, E–H). This occurred in ovaries before any response of fresh weight accumulation, suggesting a role for osmotic adjustment in growth maintenance. The osmolyte content due to soluble sugars, calculated from soluble sugar concentration and organ water content, was the main component of total osmolyte content, especially in ovaries and cobs (Fig. 7, E–H).

Suc, Glc, and Fru concentrations were at least equal in reproductive organs of WD1 compared with WW plants, regardless of date and position on the ear (Fig. 7, A–D). WD significantly increased the Suc concentration in ovaries and silks at both basal and apical positions and in the cob on the first two sampling dates, when no difference in growth rate was observable yet (Figs. 3 and 7, A–D). Suc concentration was maintained in the peduncle, for which growth was reduced from the first sampling date onward (Fig. 3; Supplemental Fig. S4). Five days after SE, the Suc concentration continued to

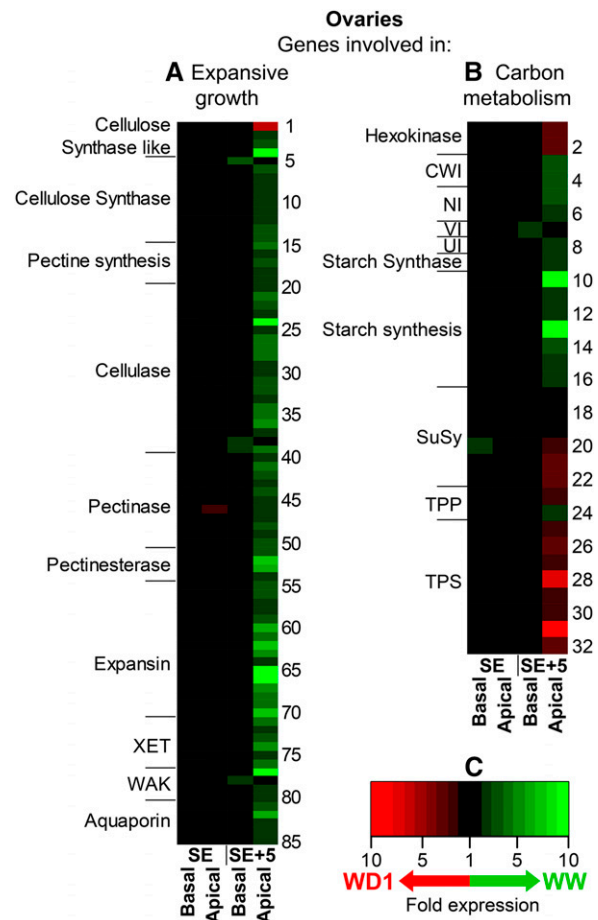


**Figure 6.** Transcriptome analysis for ovaries located at either basal or apical positions on the ear at SE and SE + 5 d (SE+5) in inbred line B73 in experiment 2. A, Genes involved in expansive growth and/or in cell walls, B, Genes involved in carbon metabolism. C, Color chart for the ratio of expression between WW and WD1 plants: green, higher expression in WW; red, higher expression in WD1. The details corresponding to each probe, identified with the numbers at right and selected with the criteria described in Figure 5, are presented as Supplemental Table S1 (carbon metabolism) and Supplemental Table S3 (expansive growth). Insignificant differences (Student's *t* test,  $P > 0.05$ ;  $n \geq 3$ ) and differences less than 2-fold are represented as black rectangles. AGP, Arabinogalactan protein; CWI, cell wall invertase; NI, neutral invertase; TPS, trehalose 6-phosphate synthase; UI, uncharacterized invertase; VI, vacuolar invertase; WAK, wall-associated kinase; XET, xyloglucan endotransglycosylase.

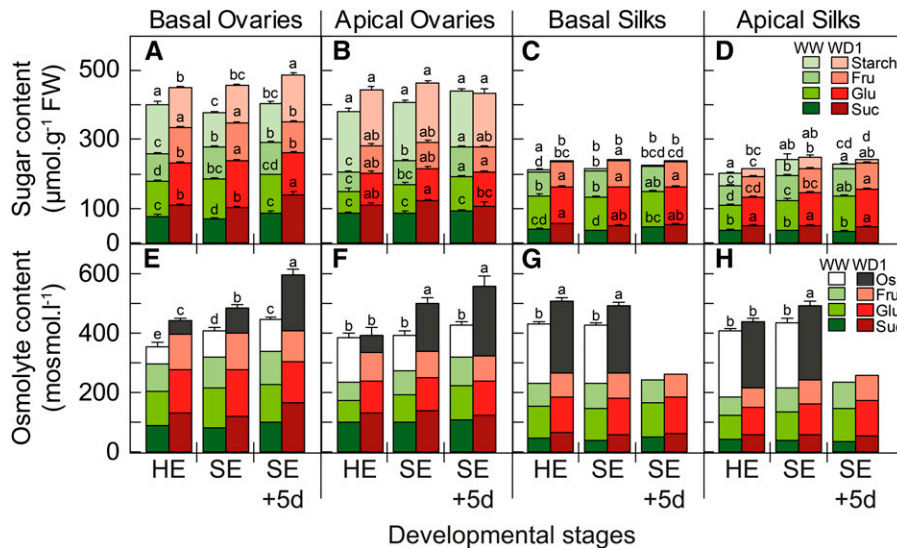


**Figure 7.** Sugar content per unit of fresh weight (FW; top row) and osmolyte content (bottom row) as a function of developmental stage in basal ovaries (A and E), apical ovaries (B and F), basal silks (C and G), and apical silks (D and H) in hybrid B73xUH007 in experiment 1. From the bottom up in each bar: Suc, Glc (Glu), Fru, and starch for sugars and Suc, Glc, Fru, and other osmolytes (Os) for osmolyte content. Other osmolytes correspond to the difference between the total osmolyte content, calculated from osmotic potential, and the accumulated osmolyte contents due to soluble sugars. Green gradient, WW; red gradient, WD1. HE, Husk emergence; SE+5d, 5 d after SE. Values are means of samples harvested at the end of the day and 10 to 11 h later at the end of the night. Error bars represent  $se$  ( $n \geq 6$ ). Different letters indicate significant differences in a Kruskal-Wallis test ( $P < 0.05$ ).

be equal or higher in reproductive organs of WD1 plants compared with WW plants. These trends also applied to Glc and Fru concentrations (Fig. 7, A–D) in this experiment and to soluble sugars in experiment 2 carried out on line B73 (Table I).

Starch content was not affected by WD, regardless of the considered organs, except at the first sampling date in basal ovaries and silks, in which growth was not reduced yet. The maintenance of starch storage in all reproductive organs during the whole period of WD suggests that carbon availability was not limiting.

The amounts of sugars and starch also were calculated on an organ basis (Supplemental Fig. S5). The effect of WD on metabolite amounts per organ closely followed the effect on concentrations on the first two sampling dates, because growth was marginally affected by WD for ovaries, silks, and cobs at this time. The WD induced an accumulation of Suc and a maintenance of hexose and starch amounts per organ until SE, indicating that the fluxes of photosynthates toward these organs were at least maintained during the early phase of WD. Five days after SE, the amounts per ovary and per silk were lower for all sugars in WD1 plants. This was due to the drought-associated reduction in growth at this stage. This reduction of growth was not accompanied by a change in the pattern of sugar concentrations in WD1 plants in ovaries and silks, regardless of their position on the ear. In particular, the pattern of contents of different sugars was similar in apical and basal ovaries, indicating a similar carbon status in

spite of the putative switch to abortion in apical but not basal ovaries. This suggests that the decrease in sugar amounts per organ probably followed, rather than preceded, the reduction in expansive growth due to WD.

#### WD Caused Limited Changes in Enzyme Activities in Ovaries

The activity of SPS, involved in Suc synthesis, was at least maintained under WD in all reproductive organs until 5 d after SE (significant increases at the first and third sampling dates except in silks; Fig. 8). This maintained or enhanced SPS activity in WD1 plants is consistent with the increase in Suc content (Fig. 7, A–D). The high level of SPS activity in WD1 plants, therefore, maintained Suc availability for its cleavage by invertases and SuSy (EC 2.4.1.13).

Changes with time and between organs in vacuolar and neutral invertase (EC 3.2.1.26) activities (Fig. 8) paralleled those of growth in WD1 plants (Fig. 3). Activities were reduced significantly by WD1 at the first sampling date in peduncle and silks but only at the last sampling date in ovaries and cobs. Vacuolar invertase activity was correlated significantly with the relative growth rate of organ fresh weight at pollination (Fig. 9). Vacuolar and neutral invertase activities increased significantly in all reproductive organs during the dark period, known to be favorable for expansive growth processes (Supplemental Fig. S6).

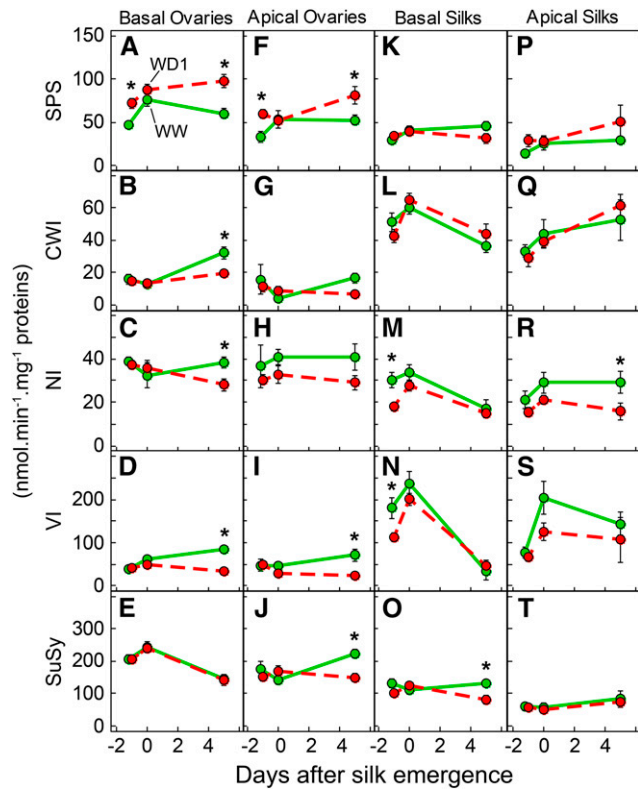


**Figure 8.** Time courses of enzymes activities in ovaries and silks in hybrid B73xUH007 in experiment 1. From top to bottom: SPS (A, F, K, and P), cell wall invertase (CWI; B, J, L, and Q), neutral invertase (NI; C, H, M, and R), vacuolar invertase (VI; D, I, N, and S), and SuSy (E, J, O, and T) activities in basal ovaries (A–E), apical ovaries (F–J), basal silks (K–O), and apical silks (P–T) at three sampling stages in WW plants (green solid lines and circles) or WD1 plants (red dashed lines and circles). Values are means of samples harvested at the end of the day and 10 to 11 h later at the end of night. Error bars represent se ( $n \geq 3$ ). Asterisks indicate significant differences in a Kruskal-Wallis test ( $P < 0.05$ ).

**DISCUSSION**

**A Limitation of Water-Induced Expansive Growth Rather a Carbon Limitation in Reproductive Organs under Moderate WD**

Even if we cannot exclude that some responses in gene expression might be specific to the inbred line in relation to the hybrid, we have hypothesized that the risk of false positive or negative results would have been increased if we had used in the hybrid a chip designed for the inbred line. The time course of events (photosynthesis, sugar accumulation, and position-time model of silk and ovule growth) leading to abortion was similar in the inbred line and the hybrid and is consistent with our position-time model of abortion (Oury et al., 2016).

Reproductive organs were rapidly expanding during the studied period, as indicated by growth in fresh weight, high expression of genes involved in cell wall mechanical properties, and high hexose contents and

acid invertase activities (both cell wall and vacuolar). The latter is involved in cell and tissue expansion in numerous studies (Morris and Arthur, 1984; Sturm and Tang, 1999; Tang et al., 1999; Kohorn et al., 2006; Wang et al., 2010; Ma et al., 2014). WD reduced expansive growth without altering the carbon status of ovaries and silks as measured on a fresh weight basis; in particular, it induced soluble sugar accumulation and starch synthesis in all reproductive organs, as did an osmotic stress due to salt (Henry et al., 2015). This is confirmed by results concerning the trehalose biosynthetic pathway in reproductive tissues of maize plants subjected to osmotic stress. Trehalose-6-phosphate (T6P) functions as a signaling intermediate for reporting the cellular Suc status (Lunn et al., 2006; Yadav et al., 2014), and its content is increased in maize ovaries during salt stress (Henry et al., 2015) and WD (Nuccio et al., 2015). The reduction of transcript abundance of TPP, the enzyme converting T6P to trehalose, observed in silks of WD1 plants in this study (Fig. 5B) suggests an increased level of T6P and, therefore, a favorable carbon status of silks in WD1 plants. This is consistent with studies indicating that moderate WDs induce a carbon satiation, because expansive growth of sink organs is more affected than photosynthesis (Hummel et al., 2010; Muller et al., 2011; Pantin et al., 2013). The facts that the ratio between total invertase and SuSy activities was lower in ovaries than in silks, especially at SE (Fig. 8), and that SuSy did not respond to WD reinforce the idea that the energy status was not limiting for silk growth. Indeed, the breakdown of Suc into hexose phosphates requires only one inorganic pyrophosphate when initiated via SuSy and two ATPs when initiated via invertase (Geigenberger, 2003). Conversely, the transcript amounts of genes involved in water movements

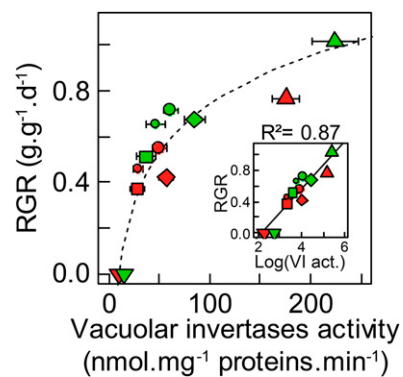


**Figure 9.** Relationship between vacuolar invertase activity (VI act.) and relative growth rate (RGR) of organs at SE in experiment 1 in hybrid B73xUH007. In the inset, the x axis is on a logarithmic scale. Green, WW; red WD1. Large circles, Basal ovaries; small circles, apical ovaries; diamonds, cob; squares, peduncle; triangles, silks; reverse triangles, leaf. Error bars represent 95% confidence intervals ( $n \geq 3$ ). The organ relative growth rates between husk emergence (t1) and SE (t2) were calculated from the average fresh weight measured at t1 (FW1) and t2 (FW2):  $RGR = \log(FW2/FW1)/(t2 - t1)$ .

(aquaporins) and in cell wall properties (expansins and XET) were more expressed in ovaries of WW than of WD1 plants. Hence, it can be considered that the growth in fresh weight was limited by expansive growth, involving water entry into cells and cell wall mechanical properties, rather than by carbon availability that is largely independent of expansive growth under WD (Hummel et al., 2010; Tardieu, 2012; Pantin et al., 2013; Tardieu et al., 2014).

No trait involved in carbon metabolism could account for the abortion of apical ovaries, except the absence of increase in the activity and transcript abundance of cell wall invertases 5 d after SE in ovaries with WD. The latter result is consistent with previous studies (Zinselmeier et al., 1995b, 1999; McLaughlin and Boyer, 2004) suggesting that the differential behavior of cell wall invertases in WW and WD plants is the cause of abortion. However, both basal and apical ovaries of plants in WD showed this absence of increase, while only apical ovaries aborted in our study. Furthermore, our companion article (Oury et al., 2016) strongly suggests that the switch to abortion occurs 1 or 2 d after SE in apical ovaries of water-deficient plants. The differential behavior of cell wall invertases, which was not yet significant at SE, therefore would occur after the switch to abortion. Thus, we suggest that it is a consequence and not a cause of ongoing abortion in apical ovaries, consistent with the fact that the mutation *miniature kernel*, which drastically reduces invertase activity in ovaries and disturbs the storage of carbohydrates in the endosperm, does not cause grain abortion (Miller and Chourey, 1992; LeClere et al., 2010).

It was demonstrated recently that the targeted overexpression of a TPP to developing maize ears improves the allocation of carbon to the ear during a WD and reduces grain abortion (Nuccio et al., 2015). Because it signals carbon starvation although Suc availability was high, the transgene probably modified sugar utilization. One could hypothesize an increased use of hexoses to contribute to osmotic potential and, therefore, maintain expansive growth in ovaries and silks. The magnitude of yield improvement due to the transgene in field studies (Nuccio et al., 2015) could be explained by a delay of 1 d in the date of silk growth arrest in our model (Fig. 2C; Oury et al., 2016).

#### Vacuolar Invertase Activity as an Indicator of Expansive Growth Rate under WD

The experiment presented here shows an early decrease in silk growth in WD before any effect on ovary growth. Consistently, the effect of WD on vacuolar invertase activity was observed 5 d earlier in silks than in ovaries and was already visible at SE (Fig. 8, D and N). The activity of vacuolar invertase was higher at the end of the night than at the end of the day (Supplemental Fig. S6G); that is, it followed the time course of expansive growth (with maximum rates during the night; Turc et al., 2016) and not that of photosynthesis (with maximum rates during the day). These differential

behaviors suggest that vacuolar invertases followed expansive growth in our experiments. High activities of vacuolar invertases are associated with rapid elongation in organs such as epicotyl of pea (*Pisum sativum*), roots of Arabidopsis (*Arabidopsis thaliana*), cotton (*Gossypium hirsutum*) fibers, or maize roots and silks (Morris and Arthur, 1984; Miller and Chourey, 1992; Wang et al., 2010), whereas decreasing the vacuolar invertase activity causes decreased organ and cell sizes (Kohorn et al., 2006).

Taken together, these arguments suggest that the time course of vacuolar invertase activity in ovaries and silks was not linked to changing Suc availability but to expansive growth, itself linked to the flux of water into growing cells and to cell wall mechanical properties (Cosgrove, 2005). The early effect of WD on vacuolar invertase activity in silks at SE, therefore, would reinforce the conclusion that silk growth was a major process involved in ovary abortion (Oury et al., 2016).

#### A Carbon-Independent Process Associated with the Sequential Emergence of Silk Cohorts, Followed by a Carbon-Dependent Cause of Abortion

The results presented here apparently contradict those of previous studies (Boyle et al., 1991; Zinselmeier et al., 1995b, 1999; McLaughlin and Boyer, 2004). In particular, the ovary carbon status differed, with a cessation of the Suc flux toward ovaries and starch depletion in ovaries in the previous studies, versus a maintained starch storage, maintained Suc and hexose contents in ovaries, and maintained Suc and starch contents in leaves in our study. We suggest that the mechanisms presented here and those in the above mentioned series of experiments coexist but at different periods and in different conditions.

In our study, the decrease in silk growth and in the expression of genes associated with silk expansive growth preceded any event affecting apical ovaries. This suggests a switch to abortion linked to silk expansive growth via the sequential emergence and pollination of silks of plants under WD, as proposed by Oury et al. (2016). The analyses of transcriptomes, of metabolite concentrations, and of enzyme activities strongly suggest a carbon-independent process. Consistent with the mechanism linked to sequential silk development, the distribution of abortion frequency on the ear had a clear base-apex pattern in our study as in most field studies (Fig. 2B; Supplemental Fig. S2A).

These developmental mechanisms were avoided in the previous studies, in which WD began after sequential SE and pollination occurred at a single date at the end of SE. Because the WD was stronger and occurred slightly after the period reported in this study, a carbon-related abortion occurred and was partly relieved by Suc feeding (Zinselmeier et al., 1999). Reductions in Suc flux to young grains and in the activities of enzymes linked to Suc cleavage were involved in the process of abortion reported in the previous studies but

also were observed in our study 5 d after SE. It is noteworthy that the carbon-driven abortion led to a random distribution of abortion frequency on the ear in plants subjected to WD, with or without Suc feeding (McLaughlin and Boyer, 2004; Supplemental Fig. S2D). This distribution is clearly different from that observed in our study.

The results presented here, therefore, suggest that two periods with different dependency on carbon supply coexist. (1) From tassel emergence to 1 to 2 d after SE in WD, processes related to expansive growth would be predominant, as shown in this study, and result in the tip abortion observed in many field studies. (2) A carbon-dependent period of sensitivity of the young grain would begin with starch storage in fertilized embryos 5 d after SE and finish when grain number becomes insensitive to WD, 20 d after SE (Claassen and Shaw, 1970; Grant et al., 1989). The first period had a major effect in our study, in which the WD was moderate during flowering time, as it is in most drought scenarios in Europe (Harrison et al., 2014). A severe WD at flowering time, causing a drastic reduction in photosynthesis, may have an appreciable effect on abortion rate via carbon limitation in the field, as it had in several studies in controlled environments (Boyle et al., 1991; Schussler and Westgate, 1991; Zinselmeier et al., 1995b, 1999; McLaughlin and Boyer, 2004). This case was estimated as 18% of drought scenarios in Europe by Harrison et al. (2014).

## MATERIALS AND METHODS

### Plant Material and Growth Conditions

Maize (*Zea mays*) plants (hybrid B73xUH007 in experiment 1 and inbred line B73 in experiment 2) were grown in a greenhouse in 9-L cylindrical plastic pots at a density of three plants  $m^{-2}$ . Three seeds per pot were sown in compost composed of clay and peat (30:70, v/v) enriched in minerals. Plants were thinned to one per pot 3 d after emergence. Each pot was placed on a scale that allowed quantifying plant transpiration and calculating soil water content every 15 min from pot weight corrected by estimated plant weight. The latter was estimated by regularly sampling plants. A water-release curve of the soil was obtained by measuring the soil water potential of soil samples with different water contents (WP4-T Dewpoint Meters; Decagon Devices), allowing calculation of the mean soil water potential in each soil column (Caldeira et al., 2014). All plants were maintained at a soil water potential above  $-0.11$  MPa by daily irrigation, except for a short period around flowering time for plants in WD treatments (Fig. 1, A and D). At tassel emergence, recorded individually for each plant, water was withheld for 2 d until soil water content reached the desired soil water potential (Fig. 1, B and E; Table I). Pots were then watered individually with the necessary volume to maintain soil water potential at the targeted value (for details, see Caldeira et al., 2014). Three levels of soil WD were performed in experiment 2, with soil water potential targeted values of  $-0.3$ ,  $-0.5$ , and  $-0.6$  MPa in WD1, WD2, and WD3 treatments, respectively, while only treatment WD1 was applied in experiment 1 (Table I). WD plants were rewatered at the level of WW plants 6 d after SE. Mean temperature and vapor pressure from tassel emergence to 6 d after SE were  $25.4^{\circ}C$  and  $1.7$  kPa during the day and  $21.8^{\circ}C$  and  $1.2$  kPa during the night. Plants of line B73 were transferred to a growth chamber with similar climatic conditions during the period of WD in experiment 2.

### Photosynthesis

Because photosynthesis measurements are often unreliable in a greenhouse because of rapid changes in light intensity, they were all performed on plants grown in the growth chamber under stable climatic conditions close to average

values experienced in the greenhouse in experiment 1. Photosynthesis was followed from 3 d after tassel emergence until 5 d after SE on the ear leaf (leaf 10 or 11) with a CIRAS-2 portable gas-exchange system (PP Systems) with a  $2.5\text{-cm}^2$  leaf chamber and an air flow rate of  $300\text{ cm}^3\text{ s}^{-1}$ . Light intensities were similar in the growth chamber at leaf level and in the gas-exchange system ( $300\text{ }\mu\text{mol m}^{-2}\text{ s}^{-1}$ ). Air temperature and vapor pressure deficit in the leaf chamber unit of the CIRAS-2 system also mimicked the environmental conditions in the growth chamber (i.e.  $25^{\circ}C$  and  $1.5$  kPa). Measurements were carried out for the whole photoperiod (16 h;  $n = 4$  and  $17$  in WW and WD treatments, respectively).

### Plant Sampling and Measurements

Ears were sampled at husk emergence, SE, 5 d after SE just before rewatering, and 15 d after SE. At the first three sampling dates, a subsample of plants was harvested at the end of the day (before irrigation) and another subsample was harvested at the end of the night. Leaf discs were sampled with a punch, frozen in liquid nitrogen, and stored at  $-60^{\circ}C$ . Ears enclosed in husks were detached from the plant and dissected immediately. Fresh weights of peduncle, ear, and silks were measured immediately, before these organs were frozen in liquid nitrogen and stored at  $-60^{\circ}C$ . Ears were sliced into six to seven sections, each of them including five ovary positions along the ear rows (positions 1–5, 6–10, etc., counted from the ear base). Ovaries and cob were separated in liquid nitrogen and weighed. Ovaries were counted to calculate fresh weight per ovary. Organs were then ground in liquid nitrogen. Fifteen days after SE, plants were sampled at the end of the day. Fresh weights of husks, peduncle, ear, and silks were measured immediately, ears were photographed, and ovary or grain number and dimensions were measured with the software ImageJ. Ovaries or grain volumes were estimated as described by Oury et al. (2016).

### Metabolites

Metabolites were extracted as described by Hendriks et al. (2003). Suc, Glc, and Fru (Jelitto et al., 1992), malate and fumarate (Nunes-Nesi et al., 2007), total amino acids (Bantan-Polak et al., 2001), and Pro (adapted from Troll and Lindsley [1955]; see also Carillo and Gibon [2011]) were determined in the ethanolic supernatant. Starch (Hendriks et al., 2003) and total protein (Bradford, 1976) contents were determined on the pellet resuspended in  $100\text{ mM}$  NaOH. Assays were prepared on 96-well microplates using Starlet pipetting robots (Hamilton), and absorbance was read at 340, 570, or 595 nm in MP96 microplate readers (SAFAS). Ovary metabolite content was measured in all ear sections described above. Sections 1 to 3 counted from the ear base were used as replicates of basal ovaries, while sections 4 and above were used as replicates of apical ovaries. Only soluble sugar content (Suc, Glc, and Fru) was assayed in experiment 2.

### Enzyme Activities in Experiment 1

Aliquots of 20 mg fresh weight were extracted as described by Biais et al. (2014), and enzyme activities were measured according to Gibon et al. (2004, 2006, 2009), Sulpice et al. (2007), and Biais et al. (2014). Assays for neutral invertase and acid invertase were performed after desalting (PD Multitrap G-25; GE Healthcare). For the determination of cell wall invertase, pellets obtained after centrifugation of the extracts were washed three times by resuspension in  $500\text{ }\mu\text{L}$  of extraction buffer without leupeptin, dithiothreitol, and Triton X-100 followed by centrifugation (15 min at  $4,000g$ ). Cell walls were then washed in  $300\text{ }\mu\text{L}$  of extraction buffer containing  $1\text{ M}$  NaCl, leupeptin, dithiothreitol, and Triton X-100 and vigorously shaken for 5 min in a Qiagen Tissue Lyser II. After centrifugation (15 min at  $4,000g$ ), cell wall invertase was measured in aliquots of the supernatant, of which  $5\text{ }\mu\text{L}$  was assayed with the same protocol as for acid invertase.

### Water Content and Osmotic Potential

Lyophilization was used to estimate the dry matter content of aliquots, and water content was calculated as the difference between fresh weight and dry weight. About 20 mg of frozen ground samples was put in a tube on ice until thawing. After centrifugation (15 min at  $13,000\text{ rpm}$ ), cell fluid was collected and osmotic potential was measured by psychrometry using a Roebbling micro-osmometer (type 13). The total osmolyte content ( $\text{mosmol L}^{-1}$ ) in each sample was calculated from its osmotic potential.

## Transcript Abundance in Experiment 2

Ovaries were sampled as described above at SE and 5 d later in WW and WD1 plants of line B73 grown in a growth chamber under stable climatic conditions close to average values experienced in the greenhouse. Silks were only sampled on day 1 of SE, but not 5 d later, because of the risks of confusing effects of pollination at SE plus 5 d (presence of pollen RNA and silk senescence due to fertilization). Line B73 was chosen rather than the hybrid in order to guarantee a good match with the probes of the chip. Samples were sorted into silks, basal ovaries (positions 1–15 along the row), and apical ovaries (beyond position 15). Three samples per ovary position and four samples for silks (one plant each) were collected at each sampling time and flash frozen less than 30 s after sampling. Expression levels were estimated with the custom oligonucleotide microarray Mais 45K developed by Biogemma (Roche NimbleGen). This chip displays a set of 45,000 probes designed using pseudomolecules and gene models (FilterGeneSet) provided by the Maize Genome Sequencing Project ([www.maizesequence.org](http://www.maizesequence.org), version 4a53), allowing for each probe a corresponding maize gene identifier. One to three probes were used to represent a gene. A total of 2,563 random probes were used for technical and internal hybridization controls. Total RNA was isolated from the tissues with the RNeasy Plant Mini Kit (Qiagen) following the manufacturer's protocol. After controlling the RNA integrity by capillary electrophoresis (Bioanalyzer; Agilent), complementary DNA was synthesized using the Superscript Double-Stranded cDNA Synthesis Kit (Invitrogen/Fisher Bioblock no. W34277). The complementary DNAs were then purified by a phenol/chloroform step and further labeled with fluorescent Cy3 (One-Color DNA Labeling Kit; Roche NimbleGen). After overnight hybridization (16 h at 42°C), the microarray slides were washed and scanned with an MS200 Roche NimbleGen scanner. The laser power settings were optimized to the autogain mode, which determines the optimal range of acquisition for each scan (laser power was fixed at 100%). Raw hybridization intensities were normalized across all arrays with RMA Express, in which the quantile normalization method was employed (Bolstad et al., 2003).

Data were imported into R (R Development Core Team, 2014). The  $\log_2$  of the transcript abundance was calculated for each probe. Differences between treatments of the transcript abundance corresponding to a given probe were considered as significant if (1) the *P* value was lower than 0.05 in a Student's *t* test and (2) it differed by a factor greater than 2 between treatments. Identification of genes was performed on Gramene.org (<http://pathway.iplantcollaborative.org/organism-summary?object=MAIZE>; accessed May 2015). Invertase gene identification was completed with data from Kakumanu et al. (2012). Gene functions were sorted out by following the ontologies proposed in MapMan with the maize genome release Zm\_B73\_5b\_FGS\_cds\_2012 (<http://mapman.gabipd.org/web/guest/mapmanstore>). Two categories were particularly analyzed and presented in Figures 5 and 6, namely genes involved in carbon metabolism (Granot et al., 2013; Yadav et al., 2014) and those involved in expansive growth, either via water transport or via cell wall mechanical properties (Cosgrove, 2005; Wolf et al., 2012; Babu et al., 2013; Xiao et al., 2014).

## Supplemental Data

The following supplemental materials are available.

**Supplemental Figure S1.** Ovary volume and abortion frequency as a function of position along the ear.

**Supplemental Figure S2.** Spatial distributions of aborted ovaries of plants subjected to WD during flowering time.

**Supplemental Figure S3.** Relationship between ovary volume and ovary fresh weight.

**Supplemental Figure S4.** Sugar content per unit fresh weight and osmolyte content as a function of developmental stages in cob and peduncle.

**Supplemental Figure S5.** Sugar amount per organ as a function of developmental stages.

**Supplemental Figure S6.** Relationship between activities or contents measured at the end of the day and at the end of the night.

**Supplemental Figure S7.** Metabolite contents and enzyme activities in leaves as a function of treatments.

**Supplemental Table S1.** Transcriptome analysis: data for genes involved in carbon metabolism expressed in maize ovaries and silks.

**Supplemental Table S2.** Transcriptome analysis: data for genes involved in expansive growth expressed in maize silks.

**Supplemental Table S3.** Transcriptome analysis: data for genes involved in expansive growth expressed in maize ovaries.

## ACKNOWLEDGMENTS

We thank S. Berthézène, G. Rolland, M. Dauzat, I. Peironnenche, C. Check, C. Pequignot, and J. Soewarto for technical support.

Received July 21, 2015; accepted April 15, 2016; published April 19, 2016.

## LITERATURE CITED

- Andersen MN, Asch F, Wu Y, Jensen CR, Naested H, Mogensen VO, Koch KE (2002) Soluble invertase expression is an early target of drought stress during the critical, abortion-sensitive phase of young ovary development in maize. *Plant Physiol* **130**: 591–604
- Babu Y, Musielak T, Henschen A, Bayer M (2013) Suspensor length determines developmental progression of the embryo in Arabidopsis. *Plant Physiol* **162**: 1448–1458
- Bantan-Polak T, Kassai M, Grant KB (2001) A comparison of fluorescamine and naphthalene-2,3-dicarboxaldehyde fluorogenic reagents for microplate-based detection of amino acids. *Anal Biochem* **297**: 128–136
- Biais B, Bénard C, Beauvoit B, Colombié S, Prodhomme D, Ménard G, Bernillon S, Gehl B, Gautier H, Ballias P, et al (2014) Remarkable reproducibility of enzyme activity profiles in tomato fruits grown under contrasting environments provides a roadmap for studies of fruit metabolism. *Plant Physiol* **164**: 1204–1221
- Bolstad BM, Irizarry RA, Åstrand M, Speed TP (2003) A comparison of normalization methods for high density oligonucleotide array data based on variance and bias. *Bioinformatics* **19**: 185–193
- Boyer JS, McLaughlin JE (2007) Functional reversion to identify controlling genes in multigenic responses: analysis of floral abortion. *J Exp Bot* **58**: 267–277
- Boyer JS, Westgate ME (2004) Grain yields with limited water. *J Exp Bot* **55**: 2385–2394
- Boyle MG, Boyer JS, Morgan PW (1991) Stem infusion of liquid culture medium prevents reproductive failure of maize at low water potential. *Crop Sci* **31**: 1246–1252
- Bradford MM (1976) A rapid and sensitive method for the quantitation of microgram quantities of protein utilizing the principle of protein-dye binding. *Anal Biochem* **72**: 248–254
- Caldeira CF, Bosio M, Parent B, Jeanguen L, Chaumont F, Tardieu F (2014) A hydraulic model is compatible with rapid changes in leaf elongation under fluctuating evaporative demand and soil water status. *Plant Physiol* **164**: 1718–1730
- Carillo P, Gibon Y (2011) Extraction and determination of proline. <http://www.publish.csiro.au/prometheus/wiki/tiki-pagehistory.php?page=Extraction%20and%20determination%20of%20proline&preview=14> (May 13, 2014)
- Claassen MM, Shaw RH (1970) Water deficit effects on corn. II. Grain components. *Agron J* **62**: 652–655
- Cosgrove DJ (2005) Growth of the plant cell wall. *Nat Rev Mol Cell Biol* **6**: 850–861
- Geigenberger P (2003) Response of plant metabolism to too little oxygen. *Curr Opin Plant Biol* **6**: 247–256
- Gibon Y, Blaiesing OE, Hannemann J, Carillo P, Höhne M, Hendriks JHM, Palacios N, Cross J, Selbig J, Stitt M (2004) A Robot-based platform to measure multiple enzyme activities in *Arabidopsis* using a set of cycling assays: comparison of changes of enzyme activities and transcript levels during diurnal cycles and in prolonged darkness. *Plant Cell* **16**: 3304–3325
- Gibon Y, Pyl ET, Sulpice R, Lunn JE, Höhne M, Günther M, Stitt M (2009) Adjustment of growth, starch turnover, protein content and central metabolism to a decrease of the carbon supply when Arabidopsis is grown in very short photoperiods. *Plant Cell Environ* **32**: 859–874
- Gibon Y, Usadel B, Blaiesing OE, Kamlage B, Hoehne M, Trethewey R, Stitt M (2006) Integration of metabolite with transcript and enzyme activity profiling during diurnal cycles in Arabidopsis rosettes. *Genome Biol* **7**: R76

- Granot D, David-Schwartz R, Kelly G** (2013) Hexose kinases and their role in sugar-sensing and plant development. *Front Plant Sci* **4**: 44
- Grant RF, Jackson BS, Kiniry JR, Arkin GF** (1989) Water deficit timing effects on yield components in maize. *Agron J* **81**: 61–65
- Harrison MT, Tardieu F, Dong Z, Messina CD, Hammer GL** (2014) Characterizing drought stress and trait influence on maize yield under current and future conditions. *Glob Change Biol* **20**: 867–878
- Hendriks JHM, Kolbe A, Gibon Y, Stitt M, Geigenberger P** (2003) ADP-glucose pyrophosphorylase is activated by posttranslational redox-modification in response to light and to sugars in leaves of *Arabidopsis* and other plant species. *Plant Physiol* **133**: 838–849
- Henry C, Bledsoe SW, Griffiths CA, Kollman A, Paul MJ, Sakr S, Lagrimini LM** (2015) Differential role for trehalose metabolism in salt-stressed maize. *Plant Physiol* **169**: 1072–1089
- Herrero MP, Johnson RR** (1981) Drought stress and its effects on maize reproductive systems. *Crop Sci* **21**: 105–110
- Hiyane R, Hiyane S, Tang AC, Boyer JS** (2010) Sucrose feeding reverses shade-induced kernel losses in maize. *Ann Bot (Lond)* **106**: 395–403
- Hummel I, Pantin F, Sulpice R, Piques M, Rolland G, Dauzat M, Christophe A, Pervent M, Bouteillé M, Stitt M, et al** (2010) *Arabidopsis* plants acclimate to water deficit at low cost through changes of carbon usage: an integrated perspective using growth, metabolite, enzyme, and gene expression analysis. *Plant Physiol* **154**: 357–372
- Jelitto T, Sonnewald U, Willmitzer L, Hajirezaei M, Stitt M** (1992) Inorganic pyrophosphate content and metabolites in potato and tobacco plants expressing *E. coli* pyrophosphatase in their cytosol. *Planta* **188**: 238–244
- Kakumanu A, Ambavaram MMR, Klumac A, Krishnan A, Batlang U, Myers E, Grene R, Pereira A** (2012) Effects of drought on gene expression in maize reproductive and leaf meristem tissue revealed by RNA-Seq. *Plant Physiol* **160**: 846–867
- Kohorn BD, Kobayashi M, Johansen S, Riese J, Huang LF, Koch K, Fu S, Dotson A, Byers N** (2006) An *Arabidopsis* cell wall-associated kinase required for invertase activity and cell growth. *Plant J* **46**: 307–316
- LeClere S, Schmelz EA, Chourey PS** (2010) Sugar levels regulate tryptophan-dependent auxin biosynthesis in developing maize kernels. *Plant Physiol* **153**: 306–318
- Lilley JM, Fukai S** (1994) Effect of timing and severity of water deficit on 4 diverse rice cultivars. 3. Phenological development, crop growth and grain yield. *Field Crops Res* **37**: 225–234
- Lunn JE, Feil R, Hendriks JHM, Gibon Y, Morcuende R, Osuna D, Scheible WR, Carillo P, Hajirezaei MR, Stitt M** (2006) Sugar-induced increases in trehalose 6-phosphate are correlated with redox activation of ADP-glucose pyrophosphorylase and higher rates of starch synthesis in *Arabidopsis thaliana*. *Biochem J* **397**: 139–148
- Ma Y, Wang Y, Liu J, Lv F, Chen J, Zhou Z** (2014) The effects of fruiting positions on cellulose synthesis and sucrose metabolism during cotton (*Gossypium hirsutum* L.) fiber development. *PLoS ONE* **9**: e89476
- Mäkelä P, McLaughlin JE, Boyer JS** (2005) Imaging and quantifying carbohydrate transport to the developing ovaries of maize. *Ann Bot (Lond)* **96**: 939–949
- McLaughlin JE, Boyer JS** (2004) Sugar-responsive gene expression, invertase activity, and senescence in aborting maize ovaries at low water potentials. *Ann Bot (Lond)* **94**: 675–689
- Miller ME, Chourey PS** (1992) The maize invertase-deficient miniature-1 seed mutation is associated with aberrant pedicel and endosperm development. *Plant Cell* **4**: 297–305
- Morris DA, Arthur ED** (1984) Invertase activity in sinks undergoing cell expansion. *Plant Growth Regul* **2**: 327–337
- Muller B, Pantin F, Génard M, Turc O, Freixes S, Piques M, Gibon Y** (2011) Water deficits uncouple growth from photosynthesis, increase C content, and modify the relationships between C and growth in sink organs. *J Exp Bot* **62**: 1715–1729
- Nuccio ML, Wu J, Mowers R, Zhou HP, Meghji M, Primavesi LF, Paul MJ, Chen X, Gao Y, Haque E, et al** (2015) Expression of trehalose-6-phosphate phosphatase in maize ears improves yield in well-watered and drought conditions. *Nat Biotechnol* **33**: 862–869
- Nunes-Nesi A, Carrari F, Gibon Y, Sulpice R, Lytovchenko A, Fisahn J, Graham J, Ratcliffe RG, Sweetlove LJ, Fernie AR** (2007) Deficiency of mitochondrial fumarate activity in tomato plants impairs photosynthesis via an effect on stomatal function. *Plant J* **50**: 1093–1106
- Oury V, Tardieu F, Turc O** (2016) Ovary apical abortion under water deficit is caused by changes in sequential development of ovaries and in silk growth rate in maize. *Plant Physiol* **171**: 986–996
- Pantin F, Fanciullino AL, Massonnet C, Dauzat M, Simonneau T, Muller B** (2013) Buffering growth variations against water deficits through timely carbon usage. *Front Plant Sci* **4**: 483
- R Development Core Team** (2014) R: a language and environment for statistical computing. R Foundation for Statistical Computing, Vienna
- Rapoport HF, Hammami SBM, Martins P, Perez-Priego O, Orgaz F** (2012) Influence of water deficits at different times during olive tree inflorescence and flower development. *Environ Exp Bot* **77**: 227–233
- Ruan YL, Patrick JW, Bouzayen M, Osorio S, Fernie AR** (2012) Molecular regulation of seed and fruit set. *Trends Plant Sci* **17**: 656–665
- Saini HS, Westgate ME** (2000) Reproductive development in grain crops during drought. *Adv Agron* **68**: 59–96
- Schober JB, Lambert RJ, Vasilas BL** (1986) Maize pollen viability and ear receptivity under water and high temperature stress. *Crop Sci* **26**: 1029–1033
- Schober JB, Lambert RJ, Vasilas BL** (1987) Pollen viability, pollen shedding, and combining ability for tassel heat tolerance in maize. *Crop Sci* **27**: 27–31
- Schussler JR, Westgate ME** (1991) Maize kernel set at low water potential. II. Sensitivity to reduced assimilates at pollination. *Crop Sci* **31**: 1196–1203
- Schussler JR, Westgate ME** (1995) Assimilate flux determines kernel set at low water potential in maize. *Crop Sci* **35**: 1074–1080
- Sturm A, Tang GQ** (1999) The sucrose-cleaving enzymes of plants are crucial for development, growth and carbon partitioning. *Trends Plant Sci* **4**: 401–407
- Sulpice R, Tschöep H, von Korff M, Büssis D, Usadel B, Höhne M, Witucka-Wall H, Altmann T, Stitt M, Gibon Y** (2007) Description and applications of a rapid and sensitive non-radioactive microplate-based assay for maximum and initial activity of D-ribulose-1,5-bisphosphate carboxylase/oxygenase. *Plant Cell Environ* **30**: 1163–1175
- Tang GQ, Lüscher M, Sturm A** (1999) Antisense repression of vacuolar and cell wall invertase in transgenic carrot alters early plant development and sucrose partitioning. *Plant Cell* **11**: 177–189
- Tardieu F** (2012) Any trait or trait-related allele can confer drought tolerance: just design the right drought scenario. *J Exp Bot* **63**: 25–31
- Tardieu F, Parent B, Caldeira CF, Welcker C** (2014) Genetic and physiological controls of growth under water deficit. *Plant Physiol* **164**: 1628–1635
- Troll W, Lindsley J** (1955) A photometric method for the determination of proline. *J Biol Chem* **215**: 655–660
- Turc O, Bouteillé M, Fuad-Hassan A, Welcker C, Tardieu F** (2016) Vegetative and reproductive structures (leaves and silks) share a partly common hydraulic control of expansive growth in maize. *New Phytol* <http://dx.doi.org/10.1111/nph.14053>
- Wang L, Li XR, Lian H, Ni DA, He YK, Chen XY, Ruan YL** (2010) Evidence that high activity of vacuolar invertase is required for cotton fiber and *Arabidopsis* root elongation through osmotic dependent and independent pathways, respectively. *Plant Physiol* **154**: 744–756
- Wolf S, Hématy K, Höfte H** (2012) Growth control and cell wall signaling in plants. *Annu Rev Plant Biol* **63**: 381–407
- Xiao C, Somerville C, Anderson CT** (2014) POLYGALACTURONASE INVOLVED IN EXPANSION1 functions in cell elongation and flower development in *Arabidopsis*. *Plant Cell* **26**: 1018–1035
- Yadav UP, Ivakov A, Feil R, Duan GY, Walther D, Giavalisco P, Piques M, Carillo P, Hubberten HM, Stitt M, et al** (2014) The sucrose-trehalose 6-phosphate (Tre6P) nexus: specificity and mechanisms of sucrose signalling by Tre6P. *J Exp Bot* **65**: 1051–1068
- Zinselmeier C, Jeong BR, Boyer JS** (1999) Starch and the control of kernel number in maize at low water potentials. *Plant Physiol* **121**: 25–36
- Zinselmeier C, Lauer MJ, Boyer JS** (1995a) Reversing drought-induced losses in grain-yield: sucrose maintains embryo growth in maize. *Crop Sci* **35**: 1390–1400
- Zinselmeier C, Westgate ME, Schussler JR, Jones RJ** (1995b) Low water potential disrupts carbohydrate metabolism in maize (*Zea mays* L.) ovaries. *Plant Physiol* **107**: 385–391

## REVIEW PAPER

# Water deficits uncouple growth from photosynthesis, increase C content, and modify the relationships between C and growth in sink organs

Bertrand Muller<sup>1,\*</sup>, Florent Pantin<sup>1</sup>, Michel Génard<sup>2</sup>, Olivier Turc<sup>1</sup>, Sandra Freixes<sup>1</sup>, Maria Piques<sup>3</sup> and Yves Gibon<sup>4</sup>

<sup>1</sup> INRA, UMR 759 Laboratoire d'Ecophysiologie des Plantes sous Stress Environnementaux, Institut de Biologie Intégrative des Plantes, F-34060 Montpellier, France

<sup>2</sup> INRA, UR 1115 Plantes et Systèmes de culture Horticoles, Domaine Saint Paul, Site Agroparc, F-84000 Avignon, France

<sup>3</sup> Max Planck Institute of Molecular Plant Physiology, Golm, Germany

<sup>4</sup> INRA, UMR 619 Biologie du Fruit, INRA Bordeaux Aquitaine, F-33883 Villenave D'Ornon, France

\* To whom correspondence should be addressed: E-mail: muller@supagro.inra.fr

Received 16 July 2010; Revised 17 November 2010; Accepted 6 December 2010

## Abstract

In plants, carbon (C) molecules provide building blocks for biomass production, fuel for energy, and exert signalling roles to shape development and metabolism. Accordingly, plant growth is well correlated with light interception and energy conversion through photosynthesis. Because water deficits close stomata and thus reduce C entry, it has been hypothesised that droughted plants are under C starvation and their growth under C limitation. In this review, these points are questioned by combining literature review with experimental and modelling illustrations in various plant organs and species. First, converging evidence is gathered from the literature that water deficit generally increases C concentration in plant organs. The hypothesis is raised that this could be due to organ expansion (as a major C sink) being affected earlier and more intensively than photosynthesis (C source) and metabolism. How such an increase is likely to interact with C signalling is not known. Hence, the literature is reviewed for possible links between C and stress signalling that could take part in this interaction. Finally, the possible impact of water deficit-induced C accumulation on growth is questioned for various sink organs of several species by combining published as well as new experimental data or data generated using a modelling approach. To this aim, robust correlations between C availability and sink organ growth are reported in the absence of water deficit. Under water deficit, relationships weaken or are modified suggesting release of the influence of C availability on sink organ growth. These results are interpreted as the signature of a transition from source to sink growth limitation under water deficit.

**Key words:** C metabolism, C signalling, growth, model, sink limitation, source limitation, starch, sugar, water deficit.

## Introduction

Plant growth and carbon (C) metabolism are intimately connected, as carbohydrates generated by photosynthesis provide building blocks and energy for the production and maintenance of biomass. Furthermore, carbohydrates are known to exert tight control over a wide range of processes

including transcriptional, post-transcriptional and post-translational mechanisms (Koch, 1996; Rolland *et al.*, 2006). On a much broader scale, biomass accumulation in a crop is a linear and remarkably stable function of light intercepted by the canopy and its transformation into dry

Abbreviations: ABA, abscisic acid; bZIP, basic leucine zipper; HXK1, hexokinase; PEG, polyethylene glycol; RER, relative expansion rate; RGR, relative growth rate; VPD, vapour pressure deficit.

© The Author [2011]. Published by Oxford University Press [on behalf of the Society for Experimental Biology]. All rights reserved.

For Permissions, please e-mail: journals.permissions@oup.com

matter through photosynthesis (Monteith, 1965), which implies that plant growth relies on C fluxes. Because water deficit induces stomatal closure and thus reduces photosynthesis, it has been suggested that it negatively affects plant C status by impairing C metabolism (e.g. Chaves *et al.*, 2009), ultimately promoting growth failure due to C starvation (Boyle *et al.*, 1991). This article thus aims to question the impact of water deficits on the C status of plant organs and the consequences of these alterations on C signalling and sink organ growth that, in the absence of stress, strongly depends on C supply.

## Soil water deficit leads to C accumulation

Contrary to the prediction made that water deficit would induce C starvation, literature converges to support the conclusion that C compounds most often accumulate in organs resulting in increased C concentrations. Such accumulation under water deficit has been reported in several species, various plant parts, and for different (i.e. soluble or structural) C forms. Soluble carbohydrate concentrations increase under water deficit in the leaves of maize (Kim *et al.*, 2000), cotton (Timpa *et al.*, 1986), barley (Teulat *et al.*, 2001), eucalyptus and sorghum (Turner *et al.*, 1978), lupin and eucalyptus (Quick *et al.*, 1992), pine (Marron *et al.*, 2003), poplar (Bogeat-Triboulot *et al.*, 2007), and grapevine (Cramer *et al.*, 2007). Carbohydrates also accumulate in stems (Bogeat-Triboulot *et al.*, 2007), flowers, and fruits (Liu *et al.*, 2004; McLaughlin and Boyer, 2004; Mercier *et al.*, 2009), as well as in roots (Sharp *et al.*, 1990; Jiang and Huang, 2001). Accumulation occurs both after rapid osmotic shocks, e.g. using polyethylene glycol (PEG) or mannitol (Zrenner and Stitt, 1991), and during slowly developing water deficit (Cramer *et al.*, 2007; Hummel *et al.*, 2010).

Carbohydrates often accumulate in the form of abundant sugars such as hexoses and sucrose (references above). However, a wider range of C-rich compounds may also accumulate in response to soil water deficit. These include minor sugars such as trehalose (Fariás-Rodríguez *et al.*, 1998) or mannitol (Guicherd *et al.*, 1997), amino acids (Morgan, 1992), in particular those with a high C/N ratio such as proline (Hare and Cress, 1997), or pipercolic acid (Barnett and Naylor, 1966). Organic acids such as malate (Franco *et al.*, 2006), fumarate (Hummel *et al.*, 2010), or citrate (Timpa *et al.*, 1986) also accumulate in response to water deficit in a range of species including *Arabidopsis* (Hummel *et al.*, 2010). Quaternary ammonium compounds such as glycine betaine, which accumulate in particular species or families (Ashraf and Foolad, 2007; Gagneul *et al.*, 2007), may also be seen as C-rich compounds, as a quaternary ammonium results from the substitution of three protons with three alkyl groups on an amine residue (Rhodes and Hanson, 1993). Many such compounds are considered to be 'compatible solutes', as they can accumulate in large amounts without perturbing cell functions, and are thought to protect subcellular structures

against the deleterious effects of cell water loss. This has motivated considerable research, in particular the genetic engineering of pathways producing these compounds in order to increase drought tolerance (Bohnert and Jensen, 1996; Rathinasabapathi, 2000; Sakamoto and Murata, 2000). However, because most of these compounds accumulate under extreme stress leading to desiccation, the relevance of this strategy has been questioned for agricultural situations where it is not crop survival but crop productivity that is critical (e.g. Tardieu, 1996; Serraj and Sinclair, 2002).

Structural C-rich compounds such as cellulose and lignin also accumulate under water deficit. Indeed, water deficit accelerates lignification (Timpa *et al.*, 1986; Vincent *et al.*, 2005), decreases leaf intercellular air spaces (Hsiao and Acevedo, 1974), and increases leaf thickness (Hummel *et al.*, 2010). All these responses contribute to the widely reported increase in specific leaf mass occurring under water deficit (see Tardieu *et al.*, 1999 and references therein).

## Soil water deficit uncouples photosynthesis and growth while C metabolism is often maintained or increased

The increase in C concentration in organs of plants under water deficit must originate from some uncoupling between C supply and demand. Accordingly, the photosynthesis (C supply) of the *Arabidopsis* rosette is resilient to even severe water deficit while leaf expansion (accounting for a major part of C demand) is strongly reduced by stress, as quantitatively argued by Hummel *et al.* (2010). The maintenance of photosynthesis under water deficit has been repeatedly reported (Boyer, 1970b; Quick *et al.*, 1992; Bogeat-Triboulot *et al.*, 2007). The mesophytic component of CO<sub>2</sub> capture is particularly resilient to water deficit (Kaiser, 1987; Cornic, 2000; Flexas and Medrano, 2002). For instance, Rubisco activity is maintained even when leaf relative water content drops to 50% while stomata are already 75% closed (Kaiser 1987; Flexas *et al.*, 2006). In contrast, water deficit strongly reduces leaf or shoot expansion rates (Boyer, 1970a; Hsiao, 1973; Ben Haj Salah and Tardieu, 1997; Tardieu *et al.*, 1999, 2000). Analysis of published work on different plant species in which plant growth and photosynthesis were measured under a range of water deficits is shown in Fig. 1. The common feature in all species is that C demand (growth) always decays before C supply (photosynthesis) is affected by water deficit. Though this analysis does not consider other C demands such as respiration or root growth, it clearly illustrates the large domain of water deficits in which C may be present in excess in the plant.

The impact of water deficit on C metabolism has been the matter of numerous studies. They report in some cases that the enzymes involved show signs of down-regulation (Chaves *et al.*, 2009) but more often support the view of maintained or increased metabolic activity. For instance, sucrose cleaving enzymes increase their activity upon water

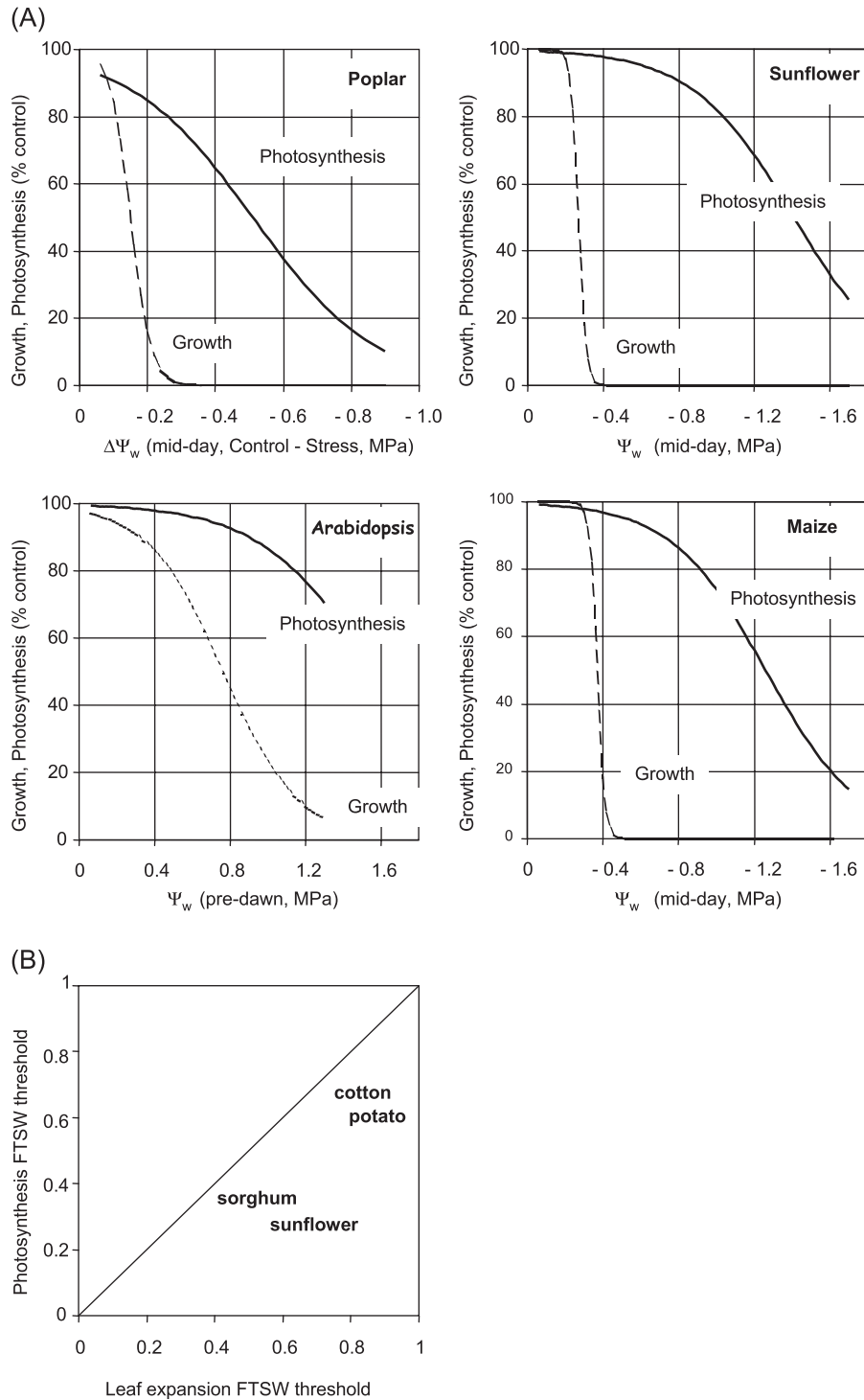


**Fig. 1.** Differential sensitivity of shoot growth and photosynthesis to soil water deficit. (A) Data originate from Bogeat-Triboullot *et al.* (2007) for poplar, Boyer (1970a) and Tardieu *et al.* (1999) for sunflower and maize, and Granier *et al.* (2006) and Hummel *et al.* (2010) for *Arabidopsis*. The x-axis refers to the level of water deficit expressed as midday leaf water potential difference between stressed and non-stressed plants (poplar), midday leaf water potential (maize, sunflower), pre-dawn water potential of the whole rosette (*Arabidopsis*). The y axis refers to both photosynthesis (A, plain lines) and organ growth (Growth, dashed line). Both are shown as a percentage of the well-watered control. Growth is expressed as shoot height increase in poplar, rosette size at bolting in *Arabidopsis*, and leaf elongation rate during day periods in maize and sunflower. In all cases, sigmoidal curves  $\{y=100/[1/(1+\exp(-(\psi-\psi_0)/b])]$  were adjusted to the data or available published curve. Note that the x and y axes do not always refer to the same variables. This figure should thus not be used to compare species sensitivities to soil water deficit. (B) Data originate from a survey performed by Sadras and Milroy (1996). They modelled leaf expansion and photosynthesis response as a function of water deficit using a bilinear model with a threshold defined as the fraction of available soil water (FTSW) at which each of these variables start to decline. Original references are found in Sadras and Milroy (1996). Only those examples from which both variables were measured in the same study by the same group are reported.

deficit in source leaves of cereals (Kim *et al.*, 2000), in pace with an increased need for osmotic adjustment in these leaves (McCree *et al.*, 1984) and a higher C demand by the seeds (Yang *et al.*, 2004). In the growing zone of maize leaves, the activities of several enzymes involved in glycolysis and TCA cycle increase (Riccardi *et al.*, 1998). In perennials such as poplar (Bogeat-Triboulot *et al.*, 2007) or grapevine (Cramer *et al.*, 2007), the triggering of particular metabolic pathways including C metabolism has been observed under moderate to severe water deficit. The activome of *Arabidopsis* plants subjected to various levels of water stress has recently been investigated by profiling a set of 30 enzymes from central C and N metabolism across rosette development (Hummel *et al.*, 2010). In most cases, enzyme activities were increased under water deficit, but these increases occurred slowly and were of low magnitude, suggesting that even in plants facing a 75% drop in aerial biomass production, there was no dramatic or specific reprogramming of metabolism.

While maintenance of C metabolism and increased C concentration in plant parts under water deficit have been reported in most studies, there are also some cases where the opposite is observed. This is notably the case when water deficit is so severe and prolonged that photosynthesis becomes inhibited over a long period. An important co-factor in that case is elevated temperature, which is usually associated with water deficit in nature and results in increased respiration, thereby negatively affecting the C status. This extreme scenario has been proposed to be responsible, along with hydraulic failure, for tree mortality under severe water deficit (McDowell *et al.*, 2008; McDowell and Sevanto, 2010).

## C signalling and possible interactions with stress

Besides their roles as bricks for structure and fuel for energy production, soluble C compounds such as glucose and sucrose (Chiou and Bush, 1998; Laby *et al.*, 2000; Moore *et al.*, 2003; Huang *et al.*, 2008), but also phosphorylated intermediates (e.g. glucose-6-phosphate or trehalose-6-phosphate; Paul, 2007; Zhang *et al.*, 2009), play key signalling roles in the overall shaping of the metabolic and developmental machinery, through both gene expression and post-translational regulation. Because water deficits are likely to alter the concentration of these metabolites, it is important to understand how C and stress signalling are integrated.

Original support for signalling roles of sugars came from single gene expression analysis, pointing towards genes coding for enzymes directly involved in the utilization of C, such as sucrose synthase and invertase (Koch *et al.*, 1992; Cierszko and Kleczkowski, 2002). Later, microarrays revealed that sugars influence the expression of hundreds of genes involved in a wide range of processes (Contento *et al.*, 2004; Price *et al.*, 2004; Thimm *et al.*, 2004; Thum *et al.*, 2004; Bläsing *et al.*, 2005; Li *et al.*, 2006). The cell cycle machinery is a key target of this control (Webster and Van't

Hof, 1969; Riou-Khamlichi *et al.*, 2000). Furthermore, ribosomal proteins and genes involved in tRNA metabolism are among the functional categories that respond the most consistently, at the transcriptional level, to fluctuations in the C resource (Thimm *et al.*, 2004; Bläsing *et al.*, 2005; Osuna *et al.*, 2007). The fact that protein synthesis represents a major sink for energy (Penning de Vries, 1975) strengthens the idea that a tight link between C metabolism and protein synthesis is necessary to prevent acute C starvation (Smith and Stitt, 2007), especially in growing tissues where most of the protein synthesis contributes to building new biomass (Piques *et al.*, 2009). In line with this, considerably more genes have been found to respond to low sugar than to high sugar (Bläsing *et al.*, 2005). It has then been proposed that sugar sensing and signalling enable the avoidance of acute C starvation under a wide range of environmental conditions, thus maintaining the ability to grow under any circumstances (Smith and Stitt, 2007). Strikingly, experiments that led to these conclusions were performed under conditions where light (and thus C) was actually the only factor limiting growth, while environmental stresses were absent.

How C and (water) stress signalling may interact is just beginning to be revealed. Among the different sugar sensing systems proposed, the best known is a pathway involving hexokinase (HXK1), which has been found to interact with abscisic acid (ABA)-, ethylene-, auxin-, and cytokinin-signalling pathways, suggesting a central role in linking C status to stress responses (Rolland *et al.*, 2006). Another glucose sensor, which is located at the plasma membrane and coupled to a G-protein complex, has recently been found in *Arabidopsis* (Grigston *et al.*, 2008). G-protein signalling is also known to be involved in responses to various biotic and abiotic stresses (e.g. Nilson and Assmann, 2010). A further pathway, which is thought to sense various sugars including glucose-6-phosphate (Toroser *et al.*, 2000) and trehalose-6-phosphate (Schluepmann *et al.*, 2004; Zhang *et al.*, 2009), involves SnRK1 protein kinases, which can act on both gene expression and enzyme activity (Halford, 2006), and are also involved in hormone (in particular ABA) signalling. Finally, while no sucrose receptor has been found so far in plants, there is a sucrose-specific pathway, also involving SnRK1, leading to translational control of a basic leucine zipper (bZIP)-type transcription factor (Wiese *et al.*, 2004), by which sucrose represses the expression of various enzymes including proline dehydrogenase (Hanson *et al.*, 2008), which is also repressed under osmotic stress (Yoshida *et al.*, 1997) and induced upon rehydration (Oono *et al.*, 2003).

Together, these results are indicative of a variety of means by which C and stress signalling could be integrated. Such a deep integration has been interpreted as resulting from the fact that most stresses would negatively affect the overall C and energy status of the plant (Baena-Gonzalez and Sheen, 2008). However, the analysis developed in the former sections tends to contradict this interpretation. One hypothesis is that such cross-talk could contribute to the bypass of critical signalling pathways, as an increase in

sugar availability provoked by water stress might otherwise be misleading. In line with this, initial mutant screens revealing such shared signalling pathways have been conducted with very high sugar concentrations (e.g. 6% w/v) ruling out the possibility that stressed plants were C starved (Arenas-Huertero *et al.*, 2000; Huijser *et al.*, 2000; Laby *et al.*, 2000; Rook *et al.*, 2001). Understanding the way water deficit modulates C sensing and signalling therefore appears to be an important topic towards the understanding of plant performance under stressing conditions.

## Water deficit differentially tunes the relationship between C availability and growth in sink organs

Growth and development of sink organs is known to be at least partly under the control of C availability. This has been repeatedly reported for roots (Aguirrezabal *et al.*, 1994; Thaler and Pagès, 1996; Freixes *et al.*, 2002; Willaume and Pagès, 2006), young leaves (Granier and Tardieu, 1999; Muller *et al.*, 2001), flowers (Guilioni *et al.*, 1997; Smith and Stitt, 2007), fruits (Borisjuk *et al.*, 2003; Liu *et al.*, 2004; Wu *et al.*, 2005), and seeds (Munier-Jolain and Ney, 1998; Munier-Jolain and Salon, 2003). Because water deficit increases C concentration and thus possibly C availability in plant tissues, it is important to understand the con-

sequences for organ growth. The analysis performed in the next paragraphs is based on the occurrence of tight relationships between C availability and the expansion or the development of different sink organs. The rationale followed is to use the modification of these relationships as diagnostic of an alteration in the C dependence of growth.

In roots, sucrose unloaded from the phloem is rapidly cleaved by invertase (Hellebust and Forward, 1962; Giaquinta *et al.*, 1983) and/or by sucrose synthase (Martin *et al.*, 1993), which are highly abundant at the site of intense phloem unloading located in the middle of the growing zone (Oparka *et al.*, 1994). This leads to very low sucrose concentrations in the root zone showing rapid expansion (Sharp *et al.*, 1990; Muller *et al.*, 1998). Concentrations of hexose released from sucrose in the growing zone are therefore a good estimate of local C availability, as they depend on the balance between C inflow and utilization. Following this rationale, hexose concentration was evaluated in growing zones of single roots whose elongation rate had been measured during 24 h prior to sampling. In well-watered *Arabidopsis* plants exposed to various light intensities or supplied with external sugars, quantitative relationships between root elongation rate and hexose concentration were found for both primary and secondary roots (Freixes *et al.*, 2002 and Fig. 2). Remarkably, these relationships were robust enough to account for the variation between primary roots of different plants, as well

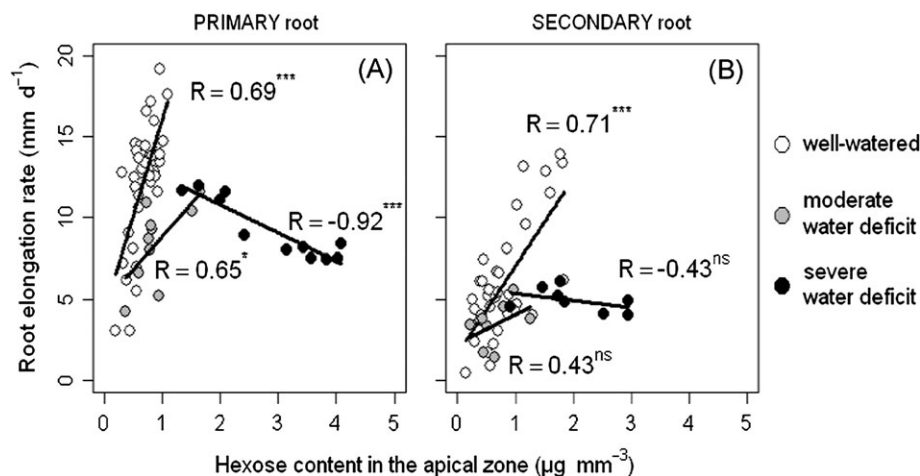


**Fig. 2.** Relationship between hexose content and elongation rate in primary and secondary roots in *Arabidopsis thaliana*. Plants were grown in agar in Petri plates at various light levels ( $5\text{--}20\text{ mol m}^{-2}\text{ d}^{-1}$ ) and were supplied with different sucrose concentrations in the root medium (0, 0.5, or 2% w/v) as in Freixes *et al.* (2002). Plants were grown under well-watered conditions (open circle) or under moderate (grey circle, solute  $\psi_w = -0.3\text{MPa}$ ) or severe (black circle, solute  $\psi_w = -0.5\text{MPa}$ ) water deficit induced by PEG, which was poured on to the surface of the agar medium before sowing. Elongation of primary (A) or secondary (B) roots was monitored during three consecutive days. The 3-mm apical region of individual primary and secondary roots encompassing the growing zone was harvested and soluble sugar content was determined as in Freixes *et al.* (2002). Results were normalized using sample volume. A linear model was fitted to each dataset. Note that the positive correlation found between root elongation rate and hexose content weakened at moderate stress and totally vanished or became negative under severe stress. The statistical significance of correlation changes was given by an analysis of covariance (ANCOVA) performed with the R software (R Development Core Team, 2008), using the water potential as factor and the apical hexose content as continuous variable. The interaction term between water potential and hexose content was high enough ( $P < 10^{-8}$  and  $P < 10^{-4}$  for the primary and secondary roots, respectively) to indicate that the effect of sugar content on growth was dependent on the water potential. Symbols \*\*\*, \*\*, \*, -, and 'ns' indicate that the  $P$  value of a Pearson's correlation test was  $<10^{-3}$ ,  $<10^{-2}$ ,  $<0.05$ ,  $<10^{-1}$ , or non-significant, respectively.

as for the variation between secondary roots of the same plant (Freixes *et al.*, 2002).

When plants were subjected to a moderate ( $\psi_{\text{medium}} = -0.3$  MPa) or severe ( $\psi_{\text{medium}} = -0.5$  MPa) water deficit by adding PEG in the root medium, root elongation rate was reduced (Fig. 2). Furthermore, hexose content increased dramatically in response to stress, i.e. up to four times at the lowest water potential when compared with controls supplied or not with sugars. Hence, the positive correlation between root elongation rate and hexose content weakened at moderate stress and totally vanished or became negative at severe stress. This accumulation can be interpreted as the result of root elongation (and hence C utilization) being more reduced than C inflow. It is thus indicative of some uncoupling between C availability and root elongation.

Growth of young, sink leaves is also highly sensitive to available C, whereas rapidly expanding leaves grow more independently of C supply. For instance, 80% shading strongly decreases expansion rates at early stages of leaf development, but has no effect at later stages (Granier and Tardieu, 1999; Muller *et al.*, 2001). Moreover, C dependence of leaf growth is different between the day and the night. Grimmer and Komor (1999) suggested that leaf growth in *Ricinus* is sink limited during the day but source limited at night. In *Arabidopsis*, the starchless mutant *pgm* shows a 2-fold reduction in leaf relative expansion rate (RER) at night as compared with the wildtype, but there is only a little difference during the day (Wiese *et al.*, 2007).

In leaves, the amount of C available for growth is the result of the balance between net photosynthesis, the accumulation of starch and various C-containing metabolites such as organic acids during the day and their remobilization at night, and C export to sink organs (Kerr *et al.*, 1985; Hendrix and Huber, 1986). Starch turnover, defined as the variation in starch content between the end of the day and the end of the night, provides a good estimate of C availability, especially for night growth (Sulpice *et al.*, 2009). Indeed, starch production proceeds at a stable rate throughout the photoperiod, and the maximum concentration reached at the end of the day is well related to C availability under a range of photoperiods (Gibon *et al.*, 2009), light intensities, or CO<sub>2</sub> levels (Sharkey *et al.*, 1985). In order to establish links between C availability and leaf growth, a set of mutants affected in starch production or utilization (*pgm*, *sex1*, *mex1*, and *dpe2*) was used. Diurnal RER of well-watered plants (Fig. 3A) showed slight negative correlation with starch turnover, which may be suggestive of a trade-off between expansion and storage during the day (Walter *et al.*, 2002). The correlation was moderately affected by water deficit (i.e. steeper slope and lower *p*-value) although no significant difference was found between slopes. In contrast and as expected, well-watered genotypes displayed large variability in starch turnover, which was positively related to leaf RER at night (Fig. 3B). This correlation was still significant at moderate stress, but vanished at severe water deficit, indicating that severe water deficit released the reliance of leaf expansion on C availability at night.

Flower set is highly sensitive to assimilate availability. In sunflower, tissue expansion in the reproductive shoot apical meristem (capitulum) directly impacts crop productivity because the number of initiated florets, a crucial component of grain yield (Cantagallo and Hall, 2002), depends on the rate and duration of tissue expansion in the meristem (Dosio *et al.*, 2006). The duration depends on the balance between the rate of centripetal progression of the generative front where florets initiate and the expansion rate of the central meristematic zone (Palmer and Steer, 1985 and Fig. 4A). A low value of the expansion rate leads to accelerated meristem exhaustion, a low number of initiated primordia, and low yield (Dosio *et al.*, 2006). In order to evaluate the dependency of meristem expansion on C availability, sunflower plants were grown in field and greenhouse, at high or low plant density (Dosio *et al.*, 2006). Plants were also subjected or not to a period of shading or of soil water deficit. Soluble sugar content was measured in synchrony with capitulum expansion rate (Dosio *et al.*, 2011). In the absence of soil water deficit, the changes in RER of the capitulum paralleled the changes in soluble sugars induced by the treatments affecting light supply (Fig. 4B), suggesting a strong role for C availability in the expanding activity of the capitulum meristematic zone. When soil water deficit developed, soluble sugars accumulated in the capitulum, while the rate of tissue expansion in the meristem decreased. Maximum sugar concentrations were measured at the end of the late water deficit. Remarkably, re-irrigation increased meristem expansion and decreased sugar content in such a way that corresponding points fit on the same relationship as in the absence of stress. Taken together, these data suggest that water deficit altered the dependence of meristem expansion on C availability.

Growth and development of fruits also rely strongly on a continuous supply of carbohydrates from source organs (Ho, 1988; Lebon *et al.*, 2008). Both fruit load and leaf shading have a considerable impact on carbohydrate partitioning and fruit size (Baldet *et al.*, 2002), possibly through the regulation of genes related to cell proliferation at very early stages of flower development (Baldet *et al.*, 2006). C starvation is also known to provoke the abortion of flowers or fruits at early stages of their development (Boyle *et al.*, 1991; Guillioni *et al.*, 1997, 2003; Smith and Stitt, 2007). Interestingly, kernel abortion provoked by extreme water stress in maize can be strongly reduced when stems are infused with sucrose (McLaughlin and Boyer, 2004) suggesting that water deficit impairs phloem and thus sugar transport into the ovaries (Makela *et al.*, 2005). In peach, water deficit decreases fruit growth whatever the fruit load and thus C availability (Berman and DeJong, 1996).

Beyond these examples, only a few studies have questioned how water deficit modifies the dependence of fruit growth on C. To address this question, a modelling approach was used, enabling the simulation of a wide range of environmental scenarios. The model used was developed for peach fruits, and validated under various situations

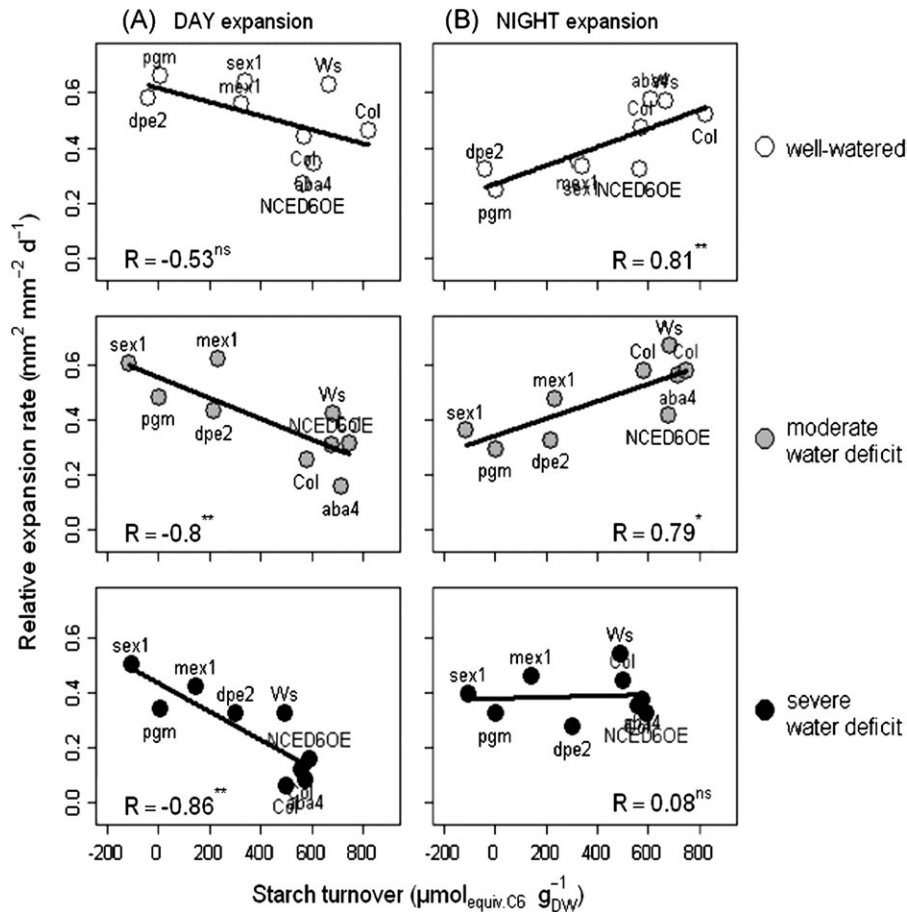


**Fig. 3.** Relationship between starch turnover and day or night leaf expansion in *A. thaliana*. Nine *Arabidopsis* genotypes (including accessions and mutants) were grown at three levels of soil water content as in Hummel *et al.* (2010). In brief, pot-grown plants were irrigated to a target soil water content corresponding to a well-watered situation (pre-dawn leaf  $\psi_w = -0.35$  MPa), moderate soil water deficit (pre-dawn leaf  $\psi_w = -0.6$  MPa), or severe deficit (pre-dawn leaf  $\psi_w = -1.1$  MPa). Genotypes included two wildtypes: Col-0 (replicated twice) and Ws; four starch-related mutants: *pgm* (Caspar *et al.*, 1985), *mex1* (Niittylä *et al.*, 2004), *sex1* (Caspar *et al.*, 1991), and *dpe2* (Chia *et al.*, 2004; Lu and Sharkey, 2004); and two ABA-related genotypes: *aba4* KO mutant (North *et al.*, 2007) and *NCED6* overexpressing line (Lefebvre *et al.*, 2006). At 45 d after sowing, the plants displayed steady-state rates of leaf production and successive leaves showed comparable behaviour (F. Pantin, T. Simonneau, B. Muller *et al.*, unpublished). Zenithal images of eight plants were taken twice a day for 3 d, at the end of both the dark and the light period. A semi-automated program developed on ImageJ software (<http://rsb.info.nih.gov/ij/>) was used to extract the area of individual leaves. Day and night RERs were computed from several individual leaves and averaged to obtain a single representative value. Four samples of actively growing leaves were then harvested at the end of day and at the end of night for evaluation of starch turnover. The day (A, left panels) or night (B, right panels) RER was plotted against starch turnover. A linear model was fitted to each dataset. Note that the positive correlation between night RER and starch turnover weakened under severe water deficit as shown by an ANCOVA performed with the R software, using the water potential as factor and the starch turnover as continuous variable. The interaction term between water potential and starch turnover indicated that the effect of starch turnover on night RER was dependent on the water potential ( $P < 10^{-1}$ ). In contrast, no significant interaction was detected for the correlations for day RER indicating that water deficit did not alter relationships between starch turnover and day RER. Symbols \*\*\*, \*\*, \*, ., and 'ns' indicate that the  $P$ -value of a Pearson's correlation test was  $<10^{-3}$ ,  $<10^{-2}$ ,  $<0.05$ ,  $<10^{-1}$ , or non-significant, respectively.

(Fishman and Génard, 1998; Lescourret and Génard, 2005). This model (details can be found as Supplementary data, available at *JXB* online) predicts dry matter accumulation as the balance between phloem sugar unloading and fruit respiration, fresh matter (dry matter plus water) accumulation, as the result of water fluxes driven by water potential gradients, and volumetric fruit expansion by using the Lockhart (1965) equation, which relates tissue expansion to

cell wall rheology and turgor. C availability was virtually affected, by modifying sucrose concentrations in the phloem reaching the fruit (from 0.02 to 0.2  $\text{g g}^{-1}$ ). Then, to investigate the effects of water deficit, simulations were also run with xylem water potential ranging from  $-0.2$  to  $-2.8$  MPa. Data of air temperature and humidity corresponding to a natural climatic scenario were provided to the model. Figure 5A, B gives the simulated outputs for three

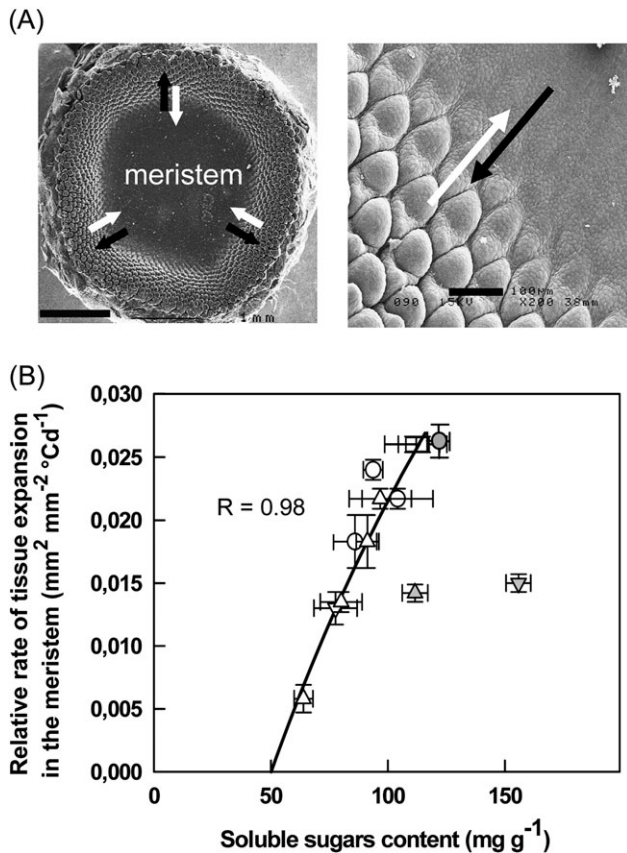


**Fig. 4.** Relationship between soluble sugar content and tissue expansion in the meristem of sunflower capitulum. (A) Top view of a sunflower capitulum during floret initiation (left; scale bar, 1 mm) and detailed view of newly initiated primordia at meristem rim (right; bar, 100  $\mu\text{m}$ ). The apparent growth of the meristem of sunflower capitulum results from the opposite effects of two processes (arrows). The expansion of the inner meristem itself (black arrows) increases meristem size while floret primordia tend to fill the expanding field of tissue with individual flowers (white arrows). The rate of tissue expansion in the meristem is thus calculated from the time courses of meristem area, primordium area, and floret number (Dosio *et al.*, 2006). (B) Relative rate of tissue expansion in the meristem as a function of soluble sugar content ( $\text{mg g}^{-1}$  dry weight) in the capitulum for plants grown in different environmental conditions, in which light (open symbols) or soil water (grey symbols) were altered. Plants were subjected to light deficit using shading or varying crop density (open triangles) or to moderate soil water deficit (grey triangles) either from capitulum initiation to first floret initiation (upward triangles), or from first floret initiation to completion of floret initiation (downward triangles). Some plants exposed to soil water deficit were re-irrigated (grey circle). Circles, control plants in the greenhouse and in field plots; squares, isolated field plants. Bars, SE. Redrawn from Dosio *et al.* (2011).

sugar concentrations in the phloem (low, intermediate, and high) at three watering regimes (well-watered, moderate, and severe water deficit). For well-watered plants, final fruit fresh weight was  $\sim 250$  g at high and intermediate sucrose concentrations, but was reduced to 90 g at low

sucrose (Fig. 5A) and fruit relative growth rate (RGR) computed from fresh weight variations (Fig. 5B) reduced accordingly (Fig. 5B). This result fits well with experimental data obtained by changing the fruit load to leaf surface ratio in tomato (Ho, 1988), coffee (Vaast *et al.*, 2001), and peach (Berman and DeJong, 1996). In plants subjected to severe water deficit, the model also predicted that fruit expansion would be reduced, resulting in a final fresh weight of 90, 60, and 20 g at high, intermediate, or low sucrose concentration in the phloem sap, respectively (Fig. 5A). However, while water deficit had a negative influence on fruit RGR during the first 20d of fruit growth, RGR remained after this time essentially driven by the phloem sugar content, independently of the xylem water potential (Fig. 5B). This was confirmed for a larger range of sugar supply in Fig. 5C where the shape of the saturating relationship between phloem sugar concentrations and fruit RGR (averaged during the rapid growth phase) was only marginally altered, even at low xylem water potential. Strikingly, due to higher fruit transpiration under well-watered conditions (Fig. 5E), RGR was not higher than under moderate stress conditions (Fig. 5C), probably in relation to higher cuticular conductance (Gibert *et al.*, 2005). As observed for other organs, water deficit strongly increased fruit sugar content, because passive concentration occurred due to reduced fruit expansion. However, the slope of the relationship between RGR and sugar content was not strongly altered, still indicating no interaction between water and sugar availability (Fig. 5D). This result differs from those found in leaves, roots, and reproductive meristem. The reason for such a discrepancy is not known but could be linked to the dominant role of sugars in fleshy fruits in which very high sugar concentrations are essential contributors to lowering the osmotic potential and thus maintaining high turgor. This role is likely to be shared among more actors in other organs (Sharp *et al.*, 1990; Hummel *et al.*, 2010). For instance, in the maize root growing zone, hexoses, together with  $\text{K}^+$ , strongly contribute to this role (Sharp *et al.*, 1990). In contrast, in the *Arabidopsis* rosette, other C-rich compounds (mainly organic acids and proline) contribute to  $> 40\%$  of osmotic adjustment whereas sugars contribute to  $< 10\%$  (Hummel *et al.*, 2010).

Does this imply that fruit water relations do not interfere in the relationships between C availability and growth? Model outputs also suggest that at later stages of development, rapidly expanding well-watered fruits showed strong fluctuations in RGR (Fig. 5B) due to fruit shrinkage during days under high evaporative demand (Days 131 and 139 in Fig. 5B) and subsequent growth boost when the air becomes wetter again, a situation commonly observed in natural conditions (Johnson *et al.*, 2006). These natural climatic variations were used to evaluate the effect of evaporative demand on the relationships between C availability and fruit growth. From the well-watered situation, days were grouped according to the mean vapour pressure deficit (VPD) occurring during those days [either high ( $> 1.25$  kPa), intermediate ( $1.25 \text{ kPa} > \text{VPD} > 0.75$  kPa), or

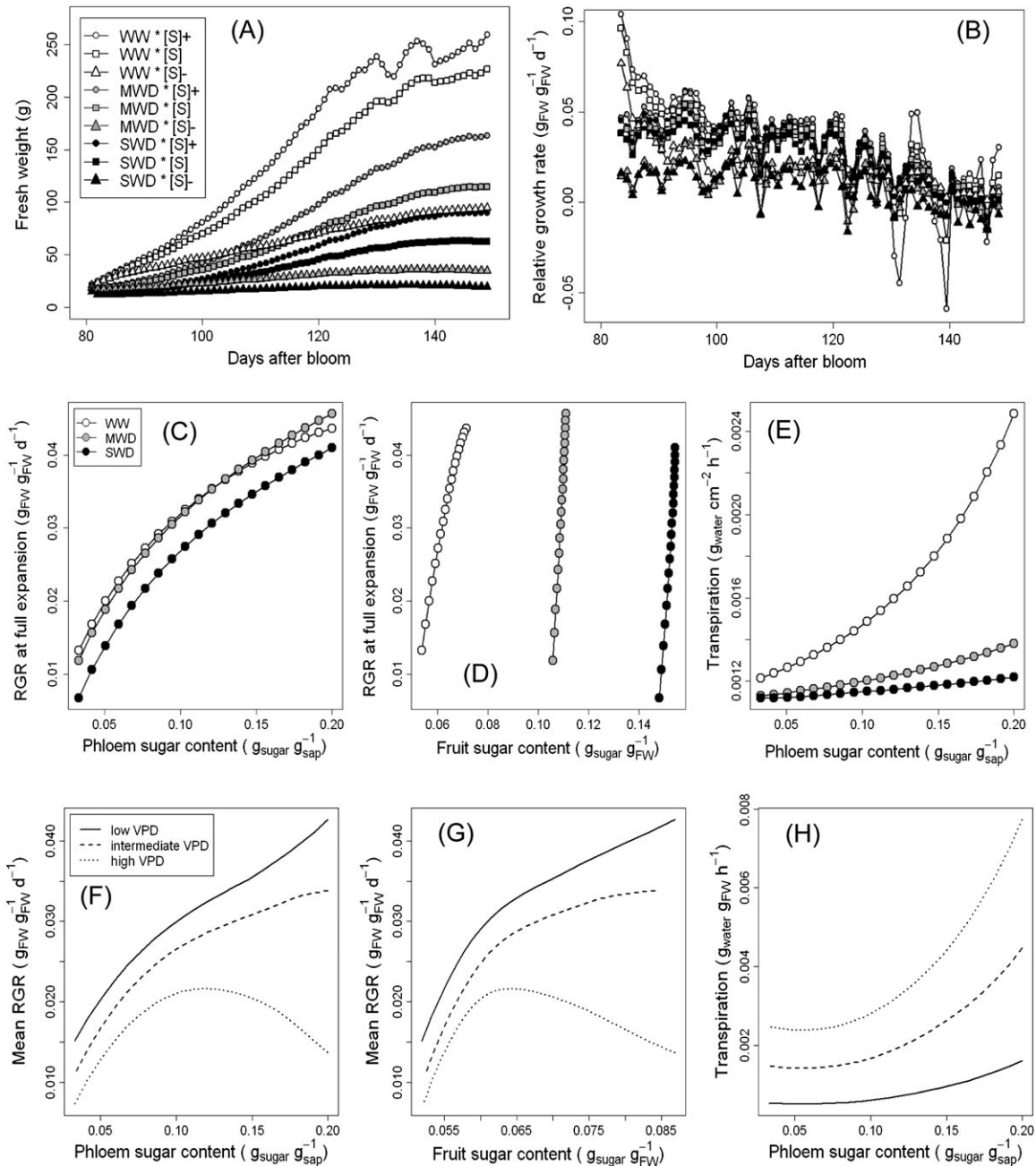


**Fig. 5.** Simulations of peach fruit growth under a wide range of phloem sugar concentrations and xylem water potentials. A biophysical model designed to simulate the transport of water and sugar into fruit (Fishman and Génard, 1998; Lescouret and Génard, 2005) was used with minor modifications to assess the effects of phloem sugar concentration and xylem water potential on peach fruit growth. The model is based on the representation of plastic fruit growth as a function of turgor pressure using the Lockhart (1965) equation. The fruit is considered as one compartment separated from xylem or phloem tissue by a membrane; flows across this membrane are described by thermodynamic equations, involving differences in hydrostatic and osmotic pressure on both sides of the membrane, and properties of the membrane towards water (hydraulic conductivity) and solutes (reflection coefficient and permeability). The total uptake of carbon from phloem is the sum of contributions due to mass flow, passive diffusion, and active transport. The virtual experiment was implemented with R software and run from 80 to 149 d after bloom in hourly time-steps. Climatic inputs are air VPD, which strongly impacted fruit transpiration and air temperature obtained from a representative natural dataset. Plant inputs are phloem sugar concentration and xylem water potential; in each simulation, they follow a sinusoidal function with fixed extremes in a period of 24 h. (A) Daily evolution of peach fresh weight for three xylem water potentials  $\times$  three phloem sugar concentrations. Open symbols represent well-watered plants (WW, daily averaged xylem water potential of  $-0.4$  MPa), grey symbols are for moderate water deficit (MWD,  $-1.1$  MPa), and dark symbols are for severe deficit (SWD,  $-1.8$  MPa). Circles are for a high sugar supply (daily averaged phloem concentration of  $0.18$  g  $g^{-1}$ ), squares for intermediate sugar supply ( $0.13$  g  $g^{-1}$ ), and triangle for low sugar supply ( $0.04$  g  $g^{-1}$ ). (B) Daily evolution of fruit RGR during the same simulations. RGR was computed as the local slope of the natural logarithm of fresh weight as a function of

low (<0.75 kPa) evaporative demand] and fruit RGR was averaged for each of these groups. Remarkably, increasing VPD in well-watered plants reduced the slope of the relationship between phloem or fruit sugar content and fruit RGR (Fig. 5F, G). In the model, VPD reduces the amount of water in the fruit by increasing transpiration according to a physical law describing the mass flow between the air-filled space of the fruit and the ambient atmosphere. Figure 5H shows to what extent high VPD increased transpiration in the well-watered plants. However, it did not alter the fruit sugar content (Fig. 5G). This fits with the view that increasing sink limitation, here by a purely hydraulic process, leads to uncoupling of growth from C availability.

### Significance of the relationships between C availability and growth, and possible reasons for their modification under water deficit

C is hypothesised to promote organ growth through a variety of mechanisms: (i) the supply of energy to highly consuming meristematic regions (Bidel *et al.*, 2000; Farrar and Jones, 2000); (ii) the generation of turgor in expanding cells via the accumulation of osmotically active C compounds (Sharp *et al.*, 1990); (iii) the supply of C bricks to the cell wall (Bret-Harte *et al.*, 1991); and (iv) the triggering of developmental or metabolic processes via C signalling (Rolland *et al.*, 2006). The positive relationships illustrated in the previous section certainly integrate some if not all of these mechanisms. Their weakening or more generally their modification may have at least two significations. First, it is possible that bulk tissue concentrations may be less relevant as an estimate of C availability under water deficit than under well-watered conditions. Thus, the importance of the vacuolar pool of C-soluble compounds is likely to increase with water deficit (Kim *et al.*, 2000) whereas the cytosolic sugars are probably more important for sugar sensing or triggering energy production. Furthermore, growth and development might be better related to sugar fluxes imported from the phloem and/or to sugar gradients (Borisjuk *et al.*, 2003; Munier-Jollain and Salon, 2003; Makela *et al.*, 2005), than to their concentrations (see Fig. 5). Another possibility is that water deficit mainly reduces growth through C-independent mechanisms, thus uncoupling growth from C availability. These C-independent mechanisms are likely

to be related to water flux to growing cells, which is reduced under soil water deficit (Tang and Boyer, 2002), or to mechanical properties of growing cell walls possibly under the influence of hormones or pH (Fan and Neumann, 2004). Accordingly, it was recently shown that the cell wall loosening proteins expansins are intimately coupled, at the transcriptional level, with local expansion in maize leaves (Muller *et al.*, 2007). This suggests that the modification (weakening) of the relationship between C availability and growth can be interpreted as the signature of the passage from source (C-based) growth limitation to less- or non-C-based (i.e. sink) limitation.

### Conclusion

When plants are facing soil water deficit, growth is reduced and C concentrations rise, possibly due to organ expansion being affected earlier and more intensively than photosynthesis and metabolism. This leads to increased concentrations in various C molecular forms in several plant parts, ruling out the idea that stress-induced energy deprivation would be the usual cause of growth reduction under water deficit. Elevated C concentrations under water deficit are also likely to interfere with C signalling in a manner that will deserve further attention. Under well-watered conditions, tight relationships linking C availability and growth illustrate the source limitation of growth in sink organs such as roots, leaves (at night), flowers, and fruits. These relationships probably reflect the different uses of C compounds, i.e. as fuel for energy supply, bricks for structure build-up, osmotica for turgor maintenance as well as signal molecules for triggering developmental and metabolic programmes. Under water deficit, these relationships are modified, suggesting that other mechanisms, possibly involving cell wall rheology or water fluxes to growing cells, override the role of C and take the lead on growth control.

### Supplementary data

Supplementary data are available at *JXB* online.

**Supplementary information:** rationale and main equations from the biophysical model of fruit growth (Fishman and Génard, 1998) used to construct Fig. 5.

time. Same symbols as in (A). (C) Effect of phloem sugar content on fruit RGR during rapid expansion (averaged between Days 110 and 115) at three selected xylem water potentials. (D) Relationship between fruit sugar concentration and RGR at full expansion in the same conditions as in (C). (E) Effect of phloem sugar content on fruit transpiration for the same set of conditions as in (C). In (C), (D), and (E), open, grey, and dark circles represent well-watered plants, moderate water deficit, and severe water deficit, respectively. (F) Effect of phloem sugar concentration and evaporative demand (estimated through the VPD) in well-watered peach plants on fruit RGR. Days were categorized according to average VPD. At all imposed phloem sugar concentrations, RGR was averaged for each VPD level. Solid line for low evaporative demand (0.75 kPa > VPD), dashed line for intermediate evaporative demand (1.25 kPa > VPD > 0.75 kPa), dotted line for high evaporative demand (VPD > 1.25 kPa). (G) Effect of fruit sugar concentration and VPD on fruit RGR in well-watered peach plants. Same conditions as in (F). (H) Effect of phloem sugar concentration and VPD on fruit transpiration. Same conditions as in (F).

## Acknowledgements

The authors thank A. Smith and S. Zeeman for sharing seeds of the *dpe2*, *sex1*, and *mex-1* mutants, A. Marion-Poll for sharing *aba4* mutant and NCED6-OE line, G. Dosio for collecting the data from Fig. 4, M. Stitt and F. Tardieu for continuous, fruitful discussions and the constructive suggestions made by two anonymous reviewers. BM thanks ANR-CASAH-BI, INRA-EA and Procope for funding.

## References

- Aguirrezabal L, Deleens E, Tardieu F.** 1994. Root elongation rate is accounted for by intercepted PPFD and source-sink relations in field and laboratory-grown sunflower. *Plant, Cell and Environment* **17**, 443–450.
- Arenas-Huertero F, Arroyo A, Zhou L, Sheen J, León P.** 2000. Analysis of *Arabidopsis* glucose insensitive mutants, *gin5* and *gin6*, reveals a central role of the plant hormone ABA in the regulation of plant vegetative development by sugar. *Genes and Development* **14**, 2085–2096.
- Ashraf M, Foolad M.** 2007. Roles of glycine betaine and proline in improving plant abiotic stress resistance. *Environmental and Experimental Botany* **59**, 206–216.
- Baena-Gonzalez E, Sheen J.** 2008. Convergent energy and stress signaling. *Trends in Plant Science* **13**, 474–482.
- Baldet P, Devaux C, Chevalier C, Brouquisse R, Just D, Raymond P.** 2002. Contrasted responses to carbohydrate limitation in tomato fruit at two stages of development. *Plant, Cell and Environment* **25**, 1639–1649.
- Baldet P, Hernould M, Laporte F, Mounet F, Just D, Mouras A, Chevalier C, Rothan C.** 2006. The expression of cell proliferation-related genes in early developing flowers is affected by a fruit load reduction in tomato plants. *Journal of Experimental Botany* **57**, 961–970.
- Barnett NM, Naylor AW.** 1966. Amino acid and protein metabolism in Bermuda grass during water stress. *Plant Physiology* **41**, 1222–1230.
- Ben Haj Salah H, Tardieu F.** 1997. Control of leaf expansion rate of droughted maize plants under fluctuating evaporative demand. A superposition of hydraulic and chemical messages? *Plant Physiology* **114**, 893–900.
- Berman ME, DeJong TM.** 1996. Water stress and crop load effects on fruit fresh and dry weights in peach (*Prunus persica*). *Tree Physiology* **16**, 859–864.
- Bidel LPR, Renault P, Pagès L, Rivière LM.** 2000. Mapping meristem respiration of *Prunus persica* (L.) Batsch seedlings: potential respiration of the meristems, O<sub>2</sub> diffusional constraints and combined effects on root growth. *Journal of Experimental Botany* **51**, 755–768.
- Bläsing OE, Gibon Y, Gunther M, Hohne M, Morcuende R, Osuna D, Thimm O, Usadel B, Scheible WR, Stitt M.** 2005. Sugars and circadian regulation make major contributions to the global regulation of diurnal gene expression in *Arabidopsis*. *The Plant Cell* **17**, 3257–3281.
- Bogeat-Triboulot MB, Brosche M, Renaut J, Jouve L, Le Thiec D, Fayyaz P, Vinocur B, Witters E, Laukens K, Teichmann T.** 2007. Gradual soil water depletion results in reversible changes of gene expression, protein profiles, ecophysiology, and growth performance in *Populus euphratica*, a poplar growing in arid regions. *Plant Physiology* **143**, 876–892.
- Bohnert HJ, Jensen RG.** 1996. Strategies for engineering water-stress tolerance in plants. *Trends in Biotechnology* **14**, 89–97.
- Borisjuk L, Rolletschek H, Wobus U, Weber H.** 2003. Differentiation of legume cotyledons as related to metabolic gradients and assimilate transport into seeds. *Journal of Experimental Botany* **54**, 503–512.
- Boyer JS.** 1970a. Leaf enlargement and metabolic rates in corn, soybean, and sunflower at various leaf water potentials. *Plant Physiology* **46**, 233–235.
- Boyer JS.** 1970b. Differing sensitivity of photosynthesis to low leaf water potentials in corn and soybean. *Plant Physiology* **46**, 236–239.
- Boyle MG, Boyer JS, Morgan PW.** 1991. Stem infusion of liquid culture medium prevents reproductive failure of maize at low water potential. *Crop Science* **31**, 1246–1252.
- Bret-Harte MS, Baskin T, Green P.** 1991. Auxin stimulates both deposition and breakdown of material in the pea outer epidermal cell wall, as measured interferometrically. *Planta* **185**, 462–471.
- Cantagallo JE, Hall AJ.** 2002. Seed number in sunflower as affected by light stress during the floret differentiation interval. *Field Crops Research* **74**, 173–181.
- Caspar T, Huber SC, Somerville C.** 1985. Alterations in growth, photosynthesis, and respiration in a starchless mutant of *Arabidopsis thaliana* deficient in chloroplast phosphoglucomutase activity. *Plant Physiology* **79**, 11–17.
- Caspar T, Lin TP, Kakefuda G, Benbow L, Preiss J, Somerville C.** 1991. Mutants of *Arabidopsis* with altered regulation of starch degradation. *Plant Physiology* **95**, 1181–1188.
- Chaves MM, Flexas J, Pinheiro C.** 2009. Photosynthesis under drought and salt stress: regulation mechanisms from whole plant to cell. *Annals of Botany* **103**, 551–560.
- Chia T, Thorneycroft D, Chapple A, Messerli G, Chen J, Zeeman SC, Smith SM, Smith AM.** 2004. A cytosolic glucosyltransferase is required for conversion of starch to sucrose in *Arabidopsis* leaves at night. *The Plant Journal* **37**, 853–863.
- Chiou TJ, Bush D.** 1998. Sucrose is a signal molecule in assimilate partitioning. *Proceedings of the National Academy of Sciences, USA* **95**, 4784–4788.
- Ciereszko I, Kleczkowski LA.** 2002. Glucose and mannose regulate the expression of a major sucrose synthase gene in *Arabidopsis* via hexokinase-dependent mechanisms. *Plant Physiology and Biochemistry* **40**, 907–911.
- Contento AL, Kim SJ, Bassham DC.** 2004. Transcriptome profiling of the response of *Arabidopsis* suspension culture cells to Suc starvation. *Plant Physiology* **35**, 2330–2347.
- Cornic G.** 2000. Drought stress inhibits photosynthesis by decreasing stomatal aperture - not by affecting ATP synthesis. *Trends in Plant Science* **5**, 187–188.
- Cramer G, Ergül A, Grimplet J, et al.** 2007. Water and salinity stress in grapevines, early and late changes in transcript and metabolite profiles. *Functional and Integrative Genomics* **7**, 111–134.

- Dosio GAA, Tardieu F, Turc O.** 2006. How does the meristem of sunflower capitulum cope with tissue expansion and floret initiation? A quantitative analysis. *New Phytologist* **170**, 711–722.
- Dosio GAA, Tardieu F, Turc O.** 2011. Floret initiation, tissue expansion and carbon availability at the meristem of the sunflower capitulum as affected by water or light deficits. *New Phytologist* **189**, 94–105.
- Fan L, Neumann PM.** 2004. The spatially variable inhibition by water deficit of maize root growth correlates with altered profiles of proton flux and cell wall pH. *Plant Physiology* **135**, 2291–2300.
- Fariás-Rodríguez R, Mellor RB, Arias C, Peña-Cabriaes JJ.** 1998. The accumulation of trehalose in nodules of several cultivars of common bean (*Phaseolus vulgaris*) and its correlation with resistance to drought stress. *Physiologia Plantarum* **102**, 353–359.
- Farrar JF, Jones DL.** 2000. The control of carbon acquisition by roots. *New Phytologist* **147**, 43–53.
- Fishman S, Génard M.** 1998. Model of fruit growth based on biophysical description of main contributing processes. Simulation of seasonal and diurnal dynamics of weight. *Plant, Cell and Environment* **21**, 739–752.
- Flexas J, Medrano H.** 2002. Drought-inhibition of photosynthesis in C3 plants, stomatal and non-stomatal limitations revisited. *Annals of Botany* **89**, 183–189.
- Flexas J, Ribas-Carbo M, Bota J, Galmes J, Henkle M, Martinez-Canellas S, Medrano H.** 2006. Decreased Rubisco activity during water stress is not induced by decreased relative water content but related to conditions of low stomatal conductance and chloroplast CO<sub>2</sub> concentration. *New Phytologist* **172**, 73–82.
- Franco AC, Ball E, Lüttge U.** 2006. Differential effects of drought and light levels on accumulation of citric and malic acids during CAM in *Clusia*. *Plant, Cell and Environment* **15**, 821–829.
- Freixes S, Thibaud M, Tardieu F, Muller B.** 2002. Root elongation and branching is related to local hexose concentration in *Arabidopsis thaliana* seedlings. *Plant, Cell and Environment* **25**, 1357–1366.
- Gagneul D, Ainouche A, Duhaze C, Lugan R, Larher FR, Bouchereau A.** 2007. A reassessment of the function of the so-called compatible solutes in the halophytic Plumbaginaceae. *Limonium latifolium*. *Plant Physiology* **144**, 1598–1611.
- Giaquinta RT, Lin W, Sadler NL, Franceschi VR.** 1983. Pathway of phloem unloading of sucrose in corn roots. *Plant Physiology* **72**, 362–367.
- Gibert C, Lescourret F, Génard M, Vercambre G, Pérez Pastor A.** 2005. Modelling the effect of fruit growth on surface conductance to water vapour diffusion. *Annals of Botany* **95**, 673–683.
- Gibon Y, Pyl E, Sulpice R, Lunn JE, Höhne M, Günther M, Stitt M.** 2009. Adjustment of growth, starch turnover, protein content and central metabolism to a decrease of the carbon supply when *Arabidopsis* is grown in very short photoperiods. *Plant, Cell and Environment* **32**, 859–874.
- Granier C, Aguirrezabal L, Chenu K, et al.** 2006. PHENOPSIS, an automated platform for reproducible phenotyping of plant responses to soil water deficit in *Arabidopsis thaliana* permitted the identification of an accession with low sensitivity to soil water deficit. *New Phytologist* **169**, 623–635.
- Granier C, Tardieu F.** 1999. Leaf expansion and cell division are affected by reducing absorbed light before but not after the decline in cell division rate in the sunflower leaf. *Plant, Cell and Environment* **22**, 1365–1376.
- Grigston JC, Osuna D, Scheible WR, Liu C, Stitt M, Jones AM.** 2008. D-Glucose sensing by a plasma membrane regulator of G signaling protein, AtRGS1. *FEBS Letters* **582**, 3577–3584.
- Grimmer C, Komor E.** 1999. Assimilate export by leaves of *Ricinus communis* L. growing under normal and elevated carbon dioxide concentrations: the same rate during the day, a different rate at night. *Planta* **209**, 275–281.
- Guicherd P, Peltier JP, Gout E, Bligny R, Marigo G.** 1997. Osmotic adjustment in *Fraxinus excelsior* L., malate and mannitol accumulation in leaves under drought conditions. *Trees Structure and Function* **11**, 155–161.
- Guilioni L, Wéry J, Lecoœur J.** 2003. High temperature and water deficit may reduce seed number in field pea purely by decreasing plant growth rate. *Functional Plant Biology* **30**, 1151–1164.
- Guilioni L, Wéry J, Tardieu F.** 1997. Heat stress-induced abortion of buds and flowers in pea. Is sensitivity linked to organ age or to relations between reproductive organs? *Annals of Botany* **80**, 159–168.
- Halford NG.** 2006. Regulation of carbon and amino acid metabolism, roles of sucrose nonfermenting-1-related protein kinase-1 and general control nonderepressible-2-related protein kinase. *Advances in Botanical Research Incorporating Advances in Plant Pathology* **43**, 93–142.
- Hanson J, Hanssen M, Wiese A, Hendriks MM, Smeekens S.** 2008. The sucrose regulated transcription factor bZIP11 affects amino acid metabolism by regulating the expression of asparagine synthetase1 and proline dehydrogenase2. *The Plant Journal* **53**, 935–949.
- Hare P, Cress W.** 1997. Metabolic implications of stress-induced proline accumulation in plants. *Plant Growth Regulation* **21**, 79–102.
- Hellebust JA, Forward DF.** 1962. The invertase of the corn radicle and its activity in successive stages of growth. *Canadian Journal of Botany* **40**, 113–126.
- Hendrix DL, Huber SC.** 1986. Diurnal fluctuations in cotton leaf carbon export, carbohydrate content, and sucrose synthesizing enzymes. *Plant Physiology* **81**, 584–586.
- Ho LC.** 1988. Metabolism and compartmentation of imported sugars in sink organs in relation to sink strength. *Annual Review of Plant Physiology and Plant Molecular Biology* **39**, 355–378.
- Hsiao TC.** 1973. Plant responses to water stress. *Annual Review of Plant Physiology* **24**, 519–570.
- Hsiao TC, Acevedo E.** 1974. Plant responses to water deficits, efficiency, and drought resistance. *Agricultural Meteorology* **14**, 59–84.
- Huang YD, Li CY, Biddle KD, Gibson SI.** 2008. Identification, cloning and characterization of sis7 and sis10 sugar-insensitive mutants of *Arabidopsis*. *BMC Plant Biology* **8**, 104.
- Huijser C, Kortstee A, Pego J, Weisbeek P, Wisman E, Smeekens S.** 2000. The *Arabidopsis* SUCROSE UNCOUPLED-6

- gene is identical to ABSCISIC ACID INSENSITIVE-4: involvement of abscisic acid in sugar responses. *The Plant Journal* **23**, 577–585.
- Hummel I, Pantin F, Sulpice R, Piques M, Rolland G, Dauzat M, Christophe A, Pervent M, Bouteillé M, Stitt M, Gibon Y, Muller B.** 2010. *Arabidopsis thaliana* plants acclimate to water deficit at low cost through changes of C usage; an integrated perspective using growth, metabolite, enzyme and gene expression analysis. *Plant Physiology* **154**, 357–372.
- Jiang Y, Huang B.** 2001. Osmotic adjustment and root growth associated with drought preconditioning-enhanced heat tolerance in Kentucky bluegrass. *Crop Science* **41**, 1168–1173.
- Johnson RW, Dixon MA, Lee DR.** 2006. Water relations of the tomato during fruit growth. *Plant, Cell and Environment* **15**, 947–953.
- Kaiser WM.** 1987. Effects of water deficit on photosynthetic capacity. *Physiologia Plantarum* **71**, 142–149.
- Kerr PS, Rufty TW, Huber SC.** 1985. Changes in nonstructural carbohydrates in different parts of soybean. *Glycine max* (L.) Merr. plants during a light/dark cycle and in extended darkness. *Plant Physiology* **78**, 576–581.
- Kim JY, Mahe A, Brangeon J, Prioul JL.** 2000. A maize vacuolar invertase, IVR2, is induced by water stress. Organ/tissue specificity and diurnal modulation of expression. *Plant Physiology* **124**, 71–84.
- Koch KE.** 1996. Carbohydrate-modulated gene expression in plants. *Annual Review of Plant Physiology and Plant Molecular Biology* **47**, 509–540.
- Koch KE, Nolte KD, Duke ER, McCarty DR, Avigne WT.** 1992. Sugar levels modulate differential expression of maize sucrose synthase genes. *The Plant Cell* **4**, 59–69.
- Laby RJ, Kincaid MS, Kim DG, Gibson SI.** 2000. The *Arabidopsis* sugar-insensitive mutants *sis4* and *sis5* are defective in abscisic acid synthesis and response. *The Plant Journal* **23**, 587–596.
- Lebon G, Wojnarowicz G, Holzapfel B, Fontaine F, Vaillant-Gaveau N, Clement C.** 2008. Sugars and flowering in the grapevine (*Vitis vinifera* L.). *Journal of Experimental Botany* **59**, 2565–2578.
- Lefebvre V, North H, Frey A, Sotta B, Seo M, Okamoto M, Nambara E, Marion-Poll A.** 2006. Functional analysis of *Arabidopsis* *NCED6* and *NCED9* genes indicates that ABA synthesized in the endosperm is involved in the induction of seed dormancy. *The Plant Journal* **45**, 309–319.
- Lescourret F, Génard M.** 2005. A virtual peach fruit model simulating changes in fruit quality during the final stage of fruit growth. *Tree Physiology* **25**, 1303–1315.
- Li Y, Lee KH, Walsh S, Smith C, Hadingham S, Sorefan K, Cawley G, Bevan MW.** 2006. Establishing glucose- and ABA-regulated transcription networks in *Arabidopsis* by microarray analysis and promoter classification using a relevance vector machine. *Genome Research* **16**, 414–427.
- Liu F, Jensen CR, Andersen MN.** 2004. Drought stress effect on carbohydrate concentration in soybean leaves and pods during early reproductive development, its implication in altering pod set. *Field Crops Research* **86**, 1–13.
- Lockhart JA.** 1965. An analysis of irreversible plant cell elongation. *Journal of Theoretical Biology* **8**, 264–275.
- Lu Y, Sharkey TD.** 2004. The role of amylomaltase in maltose metabolism in the cytosol of photosynthetic cells. *Planta* **218**, 466–473.
- Makela P, McLaughlin JE, Boyer JS.** 2005. Imaging and quantifying carbohydrate transport to the developing ovaries of maize. *Annals of Botany* **96**, 939–949.
- Marron N, Dreyer E, Boudouresque E, Delay D, Petit JM, Delmotte FM, Brignolas F.** 2003. Impact of successive drought and re-watering cycles on growth and specific leaf area of two *Populus canadensis* clones: 'Dorskamp' and 'Luisa\_Avanzo'. *Tree Physiology* **23**, 1225–1235.
- Martin T, Frommer WB, Salanoubat M, Willmitzer L.** 1993. Expression of an *Arabidopsis* sucrose synthase gene indicates a role in metabolization of sucrose both during phloem loading and in sink organs. *The Plant Journal* **4**, 367–377.
- McCree KJ, Kallsen CE, Richardson SG.** 1984. Carbon balance of sorghum plants during osmotic adjustment to water stress. *Plant Physiology* **76**, 898–902.
- McDowell N, Pockman WT, Allen CD, Breshears DD, Cobb N, Kolb T, Plaut J, Sperry J, West A, Williams DG.** 2008. Mechanisms of plant survival and mortality during drought, why do some plants survive while others succumb to drought? *New Phytologist* **178**, 719–739.
- McDowell NG, Sevanto S.** 2010. The mechanisms of carbon starvation, how, when, or does it even occur at all? *New Phytologist* **186**, 264–266.
- McLaughlin JE, Boyer JS.** 2004. Sugar-responsive gene expression, invertase activity, and senescence in aborting maize ovaries at low water potentials. *Annals of Botany* **94**, 675–689.
- Mercier V, Bussi C, Lescourret F, Génard M.** 2009. Effects of different irrigation regimes applied during the final stage of rapid growth on an early maturing peach cultivar. *Irrigation Science* **27**, 297–306.
- Monteith JL.** 1965. Light distribution and photosynthesis in field crops. *Annals of Botany* **29**, 17–37.
- Moore B, Zhou L, Rolland F, Hall Q, Cheng WH, Liu YX, Hwang I, Jones T, Sheen J.** 2003. Role of the *Arabidopsis* glucose sensor HXK1 in nutrient, light, and hormonal signaling. *Science* **300**, 332–336.
- Morgan J.** 1992. Osmotic components and properties associated with genotypic differences in osmoregulation in wheat. *Functional Plant Biology* **19**, 67–76.
- Muller B, Bourdais G, Reidy B, Bencivenni C, Massonneau A, Condamine P, Rolland G, Conéjéro G, Rogowsky P, Tardieu F.** 2007. Association of specific expansins with growth in maize leaves is maintained under environmental, genetic, and developmental sources of variation. *Plant Physiology* **143**, 278–90.
- Muller B, Reymond M, Tardieu F.** 2001. The elongation rate at the base of a maize leaf shows an invariant pattern during both the steady-state elongation and the establishment of the elongation zone. *Journal of Experimental Botany* **52**, 1259–1268.

- Muller B, Stosser M, Tardieu F.** 1998. Spatial distributions of tissue expansion and cell division rates are related to irradiance and to sugar content in the growing zone of maize roots. *Plant, Cell and Environment* **21**, 149–158.
- Munier-Jolain N, Ney B.** 1998. Seed growth rate in grain legumes II. Seed growth rate depends on cotyledon cell number. *Journal of Experimental Botany* **49**, 1971–1976.
- Munier-Jolain N, Salon C.** 2003. Can sucrose content in the phloem sap reaching field pea seeds (*Pisum sativum* L.) be an accurate indicator of seed growth potential? *Journal of Experimental Botany* **54**, 2457–2465.
- Niittylä T, Messerli G, Trevisan M, Chen J, Smith AM, Zeeman SC.** 2004. A previously unknown maltose transporter essential for starch degradation in leaves. *Science* **303**, 87–89.
- Nilson SE, Assmann SM.** 2010. Heterotrimeric G proteins regulate reproductive trait plasticity in response to water availability. *New Phytologist* **185**, 734–746.
- North HM, De Almeida A, Boutin JP, Frey A, To A, Botran L, Sotta B, Marion-Poll A.** 2007. The *Arabidopsis* ABA-deficient mutant *aba4* demonstrates that the major route for stress-induced ABA accumulation is via neoxanthin isomers. *The Plant Journal* **50**, 810–824.
- Oono Y, Seki M, Nanjo T, et al.** 2003. Monitoring expression profiles of *Arabidopsis* gene expression during rehydration process after dehydration using ca. 7000 full-length cDNA microarray. *The Plant Journal* **34**, 868–887.
- Oparka K, Duckett C, Prior D, Fisher D.** 1994. Real-time imaging of phloem unloading in the root tip of *Arabidopsis*. *The Plant Journal* **6**, 759–766.
- Osuna D, Usadel B, Morcuende R, Gibon Y, Bläsing OE, Hohne M, Gunter M, Kamlage B, Trethewey R, Scheible WR.** 2007. Temporal responses of transcripts, enzyme activities and metabolites after adding sucrose to carbon-deprived *Arabidopsis* seedlings. *The Plant Journal* **49**, 463–491.
- Palmer JH, Steer BT.** 1985. The generative area as the site of floret initiation in the sunflower capitulum and its integration to predict floret number. *Field Crops Research* **11**, 1–12.
- Paul M.** 2007. Trehalose 6-phosphate. *Current Opinion in Plant Biology* **10**, 303–309.
- Penning de Vries FWT.** 1975. The cost of maintenance processes in plant cells. *Annals of Botany* **39**, 77–92.
- Piques MC, Schulze WX, Hoehne M, Usadel B, Gibon Y, Rohwer J, Stitt M.** 2009. Ribosome and transcript copy numbers, polysome occupancy and enzyme dynamics in *Arabidopsis*. *Molecular Systems Biology* **5**, 314.
- Price J, Laxmi A, St Martin SK, Jang J.** 2004. Global transcription profiling reveals multiple sugar signal transduction mechanisms in *Arabidopsis*. *The Plant Cell* **16**, 2128–2150.
- Quick WP, Chaves MM, Wendler R, David M, Rodrigues ML, Passaharinho JA, Pereira JS, Adcock MD, Leegood RC, Stitt M.** 1992. The effect of water stress on photosynthetic carbon metabolism in four species grown under field conditions. *Plant, Cell and Environment* **15**, 25–35.
- Rathinasabapathi B.** 2000. Metabolic engineering for stress tolerance, installing osmoprotectant synthesis pathways. *Annals of Botany* **86**, 709–716.
- Rhodes D, Hanson AD.** 1993. Quaternary ammonium and tertiary sulfonium compounds in higher-plants. *Annual Review of Plant Physiology and Plant Molecular Biology* **44**, 357–384.
- Riccardi F, Gazeau P, de Vienne D, Zivy M.** 1998. Protein changes in response to progressive water deficit in maize. Quantitative variation and polypeptide identification. *Plant Physiology* **117**, 1253–1263.
- Riou-Khamlichi C, Menges M, Healy JMS, Murray JAH.** 2000. Sugar control of the plant cell cycle, differential regulation of *Arabidopsis* D-type cyclin gene expression. *Molecular and Cellular Biology* **20**, 4513–4521.
- Rolland F, Baena-Gonzalez E, Sheen J.** 2006. Sugar sensing and signaling in plants: conserved and novel mechanisms. *Annual Review of Plant Biology* **57**, 675–709.
- Rook F, Corke F, Card R, Munz G, Smith C, Bevan MW.** 2001. Impaired sucrose-induction mutants reveal the modulation of sugar-induced starch biosynthetic gene expression by abscisic acid signalling. *The Plant Journal* **26**, 421–433.
- Sadras VO, Milroy SP.** 1996. Soil-water thresholds for the responses of leaf expansion and gas exchange: a review. *Field Crops Research* **47**, 253–266.
- Sakamoto A, Murata N.** 2000. Genetic engineering of glycine betaine synthesis in plants, current status and implications for enhancement of stress tolerance. *Journal of Experimental Botany* **51**, 81–88.
- Schluepmann H, van Dijken A, Aghdasi M, Wobbes B, Paul M, Smeekens S.** 2004. Trehalose mediated growth inhibition of *Arabidopsis* seedlings is due to trehalose-6-phosphate accumulation. *Plant Physiology* **135**, 879–890.
- Serraj R, Sinclair TR.** 2002. Osmolyte accumulation, can it really help increase crop yield under drought conditions? *Plant, Cell and Environment* **25**, 333–341.
- Sharkey TD, Berry JA, Raschke K.** 1985. Starch and sucrose synthesis in *Phaseolus vulgaris* as affected by light, CO<sub>2</sub>, and abscisic acid. *Plant Physiology* **77**, 617–620.
- Sharp RE, Hsiao TC, Silk WK.** 1990. Growth of the maize primary root at low water potentials 1 ii. role of growth and deposition of hexose and potassium in osmotic adjustment. *Plant Physiology* **93**, 1337–1346.
- Smith AM, Stitt M.** 2007. Coordination of carbon supply and plant growth. *Plant, Cell and Environment* **30**, 1126–1149.
- Sulpice R, Pyl ET, Ishihara H, et al.** 2009. Starch as a major integrator in the regulation of plant growth. *Proceedings of the National Academy of Sciences, USA* **106**, 10348–10353.
- Tang AC, Boyer JS.** 2002. Growth-induced water potentials and the growth of maize leaves. *Journal of Experimental Biology* **53**, 489–503.
- Tardieu F.** 1996. Drought perception by plants: do cells of droughted plants experience water stress? *Plant Growth Regulation* **20**, 93–104.
- Tardieu F, Granier C, Muller B.** 1999. Modelling leaf expansion in a fluctuating environment, are changes in specific leaf area a consequence of changes in expansion rate? *New Phytologist* **143**, 33–43.

- Tardieu F, Reymond M, Hamard P, Granier C, Muller B.** 2000. Spatial distributions of expansion rate, cell division rate and cell size in maize leaves, a synthesis of the effects of soil water status, evaporative demand and temperature. *Journal of Experimental Botany* **51**, 1505–1514.
- Teulat B, Borries C, This D.** 2001. New QTLs identified for plant water status, water-soluble carbohydrate and osmotic adjustment in a barley population grown in a growth-chamber under two water regimes. *Theoretical and Applied Genetics* **103**, 161–170.
- Thaler P, Pagès L.** 1996. Root apical diameter and root elongation rate of rubber seedlings (*Hevea brasiliensis*) show parallel responses to photoassimilate availability. *Physiologia Plantarum* **97**, 365–371.
- Thimm O, Blaesing O, Gibon Y, Nagel A, Meyer S, Kruger P, Selbig J, Muller LA, Rhee SY, Stitt M.** 2004. MAPMAN, a user-driven tool to display genomics data sets onto diagrams of metabolic pathways and other biological processes. *The Plant Journal* **37**, 914–939.
- Thum KE, Shin MJ, Palenchar PM, Kouranov A, Coruzzi GM.** 2004. Genome-wide investigation of light and carbon signaling interactions in *Arabidopsis*. *Genome Biology* **5**, R10.
- Timpa JD, Burke JJ, Quisenberry JE, Wendt CW.** 1986. Effects of water stress on the organic acid and carbohydrate compositions of cotton plants. *Plant Physiology* **82**, 724–728.
- Toroer D, Plaut Z, Huber SC.** 2000. Regulation of a plant SNF1-related protein kinase by glucose-6-phosphate. *Plant Physiology* **123**, 403–412.
- Turner N, Begg J, Tonnet M.** 1978. Osmotic adjustment of sorghum and sunflower crops in response to water deficits and its influence on the water potential at which stomata close. *Functional Plant Biology* **5**, 597–608.
- Vaast P, Dauzat J, Génard M.** 2001. Modeling the effects of fruit load, shade and plant water status on coffee berry growth and carbon partitioning at the branch level. *VI International Symposium on Computer Modelling in Fruit Research and Orchard Management* **584**, 57–62.
- Vincent D, Lapierre C, Pollet B, Cornic G, Negroni L, Zivy M.** 2005. Water deficits affect caffeate O-methyltransferase, lignification, and related enzymes in maize leaves. A proteomic investigation. *Plant Physiology* **137**, 949–960.
- Walter A, Feil R, Schurr U.** 2002. Restriction of nyctinastic movements and application of tensile forces to leaves affects diurnal patterns of expansion growth. *Functional Plant Biology* **29**, 1247–1258.
- Webster PL, Van't Hof J.** 1969. Dependence on energy and aerobic metabolism of initiation and DNA synthesis and mitosis by G1 and G2 cells. *Chromosoma* **68**, 269–285.
- Wiese A, Christ MM, Virnich O, Schurr U, Walter A.** 2007. Spatio-temporal leaf growth patterns of *Arabidopsis thaliana* and evidence for sugar control of the diel leaf growth cycle. *New Phytologist* **174**, 752–761.
- Wiese A, Elzinga N, Wobbes B, Smeekens S.** 2004. A conserved upstream open reading frame mediates sucrose-induced repression of translation. *The Plant Cell* **16**, 1717–1729.
- Willaume M, Pagès L.** 2006. How periodic growth pattern and source/sink relations affect root growth in oak tree seedlings. *Journal of Experimental Botany* **57**, 815–826.
- Wu BH, Ben Mimoun M, Génard M, Lescourret F, Besset J, Bussi C.** 2005. Peach fruit growth in relation to the leaf-to-fruit ratio, early fruit size and fruit position. *Journal of Horticultural Science and Biotechnology* **80**, 340–345.
- Yang J, Zhang J, Wang Z, Xu G, Zhu Q.** 2004. Activities of key enzymes in sucrose-to-starch conversion in wheat grains subjected to water deficit during grain filling. *Plant Physiology* **135**, 1621–1629.
- Yoshida Y, Kiyosue T, Nakashima K, YamaguchiShinozaki K, Shinozaki K.** 1997. Regulation of levels of proline as an osmolyte in plants under water stress. *Plant and Cell Physiology* **38**, 1095–1102.
- Zhang YH, Primavesi LF, Jhurrea D, Andralojc PJ, Mitchell RAC, Powers SJ, Schlupepmann H, Delatte T, Wingler A, Paul MJ.** 2009. Inhibition of SNF1-related protein kinase1 activity and regulation of metabolic pathways by trehalose-6-phosphate. *Plant Physiology* **149**, 1860–1871.
- Zrenner R, Stitt M.** 1991. Comparison of the effect of rapidly and gradually developing water-stress on carbohydrate metabolism in spinach leaves. *Plant, Cell and Environment* **14**, 939–946.



# Floret initiation, tissue expansion and carbon availability at the meristem of the sunflower capitulum as affected by water or light deficits

Guillermo A. A. Dosio<sup>1,2,3</sup>, François Tardieu<sup>1,2</sup> and Olivier Turc<sup>1,2</sup>

<sup>1</sup>INRA, UMR 759 LEPSE, 2 place Viala, F-34000 Montpellier, France; <sup>2</sup>Montpellier SupAgro, UMR 759 LEPSE, 2 place Viala, F-34000 Montpellier, France; <sup>3</sup>Unidad Integrada (FCA UNMDP – EEA INTA) Balcarce, C.C. 276, 7620 Balcarce, Argentina

## Summary

Author for correspondence:

Olivier Turc

Tel: +33 499612 633

Email: turc@supagro.inra.fr

Received: 4 June 2010

Accepted: 19 July 2010

*New Phytologist* (2011) **189**: 94–105

doi: 10.1111/j.1469-8137.2010.03445.x

**Key words:** carbon availability, floret initiation, *Helianthus annuus* (sunflower), meristem, sunflower capitulum, tissue expansion rate, water deficit.

- The co-ordination between floret initiation and meristem expansion, and their relationships with carbon availability, were studied and quantified in sunflower (*Helianthus annuus*) plants subjected to light or water shortages.
- Meristem size, number of floret primordia, primordium size, rate of plant biomass accumulation, leaf area, photosynthetic rate, and soluble sugar content in the capitulum were measured until completion of floret initiation.
- Although treatments differentially affected tissue expansion and biomass acquisition, a common relationship between the final number of florets and the rate and duration of meristem expansion was conserved. In the absence of water deficit, changes in relative expansion rate in the meristem paralleled changes in soluble sugar content. Water deficit reduced tissue expansion both in leaves and in the capitulum, and induced the accumulation of soluble sugars in the meristem. Use of these sugars at re-watering was associated with increased meristem growth and higher floret numbers compared with control plants.
- Floret initiation and meristem tissue expansion remained strongly co-ordinated under all studied circumstances, and both depended on local carbon availability when water supply was unlimited. Transient water deficits favoured reproductive meristem growth and floret production. Equations accounting for these results constitute a framework for phenotyping the response to drought.

## Introduction

The development of the shoot apical meristem determines the number and the spatial arrangement of shoot organs (Bowman & Floyd, 2008; Wang & Li, 2008; Hamant & Traas, 2010). In sunflower (*Helianthus annuus* L.), it directly impacts crop productivity because harvested organs are initiated at the surface of the apical meristem (Palmer & Steer, 1985). The number of initiated florets is a crucial component of grain yield (Steer *et al.*, 1993; López Pereira *et al.*, 1999; Cantagallo & Hall, 2002), depending on the rate and duration of tissue expansion in the meristem (Dosio *et al.*, 2006). All florets are initiated over a short period (8–10 d) during which the capitulum is a saucer-shaped meristem measuring a few millimetres in diameter (Marc & Palmer, 1981). Floret primordia are centripetally initiated

at the generative front which divides the inner zone, or meristem proper, from the outer zone supporting the previously initiated florets (Palmer & Steer, 1985). The tissue expansion rate of the central meristematic zone of the capitulum plays an essential role in the process of floret initiation by renewing meristem area, and thus prolonging the period of primordium initiation. Numerous studies have been conducted to identify the mechanisms governing primordium initiation and patterning, and both the biomechanical (Hernández & Green, 1993; Green, 1994; Dumais & Steele, 2000) and biochemical aspects (Reinhardt *et al.*, 2003; Fleming, 2005, 2006a; Traas & Bohn-Courseau, 2005; Jönsson *et al.*, 2006) of these processes have now largely been described. Surface growth in shoot apices is also well documented, mainly in the model species *Arabidopsis thaliana* (L.) Heynh. (Grandjean *et al.*, 2004;

Kwiatkowska, 2006) and *Anagallis arvensis* L. (Dumais & Kwiatkowska, 2002; Kwiatkowska & Routier-Kierzkowska, 2009). By contrast, tissue expansion in the sunflower reproductive meristem has rarely been quantified (Hernández, 1995), and the response of this process to the environment has received little attention.

Tissue expansion depends primarily on water movements in the plant (Boyer & Silk, 2004), but assimilate supply also plays a role in tissue expansion by providing metabolites for the renewal of apical tissues and to ensure the growth of initiated primordia (Fleming, 2006b), by contributing to osmotic adjustment (Sturm & Tang, 1999) and by playing a role in signalling (Koch, 1996) to co-ordinate carbon supply and plant growth (Smith & Stitt, 2007). In the absence of water deficit, carbon availability is known to be involved in the expansion processes of heterotrophic organs such as root growing zones (Muller *et al.*, 1998) and leaf primordia (Granier & Tardieu, 1999a). By contrast, the limitation of leaf expansion under drought does not depend on photosynthesis (Boyer, 1970; Ben Haj Salah & Tardieu, 1997; Granier & Tardieu, 1999b; Munns *et al.*, 2000). The relationships among assimilate supply, tissue expansion and primordium initiation remain unclear in the reproductive organs of droughted plants. In the literature, the number of reproductive organs is classically related to plant carbon acquisition during given stages (Ritchie & Wei, 2000; Vega *et al.*, 2001), even in conditions of soil water deficit (Boyer & Westgate, 2004). Consistently, the number of initiated florets is sensitive to environmental conditions affecting plant biomass acquisition before and during the period of floret initiation, such as shading (Cantagallo & Hall, 2002) and nitrogen deficiency (Steer & Hocking, 1983). The decrease in floret initiation rate caused by a light deficit during floret initiation is related to the total apex dry weight (Cantagallo & Hall, 2002). However, mild water deficits during the vegetative period could promote floret initiation and grain production (Flénet *et al.*, 1996; Bissuel-Belaygue *et al.*, 2002; Dosio, 2002).

In a previous study, we proposed a method to quantify these two processes which affect the size of the meristem of the sunflower capitulum: tissue expansion, which tends to increase it, and floret initiation, which tends to reduce it (Dosio *et al.*, 2006). Several characteristics of floret initiation (e.g. the kinetics of the size of newly initiated primordia, and the fraction of meristem area consumed in primordia per unit time) are conserved in sunflower plants cultivated in different stable environments (Dosio *et al.*, 2006). This demonstrates that the rate of floret initiation directly depends on the rate of tissue expansion in the meristem, suggesting close co-ordination between the two processes. The above-mentioned framework (Dosio *et al.*, 2006) is used here to analyse, under various environmental conditions, the relationships among primordium initiation, tissue expansion and assimilate supply during the period in

which the number of florets is determined. The first question addressed in the present work is whether the co-ordination between floret initiation and tissue expansion remains in conditions of transient environmental constraints. Water and light deficits are considered because they have differential effects on tissue expansion and assimilate production: water deficit affects tissue expansion more than photosynthesis, and light deficit does the opposite (Boyer, 1970; Sultan, 2010), and one might expect contrasting effects on floret initiation. We then evaluated the role of carbon availability in determining the rates of floret initiation and of meristem expansion, and finally examined the eventually beneficial effect of water stress on floret initiation.

## Materials and Methods

### Experiments

Sunflower (*Helianthus annuus* L., cv Albena) seeds were sown in a field experiment conducted near Montpellier, France (43°40'N, 3°50'E) in a deep sandy loam soil (fluvio-calcaric Cambissol). Seedling emergence occurred 1 week after sowing. Nitrogen (N) fertilization was applied before sowing (80 kg ha<sup>-1</sup>). Soil water potential was monitored with five tensiometers (DTE 1000; Nardeux, Saint-Avertin, France) placed every 0.20 m from 0.30 to 1.10 m depth, and maintained by irrigation above -40 kPa in the first 0.5 m of soil during the whole crop cycle. Final plant density was 5.5 plants per m<sup>2</sup>, except for a set of isolated plants for which competition between plants was suppressed by thinning plants to 0.06 m<sup>-2</sup> after seedling emergence. Three treatments were applied to plants subjected to competition (Table 1). In the first treatment (shade before floret initiation), 75% uniform shading was achieved with a synthetic mesh cloth during the period between capitulum initiation and first floret initiation. The same shading was

**Table 1** Daily mean capitulum temperature and daily mean incident photosynthetic photon flux density (PPFD) before and during floret initiation (FI), for all applied treatments

Treatment	Temperature (°C)		PPFD (mol m <sup>-2</sup> d <sup>-1</sup> )	
	Before FI	During FI	Before FI	During FI
Control field	20.5 ± 1.9	19.8 ± 1.0	48 ± 11	53 ± 7
Shade before FI	18.5 ± 1.6	19.2 ± 1.5	12 ± 4	54 ± 8
Shade during FI	21.0 ± 1.9	18.2 ± 1.2	48 ± 11	11 ± 2
Control glasshouse	20.7 ± 1.4	21.5 ± 0.9	27 ± 9	26 ± 5
Shade before FI	20.6 ± 1.2	21.8 ± 1.0	7 ± 3	28 ± 6
WD before FI	21.1 ± 1.6	21.9 ± 0.8	27 ± 9	26 ± 5
WD during FI	20.8 ± 1.3	22.1 ± 0.9	27 ± 9	26 ± 5

Mean values ± SD are shown. WD, water deficit: soil water potential between -0.35 and -0.50 MPa. Shade treatments: 75% reduction of incident light.

applied later, during the period of floret initiation (shade during floret initiation). A plot with natural light was used as a control (control field).

A glasshouse experiment was carried out with the same hybrid at Montpellier. Seeds were sown in 156 columns (0.1 m diameter and 0.6 m height) containing a 1 : 1 loamy soil and organic compost mixture (v/v). One seedling was kept per column after thinning. Columns were irrigated with a modified one-tenth strength Hoagland solution corrected with minor nutrients. Irrigation was adjusted by daily weighing of each column to attain the desired soil water content. The fresh weight of harvested plants (measured every 3–4 d) gave an estimate of daily plant weight in each pot, which was subtracted from column weight to calculate soil water content. Available soil water content was maintained above 80% of its maximum, except during the periods of water deficit. Four treatments were applied to plants (Table 1). In the first treatment (water deficit before floret initiation), water supply was withheld 4 d before capitulum initiation until available soil water content reached 20% of its maximum, and was managed thereafter to maintain a stable soil water status (water potential between  $-0.35$  and  $-0.50$  MPa) during the period between capitulum initiation and first floret initiation. The same mild water deficit was applied later, in a second treatment (water deficit during floret initiation), during the period of floret initiation. The third treatment (shade before floret initiation) consisted of 75% uniform shading with a synthetic mesh cloth during the period between capitulum initiation and first floret initiation. Untreated columns (control glasshouse) completed the experimental design.

#### Temperature, incident light, photosynthesis and conductance

Incident light was measured continuously using a photosynthetic photon flux density sensor (LI-190SB; Li-Cor, Lincoln, NE, USA). Air temperature and relative humidity were measured every 20 s with a capacitive hygrometer (HMP35A; Vaisala Oy, Helsinki, Finland) protected from direct solar radiation. Capitulum temperature was measured on five (field experiment) or two (glasshouse experiment) plants per treatment with a fine copper-constantan thermocouple (0.4 mm diameter). As the capitulum developed, the thermocouple was successively placed inside the apical bud, inside involucre bracts when they became visible, and inside the receptacle after bract opening. All temperature data were averaged and stored every 600 s in a data-logger (LTD-CR10 Wiring Panel; Campbell Scientific, Shephed, UK). Stomatal conductance and photosynthesis were measured with a portable device (Analytical Development Company Limited LCA3, Hoddesdon, UK) every 2–5 d during each period of light or water deficit in the

glasshouse experiment and twice in the field experiment. Measurements were performed in the middle of the photoperiod, on sunny days, on at least 12 plants per treatment on fully expanded leaves receiving  $> 1000 \mu\text{mol m}^{-2} \text{s}^{-1}$  of photosynthetically active radiation (except for shaded plants where photosynthetically active radiation was much lower).

#### Plant dry matter and leaf area

Leaf area and above-ground dry matter were measured in plants every 3–4 d ( $n = 4$ ) from capitulum initiation onwards in both experiments. Detached leaves were placed under a camera coupled to an interactive image analysis system which measured leaf area (Optimas V 6.5; Media Cybernetics, Silver Spring, MD, USA). Plant leaf area was the sum of individual leaf areas. Leaves, stem and capitulum were then placed into paper bags and oven-dried (with air circulating at  $80^\circ\text{C}$ ) to constant weight and weighed. Total dry matter per plant was calculated as the sum of dry matter from each organ.

#### Measurements of areas and number of florets

Three to 10 plants were sampled three times a week in the glasshouse experiment and two times a week in the field experiment. The apical bud was dissected under a binocular microscope (MZ75; Leica, Wetzlar, Germany). Involucre bracts and floret bracts were removed, when necessary, with a fine scalpel blade to allow a clear view of florets. The area of the capitulum ( $S$ ) and that of the central meristematic zone without florets ( $S_m$ ) were estimated from the mean of four to six diameter measurements on each capitulum. The area of the parallelogram of creases that surround a primordium (Dosio *et al.*, 2006) was measured at five locations close to the generative front to estimate the projected area of newly initiated primordia. Floret area was also measured at five locations close to the capitulum edge to establish the growth kinetics of the first initiated florets. These measurements were performed on samples fixed in a mixture of ethanol (70% v/v), formaldehyde and acetic acid, and a multiplicative factor of 1.15 was applied to the measurements to take into account the retraction of tissue in the fixative solution. Diameters and areas were measured with an interactive image analysis system (Optimas 6.5; Media Cybernetics, Silver Spring, MD, USA) coupled to the binocular microscope.

The number of florets per capitulum ( $N_p$ ) was estimated at each sampling date by considering the spatial arrangement of florets in two sets of contact parastichies, the number of which conformed to the Fibonacci series. The number of parastichies  $n$  was determined at the capitulum edge, and the number of florets per parastichy,  $f$ , was determined at three locations per capitulum.  $N_p$  was calculated as:

$$N_p = n \times f, \quad \text{Eqn 1}$$

when less than two-thirds of the receptacle surface was covered by florets, that is, until floral stage 7 (Marc & Palmer, 1981). After that stage, row amalgamation occurred near the centre of the capitulum (i.e. the number of parastichies near the centre was lower than the number at the capitulum edge), and we used the following equation, derived from the empirical equation proposed in Palmer & Steer (1985):

$$N_p = (n_1 \times 0.67/p_f + n_2 \times (1 - 0.67/p_f)) \times f, \quad \text{Eqn 2}$$

( $f$ , the number of florets in a long parastichy;  $n_1$ , the number of long parastichies at the capitulum edge;  $n_2$ , the next number down in the Fibonacci series;  $p_f$ , the fraction of receptacle area  $S$  covered by florets ( $p_f = (S - S_m)/S$ ).

After completion of floret initiation, this equation becomes (Palmer & Steer, 1985):

$$N_p = n_1 \times 0.67 \times f + n_2 \times 0.33 \times f. \quad \text{Eqn 3}$$

The validity of Eqns 1 and 2 during the whole period of floret initiation was checked by exhaustive counting on scanning electron micrographs (JSM-6300F; JEOL, Tokyo, Japan) of dissected capitula. Calculated numbers were closely correlated with those obtained by counting ( $r^2 = 0.996$ , slope =  $0.995 \pm 0.015$ ).

#### Determination of developmental stages and expression of time

The dates of occurrence of capitulum developmental stages were deduced from observations of the apex of sampled plants under the binocular microscope. Capitulum initiation corresponded to the characteristic swelling and broadening of the shoot apical meristem described by Marc & Palmer (1981) as floral stage 1.3 (FS1.3). The date of capitulum initiation was determined as the day on which the projected area of the meristem was between 0.1 and 0.2 mm<sup>2</sup>. Floret initiation began on the day on which the first floret primordia were visible at the rim of the receptacle (equivalent to FS5 (Marc & Palmer, 1981)), and ended when the number of florets per capitulum did not increase compared with the previous sample. The latter date coincided with the time at which the entire receptacle was covered by florets (equivalent to FS8 (Marc & Palmer, 1981)). The date of the end of meristem growth (Dosio *et al.*, 2006) was estimated as the day on which more than two-thirds of the receptacle surface was covered with initiated florets (equivalent to FS7 (Marc & Palmer, 1981)). Time was expressed on a thermal time basis by daily integration of capitulum temperature with a threshold temperature of 4.8°C (Granier & Tardieu, 1998) and with capitulum initiation as thermal time origin.

#### Soluble sugar content

Capitulum samples were harvested at midday during both field and glasshouse experiments on several sampling dates during and after the periods of light or water deficits. Samples were immediately frozen and stored at -30°C until measurement. Soluble sugars were extracted in three steps: two consecutive extractions in ethanol (80% v/v), and a third extraction in water, each for 15 min at 95°C. The three extracts were collected and mixed, and soluble sugars were quantified by a colorimetric method (Dubois *et al.*, 1956). After a colour reaction with a mixture of phenol/sulphuric acid, optical density was measured with a colorimeter (Colorimeter 257; CIBA Corning Diagnostics, Halstead, UK). Sugar content was deduced from a standard curve established with glucose standard solutions (0–15 µg µl<sup>-1</sup>). Capitulum samples were weighed after 5 d in an oven at 80°C, and sugar content was expressed on a capitulum dry matter basis.

#### Calculations and curve fit

The increases in biomass and in meristem area were assumed to be exponential against thermal time during the period from capitulum initiation to completion of meristem growth, with rates depending on current light and/or water regimes. The parameters of the following equations were all estimated simultaneously for each given treatment by least squares fitting, using an algorithm of generalized reduced gradient (Marquardt–Levenberg algorithm in the software SIGMA PLOT 2001 V7.1; SPSS Science, Chicago, IL, USA). Standard errors on parameters are provided by the software.

The relative plant growth rates ( $PGR$ ) and the relative rates of tissue expansion in the meristem ( $Rm$ ) were first estimated for control plants ( $PGR_c$  and  $Rm_c$ ), and then calculated for 'treated' plants.

Data for the plant biomass,  $B$ , of control plants were fitted to:

$$0 < t < t_2 \quad B = B_0 \times \exp(PGR_c \times t), \quad \text{Eqn 4}$$

to calculate  $PGR_c$ .

Experimental data for the meristem area,  $Sm$ , of control plants were fitted to the following equations to calculate  $Rm_c$  and its component  $Ri_c$  consumed in primordia (Dosio *et al.*, 2006):

$$\begin{aligned} 0 < t < t_0 \quad Sm &= S_0 \times \exp(Rm_c \times t) \\ t_0 < t < t_1 \quad Sm &= S_0 \times \exp(Rm_c \times t) \\ &\quad \times \exp[(Rm_c - Ri_c) \times (t - t_0)], \quad \text{Eqn 5} \\ t_1 < t < t_2 \quad Sm &= Sm(t_1) \times (t_2 - t) / (t_2 - t_1) \end{aligned}$$

where  $t_0$ ,  $t_1$  and  $t_2$  correspond to the developmental stages of the capitulum: respectively, initiation of the first floret,

the end of tissue expansion in the meristem and the completion of floret initiation. They were determined by visual inspection of the capitulum as described in the paragraph 'Determination of developmental stages and expression of time'.

For a treatment applied before  $t_0$  (initiation of the first floret), for example shading of plants in the field applied at  $t_b$  (beginning of treatment) and removed at  $t_e$  (end of treatment), equations were:

$$\begin{aligned} 0 < t < t_b & \text{ as control} \\ t_b < t < t_e & Sm = Sm(t_b) \times \exp[Rm_d \times (t - t_b)] \\ & B = B(t_b) \times \exp[PGR_d \times (t - t_b)] \\ t_e < t < t_0 & Sm = Sm(t_e) \times \exp[Rm_a \times (t - t_e)] \\ t_0 < t < t_1 & Sm = Sm(t_0) \times \exp[(Rm_a - Ri_a) \times (t - t_0)] \\ t_1 < t < t_2 & Sm = Sm(t_1) \times (t_2 - t) / (t_2 - t_1) \\ t > t_e & B = B(t_e) \times \exp[PGR_a \times (t - t_e)] \end{aligned} \quad \text{Eqn 6}$$

allowing us to calculate  $Rm_d$ ,  $PGR_d$  (during treatment),  $Rm_a$  and  $PGR_a$  (after treatment).

The same rationale was applied to all experimental treatments to calculate  $R_m$  and  $PGR$  during and after the treatment period. In the greenhouse experiment, because sampling was more frequent, it was possible to perform calculations for two subperiods during and after treatment. The results of fitting are presented as lines in Figs 1 and 2.

Because periods of treatment did not exactly match developmental phases (e.g.  $t_b > 0$ ), we calculated a corrected duration of phases corresponding to the effect of treatment during its imposition. We considered that the progression of development was equivalent to that of control plants

before and after treatment, and was affected only during treatment imposition. In addition to  $d$ , the measured duration of each developmental phase in each experimental condition, we calculated  $d_t$ , the theoretical duration if treatment was imposed during the whole phase, as:

$$d_t = d_c \times (d - t_b) / (d_c - t_b), \quad \text{Eqn 7}$$

( $d_c$ , the duration in control plants.)

## Results

Effects of experimental treatments on photosynthesis, stomatal conductance, plant growth, leaf expansion, floret number and akene number

Water and light deficits were imposed for 7–10 d before or during floret initiation (Table 1). Shading in the field induced a decrease in capitulum temperature by  $c. 2^\circ\text{C}$  during the two periods, while shading in the glasshouse did not affect capitulum temperature (Table 1). Water deficit increased capitulum temperature by  $< 1^\circ\text{C}$ . These differences in temperature resulting from experimental treatments were taken into account for calculations of thermal time presented hereafter. Treatments induced reductions in photosynthesis, stomatal conductance and plant growth rate (Table 2). Photosynthesis was affected to a lesser extent than stomatal conductance during both water deficit treatments (Table 2). Shading resulting in a 75% reduction in incident photosynthetic photon flux density (PPFD) (Table 1) caused a steep decrease in net photosynthesis with a smaller effect on stomatal conductance (Table 2). Both photosynthesis and conductance were restored just after the return to control conditions (Table 2). In the field experiment, the

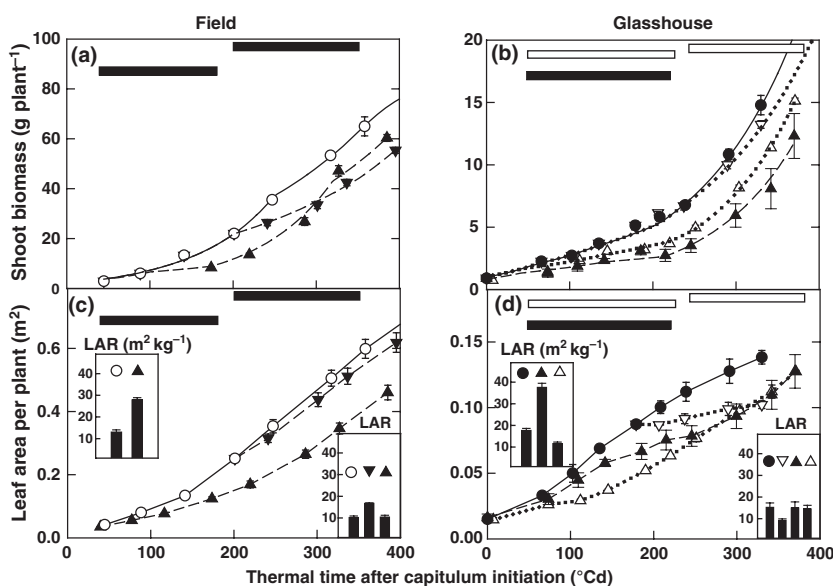


**Fig. 1** Shoot biomass accumulation per plant (a, b) and leaf area per plant (c, d) as a function of thermal time cumulated from capitulum initiation. Insets in (c) and (d) show the leaf area ratio (LAR), calculated by dividing leaf area by shoot biomass, averaged over the periods of treatment before (left histogram) or during (right histogram) floret initiation. Plants were subjected to light deficits (closed triangles) or soil water deficits (open triangles) either before (upward triangles) or during (downward triangles) floret initiation. Circles, control plants in the glasshouse (closed circles) and in the field (open circles); horizontal bars, periods of soil water deficit (white bars) and of plant shading (black bars); vertical bars, SD.

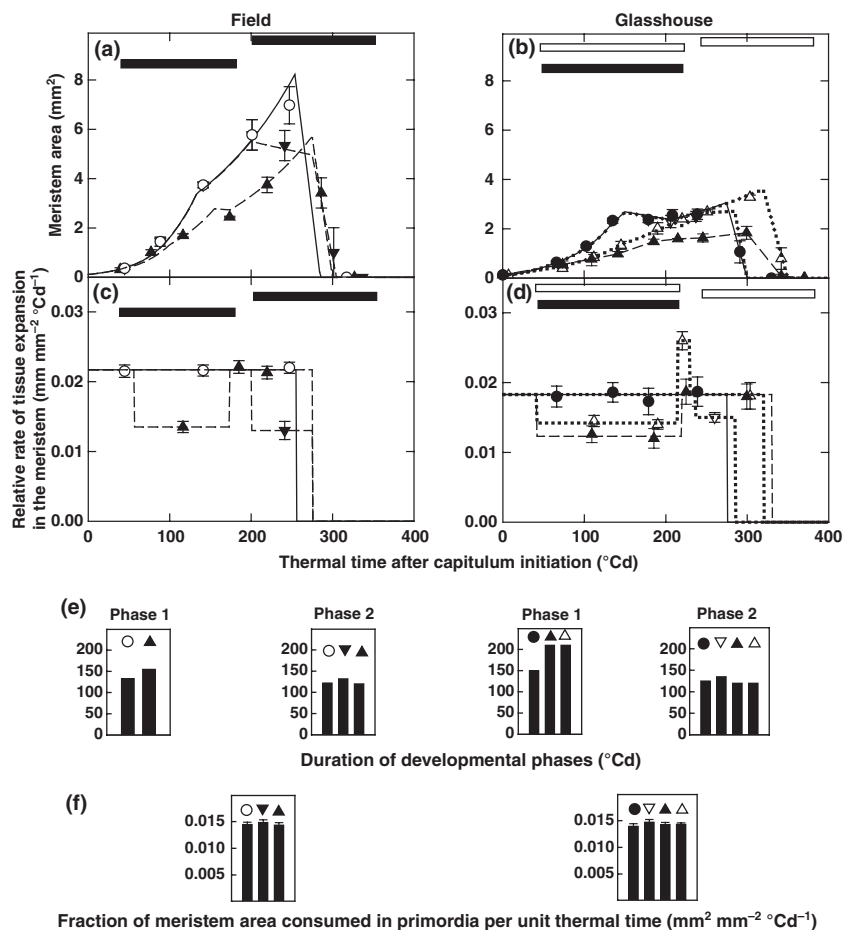


**Fig. 2** Meristem area (a, b), relative rate of tissue expansion in the meristem (c, d) as a function of thermal time cumulated from capitulum initiation, duration of the developmental phases of the capitulum meristem (e), and fraction of meristem area consumed in primordia per unit thermal time (f). Phase 1, from capitulum initiation to initiation of the first floret; phase 2, from initiation of the first floret to the end of tissue expansion in the meristem. Plants were subjected to light deficits (closed triangles) or soil water deficits (open triangles) either before (upward triangles) or during (downward triangles) floret initiation. Circles, control plants in the glasshouse (closed circles) and in the field (open circles); horizontal bars, periods of soil water deficit (white bars) and of plant shading (black bars); vertical bars, SD.

**Table 2** Photosynthesis, stomatal conductance and plant relative growth rate during and after the period of treatment, and numbers of florets and of mature akenes measured at harvest

Treatment	Photosynthesis ( $\mu\text{mol m}^{-2} \text{s}^{-1}$ )		Stomatal conductance ( $\text{mol m}^{-2} \text{s}^{-1}$ )		Plant relative growth rate ( $\text{mg g}^{-1} \text{Cd}^{-1}$ )		Floret number	Number of mature akenes
	During treatment	After treatment	During treatment	After treatment	During treatment	After treatment		
Control field	29.7 ± 3.7	29.7 ± 3.7	1.78 ± 0.21	1.78 ± 0.21	10.8 ± 0.8	10.8 ± 0.8	2388 ± 79a	1843 ± 150a
Shade before FI	9.9 ± 1.3	30.8 ± 3.6	1.10 ± 0.10	1.61 ± 0.16	4.0 ± 0.8	11.0 ± 1.2	1658 ± 229b	1456 ± 155b
Shade during FI	11.1 ± 1.2	29.5 ± 3.3	1.27 ± 0.11	1.65 ± 0.15	4.7 ± 0.5	10.4 ± 0.9	2251 ± 182a	1765 ± 190a
Control glasshouse	24.3 ± 1.5	24.3 ± 1.5	1.21 ± 0.05	1.21 ± 0.05	8.3 ± 0.3	8.3 ± 0.3	1034 ± 112d	805 ± 117d
Shade before FI	3.9 ± 0.5	23.9 ± 2.2	0.80 ± 0.02	1.16 ± 0.08	4.2 ± 1.3	8.6 ± 0.4	802 ± 130e	590 ± 172e
WD before FI	18.0 ± 2.3	24.4 ± 1.5	0.51 ± 0.14	1.22 ± 0.11	5.6 ± 1.3	8.0 ± 0.7	1394 ± 144c	981 ± 64c
WD during FI	19.6 ± 2.0	24.4 ± 1.6	0.41 ± 0.07	1.09 ± 0.12	7.0 ± 0.6	8.1 ± 0.6	1138 ± 100d	842 ± 110d

Mean values ± SD are shown. Means in columns followed by the same letter do not differ significantly ( $P < 0.05$ ) (standard ANOVA and  $t$ -test analysis). FI, floret initiation; WD, water deficit: soil water potential between  $-0.35$  and  $-0.50$  MPa. Shade treatments: 75% reduction of incident light.

daily mean incident PPFD was approximately twice that in the glasshouse (Table 1). Midday photosynthesis of control plants in the field ( $c. 30 \mu\text{mol m}^{-2} \text{s}^{-1}$ ) was slightly higher than that measured on control plants in the glasshouse ( $24 \mu\text{mol m}^{-2} \text{s}^{-1}$ ) (Table 2). Shading in the field experi-

ment reduced photosynthesis by  $c. 65\%$  ( $10\text{--}11 \mu\text{mol m}^{-2} \text{s}^{-1}$ ), that is, to a lesser extent than it did in the glasshouse experiment ( $c. 4 \mu\text{mol m}^{-2} \text{s}^{-1}$ ).

The studied range of environmental conditions caused large differences in biomass accumulation and leaf area per

plant during the period that followed capitulum initiation (Fig. 1). Biomass per plant was approximately 4-fold higher in the field compared with the glasshouse. In all cases, light and water deficits reduced the rate of biomass accumulation during treatment imposition, while the rate was restored at control level after recovery (Table 2). Biomass accumulation was reduced to a greater extent by light deficit than by water deficit when the deficit was imposed during the same period in the glasshouse experiment (Fig. 1b). Conversely, leaf area per plant was more affected by water depletion than by shading (Fig. 1d). The late, moderate water deficit in the glasshouse had a small effect on the biomass accumulation rate (Fig. 1b), while leaf expansion was significantly reduced (Fig. 1d). The leaf area ratio (LAR), that is, the leaf area per unit shoot biomass, increased during shading and decreased during water deficit (Fig. 1c,d insets).

Field-grown plants produced approximately twice the numbers of florets and akenes observed in the glasshouse (Table 2). All shading treatments, before or during floret initiation, in the field and in the glasshouse, reduced both the final number of florets and the number of akenes (Table 2). The effect was more pronounced for constraints between capitulum initiation and first floret initiation. Conversely, floret and akene numbers were increased by water deficits in the glasshouse experiment. Differences were significant for the deficit occurring before floret initiation, not for the later deficit (Table 2).

As expected, soil water deficits affected leaf expansion to a greater extent than biomass accumulation, and shading treatments had the opposite effect. The effects on the numbers of reproductive organs were also contrasting, with negative responses to shading, and positive or null responses to drought, depending on the period of treatment imposition.

Treatments induced differences in meristem growth but not in primordium size or in the fraction of meristem area consumed in primordia per unit time

The growth rate of meristem area decreased during the imposition of light or water deficits (Fig. 2c,d). The meristem area of early shaded plants remained lower than that of control plants, even after the end of the shading treatment (Fig. 2a,b). Conversely, plants subjected to water deficit showed a higher meristem area than control plants after recovery (Fig. 2b). This was associated with a transient increase in the relative rate of tissue expansion in the meristem at re-watering (Fig. 2d). Effects were limited or absent in the case of late treatments.

Treatments also affected the development of the meristem by delaying the date of meristem disappearance (Fig. 2a,b). This was a result of the prolonged duration of the period between capitulum initiation and initiation of the first floret in response to constraints (phase 1; Fig. 2e). The duration of the following phase, from initiation of the first floret to arrest of tissue expansion in the meristem, was not significantly affected (phase 2; Fig. 2e).

The fraction of meristem area consumed in primordia per unit thermal time remained stable in all the studied conditions (Fig. 2f). Mathematically, this fraction is equivalent to a relative expansion rate and corresponds to the capitulum area covered by newly initiated primordia per unit time and per unit meristem area (Dosio *et al.*, 2006). Its stability indicates that the same balance between meristem size and primordium initiation rate was maintained in all treatments.

The projected area of newly initiated primordia increased with time in all treatments (Fig. 3a). Data did not differ significantly for any treatment from the relationship established for isolated plants in an experiment carried out by

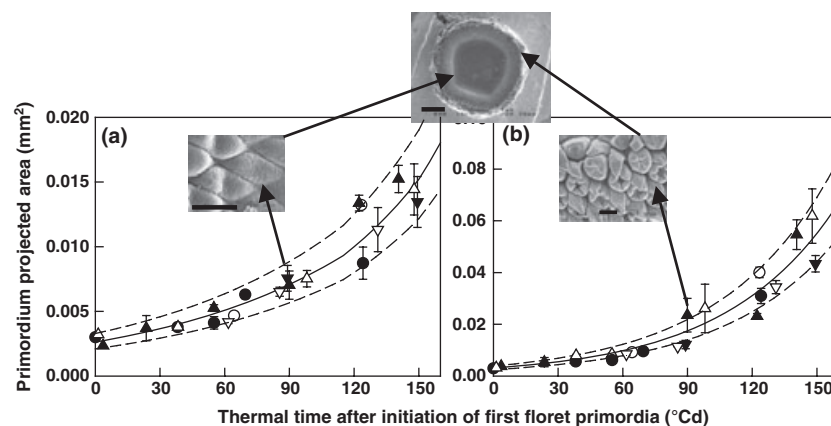


**Fig. 3** Primordium projected area, measured close to the meristem (a) or at the capitulum edge (b), as a function of capitulum age expressed in thermal time after initiation of the first floret primordia. Plants were subjected to light deficits (closed triangles) or soil water deficits (open triangles) either before (upward triangles) or during (downward triangles) floret initiation. Circles, control plants in the glasshouse (closed circles) and in the field (open circles); vertical bars, SD; solid and dashed lines, equation and confidence interval 0.05–0.95 from Dosio *et al.* (2006) for isolated field plants. Photographs show newly initiated primordia at the meristem rim (left; bar, 100  $\mu\text{m}$ ) and florets at the capitulum edge (right; bar, 100  $\mu\text{m}$ ) from the same capitulum (top; bar, 1 mm).

Dosio *et al.* (2006), indicating that the characteristics of the initiated primordia were insensitive to treatments imposed before or during floret initiation. The kinetics of the growth of florets located at the capitulum edge, corresponding to the first initiated primordia, was also conserved across experiments and treatments (Fig. 3b), suggesting that the rate of development of initiated primordia was also independent of environmental conditions.

Final numbers of initiated florets only depended on variations in meristem expansion caused by transient light or water limitations

We used the model proposed by Dosio *et al.* (2006) to predict the number of florets initiated in each experimental situation. This model includes variables related to the process of floret primordium initiation at the periphery of the meristematic zone, namely the size of the newly initiated primordia and the fraction of meristem area covered by newly initiated primordia per unit time, and variables related to the process of tissue expansion in the meristem, namely the rates and duration of expansion from capitulum initiation to arrest of meristem expansion. For the former variables, as for the duration of the period of floret initiation, we used here the values obtained in isolated plants by Dosio *et al.* (2006), because no significant difference was found among experimental treatments. For each treatment, the only input variables were therefore exclusively related to the process of tissue expansion in the meristem. They were the duration of the period between capitulum initiation and initiation of the first floret, and the relative rate of tissue expansion in the meristem between capitulum initiation and completion of meristem growth (Fig. 2c–d). Estimated values of floret number correlated well with measured values ( $y = 1.0002x$ ,  $r^2 = 0.983$ ,  $n = 8$ ), showing that the co-ordination between floret initiation and meristem expansion was conserved in conditions of transient light or water deficits (Fig. 4a). Simulated floret numbers also correlated with the final number of akenes (Fig. 4b), as the seed set ratio (number of akenes/number of florets) was almost the same in all treatments.

Are the rate and duration of tissue expansion in the meristem related to plant growth rate and/or to capitulum soluble sugar content?

For each experimental treatment, the duration of the capitulum developmental phases was plotted against the plant relative growth rate averaged over the same period. The duration of phase 1, from capitulum initiation to initiation of the first floret, increased when plant growth rate decreased (Fig. 5a), according to a common relationship for shading, water deficit and plant competition. Conversely, the duration of phase 2, from initiation of the first floret to completion of tissue expansion in the meristem, was stable,

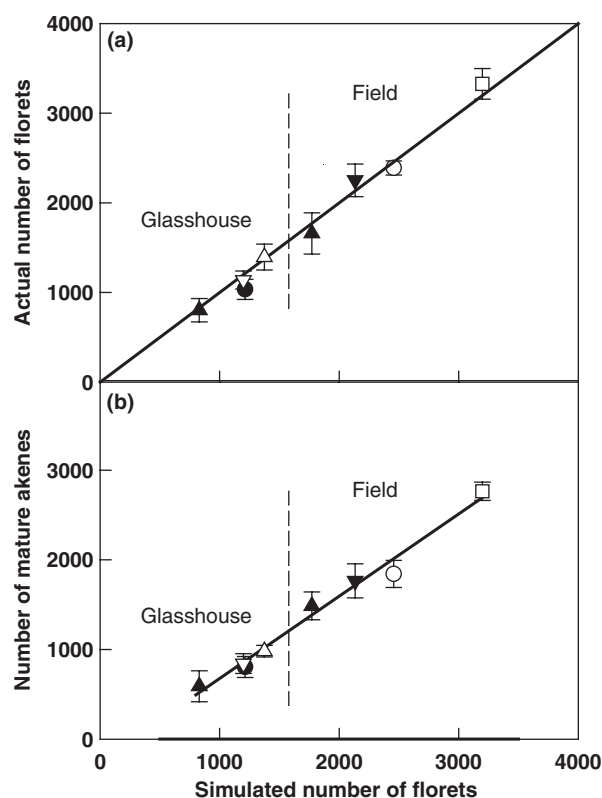


**Fig. 4** Actual numbers of florets (a) and of mature akenes (b) measured at harvest as a function of the final number of initiated florets predicted with equations from Dosio *et al.* (2006). The model calculates the kinetics of floret initiation from the rate (Fig. 2c–d) and the duration (Fig. 2e) of tissue expansion in the meristem between capitulum initiation and completion of meristem expansion. Plants were subjected to light deficits (closed triangles) or soil water deficits (open triangles) either before (upward triangles) or during (downward triangles) floret initiation. Circles, control plants in the glasshouse (closed circles) and in the field (open circles); squares, isolated field plants; vertical bars, SD.

irrespective of experimental treatment affecting plant growth rate (Fig. 5b).

In the absence of soil water deficit, the rate of tissue expansion in the meristem correlated with both the plant relative growth rate and the soluble sugar content in the capitulum (Fig. 6a,c). In other words, tissue expansion in the capitulum was positively related to the rate of assimilates produced per plant and to the carbon availability in the capitulum. The same relationship was demonstrated by different plant sets experiencing different environmental conditions at a given developmental stage (different symbols in Fig. 6a,c) and by a given plant set at successive sampling dates: before, during and after imposition of an experimental treatment (numbered 1–4 in Fig. 6a,c). Insets in Fig. 6a,b indicate the time course of the relative rate of tissue expansion in the meristem ( $R_m$ ) and that of the content of soluble sugars in the capitulum (sugars) in the case of shading before floret initiation in the field experiment

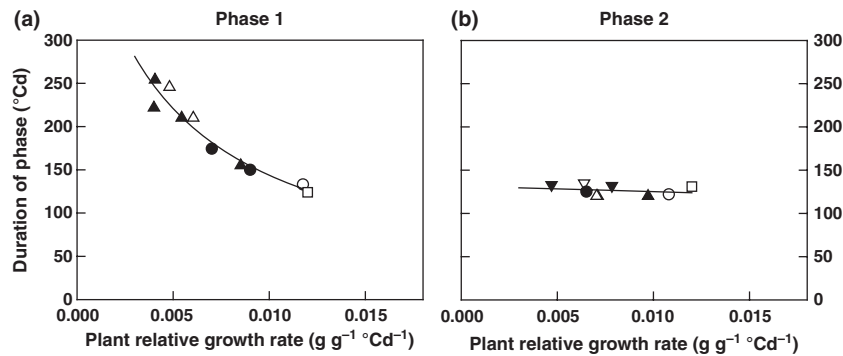


**Fig. 5** Duration of the developmental phases of the capitulum as a function of the plant relative growth rate during the corresponding phase. (a) Phase 1, from capitulum initiation to initiation of the first floret. (b) Phase 2, from initiation of the first floret to the end of tissue expansion in the meristem. Plants were subjected to light deficits (closed triangles) or soil water deficits (open triangles) either before (upward triangles) or during (downward triangles) floret initiation. Circles, control plants in the glasshouse (closed circles) and in the field (open circles); squares, isolated field plants.

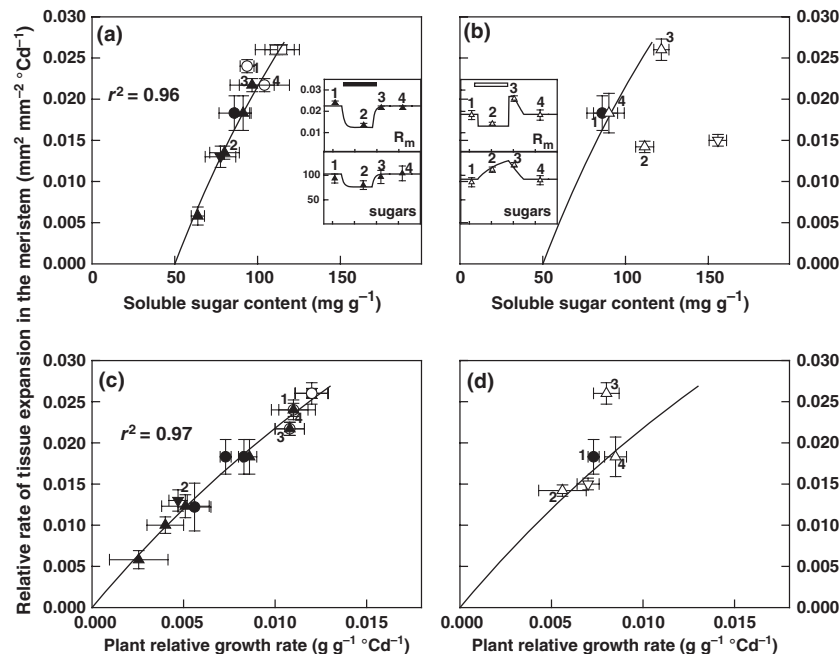


**Fig. 6** Relative rate of tissue expansion in the meristem as a function of soluble sugar content in the capitulum (a, b) and as a function of the plant relative growth rate (c, d). Left panels show data for well-watered plants (a, c) while data for plants subjected to soil water deficit are presented in the right panels (b, d); solid lines, curve fit of data for well-watered plants (a, c); the lines in (b) and (d) are the same as in (a) and (c), respectively. Insets in (a) and (b) show the time course of the relative rate of tissue expansion in the meristem ( $R_m$ ) and of the soluble sugar content (*sugars*) for treatments before floret initiation (a, field shading treatment; b, glasshouse water deficit). Numbers 1–4 (insets and main figures) represent successive measurements on plants from the same treatment: 1, before applying the treatment; 2, during the treatment; 3, just after the treatment had been removed; 4, later. Plants were subjected to light deficits (a, c; closed triangles) or soil water deficits (b, d; open triangles) either before (upward triangles) or during (downward triangles) floret initiation. Circles, control plants in the glasshouse (closed circles) and in the field (open circles); squares, isolated field plants; bars, SE; horizontal bars (insets), periods of soil water deficit (white bars) and of plant shading (black bars).

(Fig. 6a) and in the case of water deficit before floret initiation in the glasshouse (Fig. 6b).

Soluble sugars accumulated in the capitulum when soil water deficits developed, while the rate of tissue expansion in the meristem decreased (Fig. 6b, inset). The maximal value was observed at the end of the late water deficit treatment (Fig. 6b). This suggests that carbon availability in the

capitulum was not limiting for meristem expansion during water shortage. Plant re-watering restored the relationship between the rate of tissue expansion in the meristem and the sugar content in the capitulum (points 3 and 4 in Fig. 6b). This resulted in a transient increase in the relative rate of tissue expansion in the meristem above the value of control plants (point 3 in Fig. 6b). Then, meristem

expansion and sugar content decreased together until they reached the values of control plants (point 4 in Fig. 6b). Conversely, the relationship between tissue expansion in the meristem and plant biomass accumulation was conserved during soil water deficit (Fig. 6d), while the increase in meristem expansion exceeded that of plant growth rate for approximately 2 d after re-watering (point 3 in Fig. 6d). Later, meristem expansion and plant growth rate adjusted together to the common relationship (point 4 in Fig. 6d).

## Discussion

Floret initiation and capitulum expansion remain strongly co-ordinated, whatever the carbon and water status of the plant

In the absence of water deficit, the changes in soluble sugar content paralleled the changes in the relative expansion rate of the capitulum (Fig. 6). This suggests a role for carbon availability in the expanding activity of the meristematic zone of the sunflower capitulum. Such a dependence of tissue expansion on carbon status has been reported for various growing organs: root elongation (Aguirrezábal *et al.*, 1994; Muller *et al.*, 1998) and leaf growth before autotrophy (Turner *et al.*, 1978; Jones *et al.*, 1980; Granier & Tardieu, 1999a) were related to the amount of light intercepted by the plants; the rate of elongation of lateral roots in *Arabidopsis* was correlated with the local hexose content in root tips (Freixes *et al.*, 2002); the rate of cell division in the developing embryo of pea (*Pisum sativum*) seeds was explained by the sucrose content in the phloem sap reaching the seed coat (Munier-Jolain & Ney, 1998; Munier-Jolain & Salon, 2003). When plants are subjected to a soil water deficit, tissue expansion is primarily limited by water movements and cell wall rheological properties (Boyer & Silk, 2004) rather than by carbon availability. As a consequence, sugars generally accumulate in growing organs of water-stressed plants (Granier & Tardieu, 1999b), as observed in the present study.

Whatever the cause of the limitation of growth, the initiation of floret primordia was inhibited to the same extent as was meristem expansion. The set of equations calculating floret number from meristem expansion, initially established in steady growing conditions (Dosio *et al.*, 2006), was confirmed for conditions of transient light or water deficits: predicted floret numbers correlated well with measured values (Fig. 4). In all cases, floret initiation appeared to be driven by the rate of tissue expansion in the meristem. The constraints did not specifically affect the process of floret initiation: neither the size of the primordia, nor the fraction of meristem area consumed in the primordia per unit time, nor the duration of initiation was affected by light or water deficits. Because of the stability of these parameters, the rate of floret initiation at a given time depends only on

the intrinsic geometric properties of the meristem at that time (meristem area and primordium size) (Dosio *et al.*, 2006), irrespective of current environmental conditions. The close coupling between floret initiation and meristem geometry observed in all situations is probably at the origin of the well-known regular spatial arrangement of sunflower florets along parastichies (e.g. Klar, 2002). The role of such co-ordination in the maintenance of developmental patterns has recently been highlighted by several studies on the shoot apical meristem of *Arabidopsis* demonstrating that morphogenesis in the developing shoot apex is controlled by mechanical signals that are triggered by growth of the organ itself (Hamant *et al.*, 2008; Dumais, 2009; Hamant & Traas, 2010; Uyttewaal *et al.*, 2010).

Early moderate water deficits are favourable for floret and seed production

Not only floret number (Fig. 4a), but also final seed number (Fig. 4b) was largely determined by capitulum expansion during floret initiation. This was a consequence of a conserved percentage of flower or seed abortion among treatments, in spite of large differences in floret number and in light available per plant after floret initiation. The ratio of filled seeds : florets was high, *c.* 0.80 in all cases, and comparable to values obtained for a range of plant population densities (Villalobos *et al.*, 1994), and to those obtained for a set of genotypes (Paoloni *et al.*, 2000). Unlike the mean weight per seed, which differed among treatments (not shown) and according to light availability after flowering (Andrade & Ferreira, 1996; Dosio *et al.*, 2000; Lindström *et al.*, 2006), the numbers of flowers and seeds were established during floret initiation. These results underline the importance of early reproductive phases in determining seed yield components in sunflower, in agreement with other studies (Steer *et al.*, 1993; Cantagallo & Hall, 2002).

The earlier water deficit, imposed before floret initiation, was favourable for both floret and seed production per plant, compared with control plants. A similar response to moderate water stress was found for floret number in white clover (*Trifolium repens*) (Bissuel-Belaygue *et al.*, 2002). This is also in accordance with several studies indicating a positive effect of pre-anthesis water deficits on sunflower seed yield (Sobrado & Turner, 1986; Sadras *et al.*, 1993; Flénet *et al.*, 1996). This effect is generally attributed to an improved allocation of assimilates to the capitulum when soil water availability decreases. Our results, however, indicate that meristem growth is not related to carbon availability during water deficit. Because photosynthesis was affected to a lesser extent than plant growth, as classically observed for moderate water deficits (Boyer, 1970), sugars accumulated in growing organs, including the capitulum, which suggests that growth was not carbon-limited. The following sequence could explain the positive effect of

moderate water deficits: drought primarily affects expansion processes more than carbon assimilation, and carbon accumulates in growing organs; growth impairment differs among organs: shading reduces meristem expansion more than leaf expansion (Dosio *et al.*, 2003), and water deficits induce the opposite response (Figs 1 and 2). The changes in carbon allocation to the reproductive meristem should therefore be considered as a consequence of this differential effect of constraints according to organs; at re-watering, the high content of sugars accumulated during the period of soil dehydration induced an increased relative expansion rate in the meristem (Fig. 6b), and consequently an increased rate of floret initiation.

### A framework for phenotyping the response to drought

From the present results can be derived a set of equations which explicitly describe and quantify the relationships among net carbon input, capitulum growth, soluble sugar content in the capitulum, and initiation of floret primordia. This set includes: the equations of the curve fits presented in Figs 5 and 6, which calculate, respectively, the duration and the rate of meristem growth as a function of plant growth rate or capitulum sugar content; Eqns 4–7, which calculate the kinetics of the meristem area from the above-mentioned rate and duration of meristem growth; and equations described elsewhere (Dosio *et al.*, 2006) which calculate the kinetics of floret initiation from that of meristem area. These equations could be incorporated in an architectural model simulating leaf growth and light interception, and therefore plant growth rate (e.g. Rey *et al.* (2008)), in order to predict floret and seed set in various climatic scenarios and for different genotypes. This could allow an analysis of the genetic variability for traits associated with floret and seed set under water deficit, as was carried out for leaf expansion (Pereyra-Irujo *et al.*, 2008). The formalism of these equations suggests a pivotal role for the maintenance of expansion processes in the response to drought. This is in agreement with results obtained in maize (*Zea mays*), where tolerance to drought was associated with the maintenance of expansion processes (Welcker *et al.*, 2007; Fuad-Hassan *et al.*, 2008).

### Acknowledgements

G.A.A.D. is a member of CONICET, the National Research Council of Argentina, and thanks the Ministerio de Cultura y Educación de la Nación Argentina, the Ambassade de France en Argentina, the Département Environnement et Agonomie (INRA, France), and the Universidad Nacional de Mar del Plata (Argentina) for grants supporting his PhD thesis in France. We thank Benoît Suard and Jean-Jacques Thioux for technical help, and Montpellier RIO Imaging for access to scanning electron microscope facilities.

### References

- Aguirrezábal LAN, Pellerin S, Deleens E, Tardieu F. 1994. Root elongation rate is accounted for by intercepted PPFD and source-sink relations in field and laboratory-grown sunflower. *Plant, Cell & Environment* 17: 443–450.
- Andrade FH, Ferreiro MA. 1996. Reproductive growth of maize, sunflower and soybean at different source levels during grain filling. *Field Crops Research* 48: 155–165.
- Ben Haj Salah H, Tardieu F. 1997. Control of leaf expansion rate of droughted maize plants under fluctuating evaporative demand – a superposition of hydraulic and chemical messages? *Plant Physiology* 114: 893–900.
- Bissuel-Belaygue C, Cowan AA, Marshall AH, Wery J. 2002. Reproductive development of white clover (*Trifolium repens* L.) is not impaired by a moderate water deficit that reduces vegetative growth: I. Inflorescence, floret, and ovule production. *Crop Science* 42: 406–414.
- Bowman JL, Floyd SK. 2008. Patterning and polarity in seed plant shoots. *Annual Review of Plant Biology* 59: 67–88.
- Boyer JS. 1970. Leaf enlargement and metabolic rates in corn, soybean, and sunflower at various leaf water potentials. *Plant Physiology* 46: 233–235.
- Boyer JS, Silk WK. 2004. Hydraulics of plant growth. *Functional Plant Biology* 31: 761–773.
- Boyer JS, Westgate ME. 2004. Grain yields with limited water. *Journal of Experimental Botany* 55: 2385–2394.
- Cantagallo JE, Hall AJ. 2002. Seed number in sunflower as affected by light stress during the floret differentiation interval. *Field Crops Research* 74: 173–181.
- Dosio GAA. 2002. *Analyse conjointe des développements végétatif et reproducteur chez des plantes de tournesol soumises à des déficits précoces en eau et en lumière*. Thèse de Doctorat. ENSAM, Montpellier, France.
- Dosio GAA, Aguirrezábal LAN, Andrade FH, Pereyra VR. 2000. Solar radiation intercepted during seed filling and oil production in two sunflower hybrids. *Crop Science* 40: 1637–1644.
- Dosio GAA, Rey H, Lecoeur J, Turc O. 2003. La radiación solar durante etapas tempranas del desarrollo afecta al área foliar del girasol. *Revista Argentina de Agrometeorología* 2: 113–118.
- Dosio GAA, Tardieu F, Turc O. 2006. How does the meristem of sunflower capitulum cope with tissue expansion and floret initiation? A quantitative analysis *New Phytologist* 170: 711–722.
- Dubois M, Gilles KA, Hamilton JK, Rebus PA, Smith F. 1956. Colorimetric method for the determination of sugars and related substances. *Analytical Chemistry* 28: 350–356.
- Dumais J. 2009. Plant morphogenesis: a role for mechanical signals. *Current Biology* 19: R207–R208.
- Dumais J, Kwiatkowska D. 2002. Analysis of surface growth in shoot apices. *Plant Journal* 31: 229–241.
- Dumais J, Steele CR. 2000. New evidence for the role of mechanical forces in the shoot apical meristem. *Journal of Plant Growth Regulation* 19: 7–18.
- Fleming AJ. 2005. Formation of primordia and phyllotaxy. *Current Opinion in Plant Biology* 8: 53–58.
- Fleming AJ. 2006a. The co-ordination of cell division, differentiation and morphogenesis in the shoot apical meristem: a perspective. *Journal of Experimental Botany* 57: 25–32.
- Fleming AJ. 2006b. Metabolic aspects of organogenesis in the shoot apical meristem. *Journal of Experimental Botany* 57: 1863–1870.
- Flénet F, Bouniols A, Saraiva C. 1996. Sunflower response to a range of soil water contents. *European Journal of Agronomy* 5: 161–167.
- Freixes S, Thibaud MC, Tardieu F, Muller B. 2002. Root elongation and branching is related to local hexose concentration in *Arabidopsis thaliana* seedlings. *Plant, Cell & Environment* 25: 1357–1366.
- Fuad-Hassan A, Tardieu F, Turc O. 2008. Drought-induced changes in anthesis-silking interval are related to silk expansion: a spatio-temporal

- growth analysis in maize plants subjected to soil water deficit. *Plant, Cell & Environment* 31: 1349–1360.
- Grandjean O, Vernoux T, Laufs P, Belcram K, Mizukami Y, Traas J. 2004. *In vivo* analysis of cell division, cell growth, and differentiation at the shoot apical meristem in Arabidopsis. *Plant Cell* 16: 74–87.
- Granier C, Tardieu F. 1998. Is thermal time adequate for expressing the effects of temperature on sunflower leaf development? *Plant, Cell & Environment* 21: 695–703.
- Granier C, Tardieu F. 1999a. Leaf expansion and cell division are affected by reducing absorbed light before but not after the decline in cell division rate in the sunflower leaf. *Plant, Cell & Environment* 22: 1365–1376.
- Granier C, Tardieu F. 1999b. Water deficit and spatial pattern of leaf development. Variability in responses can be simulated using a simple model of leaf development. *Plant Physiology* 119: 609–619.
- Green PB. 1994. Connecting gene and hormone action to form, pattern and organogenesis: biophysical transductions. *Journal of Experimental Botany* 45: 1775–1788.
- Hamant O, Heisler MG, Jönsson H, Krupinski P, Uyttewaal M, Bokov P, Corson F, Sahlín P, Boudaoud A, Meyerowitz EM *et al.* 2008. Developmental patterning by mechanical signals in Arabidopsis. *Science* 322: 1650–1655.
- Hamant O, Traas J. 2010. The mechanics behind plant development. *New Phytologist* 185: 369–385.
- Hernández LF. 1995. Pattern formation in the sunflower (*Helianthus annuus* L.) capitulum. Biophysical considerations. *Biocell* 19: 203–212.
- Hernández LF, Green PB. 1993. Transductions for the expression of structural pattern: analysis in sunflower. *Plant Cell* 5: 1725–1738.
- Jones MM, Osmond CB, Turner NC. 1980. Accumulation of solutes in leaves of sorghum and sunflower in response to water deficits. *Australian Journal of Plant Physiology* 7: 193–205.
- Jönsson H, Heisler MG, Shapiro BE, Meyerowitz EM, Mjolsness E. 2006. An auxin-driven polarized transport model for phyllotaxis. *Proceedings of the National Academy of Sciences, USA* 103: 1633–1638.
- Klar AJS. 2002. Plant mathematics: Fibonacci's flowers. *Nature* 417: 595.
- Koch KE. 1996. Carbohydrate-modulated gene expression in plants. *Annual Review of Plant Physiology and Plant Molecular Biology* 47: 509–540.
- Kwiatkowska D. 2006. Flower primordium formation at the Arabidopsis shoot apex: quantitative analysis of surface geometry and growth. *Journal of Experimental Botany* 57: 571–580.
- Kwiatkowska D, Routier-Kierzkowska A-L. 2009. Morphogenesis at the inflorescence shoot apex of *Anagallis arvensis*: surface geometry and growth in comparison with the vegetative shoot. *Journal of Experimental Botany* 60: 3407–3418.
- Lindström LI, Pellegrini CN, Aguirrezábal LAN, Hernández LF. 2006. Growth and development of sunflower fruits under shade during pre and early post-anthesis period. *Field Crops Research* 96: 151–159.
- López Pereira M, Sadras VO, Trápani N. 1999. Genetic improvement of sunflower in Argentina between 1930 and 1995. I. Yield and its components. *Field Crops Research* 62: 157–166.
- Marc J, Palmer JH. 1981. Photoperiodic sensitivity of inflorescence initiation and development in sunflower. *Field Crops Research* 4: 155–164.
- Muller B, Stosser M, Tardieu F. 1998. Spatial distributions of tissue expansion and cell division rates are related to irradiance and to sugar content in the growing zone of maize roots. *Plant, Cell & Environment* 21: 149–158.
- Munier-Jolain N, Ney B. 1998. Seed growth rate in grain legumes II. Seed growth rate depends on cotyledon cell number. *Journal of Experimental Botany* 49: 1971–1976.
- Munier-Jolain N, Salon C. 2003. Can sucrose content in the phloem sap reaching field pea seeds (*Pisum sativum* L.) be an accurate indicator of seed growth potential? *Journal of Experimental Botany* 54: 2457–2465.
- Munns R, Passioura JB, Guo J, Chazen O, Cramer GR. 2000. Water relations and leaf expansion: importance of time scale. *Journal of Experimental Botany* 51: 1495–1504.
- Palmer JH, Steer BT. 1985. The generative area as the site of floret initiation in the sunflower capitulum and its integration to predict floret number. *Field Crops Research* 11: 1–12.
- Paoloni PJ, Hernández L, Pellegrini CN. 2000. Patrón de vaneos en capítulos de girasol (*Helianthus annuus* L.) crecidos en condiciones naturales. In: *15th International Sunflower Conference*, Vol 1. International Sunflower Association, Toulouse, France, pp. D31–D34.
- Pereyra-Irujo GA, Velazquez L, Lechner L, Aguirrezábal LAN. 2008. Genetic variability for leaf growth rate and duration under water deficit in sunflower: analysis of responses at cell, organ, and plant level. *Journal of Experimental Botany* 59: 2221–2232.
- Reinhardt D, Pesce E-R, Stieger P, Mandel T, Baltensperger K, Bennett M, Traas J, Friml J, Kuhlemeier C. 2003. Regulation of phyllotaxis by polar auxin transport. *Nature* 426: 255–260.
- Rey H, Dauzat J, Chenu K, Barczy J-F, Dosio GAA, Lecoœur J. 2008. Using a 3-D virtual sunflower to simulate light capture at organ, plant and plot levels: contribution of organ interception, impact of heliotropism and analysis of genotypic differences. *Annals of Botany* 101: 1139–1151.
- Ritchie JT, Wei J. 2000. Models of kernel number in maize. In: Westgate ME, Boote K, eds. *Physiology and modeling kernel set in maize*. Madison, WI, USA: Crop Science Society of America, 75–88.
- Sadras VO, Connor DJ, Whitfield DM. 1993. Yield, yield components and source sink relationships in water-stressed sunflower. *Field Crops Research* 31: 27–39.
- Smith AM, Stitt M. 2007. Coordination of carbon supply and plant growth. *Plant, Cell & Environment* 30: 1126–1149.
- Sobrado MA, Turner NC. 1986. Photosynthesis, dry matter accumulation and distribution in the wild sunflower *Helianthus petiolaris* and the cultivated sunflower *Helianthus annuus* as influenced by water deficits. *Oecologia* 69: 181–187.
- Steer BT, Hocking PJ. 1983. Leaf and floret production in sunflower (*Helianthus annuus* L.) as affected by nitrogen supply. *Annals of Botany* 52: 267–277.
- Steer BT, Milroy SP, Kamona RM. 1993. A model to simulate the development, growth and yield of irrigated sunflower. *Field Crops Research* 32: 83–99.
- Sturm A, Tang G-Q. 1999. The sucrose-cleaving enzymes of plants are crucial for development, growth and carbon partitioning. *Trends in Plant Science* 4: 401–407.
- Sultan SE. 2010. Plant developmental responses to the environment: eco-devo insights. *Current Opinion in Plant Biology* 13: 96–101.
- Traas J, Bohn-Courseau I. 2005. Cell proliferation patterns at the shoot apical meristem. *Current Opinion in Plant Biology* 8: 587–592.
- Turner NC, Begg JE, Tonnet ML. 1978. Osmotic adjustment of sorghum and sunflower crops in response to water deficits and its influence on water potential at which stomata close. *Australian Journal of Plant Physiology* 5: 597–608.
- Uyttewaal M, Traas J, Hamant O. 2010. Integrating physical stress, growth, and development. *Current Opinion in Plant Biology* 13: 46–52.
- Vega CRC, Andrade FH, Sadras VO, Uhart SA, Valentinuz OR. 2001. Seed number as a function of growth. A comparative study in soybean, sunflower, and maize. *Crop Science* 41: 748–754.
- Villalobos FJ, Sadras VO, Soriano A, Fereres E. 1994. Planting density effects on dry matter partitioning and productivity of sunflower hybrids. *Field Crops Research* 36: 1–11.
- Wang Y, Li J. 2008. Molecular basis of plant architecture. *Annual Review of Plant Biology* 59: 253–279.
- Welcker C, Boussuge B, Bencivenni C, Ribaut JM, Tardieu F. 2007. Are source and sink strengths genetically linked in maize plants subjected to water deficit? A QTL study of the responses of leaf growth and of Anthesis-Silking Interval to water deficit. *Journal of Experimental Botany* 58: 339–349.